

Universiteit
Leiden
The Netherlands

MicroRNA-based gene therapy for Huntington's disease : Silencing the villain

Miniarikova, J.

Citation
Miniarikova, J. (2019, January 24). *MicroRNA-based gene therapy for Huntington's disease : Silencing the villain*. Retrieved from https://hdl.handle.net/1887/68333

Version:	Not Applicable (or Unknown)
License:	Licence agreement concerning inclusion of doctoral thesis in the Institutional Repository of the University of Leiden
Downloaded from:	https://hdl.handle.net/1887/68333

Note: To cite this publication please use the final published version (if applicable).

Cover Page



Universiteit Leiden



The handle http://hdl.handle.net/1887/68333 holds various files of this Leiden University dissertation.

Author: Miniarikova, J.
Title: MicroRNA-based gene therapy for Huntington's disease : Silencing the villain
Issue Date: 2019-01-24

MicroRNA-based gene therapy for Huntington's disease: Silencing the villain



Jana Miniariková

MICRORNA-BASED GENE THERAPY FOR HUNTINGTON'S DISEASE: SILENCING THE VILLAIN

JANA MINIARIKOVÁ

PhD Thesis, Leiden University, January 2019
MicroRNA-based gene therapy for Huntington's disease: Silencing the villain
ISBN 978-94-6375-175-9
Layout: Egied Simons
Cover: Seyens
Printing: Ridderprint
Copyright © 2018, Jana Miniariková. All rights reserved. No parts of this thesis may be reproduced or transmitted in any form, by any means, without prior written permission of the author.
The printing of this thesis and graduation was financially supported by:
uniQure
Leiden University Medical Center
Baseclear
Sanbio
ttopstart
Vereniging van Huntington

MICRORNA-BASED GENE THERAPY FOR HUNTINGTON'S DISEASE: SILENCING THE VILLAIN

Proefschrift

ter verkrijging van de graad van Doctor aan de Universiteit Leiden,

op gezag van Rector Magnificus prof.mr. C.J.J.M. Stolker,

volgens besluit van het College voor Promoties

te verdedigen op donderdag 24 januari 2019

klokke 13.45 uur

door

JANA MINIARIKOVÁ

geboren te Bratislava (Slowakije)

in 1988

Promotor:	Prof. Dr. S. J. van Deventer
Co-promotor:	Dr. P. Konstantinova (uniQure, Amsterdam, The Netherlands)
Leden promotiecommissie:	Prof. Dr. R. Hoeben Prof. Dr. R. Roos Prof. Dr. A. Aartsma-Rus Prof. Dr. P. H. Reitsma Prof. MVDr. J. Motlík, DrSc. (Centrum PIGMOD, Libechov, Czech Republic)

In memory of my grandfather Dr.h.c. Prof. Ing. Eugén Jóna, DrSc.

CONTENTS

Chapter 1:	General introduction - Translation of microRNA-based huntingtin lowering therapies from preclinical studies to the clinic *Mol. Ther. (2018); **26**: 947–962*	9
Chapter 2:	Design, characterization and lead selection of therapeutic miRNAs targeting huntingtin for development of gene therapy for Huntington's disease *Mol. Ther. Nucleic Acids (2016); **5**: e297*	37
Chapter 3:	AAV5-miHTT gene therapy demonstrates suppression of mutant huntingtin aggregation and neuronal dysfunction in a rat model of Huntington's disease *Gene Ther. (2017); **24**: 630–639*	85
Chapter 4:	Therapeutic microRNAs targeting nuclear huntingtin for a development of a personalized gene therapy for Huntington's disease	111
Chapter 5:	Mature miHTT molecules are present in vesicles enriched for exosomes and secreted from Huntington's disease neuronal cultures treated with AAV5-miHTT gene therapy	135
Chapter 6:	General discussion *Mol. Ther. (2018); **26**: 947–962*	157
Addendum:	English summary	179
	Dutch summary / Nederlandse samenvatting	181
	Slovak summary / Zhrnutie v slovenčine	185
	List of abbreviations	189
	Curriculum vitae	191
	Acknowledgements	195

1

GENERAL INTRODUCTION

Translation of microRNA-based huntingtin lowering therapies from preclinical studies to the clinic

Jana Miniarikova[1,2], Melvin M. Evers[1], Pavlina Konstantinova[1]

[1]Department of Research & Development, uniQure, Amsterdam, the Netherlands

[2]Department of Gastroenterology and Hepatology, Leiden University Medical Center, Leiden, the Netherlands

*Mol. Ther. (2018); **26**: 947–962*

ABSTRACT

The single mutation underlying the fatal neuropathology of Huntington's disease (HD) is a CAG triplet expansion in exon 1 of the huntingtin (*HTT*) gene, given rise to a toxic mutant HTT protein. There has been a number of not yet successful therapeutic advances in the treatment of HD. The current excitement in the HD field is due to the recent development of therapies targeting the culprit of HD either at the DNA or RNA level to reduce the overall mutant HTT protein. In this review, we briefly describe short-term and long-term HTT lowering strategies targeting HTT transcripts. One of the most advanced HTT lowering strategies is a micro (mi)RNA-based gene therapy delivered by a single administration of an adeno-associated viral (AAV) vector to the HD patient. We outline the outcome measures for the miRNA-based HTT lowering therapy in the context of preclinical evaluation in HD animal and cell models. We highlight the strengths and ongoing queries of the HTT lowering gene therapy as an HD intervention with a potential disease-modifying effect. This review provides a perspective on the fast-developing HTT lowering therapies for HD and their translation to the clinic based on the existing knowledge in the preclinical models.

INTRODUCTION

Huntington's disease (HD) is the most common autosomal dominant neurodegenerative disorder with the prevalence rate 1-10 in 100.000 individuals worldwide.[1,2] The genetic cause of HD is an expansion of more than 39 CAG triplets in exon 1 of the huntingtin (*HTT)* gene, which results in a toxic gain of function of the mutant HTT protein containing a long polyglutamine (polyQ) tract.[3] Carriers of 36 to 39 CAG repeats show reduced penetrance.[3,4] Mutant HTT protein causes neuropathology affecting the entire brain, with medium spiny neurons of the striatum being particularly vulnerable at early stages.[5,6] The clinical symptoms include progressive motor, cognitive, and psychiatric disturbances.[5,7] The length of HD expansion on average consists of 40-55 CAGs and roughly predicts the motor onset in an inverse manner, with a 38-56% variance introduced by yet unidentified genetic modifiers.[8] The age of motor onset is typically in mid-life with a median survival of 15-18 years.[7] Occasionally, HD manifests in juveniles with a typical severe phenotype due to the very long CAG expansion.[9] Similar to other incurable neurodegenerative disorders, HD is devastating for patients and their families.

The mutant HTT protein mediates toxicity by intervening in crucial cellular pathways such as apoptosis, protein degradation, transcription, axonal transport, and mitochondrial function, leading to cellular dysfunction and cell death.[6,10] A consistent key feature of HD pathogenesis is the aggregation of mutant HTT protein in different conformations and at various cellular localizations.[11–13] Although the exact role of HTT aggregation is still under debate, several findings indicate that HTT aggregates are directly linked to HD pathology. Overexpressing an aggregating N-terminal fragment of mutant HTT is sufficient to cause HD-like neuropathology in transgenic HD mice and in a lentiviral HD rat model,[14,15] and blocking polyQ-mediated aggregation has neuroprotective effects in transgenic HD mice.[16] Interestingly, the mutant HTT aggregates can be transmitted by a prion-like mechanism to genetically unrelated fetal neural allografts within a brain of HD patients, suggesting a propagation of pathology that is similar to other neurodegenerative disorders such Alzheimer's and Parkinson's disease.[17–19] Apart from the HTT aggregation, a formation of mutant HTT fragments of different lengths has been implicated as an essential event in HD pathology.[20] The generation of these fragments is not fully understood. The mutant HTT protein undergoes a proteolytic cleavage resulting in N-terminal HTT fragments that showed toxicity in transgenic mice and have been found in HD human brains *post mortem*.[21–24] Short HTT exon 1 fragments can be translated from an aberrant splice variants in knock-in HD mice and these fragments have been also localized in the brain of HD patients *post mortem*.[25] Lastly, similar to other repeat-associated disorders, mutant HTT RNA showed repeat-associated non-ATG (RAN) translation that generates short HTT fragments of which some are toxic.[26]

Early therapeutic HD strategies focused on a development of agents to counter the downstream toxic cellular effects of mutant HTT protein or on cellular replacement strategies to compensate for the loss of neurons.[27] Unfortunately, this has not yet resulted in an effective HD treatment that would halt or delay disease progression. Because the mutant HTT protein seems to be the cardinal toxic trigger for the induction of HD pathogenesis, the HTT lowering is currently considered to be the main therapeutic objective for HD.[28] Even after the onset of symptoms, a conditional blockage of HTT expression is sufficient to clear HTT aggregates resulting in HD-like behavioral improvements in mice, which suggests that HD pathogenesis can be reversed after the onset of motor dysfunction.[29] An effective therapeutic HTT lowering approach would require a long-term HTT suppression in wide areas of the brain, which can be achieved using gene therapy technologies.[28]

Most HD patients are heterozygous for the CAG expansion and therefore, HTT lowering strategies are being developed and assessed in a non-selective or allele-selective manner by targeting both alleles or preferentially the mutant HTT allele, respectively.[30] Mutant allele-specific therapeutic strategies aim to develop molecules exclusively recognizing the longer CAG tract or sequences containing specific isoforms of heterozygous single-nucleotide polymorphisms (SNPs) that are in a linkage disequilibrium with the CAG expansion.[31–33] These approaches are challenging, because potential target SNPs are scarce within the HD population and because it is difficult to get sufficient allele selectivity.[31,32,34,35] Therefore, a majority of the most advanced projects focus on the non-selective HTT lowering.[28] Multiple lines of investigations using HD rodent and nonhuman primates indicate that the non-selective HTT lowering is feasible, reverses HD neuropathology, and –within a certain therapeutic window- is well tolerated.[36–39] The first ongoing HTT lowering clinical trial (https://clinicaltrials.gov/: NCT02519036) was initiated in 2015 and was designed to lower both HTT alleles by using antisense oligonucleotides delivered intrathecally (IT) to early stage HD patients.

Two main modes of HTT silencing are currently developed: short-term and long-term HTT lowering. The short-term HTT lowering is based on periodical re-administration of therapeutics that lower HTT, whereas the long-term HTT lowering uses viral vectors as delivery vehicles of therapeutic expression cassettes to achieve continuous drug influx in a target tissue.[20,40,41] One of the most advanced long-term HTT lowering strategies is a micro (mi)RNA-based gene therapy that comprises a single administration of an adeno-associated viral (AAV) vector delivering an expression cassette of a therapeutic miRNA precursor.[37,39,42,43] These precursors are designed to activate the endogenous mRNA silencing machinery to reduce overall HTT translation in target cells.

As for any other potential HD treatment, an AAV-miRNA gene therapy approach needs to address a representative set of outcome measures that are clinically relevant and support the translation of the therapy to the clinical setting. A great number of HD animal models, ranging from fruit flies to higher species such as a minipig or a sheep, have been

generated to evaluate early and late stage preclinical therapeutic approaches for HD.[44–46] Unfortunately, due to the complex nature of the disease, there is not a single model that addresses all necessary treatment outcome measures required for the initiation of a clinical trial. Therefore, the preclinical development of a therapy for HD must include a combination of several *in vitro* and *in vivo* studies in various disease models. The therapeutic benefit observed in a combination of HD cell and animal models is critical to support the rational for further clinical development.

In this review, we briefly discuss short-term and long-term HTT lowering strategies with a focus on miRNA-based gene therapies. We characterize the available HD animal or cell systems that enable preclinical testing of the AAV-delivered-miRNA-based gene therapy. The outcome measures that support the transition from preclinical studies to the clinic are thoroughly discussed. Ultimately, we propose a preclinical framework that should facilitate the preclinical study design for the RNA interference (RNAi)-based and other HTT lowering strategies.

HTT lowering strategies

Artificial DNA or RNA molecules to achieve lowering of HTT translation as a potential therapy for HD have been broadly investigated.[20] Here below, we will discuss these HTT lowering therapies into more detail.

Short-term HTT lowering

A wide range of small DNA and RNA molecules demonstrated efficacious short-term HTT lowering in HD rodent models and nonhuman primates.[20] Antisense oligonucleotides and small interfering (si)RNAs are designed to bind to HTT transcripts to halt HTT translation using either RNase H- or RNAi-based cellular silencing mechanisms, respectively. The chemical characteristics and mode of action of these therapeutics were extensively reviewed elsewhere.[41,47–51] Antisense oligonucleotides can dose-dependently suppress HTT, delay formation of mutant HTT aggregates, and improve neuropathology, as well as behavioral function in rodent HD models.[52–55]

Although HTT is widely expressed throughout the brain, the neuronal damage is more prominent within the corticostriatal circuitry involving cortex and deep brain structures of the striatum.[5,56] Wang et al. showed in a conditional transgenic HD mouse model that it will be crucial for drugs that lower HTT to reach in a sufficient amount not only the surface areas of the brain but also the striatum.[56] Although the infusions of antisense oligonucleotides to the cerebrospinal fluid (CSF) induced short-term non-selective HTT lowering in a nonhuman primate brain, the reduction of HTT was more extensive at approximately 50% in the cortex compared with 20% in the caudate nucleus.[57] The effect of HTT lowering was declining up to the termination of the study at three months. For siRNA therapeutics, >45% suppression of HTT in the nonhuman primate striatum was achieved in two studies using

chemically modified siRNAs administered stereotactically into the brain.[58,59] Comparison of these studies revealed that the duration of siRNA infusions into the brain strongly effects the duration of HTT suppression. Clinically more relevant shorter continuous three-day infusions lead up to 39-day therapeutic lowering till HTT suppression returned to zero.[59] An overall advantage of short-term "non-viral" induction of HTT lowering is a possibility to discontinue the treatment at any time. On the other hand, the results from nonhuman primate studies indicate that repeated administration either to the spinal cord or deep brain structures is required for persistent therapeutic effect. Periodical re-administrations present a lifelong burden for HD patients, which is higher if a treatment would need to be delivered directly into the striatum. The current clinical trial (https://clinicaltrials.gov/: NCT02519036) in humans will provide first insights into the safety and efficacy of CSF-delivered short-term therapies for HD that will require persistent re-administrations to the spinal cord.

Long-term HTT lowering

The limited drug accessibility to the human brain is one of the major challenges in the development of HD therapies and one-time delivery of a therapeutic that provides long-term benefit would have major advantages. Long-term HTT lowering can be realized by viral delivery of an expression cassette of RNAi precursors, such as miRNAs and short hairpin (sh)RNAs.[40,43,47] Similar to siRNA therapeutics, artificial miRNAs and shRNAs are designed to operate post-transcriptionally in a sequence-specific manner after being processed by the endogenous RNAi machinery (**Figure 1**).[60] shRNAs expressed from strong polymerase III promoters showed toxicity at high doses in mice.[61–63] In some cases, the shRNA toxicity correlated with high production of the passenger strand, a byproduct of RNAi processing, independent from the HTT mRNA silencing.[64] The latter was circumvented when the miRNA-based expression system was used instead.[64]

The most common delivery systems of RNAi expression cassettes are recombinant AAV or lentiviral (LV) vectors.[65,66] Whereas LV vectors integrate in the host genome, AAV genomes remain mostly episomal after transduction and therefore are less likely to cause random insertional mutagenesis and inadvertent activation of oncogenes.[67] AAVs are also know to effectively transduce non-dividing cells.[65,68] AAV vectors with increased cell- and tissue-specific tropism have been designed, and some AAV vectors exhibit anterograde and retrograde neuronal transport.[66,68] To date, AAV serotypes 1, 2, 5, 6, 8, 9, and recombinant human (rh)10 are the widely studied as delivery vectors for the central nervous system (CNS) indications.[68]

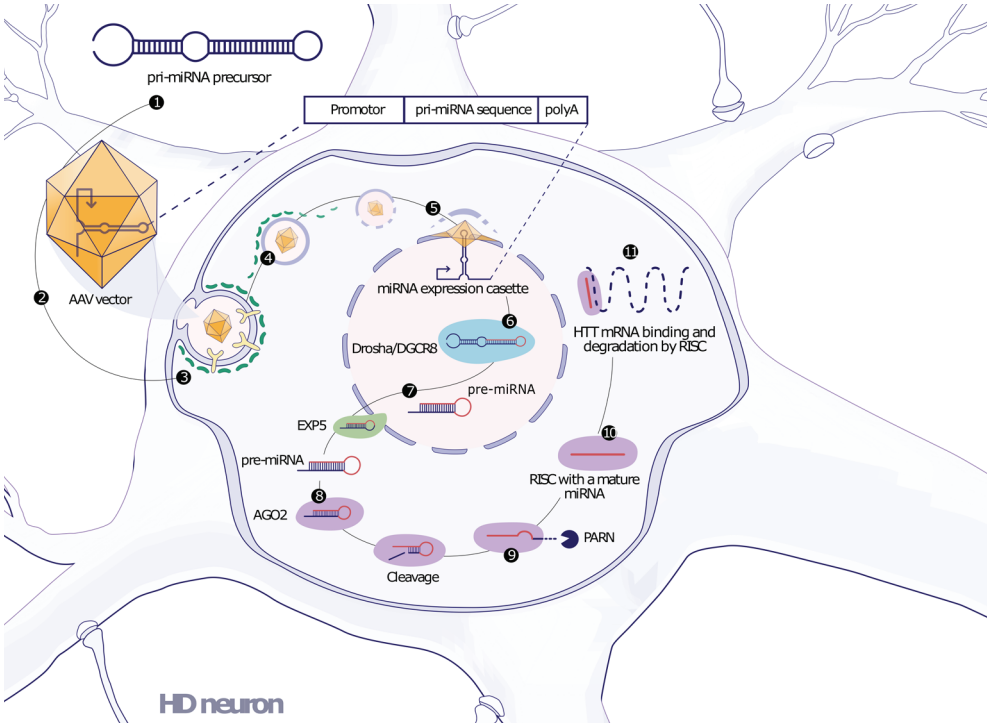


Figure 1. A therapeutic concept of an AAV-miRNA gene therapy using optimized miRNA precursors. An AAV-miRNA construct is generated by incorporating an expression cassette of a therapeutic miRNA precursor in an AAV vector (**1**). The resultant AAV-miRNA construct is delivered to the target cells, where it binds to cell-surface markers to induce endocytosis (**2**). Inside the cell, the AAV capsid is hydrolyzed (**3**) and AAV genome enters the nucleus (**4**). In the nucleus, the artificial miRNA is transcribed as a primary (pri)-miRNA precursor. The precursor folds into a typical stem-loop RNA structure and is further cleaved by DROSHA/DGCR8 complex at specific positions to render a pre-miRNA precursor (**5**). The pre-miRNA is exported out of the nucleus to the cytoplasm by Exportin 5 (EXP5) (**6**). In the cytoplasm, the precursor is recognized by RNA-induced silencing complex (RISC), from which Argonaute 2 (AGO2) enables artificial pre-miRNA cleavage, generation of the guide strand, and degradation of the passenger strand (**7**). The guide strand is further trimmed by poly(A)-specific ribonuclease (PARN) to render a mature miRNA therapeutic (**8**). RISC together with a mature miRNA bind to target HTT mRNA (**9**), which ultimately results in HTT protein lowering (**10**).

The efficacy and safety of RNAi-based gene therapies were first evaluated in HD rodent models and HTT lowering of 55% has been reported.[69] Following the initial report, more than twenty studies have been published using RNAi molecules as potential therapeutic compounds for HD treatment (**Supplementary table 1**).[70] Several studies reported inhibition of mutant HTT aggregate formation, and this reduced neuronal dysfunction in HD rats.[38,71,72] In a nonhuman primate study, AAV1-miRNA targeting rhesus HTT was magnetic resonance imaging (MRI)-guided stereotactically injected in the right and left putamen, which induced 45% HTT reduction in the mid- and caudal putamen without inducing neuronal degeneration, astrogliosis, or an immune response till the termination of the study at six weeks.[37] Similarly, injections of AAV2-shRNA targeting rhesus HTT induced well-tolerated 30% HTT reduction in the injected putamen measured at six months post injections.[73] More recently, AAV9-miRNA

unilateral injections in the striatum of the HD sheep induced 50-80% HTT protein lowering at six months post injections.[74] A dose-dependent distribution of AAV5-miRNA was achieved as well in a transgenic minipig model of HD (M.M.E. et al., unpublished data). Our study showed a significant lowering of human mutant HTT mRNA and protein in the striatum and more distal cortical areas at three months post injections (M.M.E. et al., unpublished data). Together, these data demonstrate a proof-of-concept in HD animal models, supporting the transition of RNAi-based gene therapy to the clinic.

Animal models and cell systems addressing key preclinical outcome measures relevant for the HTT lowering

Many HD animal models that represent the progressive degenerative phenotype of HD allow fast and clinically relevant assessments of novel treatment paradigms.[44–46,75,76] However, the different models represent only specific aspects of HD symptomatology,[44] No single model can be used to properly address all clinically relevant aspects of HTT lowering gene therapies. Therefore, preclinical development of an HTT-targeting gene therapy demands a combination of experiments including various HD cell and animal models addressing a broad spectrum of outcome measures.[28,77] In this section, we discuss HD animal and cell models based on their genetic and phenotypic aspects in relation to HTT lowering strategies.

Nematodes and fruit flies have been used for HD drug discovery, but we limit the scope of this review to the more relevant rodent and large animal models. HD animal models can be categorized based on the following genetic aspects: **1**) location of *HTT* gene insertion as knock-in or transgenic, **2**) construct engineering as full-length or partial mutant HTT, **3**) use of cDNA or genomic DNA, **4**) length of CAG expansion, **5**) use of the HTT or other promoters, and **6**) presence or absence of the host HTT.[44,78] The genetic background of HD animal models not only determines the phenotype, but also defines the availability for therapeutic targeting and subsequent translation of the approach to the clinic. As such, genetic therapies targeting directly DNA or RNA sequences of HTT require a presence of human target sequences in the animal model for preclinical testing. For instance, the efficacy of artificial miRNAs designed to target HTT exons closer to the 3' UTR cannot be assessed in HD animals expressing only the N-terminal fragment of human mutant HTT. Similarly, when addressing the allele-selective potential of miRNAs or antisense oligonucleotides based on a SNP in the *HTT* gene, the chosen animal model should not only carry the polymorphism but the SNP should be heterozygous. Ultimately, when selecting HD animal models, the conservation of target sequences between various species should be closely considered, as well as the effects of simultaneous targeting of the mutant and endogenous HTT. The latter is crucial for assessment of tolerability of non-selective HTT lowering, in which case the remaining levels of endogenous HTT are relevant.

Rodent HD models

Mice and rats are the most commonly tested species to address activity of therapeutic compounds in the preclinical development of HD and currently more than two dozens of rodent models have become available.[14,44,78] The most utilized mouse model of HD is a transgenic R6/2 developed by a random insertion of the human mutant HTT exon 1, originally containing 144 CAG repeats, into the mouse genome.[79,80] The gene expression is driven by the human HTT promoter and the mutant HTT is expressed at three quarters of the level of wild-type murine Htt, which has two copies.[79] Similar to juvenile HD patients, higher CAG repeat number manifests in these mice with earlier onset of disease, formation of HTT aggregates, rapidly progressive motor and cognitive deficits, and premature death. These characteristics distinguish this model from most of knock-in and full-length murine models, that have a less progressive phenotype.[81] Notably, somatic instability has been reported in R6/2 mice that manifest in variable CAG lengths.[82] This results in differential behavioral and neuropathological patterns that should be considered when testing HTT lowering therapies and comparing different studies. Another widely used transgenic HD mouse model N171-Q82 was generated with a HTT fragment containing 171 amino acids and 82 glutamines.[83] The gene is expressed from the mouse prion promoter as 20% of murine Htt. This model expresses less HTT and has shorter CAG repeats compared with R6/2 mice and subsequently it presents with later onset of symptoms.[81]

YAC128 and BACHD mice are well-known full-length mutant HTT models with 128 and 97 CAG repeats, respectively.[84–86] The transgenes are expressed from the human HTT promoter as 75% and 150% of Htt, respectively.[75,85,86] Both models show progressive motor, cognitive and psychiatric disturbances. The recent development of full-length transgenic humanized Hu128/21 (YAC128/BAC21) and Hu97/18 (BACHD/YAC18) mice by intercrossing YAC and BAC models with the Hdh-/- background now allows evaluation of the efficacy of new therapies in mice that do not express murine Htt and have two copies of the mutant human *HTT* gene.[87,88] Both Hu128/21 and Hu97/18 exhibit progressive motor, cognitive and psychiatric disturbances. Hu128/21 mice also show EM48 positive inclusions at nine months of age. These humanized HD mice offer unique opportunities to address the window of safety and efficacy of the non-selective HTT lowering as the murine HTT has been replaced by two human copies. Additionally, the humanized Hu128/21 model is also suitable for assessing the allele selectivity of HTT lowering agents targeting heterozygous SNPs or different CAG lengths. Hu97/18 is not a suitable model for assessing CAG-targeting therapeutics because of the mixed CAG-CAA tract.

The knock-in HD mouse models should represent, in theory, more accurately HD pathology since they are created by inserting a human HTT fragment with 50-200 CAGs into a part of or the entire murine Htt gene and the expression remains driven by the murine Htt promoter.[89,90] These mice are generated either homozygous or heterozygous for the human HTT fragment.[91] Overall, the behavioral deficits are reported to be not striking compared

to other murine models, which is important to consider when addressing the treatment efficacy.[14,81]

Notably, either weight gain or loss has been described in many murine HD models. R6/2 mice showed weight loss, whereas full-length murine HD models such as YAC128, BACHD, Hu97/18 and Hu128/21 mice demonstrate weight gain.[44,87,88] Hence, animal model-specific changes in body weight should be monitored since such changes could influence the results of motor and behavioral performances.

Whereas mouse models are plentiful, only three HD rat models have been described to date. The first HD rats were generated by a lentiviral delivery of a HTT fragment containing various CAG repeats.[15] These rats manifest with a rapid local neuropathology, including HTT aggregation, but do not display behavioral deficits.[15] Those models are suitable for evaluating suppression of neurodegeneration, as indeed was demonstrated for different miRNAs and shRNAs that lower HTT.[71,72] The second HD rat model is transgenic with a human HTT cDNA fragment containing 51 CAGs, whereas expression is under control of the rat Htt promoter.[92] These rats manifest with adult-onset neurodegeneration, motor, cognitive and behavioral deficits. Recently, a full-length transgenic BACHD rat model was generated that exhibits behavioral deficits, HTT aggregation and striatal neuronal loss.[93] In contrast to BACHD mice, these rats do not show increased body weight.

In summary, the progressive HD models that develop a severe neurodegeneration are suitable to evaluate the suppression of neuropathology related to HTT lowering. The slow models are suitable to study improvements of motor and behavioral deficits during a longer period of time after administrating the HTT lowering therapy. Therefore, a preclinical portfolio would ideally include studies with rapid- and slow-progression HD rodent models to gain a comprehensive understanding of the therapeutic efficacy, pharmacodynamics and potential toxicity of the treatment.

Large HD animal models

In the recent years, considerable efforts have resulted in the development of large HD animal models. These large animal models allow to study efficacy, safety, biomarker discovery, long-term HTT lowering in an animal model with a larger brain and closer similarities in immunophysiology to humans compared with rodents.[94] Two important models, the HD minipig and sheep, have been generated with the support of CHDI foundation.[95,96] The knock-in HD minipig was developed by an insertion of a fragment of mutant HTT encoding the first 548 amino acids (12 exons) containing 124 glutamines under control of the human HTT promoter.[96] The transgenic sheep was generated with a full-length human HTT cDNA encoding 73 glutamines under control of the human HTT promoter.[95] Having been recently developed, these large animal models do not yet show the HD phenotype, which is being carefully monitored. Thus, the use of large HD animal models for preclinical studies is currently restricted to direct measures related to lowering of mutant HTT. Large animal studies are

costly and lengthy as compared to rodent studies, and still need to be sufficiently powered to reach meaningful outcomes. Nevertheless, these studies should not be omitted from the preclinical development because they offer a much more realistic system regarding the delivery of gene therapy. Consequently, such studies are usually conducted after obtaining efficacy and safety signals in rodent models. Undoubtedly, a sufficient body of knowledge from the rodent studies is a requirement for a successful large animal study.

Cell systems modelling HD

During the last years, induced pluripotent stem cells (iPSCs) -derived neuronal cultures have become an accepted model of neurodegenerative diseases including HD, that enables early testing of the treatment efficacy and some aspects of the safety.[97–99] iPSCs are somatic cells, such as fibroblasts, reprogrammed to a pluripotent state by an addition of essential transcription factors, which can be subsequently differentiated into various cell types.[97] HD patient-derived iPSCs are being differentiated and matured into various neuronal lineages, astrocytes, or microglia and provide a unique platform to study the therapeutic efficacy of HTT lowering strategies in human patient cells.[100–103] Currently, the read-out of therapeutic efficacy in these HD neuronal cultures is the percentage of HTT lowering. However, several studies have been conducted to identify a functional phenotype as measurements of therapeutic efficacy, such as protein clearance, cell growth, adhesion, differentiation, survival, stress response. [reviewed 100] Dozens of transcribed polymorphisms have been found in various local HD patient cohorts that are in a linkage disequilibrium with the HD mutation, thus delineating different HD haplotypes.[34] This allows for an evaluation of HTT lowering compounds targeting a specific polymorphism present in different patient haplogroups. It should be noted that an inherent variability has been found among control iPSCs. Efforts are being made to generate more isogenic iPS lines by gene editing to more accurately define effects linked to the HD mutation.[100] Because gene expression signatures are often species-specific, these human cell-based models have become the preferred test system in parallel to animal studies to study therapy-induced neuronal protection as well as specific off-target silencing of other genes.[71,104]

Preclinical outcome measures for AAV-miRNA gene therapies

Translating preclinical studies to the clinic for an AAV-miRNA-based gene therapy involves establishing a therapeutic safety and efficacy window **(Figure 2)**. While designing preclinical studies, the emphasis should be placed on identification of a translatable framework that will provide sufficient understanding on the efficacy and safety for a given compound, as well as considering the overall financial cost and animal welfare.

Table 1: RNAi-based HTT lowering gene therapy approaches to date.

	Lowering/Improvement								
	Reference	**RNAi therapeutics**	**Vector**	**Human Target**	**HD Animal**	**Delivery**	**HTT RNA (%)**	**HTT protein or inclusions (%)**	**Motor or Behavioural**
HD rodents	Harper et al., 2005	shRNA (shHD2.1)	AAV1	Exon 2	N171-82Q	Striatum	51-55%	10-50%	Rotarod and Gait
	Rodriguez-Lebron et al., 2005	shRNA (siHUNT -1 and -2)	AAV5	Exon 1	R6/1	Striatum	78%	28%	Clasping
	Machida et al., 2006	shRNA (shEGFP)	AAV5	N/A	(eGFP) HD190QG	Striatum	N/A	82%	Rotarod and Clasping
	Huang et al., 2007	shRNA+Ad-HttQ103GFP	Ad	Exon 1	R6/2 (Ad-HttQ103GFP)	Striatum	N/A	Yes: in transduced areas, not quantified	N/A
	Franich et al., 2008	shRNA (shHD2	AAV1	Exon 1	Rat AAV1-HD70	Striatum	80-90%	50%	Forepaw use
	McBride et al., 2008	miRNA (mi2.4)	AAV1	Exon 2	CAG140	Striatum	70%	N/A	N/A
	Boudreau et al., 2009	miRNA (mi2.4)	AAV1	Exon 2	N171-82Q	Striatum	85%	Yes, not quantified	N/A
	Drouet et al., 2009	shRNAs	Lentivirus	Exon 1-4	Rat lenti-htt 171-82Q	Striatum	N/A	70-80%	N/A
	Stanek et al., 2014	miRNA	AAV1	N/A	YAC128	Striatum	45%	55%	Rotarod and Porsolt swim test
	Miniarikova et al.,2016	miRNA (miHTT)	AAV5	Exon1	Hu128/21	Striatum	N/A	80%	N/A
	Miniarikova et al.,2017	miRNA (miHTT)	AAV5	Exon1	Rat lenti-htt 171-82Q	Striatum	62%	98%	N/A
	McBride et al., 2011	miRNA (miHDS1)	AAV1	N/A	wild-type non-human primate	Striatum	45%	N/A	N/A
HD large animals	Grondin et al., 2012	shRNA (shHD5)	AAV2	N/A	wild-type non-human primate	Striatum	30%	45%	N/A
	Pfister et al., 2017	miRNA (miRHTT)	AAV9	Exon 48	HD sheep	Striatum	20-30%	49-81%	N/A
	Evers et al., 2018	miRNA (miHTT)	AAV5	Exon1	HD minipig	Striatum	40-73%	50-54%	N/A

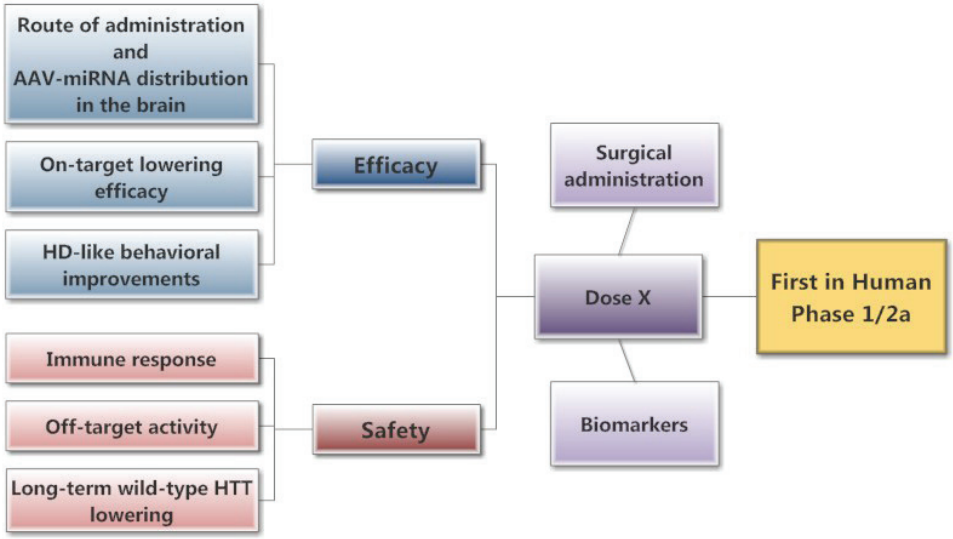


Figure 2. Preclinical measures of an AAV-miRNA gene therapy. The preclinical measures addressing the efficacy and safety aspects of an AAV-miRNA based HTT lowering gene therapy are outlined (in red and blue). Positive findings indicating a sufficient efficacy and no safety concerns demonstrated across multiple animal and cell models enable the selection of the adequate AAV dose and surgical procedure for the First in Human Phase 1/2a (in purple). Various biomarkers should be included in Human Phase 1/2a (in purple) and outlined as exploratory endpoints.

Evaluating efficacy for miRNA-based HTT lowering therapies

Many preclinical studies with potentially disease-modifying compounds have demonstrated a proof-of-principle in HD rodent models, but to date none of these putative treatments has yet successfully been translated to the clinic.[28] As discussed, several aspects of rodent models including their relatively small brain and simple anatomy, make a successful translation to the HD patient difficult. Adequate distribution is of paramount importance for AAV-miRNA gene therapy approaches, and this is dependent on the brain size and structure, the delivery vehicle, and the surgical procedure. All these require the use of a large animal model with a gyrencephalic brain similar to humans, as opposed to rodents with a lissencephalic brain.[45,105] The efficacy parameters of an AAV-miRNA gene therapy that should be explored in preclinical models are:

1. a route of administration to achieve optimal AAV distribution in the brain areas strongly affected by HD
2. mode of action or on-target lowering efficacy
3. HD-like behavioral improvements upon treatment

Route of administration and AAV-miRNA distribution in the brain

The development of AAV-based CNS deliveries has significantly progressed in recent years and multiple clinical studies have been initiated for Alzheimer's, Parkinson's, Canavan's

disease, late infantile neuronal ceroid lipofuscinosis, and Sanfilippo B syndrome.[106] The increased popularity of AAV vectors as drug vehicles for the treatment of neurodegenerative disorders reflects the long-term therapeutic benefits, the ability to transduce nondividing cells such neurons, and a relatively low immune response demonstrated in different models.[65,68] For CNS disorders, the therapeutic AAVs need to target specific brain areas, that are usually difficult to reach, or require a broad CNS coverage. In case of HD, sufficient AAV distribution in the striatum and cortex is crucial.[56] Several AAV serotypes showed efficacious transduction of neurons with different tropisms to immune cells of the brain such as astrocytes, microglia, and oligodendrocytes.[107] Given the brain complexity, the route of administration and the subsequent efficient vector genome delivery is one of the critical obstacles in a gene therapy for HD to eventually reach a clinical benefit.[108]

The three most frequently studied delivery routes of AAV vectors for CNS indications are: **A**) systemic administration through intravenous injection, **B**) direct infusions into the CSF, and **C**) local administration into the brain parenchyma. The CNS transduction efficacy and distribution of most AAV serotypes is being evaluated in large animals such as dogs, cats, minipigs and nonhuman primates (M.M.E. et al., unpublished data.[65,68,109–115] Here below, we will discuss the delivery routes in the HD context.

Intravenous injection

To reach the CNS upon the intravenous injection, AAV vectors carrying the expression cassette of the artificial miRNA precursors need to cross the blood-brain-barrier (BBB) or the blood-spinal cord barrier. These vascular barriers prevent most molecules from entering the CNS, thus providing protection against toxic or infective agents in the blood, as well as maintaining the chemical composition of the interstitial fluid.[116] Most of AAVs are not able to cross the BBB, with an exception of AAV9 which transduces the brain following intravenous injections.[117] The natural capacity of AAV9 to cross the BBB has been greatly augmented by further engineering the capsid, which led to a 40-fold and greater transduction in the murine brain when compared to the native AAV9 serotype.[118,119] Disappointingly, a recent results in marmosets did not recapitulate the enhanced transduction efficacy of these engineered capsids.[120] It still needs to be determined in other large species whether the engineered AAV capsids, when injected intravenously, specifically transduce the relevant target structures that are affected in HD. Thus, the intravenous delivery has an advantage of a low invasive nature, but the translational feasibility is challenging as extremely high doses would be necessary to therapeutically target the deeper structures in the CNS.

Direct infusion in the CSF

AAV vectors can be delivered to the brain by direct infusions in the CSF via intracerebroventricular (ICV) infusions into the lateral ventricles, IT injections in the spinal canal, or by direct administration to the cisterna magna or subarachnoid space. [68,73,109–111,121–123]

To reach the target brain structure of HD upon ICV or IT injections, the AAV needs to pass the ependymal cell layer surrounding the ventricular system or the pia mater, respectively. AAV serotypes 2, 4, 5, and 9 mainly transduce the ependymal cell layer once injected ICV, with a limited penetration into the brain parenchyma.[124] Most of studies using IT injections of various AAV serotypes have been conducted in rodents with a common outcome: the spinal cord is generally effectively transduced, but the vectors poorly reach deeper brain structures such as the striatum.[125–127] Therapeutic administration of AAV vectors to the CSF requires higher doses compared to a local administration and therefore, it may be associated with a higher likelihood of causing an immune reaction. Additionally, ICV and IT deliveries have been reported to cause a vector leakage into the periphery, limiting the clinical efficacious dose in the required brain structures.[68,111,122] On the other hand, in the case of HD, vector leakage is not unwanted *per se*, as (mutant) HTT is widely expressed outside the CNS and may be the cause of peripheral signs of the disease.[128] If IT administration of AAV vectors would result in sufficient striatal transduction, this would offer a major advantage for the clinical development of therapeutic products for HD, and promising results have been reported using AAV5 and AAV9 in nonhuman primates.[112,122]

Intracranial parenchymal administration

Despite recent improvements in an AAV-delivery following systemic or IT administration, at present, direct delivery to the parenchyma will most likely be preferred for HD-disease modifying therapies, because this method ensures sufficient transduction of deep brain structures. To date, more than ten clinical trials have been conducted or are ongoing using direct parenchymal injections of gene therapy products to the brain. [125,129–135] These studies have built on experience with therapeutic electrophysiological procedures. For example, the implantation of electrodes in the pallidus for deep brain stimulation was safe in an already degenerated HD brain.[136] None of the trials completed to date have demonstrated significant clinical benefit, possibly related to the low amount of vector used in the initial trials.[108] Nevertheless, these clinical studies did show that direct injections subcortically, in the substantia nigra or in the putamen, are safe and not associated with serious adverse events.

Optimizations of intracranial parenchymal deliveries show promises as the convection-enhanced delivery (CED) demonstrated an efficacious transmission of molecules to the brain that do not diffuse well.[137] In contrast to diffusive therapies, which are limited by concentration gradients, CED resulted in a high local concentration of drugs with a low systemic absorption.[137] For clinical applications, one or more catheters are stereotactically positioned using imaging methods into the interstitial space of the brain.[138] An infusion pump that is connected to the catheter creates a pressure gradient and drives the drug flow by replacing the extracellular fluid. To increase the safety and efficacy of CED, a reflux-resistant cannula has been developed.[139] CED resulted in improved distribution patterns

of AAV serotypes 1, 2, 5, 8, and 9 in the brain of rodents and nonhuman primates after direct injections into the brain.[109,110,140,141] This technique also showed improved diffusions throughout the brain in the clinical trial for Parkinson's disease and is currently being tested in other trials.[142]

Notably, the viral spread upon a local delivery is dependent on the intracellular transport, which occurs in either the anterograde or retrograde direction along axons.[107,143] The extent of axonal transport and distal transduction differs between the AAV serotypes and the mechanisms responsible for this variability are not clear yet.[107] For the HD treatment, the cortico-striatal circuitry in humans and large animals allows for transductions of distal areas, such as the cortex, from the striatal injection sites.[109,143] To date, all AAV1-, AAV5-, and AAV9-miRNA or AAV2-shRNA-based preclinical studies in HD animal models applied direct injections into the striatum to show a widespread AAV distribution in the CNS (M.M.E. et al., unpublished data).[39,64,72,104,144]

Measurements of on-target lowering efficacy

miRNA-based lowering strategies are designed to lower HTT mRNA levels and thereby to reduce the overall mutant HTT protein. Already in the early preclinical development, it is essential to establish the on-target activity of therapeutics by measuring their effects on HTT mRNA and protein levels. Usually, the initial assessment of a mode of action of therapeutic miRNAs is addressed using *in vitro* cell and reporter systems.[39,144] As discussed, a further extrapolation of observed HTT lowering into both slow- and rapid-progression rodent models is necessary to assess pharmacodynamics, aggregation, functional signs, and symptoms. In 2005, Harper et al. showed for the first time the feasibility of lowering human HTT in N171-82Q mice after injections of AAV1-shRNA vectors into the striatum.[69] In subsequent studies, R6/1, R6/2, CAG140, lenti-htt171-82Q, lenti-htt853-82Q and Hu128/21 rodent models have been successfully used to evaluate the efficacy of RNAi therapeutics.[36,39,64,72,145,146] In contrast to large HD animal models, HD rodents offer measurements of lowering HTT aggregation as an HTT-dependent readout.[69,72,146] The final assessment of a mode of action should be evaluated in a large HD animal model since the physiological, neurological and genetic background relates closer to the human. Although large HD animal models have been available for several years, only two studies have been described so far (M.M.E. et al., unpublished data).[74] A single AAV5-miRNA or AAV9-miRNA administration into a minipig or sheep striatum resulted in the mutant HTT mRNA and protein lowering up to 75%-80% in injected structures lasting at least three and six months post-injections, respectively. Altogether, these data highlight the importance of a careful characterization of on-target lowering efficacy in various HD models.

HD-like behavioral improvements in rodents

Deterioration of motor, cognitive, and psychiatric disturbances are a hallmark of progressive HD and studying these abnormalities in animals is important as it allows an evaluation of the clinical benefit for a specific HTT-targeting intervention.[44] Since the current HD animal models are quadrupeds or invertebrates, the correlations between the behavioral changes in these models and humans should be carefully evaluated nevertheless, a large battery of behavioral changes reported in HD rodents can be used to study efficacy of an AAV-miRNA gene therapy.[Reviewed in 44] To study improvements of motor functions, HD rodents are usually assessed using rotarod, climbing performance, gait analysis, and the balance beam test. [36,69,147] To measure cognitive improvements, learning capacity and memory of rodents are being addressed,[44] and anxiety-like and depression-like changes are used to study improvements in psychiatric measures.[44] Noteworthy, positive findings in behavioral improvements are usually challenging to conclude from a small subset of studied measures and a difficulty is added if the improvement window is not large enough to evaluate a dose response. Therefore, behavioral studies should be efficiently powered and include multiple measures that offer a highest outcome difference between the HD and control animals. Unfortunately, large HD animal models do not -yet- show HD-like symptoms, which precludes their use to study disease-specific functional, behavioral or psychiatric complications.

REFERENCES

1. Rawlins, MD, Wexler, NS, Wexler, AR, Tabrizi, SJ, Douglas, I, Evans, SJW, *et al.* (2016). The prevalence of huntington's disease. *Neuroepidemiology* **46**: 144–153.
2. Fisher, ER and Hayden, MR (2014). Multisource ascertainment of Huntington disease in Canada: Prevalence and population at risk. *Mov. Disord.* **29**: 105–114.
3. Macdonald, ME, Ambrose, CM, Duyao, MP, Myers, RH, Lin, C, Srinidhi, L, *et al.* (1993). A Novel Gene Containing a Trinucleotide That Is Expanded and Unstable on Huntington's Disease Chromosomes. *Cell* **72**: 971–983.
4. Langbehn, DR, Brinkman, RR, Falush, D, Paulsen, JS and Hayden, MR (2004). A new model for prediction of the age of onset and penetrance for Huntington's disease based on CAG length. *Clin. Genet.* **65**: 267–277.
5. Bates, GP, Dorsey, R, Gusella, JF, Hayden, MR, Kay, C, Leavitt, BR, *et al.* (2015). Huntington disease. *Nat. Rev. Dis. Prim.* **1**: 1–21.
6. Ross, CA and Tabrizi, SJ (2011). Huntington's disease: From molecular pathogenesis to clinical treatment. *Lancet Neurol.* **10**: 83–98.
7. Ross, CA, Aylward, EH, Wild, EJ, Langbehn, DR, Long, JD, Warner, JH, *et al.* (2014). Huntington disease: natural history, biomarkers and prospects for therapeutics. *Nat. Rev. Neurol.* **10**: 204–16.
8. Gusella, JF, MacDonald, ME and Lee, J-M (2014). Genetic modifiers of Huntington's disease. *Mov. Disord.* **29**: 1359–1365.
9. Sun, Y-M, Zhang, Y-B and Wu, Z-Y (2016). Huntington's Disease: Relationship Between Phenotype and Genotype. *Mol. Neurobiol.* **54**: 342–348.
10. Saudou, F and Humbert, S (2016). The Biology of Huntingtin. *Neuron* **89**: 910–926.
11. Davies, SW, Turmaine, M, Scherzinger, E, Wanker, EE, Mangiarini, L and Bates, GP (1997). Formation of Neuronal Intranuclear Inclusions Underlies the Neurological Dysfunction in Mice Transgenic for the HD Mutation. *Cell* **90**: 537–548.
12. Poirier, MA, Jiang, H and Ross, CA (2005). A structure-based analysis of huntingtin mutant polyglutamine aggregation and toxicity: evidence for a compact beta-sheet structure. *Hum. Mol. Genet.* **14**: 765–774.
13. Difiglia, M, Sapp, E, Chase, KO, Davies, SW, Bates, GP, Vonsattel, JP, *et al.* (1997). Aggregation of huntingtin in neuronal intranuclear inclusions and dystrophic neurites in brain. *Science (80-.).* **277**: 1990–3.
14. Ferrante, RJ (2009). Mouse models of Huntington's disease and methodological considerations for therapeutic trials. *Biochim. Biophys. Acta* **1792**: 506–520.
15. de Almeida, LP, Ross, C, Zala, D, Aebischer, P and Deglon, N (2002). Lentiviral-mediated delivery of mutant huntingtin in the striatum of rats induces a selective neuropathology modulated by polyglutamine repeat size, huntingtin expression levels, and protein length. *J Neurosci* **22**: 3473–3483.
16. Sánchez, I, Mahlke, C and Yuan, J (2003). Pivotal role of oligomerization in expanded polyglutamine neurodegenerative disorders. *Nature* **421**: 373–379.
17. Frost, B and Diamond, MI (2010). Prion-like mechanisms in neurodegenerative diseases. *Nat. Rev. Neurosci.* **11**: 155–159.
18. Jeon, I, Cicchetti, F, Cisbani, G, Lee, S, Li, E, Bae, J, *et al.* (2016). Human-to-mouse prion-like propagation of mutant huntingtin protein. *Acta Neuropathol.* **132**: 577–592.
19. Cicchetti, F, Lacroix, S, Cisbani, G, Vallières, N, Tolouei, R, Jn, S, *et al.* (2014). Mutant huntingtin is present in neuronal grafts in Huntington's disease patients. *Ann. Neurol.* **76**: 31–42.
20. Wild, EJ and Tabrizi, SJ (2017). Therapies targeting DNA and RNA in Huntington's disease. *Lancet Neurol.* **16**: 837–847.

21. Ehrnhoefer, DE, Sutton, L and Hayden, MR (2011). Small changes, big impact: Posttranslational modifications and function of huntingtin in Huntington disease. *Neuroscientist* **17**: 475–492.
22. Kim, YJ, Yi, Y, Sapp, E, Wang, Y, Cuiffo, B, Kegel, KB, *et al.* (2001). Caspase 3-cleaved N-terminal fragments of wild-type and mutant huntingtin are present in normal and Huntington's disease brains, associate with membranes, and undergo calpain-dependent proteolysis. *Proc. Natl. Acad. Sci. U. S. A.* **98**: 12784–12789.
23. Pouladi, MA, Graham, RK, Karasinska, JM, Xie, Y, Santos, RD, Petersn, Â, *et al.* (2009). Prevention of depressive behaviour in the YAC128 mouse model of Huntington disease by mutation at residue 586 of huntingtin. *Brain* **132**: 919–932.
24. Waldron-Roby, E, Ratovitski, T, Wang, X, Jiang, M, Watkin, E, Arbez, N, *et al.* (2012). Transgenic mouse model expressing the caspase 6 fragment of mutant huntingtin. *J. Neurosci.* **32**: 183–93.
25. Wellington, CL, Ellerby, LM, Gutekunst, C-A, Rogers, D, Warby, S, Graham, RK, *et al.* (2002). Caspase cleavage of mutant huntingtin precedes neurodegeneration in Huntington's disease. *J. Neurosci.* **22**: 7862–7872.
26. Banez-Coronel, M, Ayhan, F, Tarabochia, AD, Zu, T, Perez, BA, Tusi, SK, *et al.* (2015). RAN Translation in Huntington Disease. *Neuron* **88**: 667–677.
27. Kumar, A, Singh, KS, Kumar, V, Kumar, D, Agarwal, S and Rana, MK (2015). Huntington's disease: An update of therapeutic strategies. *Gene* **556**: 91–97.
28. Mestre, TA and Sampaio, C (2017). Huntington Disease: Linking Pathogenesis to the Development of Experimental Therapeutics. *Curr. Neurol. Neurosci. Rep.* **17**: 1–8.
29. Yamamoto, A, Lucas, JJ and Hen, R (2000). Reversal of neuropathology and motor dysfunction in a conditional model of Huntington's disease. *Cell* **101**: 57–66.
30. Wexler, NS, Young, AB, Tanzi, RE, Travers, H, Starosta-Rubinstein, S, Penney, JB, *et al.* (1987). Homozygotes for Huntington's disease. *Nature* **326**: 194–7.
31. Pfister, EL, Kennington, L, Straubhaar, J, Wagh, S, Liu, W, DiFiglia, M, *et al.* (2009). Five siRNAs targeting three SNPs in Huntingtin may provide therapy for three-quarters of Huntington's disease patients. *Curr Biol.* **19**: 774–778.
32. Lombardi, MS, Jaspers, L, Spronkmans, C, Gellera, C, Taroni, F, Di Maria, E, *et al.* (2009). A majority of Huntington's disease patients may be treatable by individualized allele-specific RNA interference. *Exp. Neurol.* **217**: 312–319.
33. Warby, SC, Montpetit, A, Hayden, AR, Carroll, JB, Butland, SL, Visscher, H, *et al.* (2009). CAG expansion in the Huntington disease gene is associated with a specific and targetable predisposing haplogroup. *Am. J. Hum. Genet.* **84**: 351–66.
34. Kay, C, Collins, JA, Skotte, NH, Southwell, AL, Warby, SC, Caron, NS, *et al.* (2015). Huntingtin Haplotypes Provide Prioritized Target Panels for Allele-specific Silencing in Huntington Disease Patients of European Ancestry. *Mol. Ther.* **23**: 1759–1771.
35. Kay, C, Skotte, N, Southwell, A and Hayden, M (2014). Personalized gene silencing therapeutics for Huntington disease. *Clin. Genet.* **86**: 29–36.
36. Boudreau, RL, Mcbride, JL, Martins, I, Shen, S, Xing, Y, Carter, BJ, *et al.* (2009). Nonallele-specific silencing of mutant and wild-type huntingtin demonstrates therapeutic efficacy in Huntington's disease mice. *Mol. Ther.* **17**: 1053–1063.
37. McBride, JL, Pitzer, MR, Boudreau, RL, Dufour, B, Hobbs, T, Ojeda, SR, *et al.* (2011). Preclinical Safety of RNAi-Mediated HTT Suppression in the Rhesus Macaque as a Potential Therapy for Huntington's Disease. *Mol. Ther.* **19**: 2152–2162.
38. Drouet, V, Perrin, V, Hassig, R, Dufour, N, Auregan, G, Alves, S, *et al.* (2009). Sustained effects of nonallele-specific Huntingtin silencing. *Ann. Neurol.* **65**: 276–85.

39. Miniarikova, J, Zanella, I, Huseinovic, A, van der Zon, T, Hanemaaijer, E, Martier, R, *et al.* (2016). Design, Characterization, and Lead Selection of Therapeutic miRNAs Targeting Huntingtin for Development of Gene Therapy for Huntington's Disease. *Mol. Ther. Acids* **5**: e297.
40. Keiser, MS, Kordasiewicz, HB and Mcbride, JL (2016). Gene suppression strategies for dominantly inherited neurodegenerative diseases: lessons from Huntington's disease and spinocerebellar ataxia. *Hum. Mol. Genet.* **25**: 53–64.
41. Sah, DWY and Aronin, N (2011). Review series Oligonucleotide therapeutic approaches for Huntington disease. *J. Clin. ingestigation* **121**: 500–507.
42. Stanek, LM, Sardi, SP, Mastis, B, Richards, AR, Treleaven, CM, Taksir, T, *et al.* (2014). Silencing mutant huntingtin by adeno-associated virus-mediated RNA interference ameliorates disease manifestations in the YAC128 mouse model of Huntington's disease. *Hum. Gene Ther.* **25**: 461–74.
43. Davidson, BL, Boudreau, RL, Rodrı, E, Rodríguez-Lebrón, E and Davidson, BL (2011). RNAi medicine for the brain: Progresses and challenges. *Hum. Mol. Genet.* **20**: 21–27.
44. Pouladi, M a, Morton, a J and Hayden, MR (2013). Choosing an animal model for the study of Huntington's disease. *Nat. Rev. Neurosci.* **14**: 708–21.
45. Howland, DS and Munoz-Sanjuan, I (2014). Mind the gap: Models in multiple species needed for therapeutic development in Huntington's disease. *Mov. Disord.* **29**: 1397–1403.
46. Philips, T, Rothstein, JD and Pouladi, MA (2014). Preclinical models: Needed in translation? A Pro/Con debate. *Mov. Disord.* **29**: 1391–1396.
47. Watts, JK and Corey, DR (2012). Silencing disease genes in the laboratory and the clinic. *J. Pathol.* **226**: 365–79.
48. Fiszer, A and Krzyzosiak, WJ (2014). Oligonucleotide-based strategies to combat polyglutamine diseases. *Nucleic Acids Res.* **42**: 6787–6810.
49. Chery, J (2016). RNA therapeutics: RNAi and antisense mechanisms and clinical applications. *Postdoc J.* **4**: 35–50.
50. Evers, MM, Toonen, LJA and van Roon-Mom, WMC (2015). Antisense oligonucleotides in therapy for neurodegenerative disorders. *Adv. Drug Deliv. Rev.* **87**: 90–103.
51. Southwell, AL, Skotte, NH, Bennett, CF and Hayden, MR (2012). Antisense oligonucleotide therapeutics for inherited neurodegenerative diseases. *Trends Mol. Med.* **18**: 634–643.
52. Evers, MM, Tran, H-D, Zalachoras, I, Meijer, OC, den Dunnen, JT, van Ommen, G-JB, *et al.* (2014). Preventing formation of toxic N-terminal huntingtin fragments through antisense oligonucleotide-mediated protein modification. *Nucleic Acid Ther.* **24**: 4–12.
53. Southwell, AL, Skotte, NH, Kordasiewicz, HB, Ostergaard, ME, Watt, AT, Carroll, JB, *et al.* (2014). In vivo evaluation of candidate allele-specific mutant huntingtin gene silencing antisense oligonucleotides. *Mol. Ther.* **22**: 2093–2106.
54. Østergaard, ME, Southwell, AL, Kordasiewicz, H, Watt, AT, Skotte, NH, Doty, CN, *et al.* (2013). Rational design of antisense oligonucleotides targeting single nucleotide polymorphisms for potent and allele selective suppression of mutant Huntingtin in the CNS. *Nucleic Acids Res.* **41**: 9634–9650.
55. Carroll, JB, Warby, SC, Southwell, AL, Doty, CN, Greenlee, S, Skotte, N, *et al.* (2011). Potent and selective antisense oligonucleotides targeting single-nucleotide polymorphisms in the Huntington disease gene / allele-specific silencing of mutant huntingtin. *Mol. Ther.* **19**: 2178–85.
56. Wang, N, Gray, M, Lu, X-H, Cantle, JP, Holley, SM, Greiner, E, *et al.* (2014). Neuronal targets for reducing mutant huntingtin expression to ameliorate disease in a mouse model of Huntington's disease. *Nat. Med.* **20**: 536–541.
57. Kordasiewicz, HB, Stanek, LM, Wancewicz, E V., Mazur, C, McAlonis, MM, Pytel, KA, *et al.* (2012). Sustained Therapeutic Reversal of Huntington's Disease by Transient Repression of Huntingtin Synthesis. *Neuron* **74**: 1031–1044.

58. Stiles, DK, Zhang, Z, Ge, P, Nelson, B, Grondin, R, Ai, Y, *et al.* (2012). Widespread suppression of huntingtin with convection-enhanced delivery of siRNA. *Exp. Neurol.* **233**: 463–471.

59. Grondin, R, Ge, P, Chen, Q, Sutherland, JE, Zhang, Z, Gash, DM, *et al.* (2015). Onset Time and Durability of Huntingtin Suppression in Rhesus Putamen After Direct Infusion of Antihuntingtin siRNA. *Mol. Ther. Acids* **4**: e245.

60. Ha, M and Kim, VN (2014). Regulation of microRNA biogenesis. *Nat. Rev. Mol. Cell Biol.* **15**: 509–524.

61. Borel, F, van Logtenstein, R, Koornneef, A, Maczuga, P, Ritsema, T, Petry, H, *et al.* (2011). In vivo knock-down of multidrug resistance transporters ABCC1 and ABCC2 by AAV-delivered shrnas and by artificial miRNAs. *J. RNAi Gene Silenc.* **7**: 434–442.

62. Bish, LT, Sleeper, MM, Reynolds, C, Gazzara, J, Withnall, E, Singletary, GE, *et al.* (2011). Cardiac gene transfer of short hairpin RNA directed against phospholamban effectively knocks down gene expression but causes cellular toxicity in canines. *Hum. Gene Ther.* **22**: 969–977.

63. Grimm, D, Streetz, KL, Jopling, CL, Storm, T a, Pandey, K, Davis, CR, *et al.* (2006). Fatality in mice due to oversaturation of cellular microRNA/short hairpin RNA pathways. *Nature* **441**: 537–541.

64. McBride, JL, Boudreau, RL, Harper, SQ, Staber, PD, Monteys, AM, Martins, I, *et al.* (2008). Artificial miRNAs mitigate shRNA-mediated toxicity in the brain: implications for the therapeutic development of RNAi. *Proc. Natl. Acad. Sci. U. S. A.* **105**: 5868–5873.

65. Kantor, B, McCown, T, Leone, P and Gray, SJ (2014). *Clinical applications involving CNS gene transfer*. *Adv. Genet.* **87**, Elsevier, 71-124pp.

66. Kantor, B, Bailey, RM, Wimberly, K, Kalburgi, SN and Gray, SJ (2014). *Methods for gene transfer to the central nervous system*. *Adv. Genet.* **87**, Elsevier, 125-197pp.

67. Knight, S, Collins, M and Takeuchi, Y (2013). Insertional mutagenesis by retroviral vectors: current concepts and methods of analysis. *Curr. Gene Ther.* **13**: 211–27.

68. Hocquemiller, M, Giersch, L, Audrain, M, Parker, S and Cartier, N (2016). Adeno-Associated Virus-Based Gene Therapy for CNS Diseases. *Hum. Gene Ther.* **27**: 478–496.

69. Harper, SQ, Staber, PD, He, X, Eliason, SL, Martins, IH, Mao, Q, *et al.* (2005). RNA interference improves motor and neuropathological abnormalities in a Huntington's disease mouse model. *Proc. Natl. Acad. Sci. U. S. A.* **102**: 5820–5825.

70. Godinho, BMDC, Malhotra, M, O'Driscoll, CM and Cryan, JF (2014). Delivering a disease-modifying treatment for Huntington's disease. *Drug Discov. Today* **20**: 50–64.

71. Drouet, V, Ruiz, M, Zala, D, Feyeux, M, Auregan, G, Cambon, K, *et al.* (2014). Allele-specific silencing of mutant huntingtin in rodent brain and human stem cells. *PLoS One* **9**.

72. Miniarikova, J, Zimmer, V, Martier, R, Brouwers, CC, Pythoud, C, Richetin, K, *et al.* (2017). AAV5-miHTT gene therapy demonstrates suppression of mutant huntingtin aggregation and neuronal dysfunction in a rat model of Huntington's disease. *Gene Ther.* **24**: 630–639.

73. Grondin, R, Kaytor, MD, Ai, Y, Nelson, PT, Thakker, DR, Heisel, J, *et al.* (2012). Six-month partial suppression of Huntingtin is well tolerated in the adult rhesus striatum. *Brain a J. Neurol.* **135**: 1197–1209.

74. Pfister, E, Dinardo, N, Mondo, E, Borel, F, Conroy, F, Fraser, C, *et al.* (2017). Artificial miRNAs reduce human mutant Huntingtin throughout the striatum in a transgenic sheep model of Huntington's disease. *Hum. Gene Ther.*doi:10.1089/hum.2017.199.

75. Menalled, L and Brunner, D (2014). Animal models of Huntington's disease for translation to the clinic: Best practices. *Mov. Disord.* **29**: 1375–1390.

76. Munoz-Sanjuan, I and Bates, GP (2011). The importance of integrating basic and clinical research toward the development of new therapies for Huntington disease. *J. Clin. Invest.* **121**: 476–483.

77. Sampaio, C, Borowsky, B and Reilmann, R (2014). Clinical trials in Huntington's disease: Interventions in early clinical development and newer methodological approaches. *Mov. Disord.* **29**: 1419–1428.

78. Ramaswamy, S, Mcbride, JL and Kordower, JH (2007). Animal Models of Huntington's Disease. *ILAR* **48**: 356–373.

79. Laura Mangiarini, Kirupa Sathasivam, Seller, M, Cozens, B, Harper, A, Hetherington, C, *et al.* (1996). Exon 1 of the HD Gene with an Expanded CAG Repeat Is Sufficient to Cause a Progressive Neurological Phenotype in Transgenic Mice. *Cell* **87**: 493–506.

80. Dragatsis, I, Goldowitz, D, Mar, N, Deng, Y, Meade, C, Liu, L, *et al.* (2015). CAG repeat lengths ≥335 attenuate the phenotype in the R6/2 Huntington's disease transgenic mouse. *Neurobiol Dis.* **33**: 315–330.

81. Menalled, L, El-khodor, BF, Patry, M, Suarez-farinas, M, Zahasky, B, Leahy, C, *et al.* (2009). Systematic behavioral evaluation of Huntington's disease transgenic and knock-in mouse models. *Neurobiol. Dis.* **35**: 319–336.

82. Gonitel, R, Moffitt, H, Sathasivam, K, Woodman, B, Detloff, PJ, Faull, RLM, *et al.* (2008). DNA instability in postmitotic neurons. *Proc. Natl. Acad. Sci.* **105**: 3467–3472.

83. Schilling, G, Becher, MW, Sharp, AH, Jinnah, HA, Duan, K, Kotzuk, JA, *et al.* (1999). Intranuclear inclusions and neuritic aggregates in transgenic mice expressing a mutant N-terminal fragment of huntingtin. *Hum. Mol. Genet.* **8**: 397–407.

84. Hodgson, JG, Agopyan, N, Gutekunst, CA, Leavitt, BR, Lepiane, F, Singaraja, R, *et al.* (1999). A YAC mouse model for Huntington's disease with full-length mutant huntingtin, cytoplasmic toxicity, and selective striatal neurodegeneration. *Neuron* **23**: 181–192.

85. Slow, EJ, van Raamsdonk, J, Rogers, D, Coleman, SH, Graham, RK, Deng, Y, *et al.* (2003). Selective striatal neuronal loss in a YAC128 mouse model of Huntington disease. *Hum. Mol. Genet.* **12**: 1555–1567.

86. Gray, M, Shirasaki, DI, Cepeda, C, Andre, VM, Wilburn, B, Lu, X-H, *et al.* (2008). Full-Length Human Mutant Huntingtin with a Stable Polyglutamine Repeat Can Elicit Progressive and Selective Neuropathogenesis in BACHD Mice. *J. Neurosci.* **28**: 6182–6195.

87. Southwell, AL, Skotte, NH, Villanueva, EB, Østergaard, ME, Gu, X, Kordasiewicz, HB, *et al.* (2017). A novel humanized mouse model of Huntington disease for preclinical development of therapeutics targeting mutant huntingtin alleles. *Hum. Mol. Genet.* **26**: 1115–1132.

88. Southwell, AL, Warby, SC, Carroll, JB, Doty, CN, Skotte, NH, Zhang, W, *et al.* (2013). A fully humanized transgenic mouse model of Huntington disease. *Hum. Mol. Genet.* **22**: 18–34.

89. Menalled, LB, Sison, JD, Wu, Y, Olivieri, M, Li, X-J, Li, H, *et al.* (2002). Early motor dysfunction and striosomal distribution of huntingtin microaggregates in Huntington's disease knock-in mice. *J. Neurosci.* **22**: 8266–8276.

90. Menalled, LB, Sison, JD, Dragatsis, I, Zeitlin, S and Chesselet, M-F (2003). Time course of early motor and neuropathological anomalies in a knock-in mouse model of Huntington's disease with 140 CAG repeats. *J. Comp. Neurol.* **465**: 11–26.

91. Menalled, LB (2005). Knock-In Mouse Models of Huntington's Disease. *NeuroRx* **2**: 465–470.

92. Horsten, S, Schmitt, I, Nguyen, HP, Holzmann, C, Schmidt, T, Walther, T, *et al.* (2003). Transgenic rat model of Huntington's disease. *Hum. Mol. Genet.* **12**: 617–624.

93. Yu-Taeger, L, Petrasch-Parwez, E, Osmand, AP, Redensek, A, Metzger, S, Clemens, LE, *et al.* (2012). A Novel BACHD Transgenic Rat Exhibits Characteristic Neuropathological Features of Huntington Disease. *J. Neurosci.* **32**: 15426–15438.

94. Eaton, SL and Wishart, TM (2017). Bridging the gap: large animal models in neurodegenerative research. *Mamm. Genome* **28**: 324–337.

95. Jacobsen, JC, Bawden, CS, Rudiger, SR, McLaughlan, CJ, Reid, SJ, Waldvogel, HJ, *et al.* (2010). An ovine transgenic Huntington's disease model. *Hum. Mol. Genet.* **19**: 1873–1882.

96. Baxa, M, Hruska-plochan, M, Juhas, S, Vodicka, P, Pavlok, A, Juhasova, J, *et al.* (2013). A Transgenic Minipig Model of Huntington's Disease. *J. Huntington's Dis.* **2**: 47–68.

97. Takahashi, K and Yamanaka, S (2006). Induction of Pluripotent Stem Cells from Mouse Embryonic and Adult Fibroblast Cultures by Defined Factors. *Cell* **126**: 663–676.

98. Marchetto, MCN, Winner, B and Gage, FH (2010). Pluripotent stem cells in neurodegenerative and neurodevelopmental diseases **19**: 71–76.

99. Park, I, Arora, N, Huo, H, Maherali, N, Ahfeldt, T, Shimamura, A, *et al.* (2008). Disease-Specific Induced Pluripotent Stem Cells. *Cell* **134**: 877–886.

100. Tousley, A and Kegel-gleason, KB (2016). Induced Pluripotent Stem Cells in Huntington's Disease Research : Progress and Opportunity. *J. Huntingtons. Dis.* **5**: 99–131.

101. Jeon, I, Lee, N, Li, J-Y, Park, I-H, Park, KS, Moon, J, *et al.* (2012). Neuronal Properties, In Vivo Effects, and Pathology of a Huntington's Disease Patient-Derived Induced Pluripotent Stem Cells. *Stem Cells* **30**: 2054–2062.

102. Nekrasov, ED, Vigont, VA, Klyushnikov, SA, Lebedeva, OS, Vassina, EM, Bogomazova, AN, *et al.* (2016). Manifestation of Huntington's disease pathology in human induced pluripotent stem cell-derived neurons. *Mol. Neurodegener.* **11**: 1–15.

103. Russo, FB, Cugola, FR, Fernandes, IR, Pignatari, GC and Beltrão-braga, PCB (2015). Induced pluripotent stem cells for modeling neurological disorders. *World J Transpl.* **5**: 209–221.

104. Cambon, K, Zimmer, V, Martineau, S, Gaillard, M, Jarrige, M, Bugi, A, *et al.* (2017). Preclinical Evaluation of a Lentiviral Vector for Huntingtin Silencing. *Mol. Ther. Methods Clin. Dev.* **5**: 259–276.

105. Schramke, S, Schubert, R, Frank, F, Wirsig, M, Fels, M, Kemper, N, *et al.* (2017). The Libechov Minipig as a Large Animal Model for Preclinical Research in Huntington's disease–Thoughts and Perspectives. *Ces. Slov Neurol N* **78**: 55–60.

106. Ojala, DS, Amara, DP and Schaffer, D V (2015). Adeno-Associated Virus Vectors and Neurological Gene Therapy. *Neurosci.* **21**: 84–98.

107. Aschauer, DF, Kreuz, S and Rumpel, S (2013). Analysis of Transduction Efficiency, Tropism and Axonal Transport of AAV Serotypes 1, 2, 5, 6, 8 and 9 in the Mouse Brain. *PLoS One* **8**: 1–16.

108. Blits, B and Petry, H (2017). Perspective on the Road toward Gene Therapy for Parkinson's Disease. *Front. Neuroanat.* **10**: 1–8.

109. Samaranch, L, Blits, B, San Sebastian, W, Hadaczek, P, Bringas, J, Sudhakar, V, *et al.* (2017). MR-guided parenchymal delivery of adeno-associated viral vector serotype 5 in non-human primate brain. *Gene Ther.* **24**: 253–261.

110. Hadaczek, P, Stanek, L, Ciesielska, A, Sudhakar, V, Samaranch, L, Pivirotto, P, *et al.* (2016). Widespread AAV1- and AAV2-mediated transgene expression in the nonhuman primate brain: implications for Huntington's disease. *Mol. Ther. Methods Clin. Dev.* **3**: 16037.

111. Gray, SJ, Matagne, V, Bachaboina, L, Yadav, S, Ojeda, SR and Samulski, RJ (2011). Preclinical Differences of Intravascular AAV9 Delivery to Neurons and Glia: A Comparative Study of Adult Mice and Nonhuman Primates. *Mol. Ther.* **19**: 1058–1069.

112. Samaranch, L, Kells, AP, Foust, KD, Salegio, EA, Sebastian, WS, Bringas, JR, *et al.* (2012). Adeno-Associated Virus Serotype 9 Transduction in the Central Nervous System of Nonhuman Primates. *Hum. Gene Ther.* **23**: 382–389.

113. Markusic, DM, Nichols, TC, Merricks, EP, Palaschak, B, Zolotukhin, I, Marsic, D, *et al.* (2017). Evaluation of engineered AAV capsids for hepatic factor IX gene transfer in murine and canine models. *J. Transl. Med.* **15**: 1–11.

114. Bradbury, AM, Gurda, BL, Casal, ML, Ponder, KP, Vite, CH and Haskins, ME (2015). A Review of Gene Therapy in Canine and Feline Models of Lysosomal Storage Disorders. *Hum. gene Ther. Clin. Dev.* **26**: 27–37.

115. Hinderer, C, Bell, P, Katz, N, Vite, CH, Louboutin, J, Bote, E, *et al.* (2017). Evaluation of intrathecal routes of administration for adeno-associated virus vectors in large animals. *Hum. Gene Ther.*doi:10.1089/hum.2017.026.

116. Palmer, AM (2010). Neurobiology of Disease The role of the blood–CNS barrier in CNS disorders and their treatment. *Neurobiol. Dis.* **37**: 3–12.

117. Foust, KD, Nurre, E, Montgomery, CL, Hernandez, A, Curtis, M and Kaspar, BK (2010). Intravascular AAV9 preferentially targets neonatal-neurons and adult-astrocytes in CNS. *Nat. Biotechnol.* **27**: 59–65.

118. Deverman, BE, Pravdo, PL, Simpson, BP, Kumar, SR, Chan, KY, Banerjee, A, *et al.* (2016). Cre-dependent selection yields AAV variants for widespread gene transfer to the adult brain. *Nat. Biotechnol.* **34**: 204–209.

119. Chan, KY, Jang, MJ, Yoo, BB, Greenbaum, A, Ravi, N, Wu, W, *et al.* (2017). Engineered adeno-associated viruses for efficient and noninvasive gene delivery throughout the central and peripheral nervous systems. *Nat. Neurosci.* **20**: 1172–1179.

120. Matsuzaki, Y, Konno, A, Mochizuki, R, Shinohara, Y, Nitta, K, Okada, Y, *et al.* (2017). Intravenous administration of the adeno-associated virus-PHP.B capsid fails to upregulate transduction efficiency in the marmoset brain. *Neurosci. Lett.* **665**: 182–188.

121. Markakis, EA, Vives, KP, Bober, J, Leichtle, S, Leranth, C, Beecham, J, *et al.* (2010). Comparative Transduction Efficiency of AAV Vector Serotypes 1–6 in the Substantia Nigra and Striatum of the Primate Brain. *Mol. Ther.* **18**: 588–593.

122. Gray, S, Kalburgi, S, Mccown, T and Samulski, R (2013). Global CNS gene delivery and evasion of anti-AAV-neutralizing antibodies by intrathecal AAV administration in non-human primates. *Gene Ther.* **20**: 450–459.

123. Federici, T, Taub, JS, Baum, GR, Gray, SJ, Grieger, JC, Matthews, KA, *et al.* (2011). Robust spinal motor neuron transduction following intrathecal delivery of AAV9 in pigs **19**: 852–859.

124. Davidson, BL, Stein, CS, Heth, JA, Kotin, RM, Derksen, TA, Zabner, J, *et al.* (2000). Recombinant adeno-associated virus type 2, 4, and 5 vectors: Transduction of variant cell types and regions in the mammalian central nervous system. *Proc. Natl. Acad. Sci.* **97**: 3428–3432.

125. Mittermeyer, G, Christine, CW, Rosenbluth, KH, Baker, SL, Starr, P, Larson, P, *et al.* (2012). Long-Term Evaluation of a Phase 1 Study of AADC Gene Therapy for Parkinson's Disease. *Hum. Gene Ther.* **23**: 377–381.

126. Kao, J, Chen, S, Ma, H, Law, P, Tao, P and Loh, H (2010). Intrathecal Delivery of a Mutant u-Opioid Receptor Activated by Naloxone as a Possible Antinociceptive Paradigm. *J. Pharmacol. Exp. Ther.* **334**: 739–745.

127. Schuster, DJ, Belur, LR, Riedl, MS, Schnell, SA, Podetz-pedersen, KM, Kitto, KF, *et al.* (2014). Supraspinal gene transfer by intrathecal adeno-associated virus serotype 5. *Front. Neuroanat.* **8**: 1–10.

128. Carroll, JB, Bates, GP, Steffan, J, Saft, C and Tabrizi, SJ (2015). Treating the whole body in Huntington's disease. *Lancet Neurol.* **14**: 1135–1142.

129. Bartus, RT, Baumann, TL, Herzog, CD, Alterman, R, Boulis, N, Turner, DA, *et al.* (2013). Safety/feasibility of targeting the substantia nigra with AAV2-neurturin in Parkinson patients. *Neurology* **80**: 1698–1702.

130. LeWitt, PA, Rezai, AR, Leehey, MA, Ojemann, SG, Flaherty, AW, Eskandar, EN, *et al.* (2011). AAV2-GAD gene therapy for advanced Parkinson's disease: a double-blind, sham-surgery controlled, randomised trial. *Lancet Neurol.* **10**: 309–319.

131. Kaplitt, MG, Feigin, A, Tang, C, Fitzsimons, HL, Mattis, P, Lawlor, PA, *et al.* (2007). Safety and tolerability of gene therapy with an adeno-associated virus (AAV) borne GAD gene for Parkinson's disease: an open label, phase I trial. *Lancet* **369**: 2097–2105.

132. Tuszynski, MH, Thal, L, Pay, M, Salmon, DP, U, HS, Bakay, R, *et al.* (2005). A phase 1 clinical trial of nerve growth factor gene therapy for Alzheimer disease. *Nat. Med.* **11**: 551–555.

133. Muramatsu, S, Fujimoto, K, Kato, S, Mizukami, H, Asari, S, Ikeguchi, K, *et al.* (2010). A Phase I Study of Aromatic L-Amino Acid Decarboxylase Gene Therapy for Parkinson's Disease. *Mol. Ther.* **18**: 1731–1735.

134. Olanow, CW, Bartus, RT, Volpicelli-daley, LA and Kordower, JH (2015). Trophic Factors for Parkinson's Disease: To Live or Let Die. *Mov. Disord.* **30**: 1715–1723.

135. Palfi, S, Gurruchaga, JM, Ralph, GS, Lepetit, H, Lavisse, S, Buttery, PC, *et al.* (2014). Long-term safety and tolerability of ProSavin, a lentiviral vector-based gene therapy for Parkinson's disease: a dose escalation, open-label, phase 1/2 trial. *Lancet* **383**: 1138–1146.

136. Wojtecki, L, Groiss, SJ, Hartmann, CJ, Elben, S, Omlor, S, Schnitzler, A, *et al.* (2016). Deep Brain Stimulation in Huntington's Disease — Preliminary Evidence on Pathophysiology, Efficacy and Safety. *Brain Sci.* **6**: 1–15.

137. Mehta, AM, Sonabend, AM and Bruce, JN (2017). Convection-Enhanced Delivery. *Neurotherapeutics* **14**: 358–371.

138. Zhou, Z, Singh, R and Souweidane, M (2016). Convection-Enhanced Delivery for Diffuse Intrinsic Pontine Glioma Treatment. *Curr. Neuropharmacol.* **15**: 116–128.

139. Krauze, MT, Saito, R, Ph, D, Noble, C, Ph, D, Tamas, M, *et al.* (2013). Reflux-free cannula for convection-enhanced high-speed delivery of therapeutic agents. *J Neurosurg.* **103**: 1–12.

140. Carty, N, Lee, D, Dickey, C, Ceballos-diaz, C, Jansen-west, K, Golde, TE, *et al.* (2010). Convection-enhanced delivery and systemic mannitol increase gene product distribution of AAV vectors 5, 8, and 9 and increase gene product in the adult mouse brain. *J. Neurosci.* **194**: 144–153.

141. Kells, AP, Hadaczek, P, Yin, D, Bringas, J, Varenika, V, Forsayeth, J, *et al.* (2009). Efficient gene therapy-based method for the delivery of therapeutics to primate cortex. *Proc. Natl. Acad. Sci. U. S. A.* **106**: 2407–2411.

142. Eberling, JL, Jagust, WJ, Christine, CW, Starr, P, Larson, P, Bankiewicz, KS, *et al.* (2008). Results from a phase I safety trial of hAADC gene therapy for Parkinson disease. *Neurology* **70**: 1980–1983.

143. Salegio, EA, Samaranch, L, Kells, AP, Mittermeyer, G, Sebastian, WS, Zhou, S, *et al.* (2013). Axonal transport of adeno-associated viral vectors is serotype-dependent. *Gene Ther.* **20**: 348–352.

144. Monteys, AM, Wilson, MJ, Boudreau, RL, Spengler, RM and Davidson, BL (2015). Artificial miRNAs Targeting Mutant Huntingtin Show Preferential Silencing In Vitro and In Vivo. *Mol. Ther. Acids* **4**: e234.

145. Franich, NR, Fitzsimons, HL, Fong, DM, Klugmann, M, During, MJ and Young, D (2008). AAV vector-mediated RNAi of mutant huntingtin expression is neuroprotective in a novel genetic rat model of Huntington's disease. *Mol. Ther.* **16**: 947–956.

146. Rodriguez-Lebron, E, Denovan-Wright, EM, Nash, K, Lewin, AS and Mandel, RJ (2005). Intrastriatal rAAV-mediated delivery of anti-huntingtin shRNAs induces partial reversal of disease progression in R6/1 Huntington's disease transgenic mice. *Mol. Ther.* **12**: 618–33.

147. DiFiglia, M, Sena-Esteves, M, Chase, K, Sapp, E, Pfister, E, Sass, M, *et al.* (2007). Therapeutic silencing of mutant huntingtin with siRNA attenuates striatal and cortical neuropathology and behavioral deficits. *Proc. Natl. Acad. Sci. U. S. A.* **104**: 17204–17209.

Acknowledgements

The authors thank Prof. Sander van Deventer for critically reviewing the manuscript.

SCOPE OF THE THESIS

HD is a fatal polyglutamine (polyQ)-associated monogenic neurodegenerative disorder with no disease-modifying treatment currently available. The underlying cause of HD pathology is an expansion of CAG repeats in the huntingtin (*HTT*) gene, translated into a polyQ region, and generating a toxic mutant HTT protein. Therapeutic strategies that are designed to lower the production of the mutant HTT are currently of primary interest for the scientific community and industry.

This thesis focuses on *in vitro* and *in vivo* studies contributing to the preclinical development of the micro (mi)RNA-based HTT lowering gene therapy to treat HD. It includes the pioneering preclinical studies of the lead AAV5-miHTT construct (AMT-130), which is planned to enter the clinic in 2019 (www.uniQure.com). More specifically, we have developed and preclinically tested therapeutic miRNAs, delivered and expressed from an adeno-associated viral serotype 5 (AAV5) vector, targeting HTT transcripts to reduce the formation of toxic HTT protein. The results published in this thesis contribute to the translation of the AAV-delivered-miRNA-based gene therapy approach from preclinical to the clinical setting.

In chapter 1, we summarize the current knowledge on the promising HTT lowering therapies as a treatment for HD with a focus on the miRNA-based gene therapy. We outline the animal and cell systems modelling HD that allow for the preclinical testing of HTT lowering therapies, emphasizing that there is no single model that can be used to fully address all clinically relevant aspects of HD treatments. We discuss the preclinical outcome measures of efficacy suitable for an AAV-miRNA-based gene therapy that support the translation to the clinic.

To develop an HD therapy that continuously lowers HTT transcripts and thereby reduces the mutant HTT protein, **in chapter 2**, we have designed dozens of therapeutic miRNAs targeting different regions in human HTT transcripts and analysed their efficacy *in vitro* and *in vivo*. Two approaches have been addressed. The non-selective HTT lowering was achieved by targeting sequences located on both HTT alleles. We showed efficacious mutant HTT knock-down induced by the miHTT construct delivered by the AAV5 vector *in vitro* and in the striatum and cortex of the humanized Hu128/21 HD mouse model. Furthermore, we have evaluated the efficacy and allele-selectivity of therapeutic miRNAs targeting CAG repeats and heterozygous single nucleotide polymorphisms (SNPs) in linkage disequilibrium with the mutant HTT allele. In this study, we also evaluated the role of pre-miRNA scaffolds in the efficacy and preliminary safety of therapeutic miRNA constructs and identified the pre-miR-451 precursor suitable for the miRNA-based gene therapy to treat HD.

To further address the efficacy in suppressing the HD-like neuropathology, **in chapter 3,** we performed a second preclinical study with the selected miHTT construct targeting both HTT alleles, processed from the pre-miR-451 precursor, and delivered by AAV5 vectors

(named as the AAV5-miHTT throughout the thesis) in the striata of the lentiviral HD rat model. We have shown a strong reduction of HTT aggregates, which resulted in a reduction of HD-like neuronal dysfunction. Moreover, we demonstrated the allele-specific HTT lowering by a therapeutic miRNA targeting T isoform of SNP rs362331 in exon 50. These results supported further testing of AAV5-miHTT construct in a minipig model of HD, which is not in the scope of this thesis.

The general concept of miRNAs being mainly active in the cytoplasm has been recently challenged, with evidence demonstrating the nuclear activity of cellular miRNAs. This concept offers new opportunities for miRNA-based therapies to target and lower disease-related transcripts in the nucleus and cytoplasm, simultaneously. In case of HD, this might be particularly of interest since there are data showing HTT RNA-associated toxicity in HD mice. To investigate the potential of artifical miRNAs to induce HTT lowering in the nucleus, **in chapter 4,** we have designed and tested several miRNAs selectively targeting a four-nucleotide deletion in HTT intron 22 (ΔACTT). We have shown a first demonstration that mature therapeutic miRNAs delivered by an AAV5 vector can shuttle to the nucleus to induce lowering of endogenous mutant HTT in induced pluripotent stem cells (iPSCs)-derived HD neuronal cultures.

In preparations for a clinical trial, it will be important to identify pharmacokinetic/pharmacodynamics (PK/PD) modeling measures and biomarkers from easily obtainable biofluids that would provide correlations between the drug dosing, concentration, and efficacy in HD patients. To identify a source of quantifiable PK/PD measures which would signal the presence of an active therapeutic miRNA in the patient brain, **in chapter 5,** we have investigated exosomes as potential carriers of therapeutic miRNAs, released from iPSC-derived HD neuronal cultures transduced with the AAV5-miHTT vector. We confirmed the presence of mature miHTT molecules in the vesicles secreted from these cells, prompting further investigations using large animals, which is not in the scope of this thesis.

To summarize the current knowledge on the preclinical development for the miRNA-based gene therapy approaches for HD, **in chapter 6,** we discussed additional aspects of the translation of HTT lowering gene therapy to the clinic. We outline the safety measures for the miRNA-based gene therapy and highlight the current need for quantifiable biomarkers to monitor the AAV5-miHTT treatment response and outcomes. We emphasize the intriguing opportunity to investigate exosomes as potential carries of PK/PD measures. We also provide an overview on the current knowledge for the nuclear transcript lowering by cellular miRNAs. Ultimately, we comment on the future perspectives of the miRNA-based lowering gene therapy for HD.

2

DESIGN, CHARACTERIZATION AND LEAD SELECTION OF THERAPEUTIC MIRNAS TARGETING HUNTINGTIN FOR DEVELOPMENT OF GENE THERAPY FOR HUNTINGTON'S DISEASE

Jana Miniarikova[1,2], Ilaria Zanella[1], Angelina Huseinovic[1], Tom van der Zon[1], Evelyn Hanemaaijer[1], Raygene Martier[1,2], Annemart Koornneef[1], Amber L Southwell[3], Michael R Hayden[3], Sander J van Deventer[2], Harald Petry[1], and Pavlina Konstantinova[1]

[1]Department of Research & Development, uniQure, Amsterdam, the Netherlands
[2]Department of Gastroenterology and Hepatology, Leiden University Medical Center, Leiden, the Netherlands
[3]Centre for Molecular Medicine and Therapeutics, University of British Columbia, Vancouver, Canada

*Mol. Ther. Nucleic Acids (2016); **5**: e297*

ABSTRACT

Huntington's disease *(HD)* is a neurodegenerative disorder caused by accumulation of CAG expansions in the huntingtin (HTT) gene. Hence, decreasing the expression of mutated HTT (mtHTT) is the most upstream approach for treatment of HD. We have developed HTT gene-silencing approaches based on expression cassette-optimized artificial miRNAs (miHTTs). In the first approach, total silencing of wild-type and mtHTT was achieved by targeting exon 1. In the second approach, allele-specific silencing was induced by targeting the heterozygous single-nucleotide polymorphism (SNP) rs362331 in exon 50 or rs362307 in exon 67 linked to mtHTT. The miHTT expression cassette was optimized by embedding anti-HTT target sequences in ten pri-miRNA scaffolds and their HTT knockdown efficacy, allele selectivity, passenger strand activity, and processing patterns were analyzed *in vitro*. Furthermore, three scaffolds expressing miH12 targeting exon 1 were incorporated in an adeno-associated viral serotype 5 (AAV5) vector and their HTT knock-down efficiency and pre-miHTT processing were compared in the humanized transgenic Hu128/21 HD mouse model. Our data demonstrate strong allele-selective silencing of mtHTT by miSNP50 targeting rs362331 and total HTT silencing by miH12 both *in vitro* and *in vivo*. Ultimately, we show that HTT knock-down efficiency and guide strand processing can be enhanced by using different cellular pri-miRNA scaffolds.

INTRODUCTION

Huntington's disease (HD) is a rare, fatal, neurodegenerative genetic disorder that affects muscle coordination and leads to behavioral symptoms and cognitive decline, resulting in total physical and mental deterioration over a 12- to 15-year period.[1] HD is caused by the expansions of the polyglutamine (polyQ) tract in the multifunctional huntingtin protein (HTT). Despite the ability to identify HD mutation carriers decades before onset, there is currently no available therapy that can delay onset or slow progression of the disease.

The monogenetic etiology, autosomal dominant inheritance, and the fully penetrant phenotype following a long pre-syndromatic phase place HD as a good candidate for gene therapy. Consequently, there is a wide variety of potential HD therapeutic strategies aiming at delivery of neurotrophic factors, activation of neuronal stem cells, Ca2+ and mitochondrial function normalization and mutant (mt)HTT targeting.[2] The preferred strategy by many groups including ours is direct lowering of the *mtHTT* mRNA level.

Interfering with *HTT* mRNA expression has been widely explored using synthetic antisense oligonucleotides (ASOs), single-stranded RNAs (ssRNAs), small interfering RNAs (siRNAs), expressed short hairpin RNAs (shRNAs), or artificial microRNAs (miRNAs).[3–5]

ASO and siRNA are chemically modified DNA or RNA oligos, respectively that bind to the HTT transcript. ASO-mediated HTT lowering has been successfully shown in murine HD models and holds a great promise for HD therapy.[6,7] Infusion of siRNAs targeting HTT into the striatum of nonhuman primates has demonstrated significant silencing of HTT in a dose-dependent manner.[8] However, it still needs to be determined if sufficient ASO and siRNA biodistribution, efficacy, and safety in the large animal and human brain can be achieved. Moreover, the relatively short half-life of the ASO and siRNA would require repeated administration presenting clinical burden for the HD patients.

Expressing siRNAs from shRNA or miRNA scaffolds has shown great promise for HTT lowering in murine HD models when delivered with adeno-associated viral (AAV) vectors.[4,9,10] The shRNA- or miRNA-expression can be driven by polymerase (pol) III or pol II promoters allowing for tissue- or cell-specific expression.[11] Moreover, the expressed shRNA or miRNA provide long-term silencing of the HTT transcript, avoiding the necessity for re-administration of the therapeutic.

Gene silencing may be indiscriminative between the wild type (wt) and mtHTT or can selectively silence only the mutated allele with expanded CAG repeats. Multiple lines of evidence indicate that total silencing of HTT can be performed in a certain therapeutic window.[12] Two studies used AAV2-miHTT or AAV2-shHTT to partially silence wtHTT in a healthy rhesus macaque putamen. In both studies, 45% reduction of HTT did not induce any abnormal motor phenotype, altered circadian behavior, fine motor skill deficits, neuronal loss, gliosis, or immune response at 6 weeks or 6 months post injection, respectively.[13,14] Selective silencing only of the mtHTT presents challenges as the difference from the

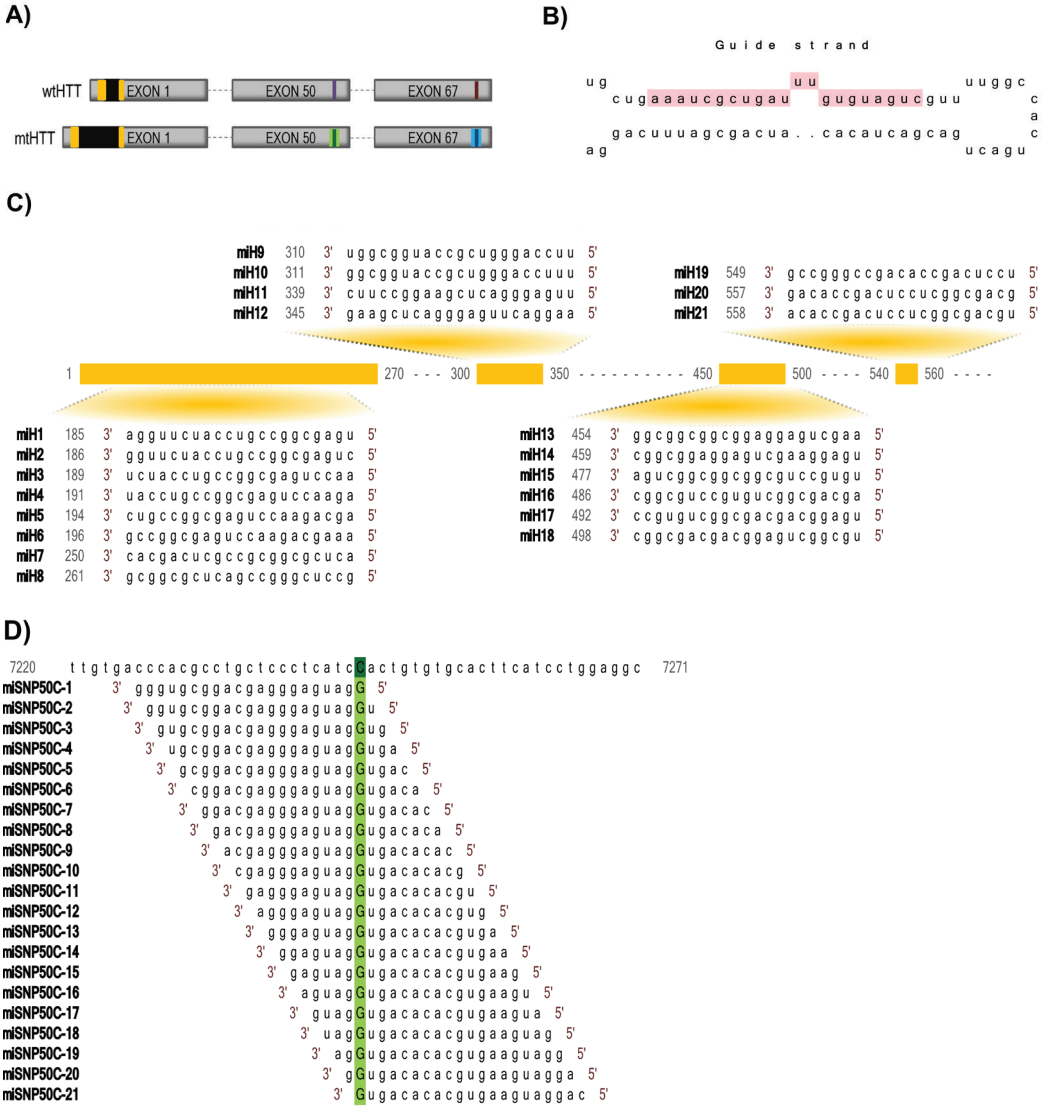
wtHTT allele is mainly in the higher number of CAG repeats. Allele-specific HTT silencing via targeting of the CAG repeat is possible using ssRNAs and can be specific to only the mutant allele.[15] Single-nucleotide polymorphism (SNP) genotyping of HD patients has identified ~41 SNPs heterozygous in at least 30% of the patients.[16] Those SNPs are good targets for silencing of only the mtHTT while maintaining the expression of the wtHTT allele. Allele-selective mtHTT silencing has been achieved with ASOs, siRNAs, shRNAs, or miRNAs directed toward heterozygous SNPs in exons 39 (rs363125), 50 (rs362331), 60 (rs2276881), or 67 (rs362307)[7,16–20]

Despite the existence of many algorithms and rules for design of therapeutic miRNAs targeting either both HTT alleles or only the mutant allele based on SNPs, the evaluation of efficacy and allele selectivity of every molecule still needs to be performed empirically. In the current study, we designed artificial miRNAs targeting human HTT exon 1 (miH), the expanded CAG repeats (miCAG), C or T isoform of SNP rs362331 in exon 50 (miSNP50C and miSNP50T) and T isoform of SNP rs362307 in exon 67 extended to 3'UTR (miSNP67T). miH12 variant silenced efficiently both wt and mtHTT reporters, while miCAG constructs failed to induce allele-specific silencing. The latter was achieved by miSNP50 and miSNP67 variants bearing secondary mismatches to the wtHTT. Furthermore, to reduce the chance of off-target effects due to passenger strand activity, artificial miRNA processing was "biased" towards high concentrations of guide strand production by using different cellular pri-miRNA scaffolds. This resulted in differential guide and passenger strand processing patterns revealed by next-generation sequencing (NGS) and HTT knockdown efficiency *in vitro*. Ultimately, to compare the HTT silencing efficiency and miH12 processing *in vivo*, three AAV5-miH12 vectors were generated and tested in the humanized Hu128/21 HD mouse model. For the first time, we show that the therapeutic pri-miRNA scaffold influences HTT knock-down and guide strand processing *in vivo*. The best therapeutic scaffolds were miH12-451, miSNP50C-451 and miSNP50T-451 as they induced strong HTT silencing and had almost undetectable passenger strand concentration with no activity.

RESULTS

Huntingtin (*HTT*) target sequences and design of artificial microRNA-expression constructs

Three regions in exon 1, 50, and 67 (extended to 3'UTR) of the human *HTT* gene were selected to design artificial anti-HTT miRNAs (miHTTs) (**Figure 1a**). All miHTT variants were generated to specifically target the human *HTT* transcripts. The miHTT sequences were embedded in the engineered mmu-pre-miR-155 scaffold (**Figure 1b**). The first miHTT group, miH1-miH21, was developed to target sequences within exon 1, hence to induce HTT knock-down of both wt and mt alleles (**Figure 1c**). An alternative strategy aims at suppressing only the mtHTT allele. The majority of HD patients are heterozygous for the CAG expansion and the selective targeting of the longer HD-associated CAG tract could potentially treat all patients.[21] Therefore, we designed miCAG1—miCAG15 targeting the CAG repeats in exon 1 to selectively suppress only the mtHTT allele. Recently, several SNPs have been identified in high linkage disequilibrium with the disease-associated allele.[3,17,20,22] Notably, heterozygosity of SNP rs362307 located in 3'UTR of HTT (the extended exon 67) was observed in 48.6% of US and European HD representative population and the T isoform of rs362307 constituted 26%. In the same study, heterozygosity (C/T) of SNP rs362331 located in exon 50 was observed in 39.4%[17] In another study, heterozygosity (C/T) of rs362331 was observed in 47.6% of Italian HD representative population.[20] Therefore, in pursuit of selective degradation of the mutant transcript from the HD allele, we selected HTT sequences that contain HD-related isoforms C or T of rs362331 in exon 50 and the isoform T of rs362307 located in exon 67 (extend to 3'UTR). Consequently, we designed miSNP50C-1—miSNP50C-21 to silence the transcripts carrying the C isoform of rs362331 (**Figure 1d**), miSNP50T-1—miSNP50T-21 to suppress the transcripts with the U isoform of rs362331 (**Figure 1e**), and miSNP67T-1—miSNP67T-21 to target transcripts with the U isoform of rs362307 (**Figure 1f**).


A)
wtHTT
EXON 1
EXON 50
EXON 67
mtHTT
EXON 1
EXON 50
EXON 67
B)
Guide strand
C)
miH9 310 3' uggcgguaccgcugggaccuu 5'
miH10 311 3' ggcgguaccgcugggaccuuu 5'
miH11 339 3' cuuccggaagcucagggaguu 5'
miH12 345 3' gaagcucagggaguucaggaa 5'
miH19 549 3' gccgggccgacaccgacuccu 5'
miH20 557 3' gacaccgacuccucggcgacg 5'
miH21 558 3' acaccgacuccucggcgacgu 5'
1
270
300
350
450
500
540
560
miH1 185 3' agguucuaccugccggcgagu 5'
miH2 186 3' gguucuaccugccggcgaguc 5'
miH3 189 3' ucuaccugccggcgaguccaa 5'
miH4 191 3' uaccugccggcgaguccaaga 5'
miH5 194 3' cugccggcgaguccaagacga 5'
miH6 196 3' gccggcgaguccaagacgaaa 5'
miH7 250 3' cacgacucgccgcggcgcuca 5'
miH8 261 3' gcggcgcucagccgggcuccg 5'
miH13 454 3' ggcggcggcggaggagucgaa 5'
miH14 459 3' cggcggaggagucgaaggagu 5'
miH15 477 3' agucggcggcggcguccgugu 5'
miH16 486 3' cggcguccgugucggcgacga 5'
miH17 492 3' ccgugucggcgacgacggagu 5'
miH18 498 3' cggcgacgacggagucggcgu 5'
D)
7220 ttgtgacccacgcctgctccctcatcCactgtgtgcacttcatcctggaggc 7271
miSNP50C-1 3' gggugcggacgagggaguagG 5'
miSNP50C-2 3' ggugcggacgagggaguagGu 5'
miSNP50C-3 3' gugcggacgagggaguagGug 5'
miSNP50C-4 3' ugcggacgagggaguagGuga 5'
miSNP50C-5 3' gcggacgagggaguagGugac 5'
miSNP50C-6 3' cggacgagggaguagGugaca 5'
miSNP50C-7 3' ggacgagggaguagGugacac 5'
miSNP50C-8 3' gacgagggaguagGugacaca 5'
miSNP50C-9 3' acgagggaguagGugacacac 5'
miSNP50C-10 3' cgagggaguagGugacacacg 5'
miSNP50C-11 3' gagggaguagGugacacacgu 5'
miSNP50C-12 3' agggaguagGugacacacgug 5'
miSNP50C-13 3' gggaguagGugacacacguga 5'
miSNP50C-14 3' ggaguagGugacacacgugaa 5'
miSNP50C-15 3' gaguagGugacacacgugaag 5'
miSNP50C-16 3' aguagGugacacacgugaagu 5'
miSNP50C-17 3' guagGugacacacgugaagua 5'
miSNP50C-18 3' uagGugacacacgugaaguag 5'
miSNP50C-19 3' agGugacacacgugaaguagg 5'
miSNP50C-20 3' gGugacacacgugaaguagga 5'
miSNP50C-21 3' Gugacacacgugaaguaggac 5'

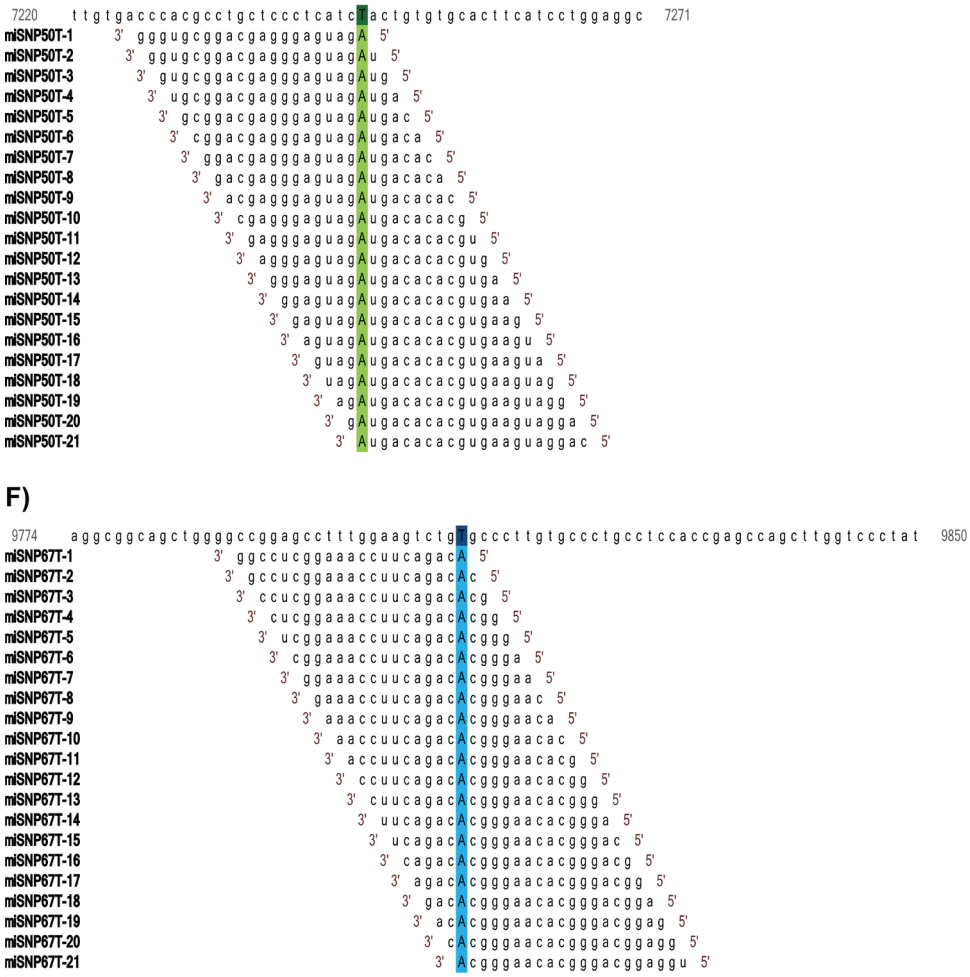


Figure 1. Design of therapeutic miHTT variants for Huntington's disease (HD) therapy. **(a)** Schematic of exons 1, 50, and 67 (extended to 3'UTR) of human wild-type (wt) or mutated (mt) huntingtin (HTT) gene (gb|L12392.1|HUMHDA) with CAG expansions in black, target sequences for miH1-miH21 in yellow, miSNP50 variants in green, and miSNP67 variants in blue. Single-nucleotide polymorphisms (SNPs) located either in exon 50 (rs362331) or exon 67 extended to 3'UTR (rs362307) are represented as dark stripes within the target regions. **(b)** The engineered mmu-pre-miR-155 scaffold used for miHTT expression with highlighted 21 nt guide strand. **(c)** Twenty-one miHTT variants were designed to target HTT exon 1. In a consecutive manner, miH1-miH21 bind to HTT exon 1 shown in yellow with the target starting nucleotide positions in gray. **(d)** miSNP50C variants targeting the C isoform of mtHTT-associated SNP rs362331 in exon 50. Micro-shifting of mature miSNP50C sequences along the C isoform generated 21 variants with the SNP-matching position 1–21 (miSNP50C-1—miSNP50C-21). The C isoform is represented in dark green and the SNP-matching nucleotide in light green. **(e)** miSNP50T variants targeting the T isoform of mtHTT-associated SNP rs362331 in exon 50. miSNP50T variants were generated similarly to miSNP50C. **(f)** miSNP67T variants targeting the T isoform of mtHTT-associated SNP rs362307 in exon 67. miSNP67T variants were generated similarly to miSNP50T. The T isoform of rs362307 is represented in dark blue and the SNP-matching nucleotide in light blue. A list of all pre-miHTT scaffolds can be found in Supplementary Table S1.

In vitro silencing efficacy of artificial miHTT constructs

To evaluate the HTT knock-down efficacy by the miHTT-expression constructs *in vitro*, we co-transfected them in human embryonic kidney (HEK)293T cells with luciferase (Luc) reporters bearing complementary HTT regions fused to the renilla luciferase (RL) gene. Independently from RL, firefly luciferase (FL) was expressed from the reporter vector to correct for transfection efficiency (**Figure 2a**). From miH1-miH21 constructs designed to target both HTT alleles, miH10, miH14, miH15, miH19, miH20, and miH21 induced mild knock-down between 25–45% of LucHTT(mt) expressing a portion of human HTT exon 1 encompassing 73 CAG repeats (**Figure 2b**). miH12 construct was highly effective and induced more than 70% inhibition of LucHTT(mt) reporter.

For the allele-specific HTT suppression based on discriminating between different lengths of the CAG expansion, we evaluated the silencing efficacy of 15 miCAG constructs on Luc reporters expressing either 19 or 73 CAG repeats, named LucHTT(wt) and LucHTT(mt) respectively (**Figure 2c**). In contrary to previously published studies using siRNAs, ss-siRNAs, ASOs, or different artificial miRNAs, all miCAG variants showed poor allele selectivity and neither of the constructs induced HTT knock-down stronger than 60%[15,19,23–25]

Previously, several small molecules such as siRNAs, ASOs, shRNAs, and different artificial miRNAs targeting the isoforms of rs362307 or rs362331 were designed and experimentally tested for the allele-specific silencing of mtHTT allele.[16,17,19,20] To estimate the ability of our miHTT constructs to induce the allele selectivity by owning only one nucleotide difference between the match and mismatch target sequences, we first co-transfected miSNP50C constructs with LucSNP50C or LucSNP50T reporters carrying target sequences of exon 50 with either C or T isoform of rs362331, respectively (**Figure 2d**). Seven miSNP50C variants with the SNP-matching nucleotide at positions 13, 14, 16, 17, 18, 20, and 21 induced mtHTT knock-down stronger than 70% with miSNP50C-18 being the most efficient and inducing ±80% knock-down of both C and T target variants. Neither of these constructs showed great potential to discriminate between the match and mismatch targets. Similarly to the miSNP50C constructs, co-transfections of the miSNP50T constructs with the match LucSNP50T and mismatch LucSNP50C reporters showed strong HTT inhibition by a number of variants but overall poor allele selectivity (**Figure 2e**). Three miSNP50T variants with the SNP-matching nucleotide at positions 14, 18, and 21 induced HTT knock-down stronger than 70% with miSNP50T-18 being again the most efficient. Finally, miSNP67T constructs were co-transfected with the match LucSNP67T and mismatch LucSNP67C reporters. miSNP67T constructs with the SNP-matching nucleotide at position 7, 8, 9, 16, 17, and 18 induced mild 50–60% knock-down of their match target and poor allele selectivity (**Figure 2f**). The most efficient was miSNP67T with the SNP-matching nucleotide at position 7 and showed HTT knock-down of ±60% with mild allele selectivity. Based on these results, miH12, miSNP50C-18, miSNP50T-18, and miSNP67T-7 were selected for further optimizations.

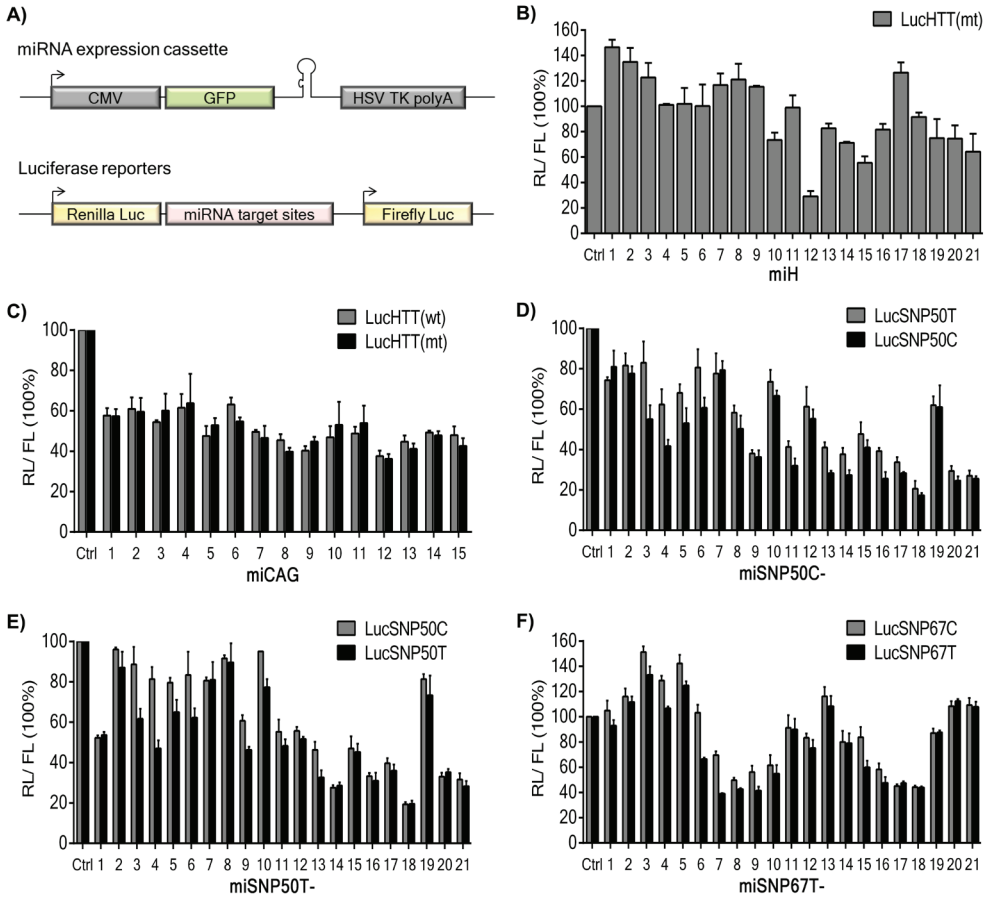


Figure 2. Luciferase reporter knock-down by different miHTT variants. **(a)** Schematic representation of pcDNA6.2-CMV-GFP-miHTT constructs and luciferase (Luc) reporters. Green fluorescent protein (GFP) and miHTT variants were expressed as one transcript from the cytomegalovirus (CMV) promoter and the expression cassette terminated with the herpes simplex virus thymidine kinase polyadenylation (HSV TK polyA) signal. For the Luc reporters, sequences from HTT exon 1 with 19 or 73 CAG repeats (LucHTT(wt) or LucHTT(mt), respectively), exon 50 (LucSNP50C, LucSNP50T), or exon 67 (LucSNP67C, LucSNP67T) were cloned behind the renilla luciferase (RL) gene. In addition, firefly luciferase (FL) was co-expressed from the vector as an internal control. **(b)** LucHTT(mt) reporter knock-down by miH1-miH21 constructs targeting sequences in HTT exon 1. Human embryonic kidney (HEK)293T cells were cotransfected with 50 ng Luc reporter and 50 ng miH1-miH21 constructs. RL and FL were measured 2 days post-transfection and RL was normalized to FL expression. Scrambled (Ctrl) served as a negative control and was set at 100%. **(c)** LucHTT(wt) and LucHTT(mt) reporter knock-down by 15 miCAG constructs targeting the CAG repeats of exon 1 measured 2 days post-transfection. The experimental setup is as described in **(b)**. **(d)** LucSNP50 reporter knock-down by miSNP50C-1—miSNP50C-21. LucSNP50C and LucSNP50T expressed a partial sequence of exon 50 with the isoform C or T of rs362331, respectively. All miSNP50C variants perfectly match to LucSNP50C and have 1 nt mismatch with LucSNP50T target sequences. HEK293T cells were co-transfected with 100 ng Luc reporter and 10 ng miSNP50C constructs. Luciferase expression was measured as described in **(b)**. **(e)** LucSNP50 reporter knock-down by miSNP50T-1—miSNP50T-21 constructs. All miSNP50T variants perfectly match to LucSNP50T and have 1 nt mismatch with LucSNP50C target sequences. Transfections and luciferase measurements were performed as described in **(d)**. **(f)** LucSNP67 reporter knock-down by miSNP67T-1—miSNP67T-21 constructs. LucSNP67C and LucSNP67T reporters expressed a partial sequence of exon 67 with the isoform C or T of rs362307, respectively. All miSNP67T variants perfectly match with LucSNP67T and have 1 nt mismatch with LucSNP67C target sequences. Transfections and luciferase measurements were performed as in **(b)**. The luciferase knock-down are representative figures of three independent experiments.

Enhancement of allele selectivity by introduction of a single base substitution in miSNP50C-18, miSNP50T-18, and miSNP67T-7 constructs

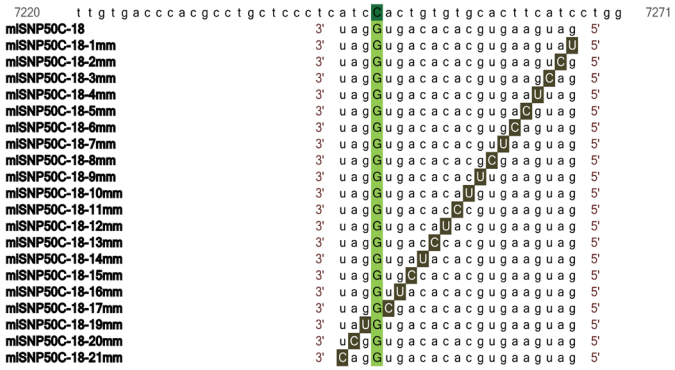
miSNP50C-18, miSNP50T-18, and miSNP67T-7 constructs showed good HTT silencing efficacy but poor allele selectivity *in vitro*. In order to enhance their potential to discriminate between two heterozygous HTT alleles, we introduced a single base change at each possible position of the guide strand while creating the mismatch with the target sequences.[26] For each base substitution, G or C were replaced by T, and A or T were replaced by C. Since the inserted guide strand sequences of all three variants are 21 nt long with one crucial SNP-matching nucleotide, we generated 20 constructs for miSNP50C-18 (**Figure 3a**), miSNP50T-18 (**Figure 3b**), and miSNP67T-7 (**Figure 3c**).

To determine whether a single base substitution can improve the allele selectivity, we first co-transfected miSNP50C-18-1mm—miSNP50C-18-21mm with LucSNP50C or LucSNP50T reporter (**Figure 3d**). Each miSNP50C-18-mm construct acquired one nucleotide mismatch with LucSNP50C reporter and a second nucleotide mismatch with LucSNP50T reporter. Overall, we observed a variation between miSNP50C-18-mm constructs in both the reporter silencing efficacy and allele discrimination. miSNP50C-18-6mm induced mild allele selectivity and ±70% knock-down of the match LucSNP50C reporter. miSNP50C-18-15mm and miSNP50C-18-16mm showed good allele selectivity and match reporter knock-down stronger than 80% with miSNP50C-18-16mm being the most efficient.

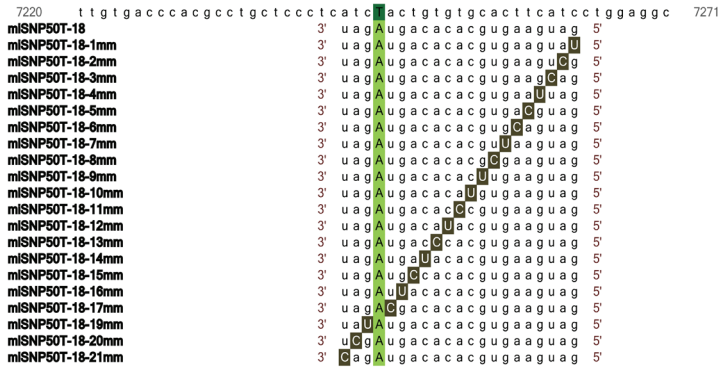
Co-transfections of miSNP50T-18-1mm—miSNP50T-18-21mm with LucSNP50C and LucSNP50T reporters showed similar trend of match reporter knock-down and allele selectivity as with miSNP50C-18-mm variants, but a greater potential to discriminate between the two reporters (**Figure 3e**). miSNP50T-18-7mm and miSNP50T-18-16mm triggered good allele selectivity and match reporter knock-down stronger than 80% with miSNP50T-18-7mm being the most efficient

Co-transfections of miSNP67T-7-1mm—miSNP67T-7-21mm with LucSNP67C and LucSNP67T showed overall poor enhancement of allele selectivity and a reduction of silencing efficacy compared with the initial miSNP67T-7 (**Figure 3f**).

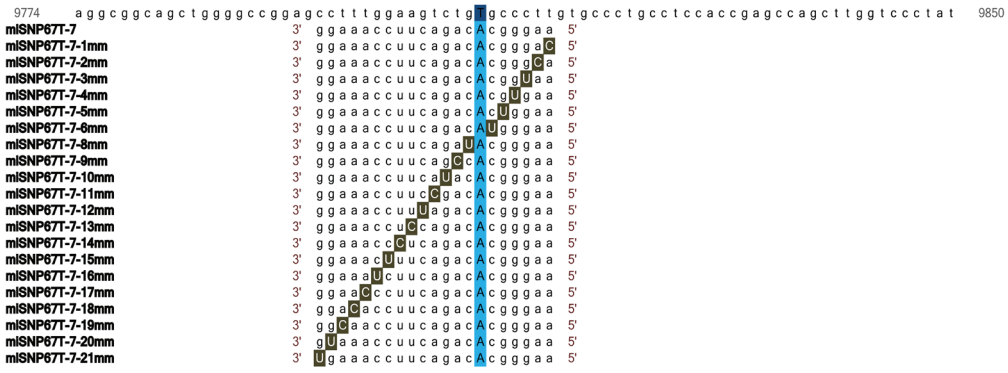
A)


7220 t t g t g a c c c a c g c c t g c t c c c t c a t c C a c t g t g t g c a c t t c a t c c t g g 7271
mISNP50C-18 3' u a g G u g a c a c a c g u g a a g u a g 5'
mISNP50C-18-1mm 3' u a g G u g a c a c a c g u g a a g u a U 5'
mISNP50C-18-2mm 3' u a g G u g a c a c a c g u g a a g u C g 5'
mISNP50C-18-3mm 3' u a g G u g a c a c a c g u g a a g C a g 5'
mISNP50C-18-4mm 3' u a g G u g a c a c a c g u g a a U u a g 5'
mISNP50C-18-5mm 3' u a g G u g a c a c a c g u g a C g u a g 5'
mISNP50C-18-6mm 3' u a g G u g a c a c a c g u g C a g u a g 5'
mISNP50C-18-7mm 3' u a g G u g a c a c a c g u U a a g u a g 5'
mISNP50C-18-8mm 3' u a g G u g a c a c a c g C g a a g u a g 5'
mISNP50C-18-9mm 3' u a g G u g a c a c a c U u g a a g u a g 5'
mISNP50C-18-10mm 3' u a g G u g a c a c a U g u g a a g u a g 5'
mISNP50C-18-11mm 3' u a g G u g a c a c C c g u g a a g u a g 5'
mISNP50C-18-12mm 3' u a g G u g a c a U a c g u g a a g u a g 5'
mISNP50C-18-13mm 3' u a g G u g a c C c a c g u g a a g u a g 5'
mISNP50C-18-14mm 3' u a g G u g a U a c a c g u g a a g u a g 5'
mISNP50C-18-15mm 3' u a g G u g C c a c a c g u g a a g u a g 5'
mISNP50C-18-16mm 3' u a g G u U a c a c a c g u g a a g u a g 5'
mISNP50C-18-17mm 3' u a g G C g a c a c a c g u g a a g u a g 5'
mISNP50C-18-19mm 3' u a U G u g a c a c a c g u g a a g u a g 5'
mISNP50C-18-20mm 3' u C g G u g a c a c a c g u g a a g u a g 5'
mISNP50C-18-21mm 3' C a g G u g a c a c a c g u g a a g u a g 5'

B)


7220 t t g t g a c c c a c g c c t g c t c c c t c a t c T a c t g t g t g c a c t t c a t c c t g g a g g c 7271
mISNP50T-18 3' u a g A u g a c a c a c g u g a a g u a g 5'
mISNP50T-18-1mm 3' u a g A u g a c a c a c g u g a a g u a U 5'
mISNP50T-18-2mm 3' u a g A u g a c a c a c g u g a a g u C g 5'
mISNP50T-18-3mm 3' u a g A u g a c a c a c g u g a a g C a g 5'
mISNP50T-18-4mm 3' u a g A u g a c a c a c g u g a a U u a g 5'
mISNP50T-18-5mm 3' u a g A u g a c a c a c g u g a C g u a g 5'
mISNP50T-18-6mm 3' u a g A u g a c a c a c g u g C a g u a g 5'
mISNP50T-18-7mm 3' u a g A u g a c a c a c g u U a a g u a g 5'
mISNP50T-18-8mm 3' u a g A u g a c a c a c g C g a a g u a g 5'
mISNP50T-18-9mm 3' u a g A u g a c a c a c U u g a a g u a g 5'
mISNP50T-18-10mm 3' u a g A u g a c a c a U g u g a a g u a g 5'
mISNP50T-18-11mm 3' u a g A u g a c a c C c g u g a a g u a g 5'
mISNP50T-18-12mm 3' u a g A u g a c a U a c g u g a a g u a g 5'
mISNP50T-18-13mm 3' u a g A u g a c C c a c g u g a a g u a g 5'
mISNP50T-18-14mm 3' u a g A u g a U a c a c g u g a a g u a g 5'
mISNP50T-18-15mm 3' u a g A u g C c a c a c g u g a a g u a g 5'
mISNP50T-18-16mm 3' u a g A u U a c a c a c g u g a a g u a g 5'
mISNP50T-18-17mm 3' u a g A C g a c a c a c g u g a a g u a g 5'
mISNP50T-18-19mm 3' u a U A u g a c a c a c g u g a a g u a g 5'
mISNP50T-18-20mm 3' u C g A u g a c a c a c g u g a a g u a g 5'
mISNP50T-18-21mm 3' C a g A u g a c a c a c g u g a a g u a g 5'

C)


9774 a g g c g g c a g c t g g g g c c g g a g c c t t t g g a a g t c t g T g c c c t t g t g c c c t g c c t c c a c c g a g c c a g c t t g g t c c c t a t 9850
mISNP67T-7 3' g g a a a c c u u c a g a c A c g g g a a 5'
mISNP67T-7-1mm 3' g g a a a c c u u c a g a c A c g g g a C 5'
mISNP67T-7-2mm 3' g g a a a c c u u c a g a c A c g g g C a 5'
mISNP67T-7-3mm 3' g g a a a c c u u c a g a c A c g g U a a 5'
mISNP67T-7-4mm 3' g g a a a c c u u c a g a c A c g U g a a 5'
mISNP67T-7-5mm 3' g g a a a c c u u c a g a c A c U g g a a 5'
mISNP67T-7-6mm 3' g g a a a c c u u c a g a c A U g g g a a 5'
mISNP67T-7-8mm 3' g g a a a c c u u c a g a U A c g g g a a 5'
mISNP67T-7-9mm 3' g g a a a c c u u c a g C c A c g g g a a 5'
mISNP67T-7-10mm 3' g g a a a c c u u c a U a c A c g g g a a 5'
mISNP67T-7-11mm 3' g g a a a c c u u c C g a c A c g g g a a 5'
mISNP67T-7-12mm 3' g g a a a c c u u U a g a c A c g g g a a 5'
mISNP67T-7-13mm 3' g g a a a c c u C c a g a c A c g g g a a 5'
mISNP67T-7-14mm 3' g g a a a c C c C u c a g a c A c g g g a a 5'
mISNP67T-7-15mm 3' g g a a a c U u u c a g a c A c g g g a a 5'
mISNP67T-7-16mm 3' g g a a a U c u u c a g a c A c g g g a a 5'
mISNP67T-7-17mm 3' g g a a C c c u u c a g a c A c g g g a a 5'
mISNP67T-7-18mm 3' g g a G a c c u u c a g a c A c g g g a a 5'
mISNP67T-7-19mm 3' g g C a a c c u u c a g a c A c g g g a a 5'
mISNP67T-7-20mm 3' g U a a a c c u u c a g a c A c g g g a a 5'
mISNP67T-7-21mm 3' U g a a a c c u u c a g a c A c g g g a a 5'

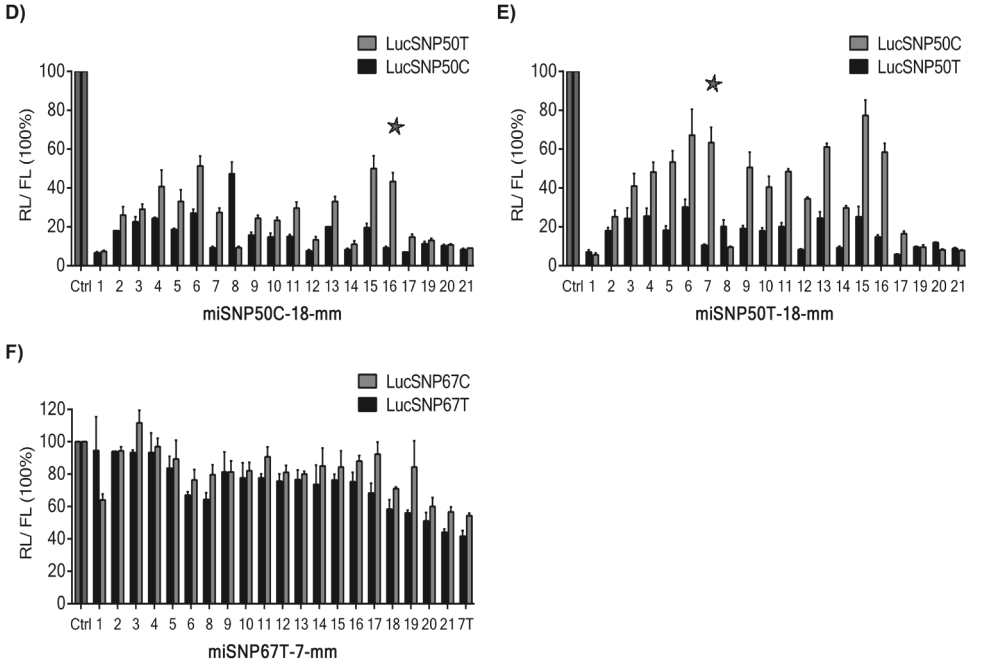


Figure 3. Introduction of a mismatch to miSNP50C-18, miSNP50T-18, and miSNP67T-7 to improve mtHTT allele selectivity. **(a)** Twenty variants named miSNP50C-18-1mm to miSNP50C-18-21mm were generated with one mismatch to the C-target sequence at positions 1–21 and two mismatches to the T-target sequence: one at position 18 and the other at positions 1–21. In all variants, G or C were replaced by T, and A or T by C. The C isoform of rs362331 is represented in dark green, the SNP-matching nucleotide in light green and the mismatch in grey. **(b)** Twenty variants named miSNP50T-18-1mm—miSNP50T-18-21mm were designed as described in **(a)**. **(c)** Twenty variants named miSNP67T-7-1mm—miSNP67T-7-21mm were designed as described in **(a)**. The T isoform of rs362307 is represented in dark blue, the SNP-matching nucleotide in light blue and the mismatch in dark gray. **(d)** LucSNP50 reporter knock-down by miSNP50C-18-1mm to miSNP50C-18-21mm constructs. Human embryonic kidney (HEK)293T cells were co-transfected with 50 ng Luc reporter and 50 ng miSNP50C-18 constructs. Renilla (RL) and firefly (FL) luciferases were measured 2 days post-transfection and RL was normalized to FL expression. Scrambled (Ctrl) served as a negative control and was set at 100%. **(e)** LucSNP50 reporter knock-down by miSNP50T-18-1mm to miSNP50T-18-21mm constructs. Transfections and luciferase measurements were performed as described in **(d)**. **(f)** LucSNP67 reporter knock-down by miSNP67T-7-1mm—miSNP67T-7-21mm constructs. HEK293T cells were co-transfected with 30 ng Luc reporter and 3 ng miSNP67T constructs. Luciferase expression was measured as in **(d)**. The miSNP50C-18-16mm and miSNP50T-18-7mm constructs selected for further optimization are indicated with the asterisk. The luciferase knock-down are representative figures of four independent experiments.

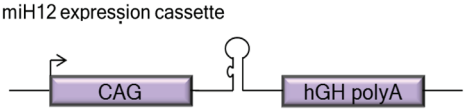
Generation and testing of miHTT expression vectors suitable for clinical use

Thus far, all miHTT variants were expressed jointly with green fluorescent protein (GFP) from the cytomegalovirus (CMV) promoter. In a vision of clinical trial preparations for the total HTT knock-down, we chose to optimize further the expression cassette of miH12. First, the CMV promoter was replaced by a ubiquitous CAG promoter that consisted of cytomegalovirus immediate-early enhancer fused to chicken β-actin promoter (**Figure 4a**). This promoter is known to drive stable high expression of a transgene and to be highly effective in the brain.[27] Second, GFP was excluded from the expression vector to eliminate the possibility of the host immune response. To address the influence of the pri-miRNA scaffold on the processing, silencing potential of miH12 and the passenger strand activity, the 21 nt guide sequence was embedded in the human miR-1–2, miR-16-1, miR-26a-1, miR-101-1, miR-122, miR-135b, miR-155, miR-203a, miR-335, miR-451a scaffolds with 200 nt 5' and 3' encompassing flanking regions (**Figure 4b**). The pri-miRNA scaffolds were selected based on their stem-loop structure and the high guide versus passenger strand ratios obtained from miRBase release 21 (http://www.mirbase.org/). The corresponding passenger strand (miH12*) was corrected in order to preserve the original pri-miRNA structure.

The silencing efficacy of ten CAG-miH12 expression constructs, named miH12-1, miH12-16, miH12-26, miH12-101, miH12-122, miH12-135, miH12-155, miH12-203, miH12-335, and miH12-451 was measured by the LucHTT(mt) knock-down in HEK293T cells (**Figure 4c**). Heterogeneity in the silencing effect was observed for the different constructs. A weak 20% HTT knock-down was induced by miH12-16 scaffold. miH12-101 and miH12-451 scaffolds triggered ±50% HTT knock-down while miH12-1, miH12-26, miH12-122, miH12-135, miH12-155, miH12-203, and miH12-335 scaffolds reached 60-70% HTT knock-down. To more precisely define the knock-down efficacy of the miH12 scaffolds, titration curves were generated for the best candidates (**Figure 4d**). Only at 1 ng of the transfected plasmid, we observed a clear difference in the LucHTT(mt) knock-down between individual scaffolds. With 50 ng and higher concentrations of the plasmid, all constructs showed more than 70% LucHTT(mt) knock-down.

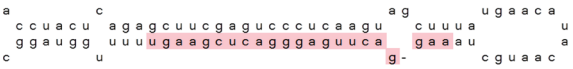
It has been shown that thermodynamic properties of double-stranded miRNA molecules play key roles in strand selection and functional assymetry.[28–30] To estimate the silencing activity of the complementary miH12* passenger strand in vitro, we generated Luc reporters carrying extended miH12* complementary sequences (LucPassenger). Cotransfections of LucPassenger constructs with the corresponding miH12 scaffolds in HEK293T cells showed variations in LucPassenger knock-down (**Figure 4e**). We detected no or low activity of the miH12* processed from miH12-101, miH12-122, miH12-135, miH12-155, and miH12-451 scaffolds. Strong LucPassenger knock-down was induced by the rest of the miH12 scaffolds.

A)

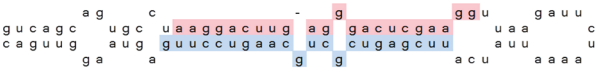


B)

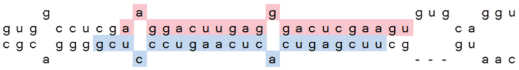
miH12_1



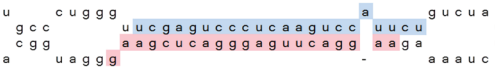
miH12_16



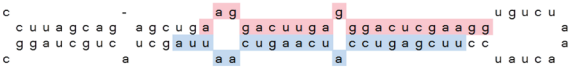
miH12_26



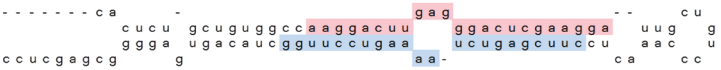
miH12_101



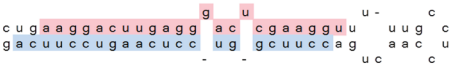
miH12_122



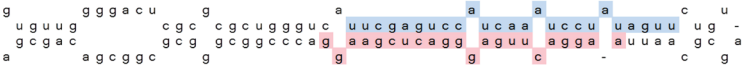
miH12_135



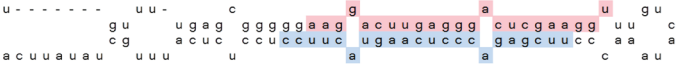
miH12_155



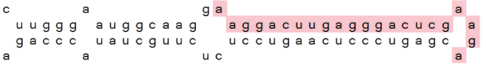
miH12_203



miH12_335



miH12_451



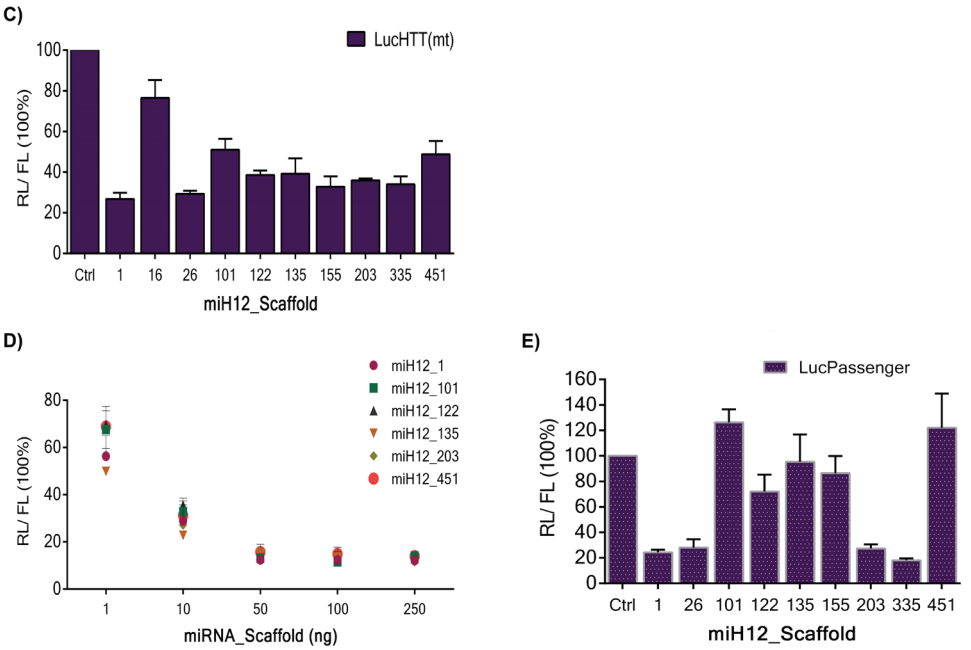
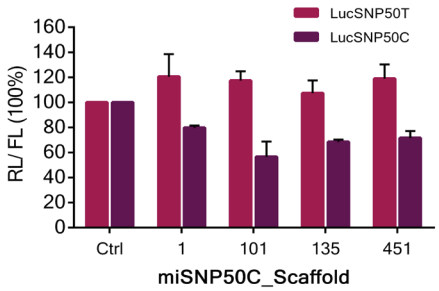


Figure 4. Optimization of the miH12 expression cassette to address efficacy and passenger strand activity. **(a)** Schematic representation of the pri-miH12 expression cassette with the CMV immediate-early enhancer fused to chicken β-actin (CAG) promoter and human growth hormone polyadenylation (hGH polyA) signal. **(b)** Ten cellular pri-miRNA scaffolds were selected from miRBase database (www.mirbase.org) based on the guide/passenger strand prevalence and RNA folding. Twenty-one nt of the guide strand were replaced by the mature miH12 sequence and the passenger strand was corrected in order to preserve pri-miH12 scaffolding. Based on miRBase, the predicted guide and passenger strand sequences of the cellular pre-miRNA scaffolds are indicated in red and blue, respectively. **(c)** LucHTT(mt) reporter knock-down by ten miH12 scaffolds. Human embryonic kidney (HEK)293T cells were co-transfected with 100 ng LucHTT(mt) reporter and 10 ng miH12 constructs. Renilla (RL) and firefly (FL) luciferases were measured 2 days post-transfection and RL was normalized to FL expression. Scrambled (Ctrl) served as a negative control and was set at 100%. **(d)** Titration curve of miH12 embedded in the human miR-1, miR-101, miR-122, miR-135, miR-203, and miR-451 scaffolds. HEK293T cells were co-transfected with 50 ng LucHTT(mt) reporter and 1, 10, 50, 100, or 250 ng of miH12 constructs. Luciferase expression was measured as described in **(c)**. **(e)** In vitro passenger strand activity of miH12-1, miH12-26, miH12-101, miH12-122, miH12-135, miH12-155, miH12-203, miH12-335, and miH12-451 scaffolds. For the LucPassenger reporters, reverse complement sequences to the miH12 passenger strand sequences were cloned behind RL. In addition, FL was co-expressed from the vector as an internal control. Transfections and luciferase measurements were performed as in **(c)**. The luciferase knock-down are representative figures of three independent experiments.

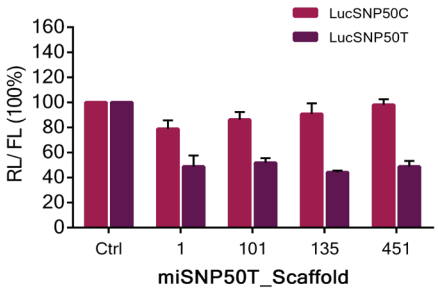
In vitro allele-selective HTT suppression by miSNP50C and miSNP50T processed from miR-1, miR-101, miR-135 and mir-451 scaffolds

In a vision of clinical trial preparations for the allele-specific HTT knock-down by targeting the HD-associated SNP rs362331, we optimized further the expression cassette for miSNP50C-18-16mm (from now referred as miSNP50C) and miSNP50T-18-7mm (from now referred as miSNP50T). Based on *in vitro* results from ten miH12 scaffolds, we selected miR-1, miR-101, miR-135, and miR-451 scaffolds for miSNP50C and miSNP50T. miH12-135 was highly efficient and together with miH12-101 and miH12-451 did not produce any passenger strand. The miR-1 scaffold was included based on the simplicity of the stem structure. To evaluate their silencing and allele-selectivity potential, we co-transfected the different scaffolds with LucSNP50C and LucSNP50T reporters (**Figure 5a,b**). We observed a similar trend of match reporter knock-down and allele selectivity for all four scaffolds with miSNP50C-101 and miSNP50T-135 being the most efficient. Further titrations of the miSNP50 scaffolds revealed a concentration-dependent silencing. Representative figures of miSNP50C-451 and miSNP50T-451 titrations are shown (**Figure 5c,d,g**). Next, we addressed the passenger strand activity of the miSNP50C and miSNP50T scaffolds on LucPassenger reporters carrying extended miSNP50C* and miSNP50T* complementary target sequences. On the contrary to our results with miH12 constructs, we observed strong LucPassenger knock-down by miSNP50C* and miSNP50T* strands processed from miR-1, miR-101, and miR-135 scaffolds (**Figure 5e,f**). miR-451 was the only scaffold that did not induce LucPassenger reporter silencing.

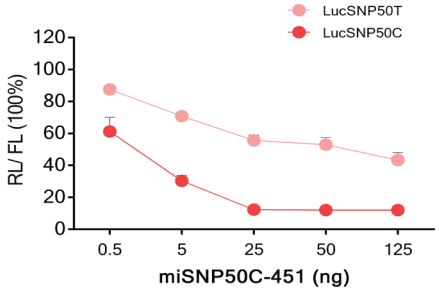
A)



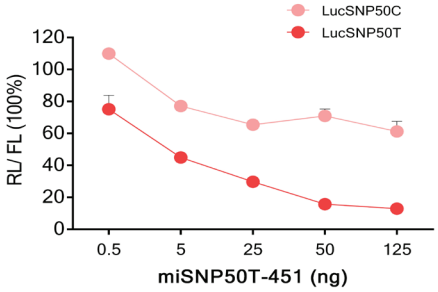
B)



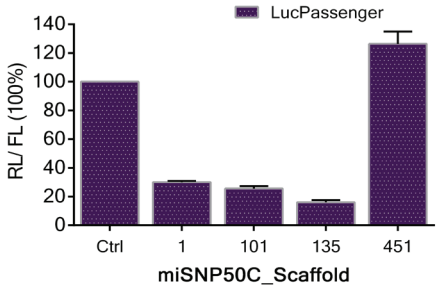
C)



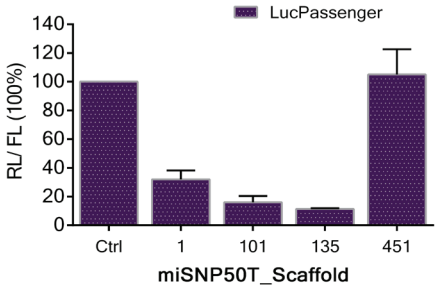
D)



E)



F)



G)

Constructs	IC50 (ng) Match	IC50 (ng) Mismatch	Selectivity Ratio
miSNP50C-1	1,1	> 125	> 113,6
miSNP50T-1	2,8	> 125	> 44,6
miSNP50C-101	1,2	> 125	> 104,2
miSNP50T-101	3,3	> 125	> 37,9
miSNP50C-135	3,1	> 125	> 40,3
miSNP50T-135	5	> 125	> 25
miSNP50C-451	2,1	50	23,8
miSNP50T-451	3,5	> 125	> 35,7

Figure 5. Optimization of the miSNP50C and miSNP50T expression cassette to address efficacy and passenger strand activity. **(a)** LucSNP50 reporter knock-down by four different pri-miSNP50C scaffolds. Twenty-one nt mature miSNP50C-18-16mm sequence, from now referred as miSNP50C, was embedded as a guide strand in the human miR-1, miR-101, miR-135, and miR-451 scaffolds and the passenger strand was corrected in order to preserve pri-miSNP50C folding. Human embryonic kidney (HEK)293T cells were cotransfected with 50 ng luciferase (Luc) reporter and 10 ng miSNP50C constructs. Renilla (RL) and firefly (FL) luciferases were measured 2 days post-transfection and RL was normalized to FL expression. Scrambled (Ctrl) served as a negative control and was set at 100%. **(b)** LucSNP50 reporter knock-down by four different pri-miSNP50T constructs. Twenty-one nt mature miSNP50T-18-7mm sequence, from now referred as miSNP50T, was embedded as a guide strand in the human miR-1, miR-101, miR-135, and miR-451 scaffolds and the passenger strand was corrected in order to preserve pri-miSNP50T folding. HEK293T cells were co-transfected with 50 ng Luc reporter and 10 ng pri-miSNP50T constructs. Luciferase expression was measured as in **(a)**. **(c)** Titration curve of miSNP50C embedded in the miR-451 scaffold, from now referred as miSNP50C-451. HEK293T cells were cotransfected with 25 ng Luc reporter and 0.5, 5, 25, 50, or 125 ng of miSNP50C-451 construct. Luciferase expression was measured as described in **(a)**. **(d)** Titration curve of miSNP50T embedded in the miR-451 scaffold, from now referred as miSNP50T-451. Transfections and luciferase measurements were performed as in **(c)**. **(e)** In vitro passenger strand activity of miSNP50C embedded in the miR-1, miR-101, miR-135, and miR-451 scaffolds. For the LucPassenger reporters, reverse complement sequences to the four miSNP50C passenger strand sequences were cloned behind RL. In addition, FL was coexpressed from the vector as an internal control. HEK293T cells were cotransfected with 25 ng Luc reporter and 5 ng miSNP50C constructs. Luciferase measurements were performed as in **(a)**. **(f)** In vitro passenger strand activity of miSNP50T embedded in the miR-1, miR-101, miR-135, and miR-451 scaffolds. Transfections and luciferase measurements were performed as in **(e)**. **(g)** Allele selectivity ratios of miSNP50C and miSNP50T embedded in the miR-1, miR-101, miR-135, and miR-451 scaffolds. IC50 indicates a concentration (ng) of miSNP50 construct that is required for 50% Luc reporter knock-down. LucSNP50C represents a match reporter for miSNP50C constructs and a mismatch reporter for miSNP50T constructs, and vice versa. The allele selectivity ratios were calculated as IC50(mismatch)/IC50(match). The luciferase knock-down are representative figures of two independent experiments.

Expression of miH12 and miSNP50 from various cellular pri-miRNA scaffolds results in different guide and passenger strand processing

To demonstrate the influence of the cellular pri-miRNA scaffolds on miH12 and miSNP50 processing, we analyzed the prevalence and sequence composition of the guide and passenger strands by NGS. NGS was performed on small RNAs isolated from HEK293T cells transfected with miH12-1, miH12-101, miH12-122, miH12-135, miH12-155, miH12-203, or miH12-451 expression constructs. For miSNP50C and miSNP50T, we analyzed the processing from miR-135 and miR-451 scaffolds. For each sample, we obtained between 15–30 mln small RNA reads that were subsequently trimmed and aligned against the corresponding reference sequence. All reads shorter than 10 nt, longer than 45 nt, and represented less than 10 times were excluded from the analysis.

Overview of the read alignments for the different pre-miH12 and pre-miSNP50 reference sequences is presented in (**Figure 6**). There was a large difference in the pri-miH12 and pri-miSNP50 processing pattern originating from different scaffolds. First, miH12-101, miH12-122, miH12-155, miH12-451, miSNP50C-451, and miSNP50T-451 scaffolds were processed to yield almost exclusively the guide strand with absent or very low concentrations of the passenger strand. The ratio between the guide and passenger strand was lower for the other miH12 scaffolds making them less attractive for future studies. Second, the analysis of the sequence length and composition of the different miH12 scaffolds revealed that the guide strands from all analyzed constructs were cleaved almost precisely at the predicted

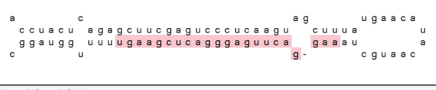
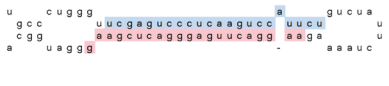
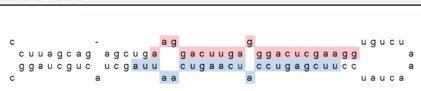
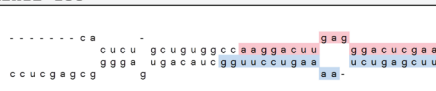
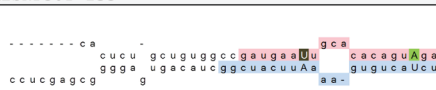
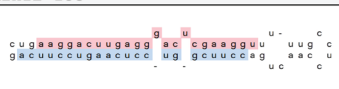
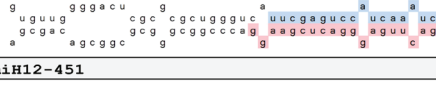
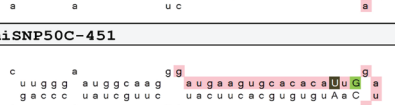
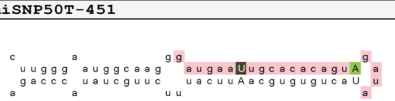
Drosha sites whereas the further downstream Dicer cleavage generated variability in the sequence length (**Figure 6a**). The latter ranged from 19–31 nt depending on the scaffold. The most prevalent miH12 length was 22 nt and originated from four scaffolds miH12-1, miH12-101, miH12-122, and miH12-203. Furthermore, the length of the most abundant read from all constructs except for miH12-101, miH12-155, miH12-451, miSNP50C-451, and miSNP50T-451 corresponded to the predicted cleavage pattern obtained from miRBase release 21.

By allowing three mismatches with the reference sequence, we observed 3' end sequence modifications for all the constructs with few that reached more than 2% threshold set for our analysis. This is in accordance with previously published data on 3'end editing events in various cell lines and tissues.[31–33] The miR-101 generated the least sequence heterogeneity and active passenger strand, but the most 3'end editing. The most abundant edited read accounted for 47.20% from all reads that aligned to the pre-miH12-101 reference sequence.

Notably, the read alignments of miH12 and miSNP50 expressed from the miR-451 scaffold showed different length and cleavage patterns of the most prevalent sequences. In the case of miH12-451, the most abundant read (59.98%) was 30 nt long encompassing the guide, loop and 8 nt from the passenger strand. The incorporated 21 nt miH12 sequence was detected in only 0.05% of the reads. No full-length passenger strand was detected. This cleavage pattern is typical for the non-canonical Drosha/Argonaute 2 processing mechanism. The read alignment analysis of miSNP50C-451 and miSNP50T-451 revealed a completely different picture; for both constructs the most abundant sequences were 23 nt long, representing 48.52 and 42.28% of the reads matching the reference sequences, respectively. Similarly to miH12-451, very little passenger strand was detected.

During miH12-135 processing, the guide strand sequences were generated from the 5' arm. Interestingly, embedding miSNP50C and miSNP50T sequences into the miR-135 scaffold reversed the preference for the 5' arm to serve as a guide strand and the 3' arm as a passenger strand (**Figure 6b**).

A)

miRNA reference sequence		Guide Strand
miH12-1		
	1	AAGGACTTGAGGGACTCGAAGT
	2	AAGGACTTGAGGGACTCGAAG
	3	AAGGACTTGAGGGACTCGA
	4	AGGACTTGAGGGACTCGAAGT
	5	GAGGACTTGAGGGACTCGAAGT
miH12-101		
	1	AAGGACTTGAGGGACTCGAAGT
	2	AAGGACTTGAGGGACTCGAAGTT
	3	AAGGACTTGAGGGACTCGAAG
	4	AAGGACTTGAGGGACTCGA
	5	AAGGACTTGAGGGACTCGAAGG
	6	AAGGACTTGAGGGACTCGAAT
	7	AAGGACTTGAGGGACTCGAAGA
miH12-122		
	1	AAGGACTTGAGGGACTCGAAGG
	2	AAGGACTTGAGGGACTCGAAGGT
	3	AAGGACTTGAGGGACTCGAAGGA
	4	AAGGACTTGAGGGACTCGAAG
	5	AAGGACTTGAGGGACTCGAAGT
	6	AAGGACTTGAGGGACTCGA
miH12-135		
	1	AAGGACTTGAGGGACTCGAAGGA
	2	AAGGACTTGAGGGACTCGAAGG
	3	AAGGACTTGAGGGACTCGAAGGAT
	4	AAGGACTTGAGGGACTCGAAGGATT
	5	AAGGACTTGAGGGACTCGAAG
	6	AAGGACTTGAGGGACTCGAAGGAA
miSNP50C-135		
	1	GATGAAGTGCACACATTGGATGA
	2	GATGAAGTGCACACATTGGATG
	3	
	4	
	5	
	6	
miSNP50T-135		
	1	GATGAATTGCACACAGTAGATGA
	2	
	3	
	4	
	5	
	6	
miH12-155		
	1	AAGGACTTGAGGGACTCGAAGGTT
	2	AAGGACTTGAGGGACTCGAAGGTTT
	3	AAGGACTTGAGGGACTCGAAGGT
	4	AAGGACTTGAGGGACTCGAAGGTTTT
	5	AAGGACTTGAGGGACTCGAAGGTTTTT
miH12-203		
	1	AAGGACTTGAGGGACTCGAAGG
	2	TAAGGACTTGAGGGACTCGAAG
	3	AAGGACTTGAGGGACTCGAAG
	4	AAGGACTTGAGGGACTCGAAGT
miH12-451		
	1	AAGGACTTGAGGGACTCGAAGACGAGTCCC
	2	AAGGACTTGAGGGACTCGAAGACGAGTCCCA
	3	AAGGACTTGAGGGACTCGAAGACGAGTCCCT
miSNP50C-451		
	1	GATGAAGTGCACACATTGGATAC
	2	GATGAAGTGCACACATTGGATACA
	3	GATGAAGTGCACACATTGGATACAATGTGT
	4	GATGAAGTGCACACATTGGAT
	5	GATGAAGTGCACACATTGGATA
miSNP50T-451		
	1	GATGAATTGCACACAGTAGATAT
	2	GATGAATTGCACACAGTAGATATAC
	3	GATGAATTGCACACAGTAGATATACTGTGT
	4	GATGAATTGCACACAGTAGATATA
	5	ATGAATTGCACACAGTAGATATAC
	6	GATGAATTGCACACAGTAGATA
	7	GATGAATTGCACACAGTAGATATACTGTG

Length	% Reads	Passenger Strand	Length	% Reads
22	65.80%	TTCGAGTCCCTCAAGTAGCT	20	3.16%
21	4.41%	TTCGAGTCCCTCAAGTAGCTTT	22	2.17%
19	3.54%			
21	2.65%			
22	2.23%			
22	47.20%	TCGAGTCCCTCAAGTCCATTCT	22	0.99%
23	7.73%			
21	6.56%			
19	5.16%			
22	3.97%			
21	3.53%			
22	2.71%			
22	38.35%	TTCGAGTCCATCAAGTCAATT	21	0.28%
23	15.56%			
23	12.91%			
21	9.69%			
22	3.35%			
19	2.71%			
23	25.42%	TTCGAGTCTAAAAGTCCTTGG	21	7.20%
22	8.35%	TTCGAGTCTAAAAGTCCTTGGC	22	5.43%
24	7.31%	CTTCGAGTCTAAAAGTCCTTGG	22	4.97%
25	6.17%	TTCGAGTCTAAAAGTCCTTGG**T**	22	2.49%
21	2.79%	TTCGAGTCTAAAAGTCCTTGGCT	23	2.14%
24	2.55%			
23	11.12%	TCCAATGTGAAACTTCATCGGCT	23	29.78%
22	2.27%	TCCAATGTGAAACTTCATCGGC	22	9.54%
		ATCCAATGTGAAACTTCATCG**T**	22	7.72%
		ATCCAATGTGAAACTTCATCGG**T**	23	5.33%
		TCCAATGTGAAACTTCATCGG**T**	22	2.39%
		TCCAATGTGAAACTTCATCGGCT**T**	24	2.34%
23	2.80%	ATCTACTGTGAAAATTCATCGG	22	39.33%
		TCTACTGTGAAAATTCATCGG	21	17.34%
		TCTACTGTGAAAATTCATCGGC	22	13.34%
		ATCTACTGTGAAAATTCATCGG**T**	23	5.61%
		TCTACTGTGAAAATTCATCGG**T**	22	4.72%
		TCTACTGTGAAAATTCATCGGCT	23	4.00%
24	48.54%	CCTTCGGTCCTCAAGTCCTTCA	22	1.44%
25	24.87%			
23	7.06%			
26	6.46%			
27	2.15%			
22	10.32%	TTCGAGTCCATCAAATCCTATAGT	24	4.42%
22	6.93%			
21	6.09%			
22	2.07%			
30	59.98%			
31	21.03%			
31	8.23%			
23	48.52%	TACAATGTGTGCACTTCATAT	21	0.30%
24	15.93%			
30	8.04%			
21	7.96%			
22	5.01%			
23	42.28%	TATACTGTGTGCAATTCATTTCT	23	0.37%
25	22.26%			
30	9.07%			
24	4.51%			
24	2.93%			
22	2.15%			
29	2.01%			

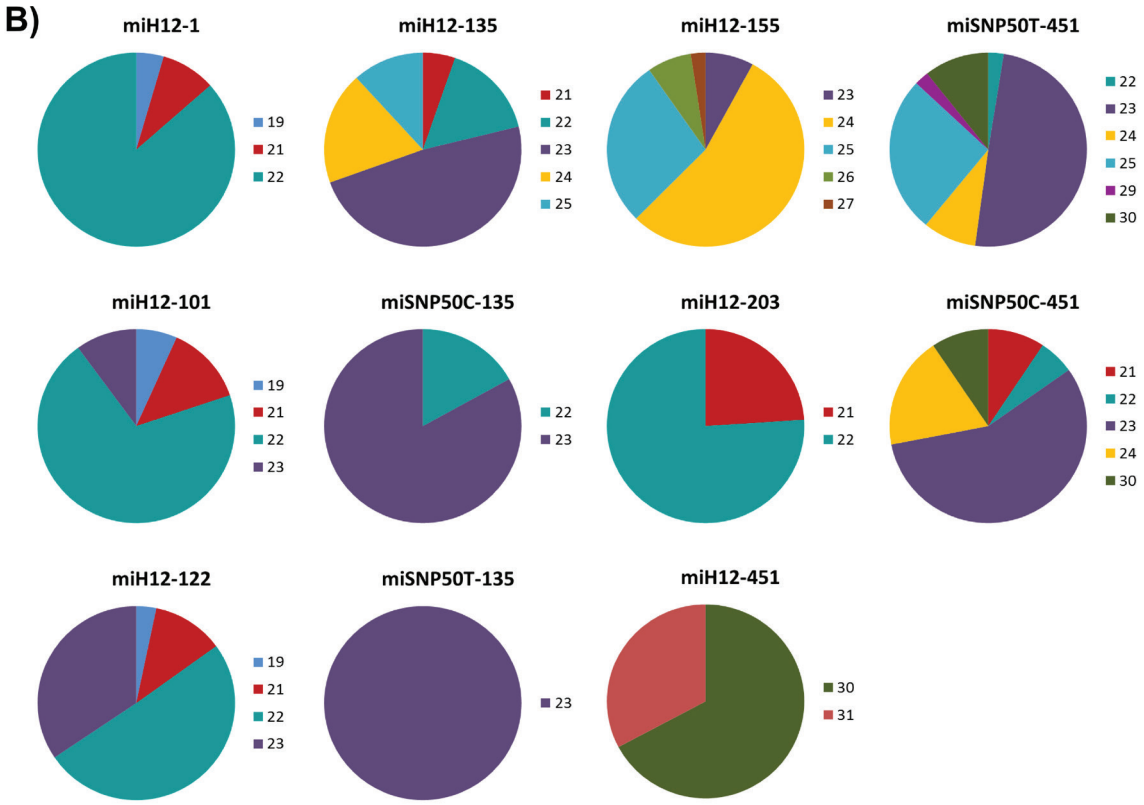


Figure 6. Next generation sequencing (NGS) analysis on the processing of miH12-1, miH12-101, miH12-122, miH12-135, miH12-155, miH12-203, miH12-451, miSNP50C-135, miSNP50T-135, miSNP50C-451 and miSNP50T-451 scaffolds. **(a)** Sequence distribution (%) of reads mapping to miH12-1, miH12-101, miH12-122, miH12-135, miH12-155, miH12-203, miH12-451, miSNP50C-135, miSNP50T-135, miSNP50C-451, and miSNP50T-451 pre-miRNA scaffold sequences. Human embryonic kidney (HEK)293T cells were transfected with 4 µg of the constructs, 48 hours post-transfection RNA was isolated and small RNA NGS was performed. For each variant, the miHTT scaffold is shown in the first column. Based on miRBase, the predicted guide and passenger strand sequences of the cellular pri-miRNA scaffolds are indicated in red and blue, respectively, 5' and 3' flanking nucleotides in black, and a mismatch with the reference sequence in green. **(b)** Length distribution of reads mapping to miH12-1, miH12-101, miH12-122, miH12-135, miH12-155, miH12-203, miH12-451, miSNP50C-135, miSNP50T-135, miSNP50C-451, and miSNP50T-451 scaffold sequences. For the read alignments, up to three mismatches with the references sequences were allowed. Reads represented with less than 2% were excluded from the figure.

In vivo silencing efficacy and pre-miH12 processing of AAV5-miH12-101, AAV5-miH12-135 and AAV5-miH12-451 vectors

To investigate the miH12 silencing efficacy and processing patterns *in vivo*, the humanized transgenic Hu128/21 HD mice were injected bilaterally in the striatum with $4x10^{11}$gc per animal of AAV5 encoding miH12-101, miH12-135, miH12-451, or Ctrl constructs. Two months post-injection, mice were sacrificed and the level of HTT silencing in the brain was evaluated by western blotting (**Figure 7a**). Similar to our *in vitro* data, miH12 induced strong more than 70% total HTT knock-down in the striatum and more than 50% HTT knock-down in the cortex. Moreover, the silencing efficiency varied between the three scaffolds with AAV5-miH12-135 showing the strongest HTT knock-down. To address the miH12 processing *in vivo*, we analyzed the prevalence and sequence composition of the guide and passenger strands by NGS. RNA was isolated from the cortices of Hu128/21 mice and small RNA NGS was performed. For each sample, we obtained between 15–30 mln small RNA reads that were subsequently adaptor-trimmed and aligned against the corresponding reference sequence. All reads shorter than 10 nt, longer than 45 nt, and represented less than 10 times were excluded from the analysis. Overview of the read alignments for pre-miH12-135 and pre-miH12-451 scaffolds is represented in (**Figure 7b**). In the case of miH12-451, the most abundant reads were 30 nt and 23 nt long, respectively. In case of miH12-135, we observed similar Dicer cleavage pattern as we observed *in vitro*. Surprisingly, the most abundant read was 19 nt long and accounted for 33.51%. We also observed similar 3'end editing events from both scaffolds compared to our *in vitro* data.

Our results demonstrate that the incorporation of identical sequences in various pri-miRNA scaffolds results in different HTT knock-down and processing of guide and passenger strands both *in vitro* and *in vivo*. As a consequence, every scaffold yielded its own "fingerprint" of mature miH12 and miSNP50 sequences. Based on the silencing efficacy and processing profile, we selected miH12-451 for further development as the artificial miRNA-based therapeutic candidate for HD.

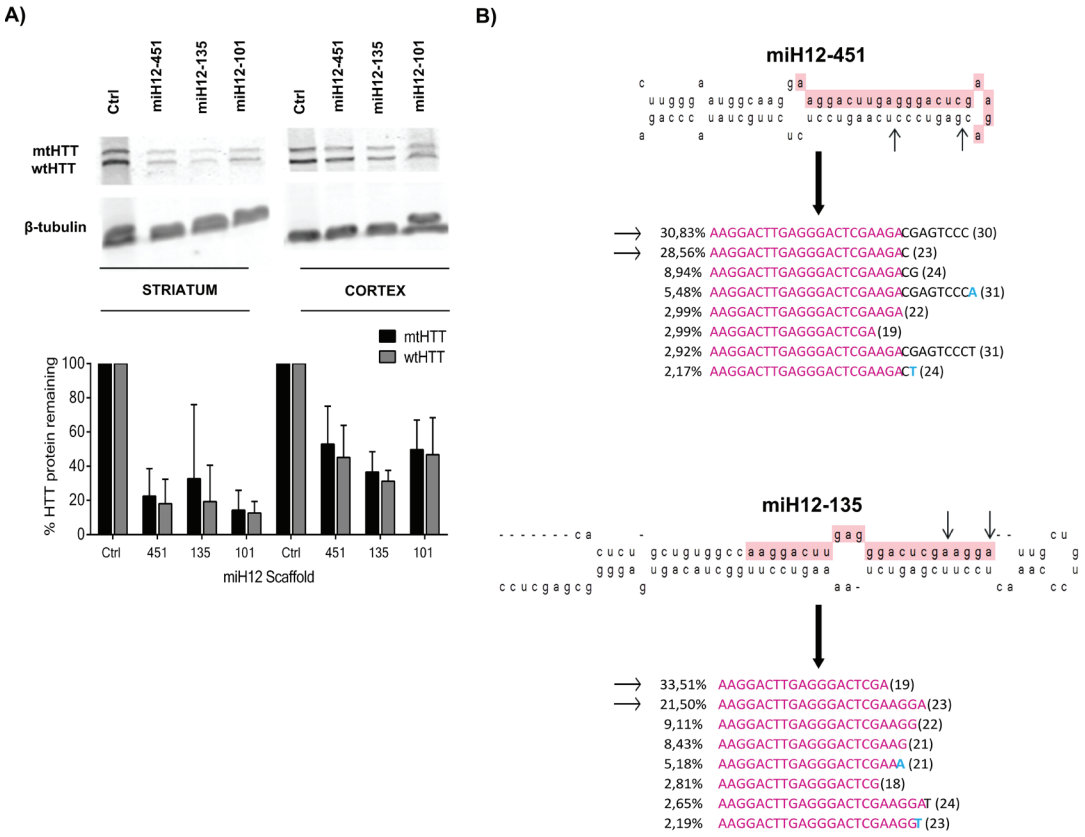


Figure 7. HTT knock-down by AAV5-miH12-101, AAV5-miH12-135, AAV5-miH12-451 scaffolds and NGS analysis on miH12 processing in the humanized Hu128/21 HD mouse model. (**a**) Top, an example western blot showing wtHTT and mtHTT knock-down by AAV5-miH12-101, AAV5-miH12-135, and AAV5-miH12-451 viruses. Bottom, quantification of HTT protein in the striata and cortices of Hu128/21 mice 2 months postinjection with AAV5-miH12-101, AAV5-miH12-135 and AAV5-miH12-451 viruses. Density of HTT bands was normalized to β-tubulin loading control and shown as a percentage of the same allele (either wtHTT or mtHTT) from Ctrl animals. (**b**) Sequence distribution (%) of reads mapping to miH12-135 and miH12-451 scaffolds. Cortices were isolated from mice 2 months postinjection of AAV5-miH12-135 and AAV5-miH12-451. RNA was isolated from tissue homogenate and small RNA NGS was performed. For each variant, the miHTT scaffold is shown on top. First two most abundant sequences are represented by the arrow. For the read alignments, up to three mismatches with the reference sequences were allowed and are shown in green. Reads represented with less than 2% were excluded from the figure.

DISCUSSION

Given the complexity of pathology and natural history of HD, HTT transcript lowering approaches come to focus since they aim to reduce the concentration of the malfunctioned protein. To date, both total and allele-specific HTT down-regulation strategies are moving forward to the clinic. siRNAs and ASOs show positive results when targeting either both alleles or only mtHTT allele *in vitro* and *in vivo.*[7,15,16,34,35] However, the periodical re-administration of these therapeutics is required which adds more risk for infections and burden on the patients. Recently, the artificial RNAi-based approach using shRNAs or miRNAs has been proposed for the sustained total and allele-selective HTT down-regulation.[10,13,18,19] In general, shRNAs are expressed from pol III promoters and miRNAs from pol II promoters. Evidence suggests that expressing artificial shRNAs from strong pol III promoters can induce severe toxicity at high doses.[36–38] In some cases, the toxicity correlates with high production of the passenger strand, independent from the target HTT mRNA inhibition.[39] Importantly, switching to miRNA-based expression system can reduce the toxic effect.[36] Thus, a promising approach for the HD therapy is considered the pol II expression of artificial miRNAs targeting HTT transcripts delivered with viral vectors. Nevertheless, a detailed analysis on miRNA processing patterns, such as sequence composition, guide/passenger strand ratios, and passenger strand activity is necessary to estimate the potential cellular toxicity *in vivo.*

In the current study, we have evaluated three different approaches for HTT silencing using expressed artificial miHTTs. Total HTT knock-down was induced by targeting both wtHTT and mtHTT alleles with miH1-miH21 directed towards exon 1. The feasibility of the allele-specific silencing was evaluated by targeting the CAG repeats or heterozygous SNPs rs362331 and rs362307 in the *HTT* gene. Construct optimization of the best miH12, miSNP50C, and miSNP50T candidates has been performed by introduction of single base substitutions in the guide strand sequences, adapting the expression cassette and using different cellular pri-miRNA scaffolds. The silencing efficacy, allele selectivity, analysis of miH12, miSNP50C, and miSNP50T processing patterns, and evaluation of the passenger strand activity supported the selection of the best therapeutic candidate for further development.

Several lines of investigation suggest that sufficient inhibition of mtHTT while maintaining wtHTT at adequate levels is achievable and therapeutically beneficial.[8,10,13,40] For instance, lentiviral delivery of shRNAs targeting both HTT alleles reduced HD-like neuropathology in the HD rat model.[10] In another study with the transgenic HD mice, more than 70% total HTT knock-down using artificial miRNAs was efficacious with no apparent toxicity 3 months post-injection.[40] The safety of the nonallele-selective HTT approach was also evaluated in nonhuman primates where it showed tolerance to 45% HTT knock-down [8,13] Additionally, from the drug manufacturing perspective, single product development and drug availability for all HD-allele carriers favor nonallele-selective HD approaches forward to the clinic. Here, we identified miH12, which induced more than 70% HTT knock-down both *in vitro*

and *in vivo* as the therapeutic candidate for further development. Also, we optimized the expression cassette of miH12 to make the vector suitable for clinical use.

Despite the promising results for the total HTT knock-down, the model therapy would inhibit only the mtHTT allele while preserving wtHTT at normal levels. To achieve this, we initially designed 15 miCAG constructs with either perfect or partial complementarity to the CAG repeats. It has been shown that introducing base changes at a specific position within siRNA sequences that target CAG repeats enhanced HD allele discrimination.[23] We applied this knowledge when generating our miCAG constructs. However, none of the constructs induced good allele selectivity. Recently, ASOs and miRNAs perfectly complementary to CAG repeats with one mismatch at position 9 showed good allele selectivity.[39,41] Differences in the mismatch position, base composition, and expression cassette could explain the contrast in allele selectivity between theirs and our CAG-targeting constructs.

To design allele-specific HD therapy by targeting the mtHTT allele-linked SNPs, ideally, HD patients would be heterozygous for a specific SNP with one isoform linked to the mtHTT. However till now, no such SNP has been discovered. Evidence shows that a combination of targetable isoforms originating from different SNPs will be required to treat the majority of HD population.[17] Very similarly to miCAG constructs, artificial miRNAs designed to target the HD-linked isoform T of rs362307 could not discriminate well between the two heterozygous alleles. Similar results have been shown in rodent HD models using siRNAs, shRNAs and different artificial miRNAs.[17–19] Moreover, the introduction of secondary mismatches did not improve the allele specificity *in vitro*. In contrast, previously it has been shown that some siRNAs targeting the isoform T of rs362307 and carrying a secondary mismatch to the wtHTT allele, showed good allele selectivity, which might be due to differences in the effective therapeutic sequence, administration, test system, and concentration.[17]

A great portion of the Caucasian HD population is heterozygous (C/T) for rs362331 in exon 50.[3] Here, we designed 42 different artificial miSNP50 by micro-shifting the 21 nt guide strand along the HTT target sequence that contained either C or T isoform of rs362331. In contrary to previously published data with shRNAs and siRNAs, none of the constructs induced immediate good allele selectivity.[18,20] Very likely, the length of the guide strand, sequence composition and miRNA processing contributed to the observed differences. The allele selectivity was achieved after introducing single nucleotide substitutions at specific positions within the guide strand, as previously suggested.[26]

In the canonical processing pathway, cellular miRNAs are expressed from the genome mainly by RNA pol II as long pri-miRNAs.[42] The pri-miRNA transcripts fold into specific stem-containing RNA scaffolds which determinate their further processing by the Microprocessor complex.[43–45] Further downstream, Dicer cleaves the loop-containing precursor into a mature double-stranded miRNA structure composed of the more active guide strand and its complementary passenger strand.[46] The main concerns when using artificial miRNAs are the off-target effects and saturation of RNAi machinery caused by events linked to cellular

processing of mature miRNA strands and target similarity with other genes.[38,39,47] Here, for the first time, we evaluated the efficacy and processing of miH12, miSNP50C, and miSNP50T from several pri-miRNA scaffolds for a single HD therapeutic. We have performed detailed NGS analysis of the artificial miRNA processing and the passenger strand activity both *in vitro* and *in vivo*, which varied depending on the scaffold. Moreover, we showed that embedding miH12, miSNP50C, and miSNP50T sequences in the same miR-135 scaffold resulted in different cellular processing of guide and passenger strands. For instance, cellular processing of miH12-135 favored production of the 5'arm over the 3'arm. However, miSNP50C-135 and miSNP50T-135 processing had reversed preferences, the 3'arm served as the predominant guide strand. Variability in the miRNA scaffold, thermodynamic properties of the duplex miRNA, 3'overhangs of the both strands could result in the observed differences.

In the noncanonical pathway, the pre-miR-451 escapes Dicer cleavage and only a 5' arm strand is active on the targets.[48,49] The mature guide strand sequence of the miR-451 is generated by cleaving the 3'arm between 10–11 nt from the stem origin which yields a 30 nt long intermediate that is subsequently trimmed by poly(a)-specific ribonuclease (PARN) into a mature ~23 nt long active molecule.[50–52] Interestingly, NGS on miH12-451 processing *in vitro* showed a 30 nt long predominant read, but for miSNP50C-451 or miSNP50T-451 the read was only 23 nt long. Moreover, miH12-451 processing *in vivo* showed equal ratios of the 30 nt and 23 nt long molecules. It has been reported that PARN-associated trimming exhibit nucleotide preferences at the 3'end of AGO2-cleaved intermediates and is not required for target silencing.[52] Construct concentration and the cellular environment could be potential reasons for the lack of a ~23 nt long active miH12 molecules *in vitro*.

Ultimately, our NGS analysis showed 3'end miRNA editing events both *in vitro* and *in vivo*. In both cases, adenosine or uracil was added to the mature guide sequences. This resulted in a formation of several mature miH12 isoforms containing the same seed region. Previous studies report that trimming and tailing influence the stability and processing of pre-miRNAs, mature miRNAs or mRNA sequences.[53–56] However, the exact roles of miH12 mono-uridylation and mono-adenylation still needs to be determined.

Altogether, our results highlight the necessity of careful selection and characterization of the therapeutic product both *in vitro* and *in vivo* before entering the clinic. A number of parameters need to be carefully evaluated including gene silencing efficacy, miRNA processing pattern, and induction of off-target effects.

MATERIALS AND METHODS

HTT target sequences

Homo sapiens HD mRNA, complete cds (gb|L12392.1|HUMHDA) obtained from http://blast.ncbi.nlm.nih.gov/Blast.cgi was used to identify target sequences for the artificial miHTTs. miH1-21 targeted sequences in exon 1 (pos.185–579), miCAG constructs targeted the CAG repeats (pos.367–429), miSNP50 constructs targeted SNP rs362331 (pos.7246), and miSNP67 constructs targeted SNP rs362307 (pos.9809).

DNA constructs

To create the miHTT vectors, miRNA sequences targeting HTT transcripts were embedded into the murine pre-miR-155 backbone of pcDNA6.2-GW/EmGFP-miR (Invitrogen, Carlsbad, CA) by annealing complementary oligonucleotides (Qiagen, Valencia, CA) and ligation into the linearized pcDNA6.2 plasmid. As a negative control, pcDNA6.2-GW/EmGFP-miR-neg control (Invitrogen) was used, named Ctrl. miH12 and miSNP50 sequences were subsequently incorporated in cellular pri-miRNA scaffolds of the human miR-1–2, miR-16-1, miR-26a-1, miR-101-1, miR-122, miR-135b, miR-155, miR-203a, miR-335, and miR-451a. 200 nt 5' and 3' flanking regions were included with EcoRV and BamHI restriction sites and the complete sequences were ordered from GeneArt gene synthesis (Invitrogen). In those constructs, the CMV promoter was replaced by the CMV immediate-early enhancer fused to chicken β-actin (CAG) promoter (Inovio, Plymouth Meeting, PA).

For generation of the luciferase reporters LucHTT(wt) or LucHTT(mt), HTT exon 1 containing 19 or 73 CAG repeats respectively was linked to 83 nt from HTT exon 67 containing C/T at SNP rs362307 (pos.9809) and the fragment was cloned in the 3'UTR of the RL gene of the psiCHECK-2 vector (Promega, Madison, WI). For generation of LucSNP50C and LucSNP50T constructs, 48 nt fragment from HTT exon 50 containing C/T at SNP rs362331 (pos.7246) was cloned in the 3'UTR of the RL gene of the psiCHECK-2 vector (Promega). For different LucPassenger reporters, reverse complements of the passenger strands with 5 nt added from the Dicer cleavage sites were generated by CLC Main Workbench (version 6.6.1) and ordered (Qiagen). Annealed complementary oligonucleotides were cloned in the 3'UTR of the psiCHECK-2 vector (Promega). The mfold program (http://mfold.rna.albany.edu/?q=mfold) was used to determine the secondary structure of the RNA transcripts. The mfold structures of the oligonucleotides used in this study are listed in Supplementary Table S1.

Cell culture and transfections

The human embryonic kidney (HEK)293T cells were maintained in Dulbecco's modified Eagle's medium (Invitrogen) containing 10% fetal calf serum (Greiner, Kremsmünster, Austria), 100 U/ml penicillin and 100 U/ml streptomycin (Thermo Fisher, Waltham, MA), at

37 °C and 5% CO2. For luciferase assays and small RNA NGS, cells were seeded in 24- or 6-well plates at a density of 1.2*105 or 0.5*105 cells per well, respectively, in Dulbecco's modified Eagle's medium (Invitrogen) 1 day prior transfection. Transfections were performed with Lipofectamine 2000 reagent (Invitrogen) according to the manufacturer's instructions.

Luciferase assays

HEK293T cells were co-transfected with miHTT expression constructs and luciferase reporters that contain both the RL gene fused to miHTT target sequences and the FL gene. Transfected cells were assayed at 48 hours post-transfection in 100 µl 1× passive lysis buffer (Promega) by gentle rocking for 15 minutes at room temperature. The cell lysates were centrifuged for 5 minutes at 4,000 rpm and 10 µl of the supernatant was used to measure FL and RL activities with the Dual-Luciferase Reporter Assay System (Promega). Relative luciferase activity was calculated as the ratio between RL and FL activities. Allele selectivity ratio of the miSNP50 and miSNP67 variants was calculated on the IC50 given as the concentration in (ng) of miSNP needed to reach the half-maximal inhibition and dividing the IC50 of the mismatch reporter against the IC50 of the match reporter..

RNA isolation and Next Generation Sequencing (NGS)

HEK293T cells were transfected with 4 µg miH12 and miSNP50 expression plasmids using Lipofectamine 2000 reagent (Invitrogen) and total RNA was isolated from cells 48 hours post-transfection using Trizol (Invitrogen) according to the manufacturer's protocol. Cortices isolated from Hu128/21 mice were tissue homogenized in Trizol (Invitrogen) using gentleMACS Dissociator (Miltenyi Biotec, Bergisch Gladbach, Germany) and total RNA was isolated from Trizol according to the manufacturer's protocol (Invitrogen). Small RNA sequencing libraries for the Illumina sequencing platform were generated using high-quality total RNA as input and the NEXTflex Small RNA Sequencing kit (Bioo Scientific, Austin, TX). Briefly, the small RNA species were subjected to ligation with 3' and 5' RNA adapters, first strand reverse transcription, and polymerase chain reaction (PCR) amplification. Sample-specific barcodes were introduced in the PCR step. The PCR products were separated on TBE-PAGE electrophoresis and the expected band around 30 bp was recovered for each sample. The resulting sequencing libraries were quantified on a BioAnalyzer (Agilent, Santa Clara, CA). The libraries were multiplexed, clustered, and sequenced on an Illumina HiSeq 2000 (TruSeq v3 chemistry) with a single-read 36 cycles sequencing protocol and indexing. The sequencing run was analyzed with the Illumina CASAVA pipeline (v1.8.2), with demultiplexing based on sample-specific barcodes. The raw sequencing data produced was processed removing the sequence reads which were of too low quality (only "passing filter" reads were selected). In total, we generated between 15–35 mln reads per sample.

NGS data analysis

NGS small RNA raw data sets were analyzed using the CLC Genomics Workbench 6 (Qiagen). The obtained reads were adaptor-trimmed, which decreased the average read size from ~50 bp to ~25 bp. The custom adapter sequenced used for trimming all the bases extending 5' was: GTGACTGGAGTTCCTTGGCACCCGAGAATTCCA. All reads containing ambiguity N symbols, reads shorter than 10 nt, longer than 45 nt, and reads represented less than 10 times were discarded. Next, the obtained unique small RNA reads were aligned to the references sequences of the pre-miHTT constructs (Supplementary Table S1) with a max. of 3 nt mismatches allowed. The percentages of reads based on the total number of reads matching the reference sequence were calculated.

AAV vector production

AAV5 vectors encoding miH12 and Ctrl were produced by a baculovirus-based AAV production system. Briefly, the miRNA constructs were synthesized and cloned in an expression vector containing the CAG promotor. The CAG-miRNA cassette was obtained by digestion with restriction enzymes HindIII and PvuI and cloned in a uniQure transfer plasmid named pVD789 in order to generate an entry plasmid. The presence of the two inverted terminal repeats (ITRs) was confirmed by restriction digestion with SmaI. The ITR-CAG-miRNA cassette was inserted in a recombinant baculovirus vector (Bac.AMT5) by homologous recombination in Sf9 cells and clones were selected by plague purification. The recombinant baculovirus containing the ITR-CAG-miRNA were further amplified till P6 in Sf+ cells and screened for the best production and stability by PCR and qPCR. To generate AAV5, Sf+ cells were triple infected with three different recombinant baculoviruses expressing the ITRs-CAG-miRNA, the replicon enzyme (rep 183) and the capsid protein (cap 765). The cells were lysed 72 hours after the triple infection and the crude lysate was treated with Benzonase (50U/ml) (Merck, Darmstadt, Germany) for 1 hour at 37 °C. AAV5 was purified on an AVB Sepharose column (GE Healthcare, Little Chalfont, UK) using an AKTA purification system (GE Healthcare) and the final concentration was determined by quantitative PCR with primers amplifying a 95bp fragment from the CAG promoter region. The final product was sequence verified by NGS.

Mice and treatments

Humanized transgenic HD mice expressing full-length genomic human mtHTT from the YAC128 transgene and full-length genomic human wtHTT from the BACWT transgene (Hu128/21, Amber L Southwell, the manuscript in preparation) were maintained under a 12-hour light: 12-hour dark cycle in a clean facility with free access to food and water. Experiments were performed with the approval of the animal care committee at the University of British Columbia. Two-month-old animals were injected bilaterally with AAV5-miRNAs as in ref. 57. Briefly, mice were anesthetized with isoflurane, placed into a

stereotaxic frame, and the scalp prepared. An incision was made along the mid-line and burr holes drilled in both hemispheres of the skull at 0.8 mm anterior and 1.8 mm lateral to Bregma. A 5 µl Hamilton syringe loaded with 3 µl of sterile saline and 2 µl of viral solution (such that the viral solution would be injected first followed by the saline) was then lowered to mid striatum at a depth of 3.5 mm and the full 5 µl was injected at a rate of 0.5 µl/minute. The needle was left in place for additional 5 minutes and withdrawn slowly.

HTT immunoblotting

Two months after treatment, mice were killed with an overdose of avertin followed by cervical dislocation. Brains were removed, briefly placed on ice to increase tissue rigidity, and microdissected by region. Striata and cortices were equilibrated in RNAlater solution (Ambion) overnight at 4 °C before storage at −80 °C. Allelic HTT protein was then quantified in the striatum and cortex of three animals per condition by immunoblot as in ref. 16. Briefly, tissue was lysed in single detergent lysis buffer, total protein quantified by DC assay (Bio-Rad, Hercules, CA), and 40 µg total protein resolved on 10% low-bis acrylamide gels (200:1 acrylamide:bis). Proteins were transferred to 0.45 µm nitrocellulose membranes, which were probed for HTT (MAB2166 1:2,000, Millipore, Billerica, MA) and β-tubulin loading control (1:5,000, Sigma-Aldrich, St. Louis, MO). Secondary IR dye 800CW goat anti-mouse (1:250, Rockland, Limerick, PA) antibody and the LiCor Odyssey infrared imaging system were used to visualize proteins. The intensity of each allele of HTT was normalized to β-tubulin and then to the mean value for the same allele from Ctrl injected animals on the same membrane.

Acknowledgments

The authors thank Jolanda Snapper (uniQure) for technical support. Qingwen Xia for assistance with genotyping. Yuanyun Xie and Louisa DalCengio for assistance with HTT quantitation. We also thank Wim Hermens (uniQure) and Olivier ter Brake (EP&C) for critically reviewing the manuscript. The authors declare no conflict of interest.

REFERENCES

1. Ross, CA and Tabrizi, SJ (2011). Huntington's disease: From molecular pathogenesis to clinical treatment. *Lancet Neurol.* 10: 83–98.
2. Southwell, AL and Patterson, PH (2011). Gene therapy in mouse models of huntington disease. *Neuroscientist* 17: 153–162.
3. Kay, C, Skotte, N, Southwell, A and Hayden, M (2014). Personalized gene silencing therapeutics for Huntington disease. *Clin. Genet.* 86: 29–36.
4. Davidson, BL, Boudreau, RL, Rodrı, E, Rodríguez-Lebrón, E and Davidson, BL (2011). RNAi medicine for the brain: Progresses and challenges. *Hum. Mol. Genet.* 20: 21–27.
5. Aronin, N and DiFiglia, M (2014). Huntingtin-Lowering Strategies in Huntington's Disease: Antisense Oligonucleotides, Small RNAs, and Gene Editing. *Mov. Disord.* 29: 1455–1461.
6. Østergaard, ME, Southwell, AL, Kordasiewicz, H, Watt, AT, Skotte, NH, Doty, CN, *et al.* (2013). Rational design of antisense oligonucleotides targeting single nucleotide polymorphisms for potent and allele selective suppression of mutant Huntingtin in the CNS. *Nucleic Acids Res.* 41: 9634–9650.
7. Southwell, AL, Skotte, NH, Kordasiewicz, HB, Ostergaard, ME, Watt, AT, Carroll, JB, *et al.* (2014). In vivo evaluation of candidate allele-specific mutant huntingtin gene silencing antisense oligonucleotides. *Mol. Ther.* 22: 2093–2106.
8. Stiles, DK, Zhang, Z, Ge, P, Nelson, B, Grondin, R, Ai, Y, *et al.* (2012). Widespread suppression of huntingtin with convection-enhanced delivery of siRNA. *Exp. Neurol.* 233: 463–471.
9. Stanek, LM, Sardi, SP, Mastis, B, Richards, AR, Treleaven, CM, Taksir, T, *et al.* (2014). Silencing mutant huntingtin by adeno-associated virus-mediated RNA interference ameliorates disease manifestations in the YAC128 mouse model of Huntington's disease. *Hum. Gene Ther.* 25: 461–74.
10. Drouet, V, Perrin, V, Hassig, R, Dufour, N, Auregan, G, Alves, S, *et al.* (2009). Sustained effects of nonallele-specific Huntingtin silencing. *Ann. Neurol.* 65: 276–85.
11. Maczuga, P, Koornneef, A, Borel, F, Petry, H, van Deventer, S, Ritsema, T, *et al.* (2012). Optimization and comparison of knockdown efficacy between polymerase II expressed shRNA and artificial miRNA targeting luciferase and Apolipoprotein B100. *BMC Biotechnol.* 12: 1–12.
12. Southwell, AL, Skotte, NH, Bennett, CF and Hayden, MR (2012). Antisense oligonucleotide therapeutics for inherited neurodegenerative diseases. *Trends Mol. Med.* 18: 634–643.
13. McBride, JL, Pitzer, MR, Boudreau, RL, Dufour, B, Hobbs, T, Ojeda, SR, *et al.* (2011). Preclinical Safety of RNAi-Mediated HTT Suppression in the Rhesus Macaque as a Potential Therapy for Huntington's Disease. *Mol. Ther.* 19: 2152–2162.
14. Grondin, R, Kaytor, MD, Ai, Y, Nelson, PT, Thakker, DR, Heisel, J, *et al.* (2012). Six-month partial suppression of Huntingtin is well tolerated in the adult rhesus striatum. *Brain a J. Neurol.* 135: 1197–1209.
15. Yu, D, Pendergraff, H, Liu, J, Kordasiewicz, HB, Cleveland, DW, Swayze, EE, *et al.* (2012). Single-stranded RNAs use RNAi to potently and allele-selectively inhibit mutant huntingtin expression. *Cell* 150: 895–908.
16. Carroll, JB, Warby, SC, Southwell, AL, Doty, CN, Greenlee, S, Skotte, N, *et al.* (2011). Potent and selective antisense oligonucleotides targeting single-nucleotide polymorphisms in the Huntington disease gene / allele-specific silencing of mutant huntingtin. *Mol. Ther.* 19: 2178–85.
17. Pfister, EL, Kennington, L, Straubhaar, J, Wagh, S, Liu, W, DiFiglia, M, *et al.* (2009). Five siRNAs targeting three SNPs in Huntingtin may provide therapy for three-quarters of Huntington's disease patients. *Curr Biol.* 19: 774–778.
18. Drouet, V, Ruiz, M, Zala, D, Feyeux, M, Auregan, G, Cambon, K, *et al.* (2014). Allele-specific silencing of mutant huntingtin in rodent brain and human stem cells. *PLoS One* 9.

19. Monteys, AM, Wilson, MJ, Boudreau, RL, Spengler, RM and Davidson, BL (2015). Artificial miRNAs Targeting Mutant Huntingtin Show Preferential Silencing In Vitro and In Vivo. *Mol. Ther. Acids* 4: e234.
20. Lombardi, MS, Jaspers, L, Spronkmans, C, Gellera, C, Taroni, F, Di Maria, E, *et al.* (2009). A majority of Huntington's disease patients may be treatable by individualized allele-specific RNA interference. *Exp. Neurol.* 217: 312–319.
21. Kremer B1, Goldberg P, Andrew SE, Theilmann J, Telenius H, Zeisler J, Squitieri F, Lin B, Bassett A, Almqvist E, et al. (1994). The New England Journal of Medicine Downloaded from nejm.org at UNIVERSITEIT VAN AMSTERDAM on March 9, 2015. For personal use only. No other uses without permission. Copyright © 1994 Massachusetts Medical Society. All rights reserved. *N Engl J Med.*
22. Kay, C, Collins, JA, Skotte, NH, Southwell, AL, Warby, SC, Caron, NS, *et al.* (2015). Huntingtin Haplotypes Provide Prioritized Target Panels for Allele-specific Silencing in Huntington Disease Patients of European Ancestry. *Mol. Ther.* 23: 1759–1771.
23. Fiszer, A, Mykowska, A and Krzyzosiak, WJ (2011). Inhibition of mutant huntingtin expression by RNA duplex targeting expanded CAG repeats. *Nucleic Acids Res.* 39: 5578–85.
24. Fiszer, A, Olejniczak, M, Galka-Marciniak, P, Mykowska, A and Krzyzosiak, WJ (2013). Self-duplexing CUG repeats selectively inhibit mutant huntingtin expression. *Nucleic Acids Res.* 41: 10426–37.
25. Gagnon, KT, Pendergraff, HM, Deleavey, GF, Swayze, EE, Potier, P, Randolph, J, *et al.* (2010). Allele-selective inhibition of mutant huntingtin expression with antisense oligonucleotides targeting the expanded CAG repeat. *Biochemistry* 49: 10166–78.
26. Ohnishi, Y, Tamura, Y, Yoshida, M, Tokunaga, K and Hohjoh, H (2008). Enhancement of allele discrimination by introduction of nucleotide mismatches into siRNA in allele-specific gene silencing by RNAi. *PLoS One* 3: e2248.
27. Klein, RL, Hamby, ME, Gong, Y, Hirko, AC, Wang, S, Hughes, J a., *et al.* (2002). Dose and Promoter Effects of Adeno-Associated Viral Vector for Green Fluorescent Protein Expression in the Rat Brain. *Exp. Neurol.* 176: 66–74.
28. Khvorova, A, Reynolds, A and Jayasena, SD (2003). Functional siRNAs and miRNAs exhibit strand bias. *Cell* 115: 209–16.
29. Meijer, H a, Smith, EM and Bushell, M (2014). Regulation of miRNA strand selection: follow the leader? *Biochem. Soc. Trans.* 42: 1135–40.
30. Gu, S, Jin, L, Zhang, F, Huang, Y, Grimm, D, Rossi, JJ, *et al.* (2011). Thermodynamic stability of small hairpin RNAs highly influences the loading process of different mammalian Argonautes. *Proc. Natl. Acad. Sci. U. S. A.* 108: 9208–13.
31. Martí, E, Pantano, L, Bañez-Coronel, M, Llorens, F, Miñones-Moyano, E, Porta, S, *et al.* (2010). A myriad of miRNA variants in control and Huntington's disease brain regions detected by massively parallel sequencing. *Nucleic Acids Res.* 38: 7219–35.
32. Aravin, A and Tuschl, T (2005). Identification and characterization of small RNAs involved in RNA silencing. *FEBS Lett.* 579: 5830–5840.
33. Landgraf, P, Rusu, M, Sheridan, R, Sewer, A, Iovino, N, Aravin, A, *et al.* (2007). A Mammalian microRNA Expression Atlas Based on Small RNA Library Sequencing. *Cell* 129: 1401–1414.
34. DiFiglia, M, Sena-Esteves, M, Chase, K, Sapp, E, Pfister, E, Sass, M, *et al.* (2007). Therapeutic silencing of mutant huntingtin with siRNA attenuates striatal and cortical neuropathology and behavioral deficits. *Proc. Natl. Acad. Sci. U. S. A.* 104: 17204–17209.
35. Kordasiewicz, HB, Stanek, LM, Wancewicz, E V., Mazur, C, McAlonis, MM, Pytel, KA, *et al.* (2012). Sustained Therapeutic Reversal of Huntington's Disease by Transient Repression of Huntingtin Synthesis. *Neuron* 74: 1031–1044.

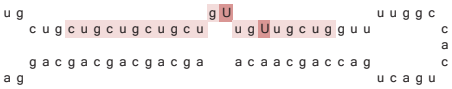
36. Borel, F, van Logtenstein, R, Koornneef, A, Maczuga, P, Ritsema, T, Petry, H, *et al.* (2011). In vivo knock-down of multidrug resistance transporters ABCC1 and ABCC2 by AAV-delivered shrnas and by artificial miRNAs. *J. RNAi Gene Silenc.* 7: 434–442.
37. Bish, LT, Sleeper, MM, Reynolds, C, Gazzara, J, Withnall, E, Singletary, GE, *et al.* (2011). Cardiac gene transfer of short hairpin RNA directed against phospholamban effectively knocks down gene expression but causes cellular toxicity in canines. *Hum. Gene Ther.* 22: 969–977.
38. Grimm, D, Streetz, KL, Jopling, CL, Storm, T a, Pandey, K, Davis, CR, *et al.* (2006). Fatality in mice due to oversaturation of cellular microRNA/short hairpin RNA pathways. *Nature* 441: 537–541.
39. McBride, JL, Boudreau, RL, Harper, SQ, Staber, PD, Monteys, AM, Martins, I, *et al.* (2008). Artificial miRNAs mitigate shRNA-mediated toxicity in the brain: implications for the therapeutic development of RNAi. *Proc. Natl. Acad. Sci. U. S. A.* 105: 5868–5873.
40. Boudreau, RL, Mcbride, JL, Martins, I, Shen, S, Xing, Y, Carter, BJ, *et al.* (2009). Nonallele-specific silencing of mutant and wild-type huntingtin demonstrates therapeutic efficacy in Huntington's disease mice. *Mol. Ther.* 17: 1053–1063.
41. Hu, J, Liu, J and Corey, DR (2010). Allele-selective inhibition of huntingtin expression by switching to an miRNA-like RNAi mechanism. *Chem. Biol.* 17: 1183–8.
42. Lee, Y, Kim, M, Han, J, Yeom, K-H, Lee, S, Baek, SH, *et al.* (2004). MicroRNA genes are transcribed by RNA polymerase II. *EMBO J.* 23: 4051–60.
43. Auyeung, VC, Ulitsky, I, McGeary, SE and Bartel, DP (2013). Beyond secondary structure: primary-sequence determinants license pri-miRNA hairpins for processing. *Cell* 152: 844–58.
44. Gregory, RI, Yan, K-P, Amuthan, G, Chendrimada, T, Doratotaj, B, Cooch, N, *et al.* (2004). The Microprocessor complex mediates the genesis of microRNAs. *Nature* 432: 235–40.
45. Han, J, Lee, Y, Yeom, K-H, Kim, Y-K, Jin, H and Kim, VN (2004). The Drosha-DGCR8 complex in primary microRNA processing. *Genes Dev.* 18: 3016–27.
46. Gurtan, AM, Lu, V, Bhutkar, A and Sharp, PA (2012). In vivo structure-function analysis of human Dicer reveals directional processing of precursor miRNAs. *RNA* 18: 1116–22.
47. Monteys, AM, Spengler, RM, Dufour, BD, Wilson, MS, Oakley, CK, Sowada, MJ, *et al.* (2014). Single nucleotide seed modification restores in vivo tolerability of a toxic artificial miRNA sequence in the mouse brain. *Nucleic Acids Res.* 42: 13315–13327.
48. Cheloufi, S, Dos Santos, CO, Chong, MMW and Hannon, GJ (2010). A dicer-independent miRNA biogenesis pathway that requires Ago catalysis. *Nature* 465: 584–589.
49. Cifuentes, D, Xue, H, Taylor, DW, Patnode, H, Mishima, Y, Cheloufi, S, *et al.* (2010). A novel miRNA processing pathway independent of Dicer requires Argonaute2 catalytic activity. *Science* 328: 1694–1698.
50. Ma, H, Zhang, J and Wu, H (2014). Designing Ago2-specific siRNA/shRNA to Avoid Competition with Endogenous miRNAs. *Mol. Ther. Nucleic Acids* 3: e176.
51. Herrera-Carrillo, E, Harwig, A, Liu, YP and Berkhout, B (2014). Probing the shRNA characteristics that hinder Dicer recognition and consequently allow Ago-mediated processing and AgoshRNA activity. *RNA* 20: 1410–1418.
52. Yoda, M, Cifuentes, D, Izumi, N, Sakaguchi, Y, Suzuki, T, Giraldez, AJ, *et al.* (2013). Poly(A)-specific ribonuclease mediates 3'-end trimming of argonaute2-cleaved precursor micrornas. *Cell Rep.* 5: 715–726.
53. Lee, M, Kim, B and Kim, VN (2014). Emerging Roles of RNA Modification: m6A and U-Tail. *Cell* 158: 980–987.
54. Ameres, SL and Zamore, PD (2013). Diversifying microRNA sequence and function. *Nat. Rev. Mol. Cell Biol.* 14: 475–88.
55. Ha, M and Kim, VN (2014). Regulation of microRNA biogenesis. *Nat. Rev. Mol. Cell Biol.* 15: 509–524.
56. D'Ambrogio, A, Gu, W, Udagawa, T, Mello, CC and Richter, JD (2012). Specific miRNA stabilization by Gld2-catalyzed monoadenylation. *Cell Rep.* 2: 1537–45.

SUPPLEMENTARY

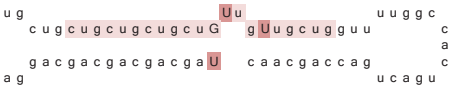
Supplementary Table 1: mfold scaffolds of pre-miRNA sequences used in the study.
(**A**) miCAG variants with the inserted guide strand sequence in pink and the nucleotide substitution in purple. (**B**) miH1-miH21 variants with the inserted guide strand sequence in pink. (**C**) miSNP50C and miSNP50T variants with the inserted guide strand sequence in pink and the SNP-matching nucleotide in green. (**D**) miSNP50C and miSNP50T -18mm variants with the inserted guide strand sequence in pink, the SNP-matching nucleotide in green and the secondary mismatch to the wtHTT in dark green. (**E**) miSNP67T variants with the inserted guide strand sequence in pink and the SNP-matching nucleotide in blue. (**F**) miSNP67T-7mm variants with the inserted guide strand sequence in pink, the SNP-matching nucleotide in blue and the secondary mismatch to the wtHTT in dark green. (**G**) miH12_Scaffolds with the predicted guide strand sequence in pink and the predicted passenger strand sequence in blue (www.mirbase.org). (**E**) miSNP50_Scaffolds with the predicted guide strand sequence in pink, the predicted passenger strand sequence in blue (www.mirbase.org), the SNP-matching nucleotide in green and the secondary mismatch to the wtHTT in dark green

Inserted guide strand sequence
Nucleotide substitutions
pre-miCAG folding was generated from (http://unafold.rna.albany.edu/?q=mfold)

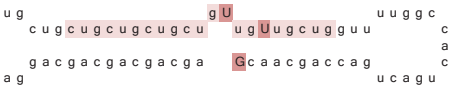
miCAG1



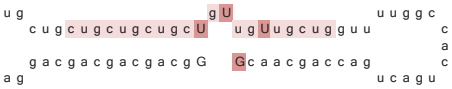
miCAG2



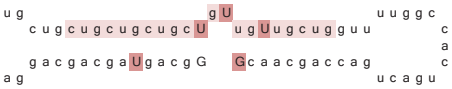
miCAG3



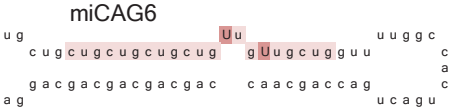
miCAG4



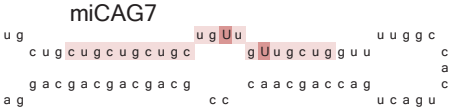
miCAG5



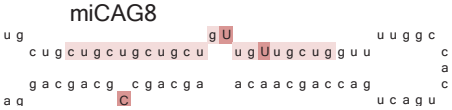
miCAG6



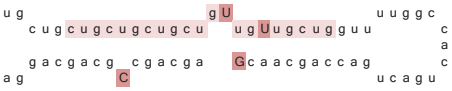
miCAG7



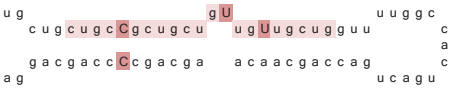
miCAG8



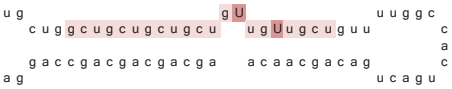
miCAG9



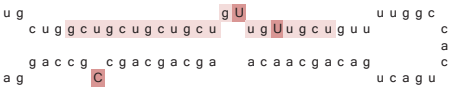
miCAG10



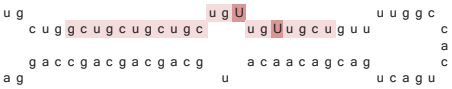
miCAG11



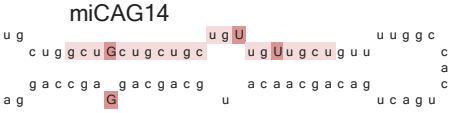
miCAG12



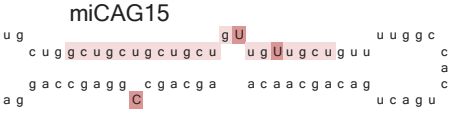
miCAG13



miCAG14

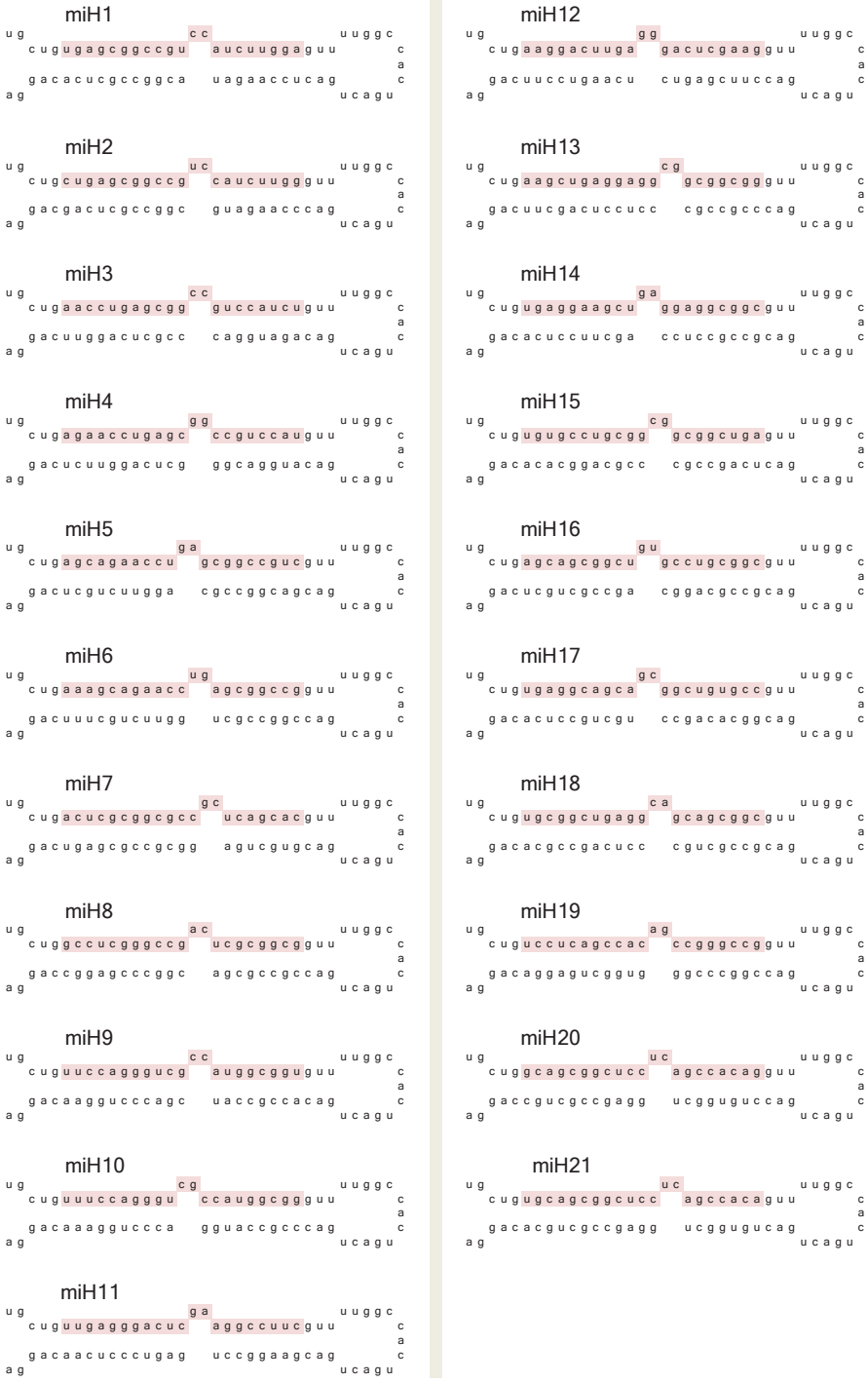


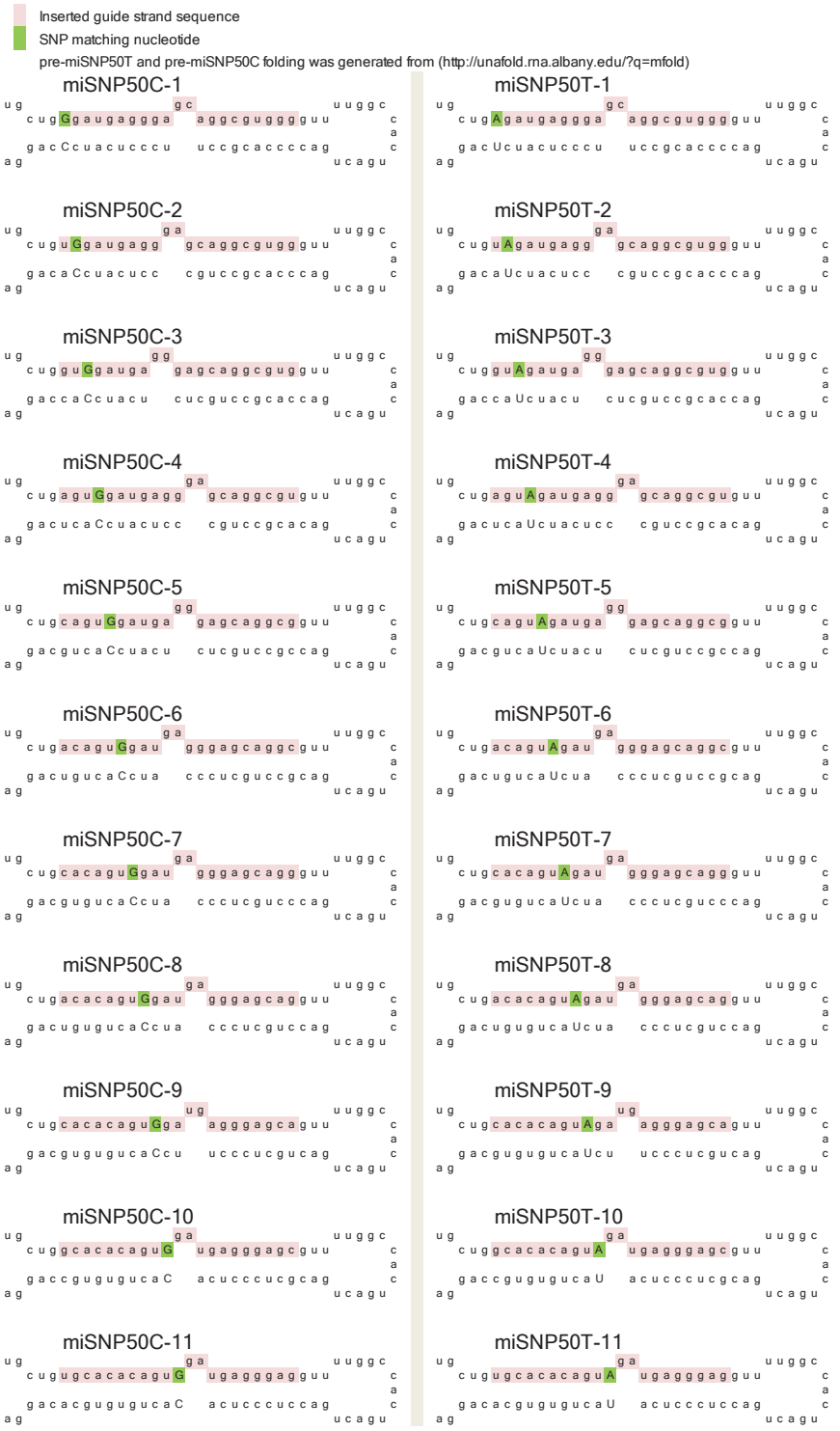
miCAG15



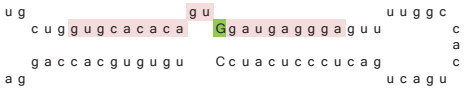
Inserted guide strand sequence

pre-miH folding was generated from (http://unafold.rna.albany.edu/?q=mfold)

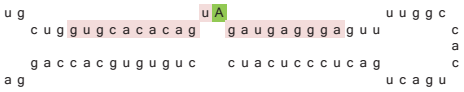



Inserted guide strand sequence
SNP matching nucleotide
pre-miSNP50T and pre-miSNP50C folding was generated from (http://unafold.rna.albany.edu/?q=mfold)
miSNP50C-1
miSNP50T-1
miSNP50C-2
miSNP50T-2
miSNP50C-3
miSNP50T-3
miSNP50C-4
miSNP50T-4
miSNP50C-5
miSNP50T-5
miSNP50C-6
miSNP50T-6
miSNP50C-7
miSNP50T-7
miSNP50C-8
miSNP50T-8
miSNP50C-9
miSNP50T-9
miSNP50C-10
miSNP50T-10
miSNP50C-11
miSNP50T-11

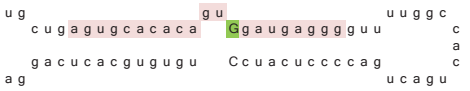
miSNP50C-12



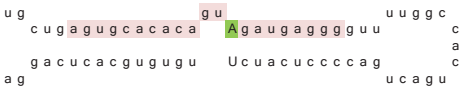
miSNP50T-12



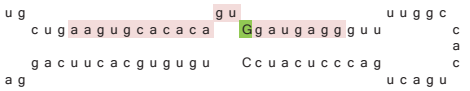
miSNP50C-13



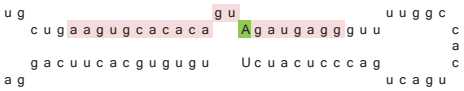
miSNP50T-13



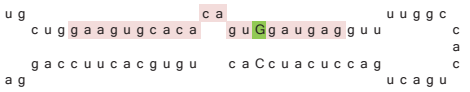
miSNP50C-14



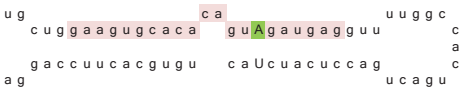
miSNP50T-14



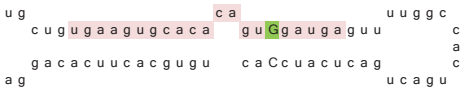
miSNP50C-15



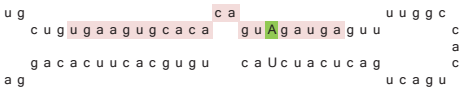
miSNP50T-15



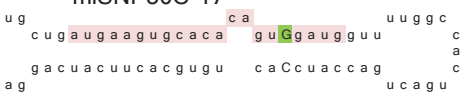
miSNP50C-16



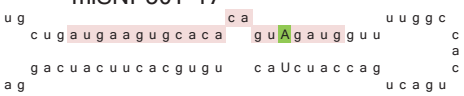
miSNP50T-16



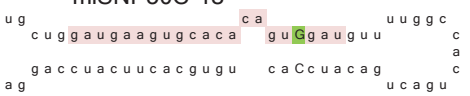
miSNP50C-17



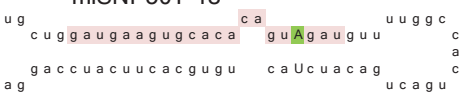
miSNP50T-17



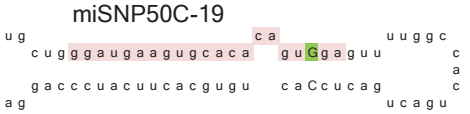
miSNP50C-18



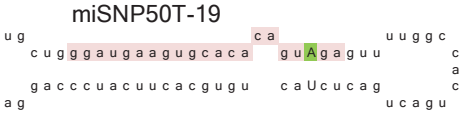
miSNP50T-18



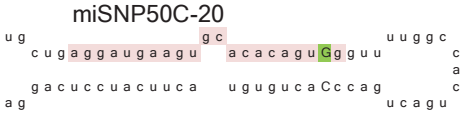
miSNP50C-19



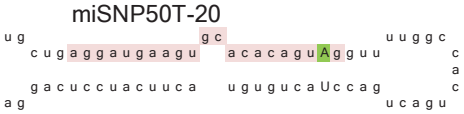
miSNP50T-19



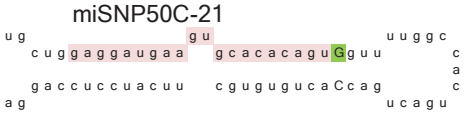
miSNP50C-20



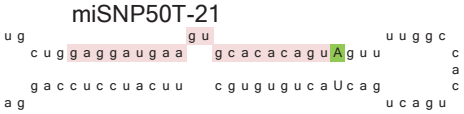
miSNP50T-20



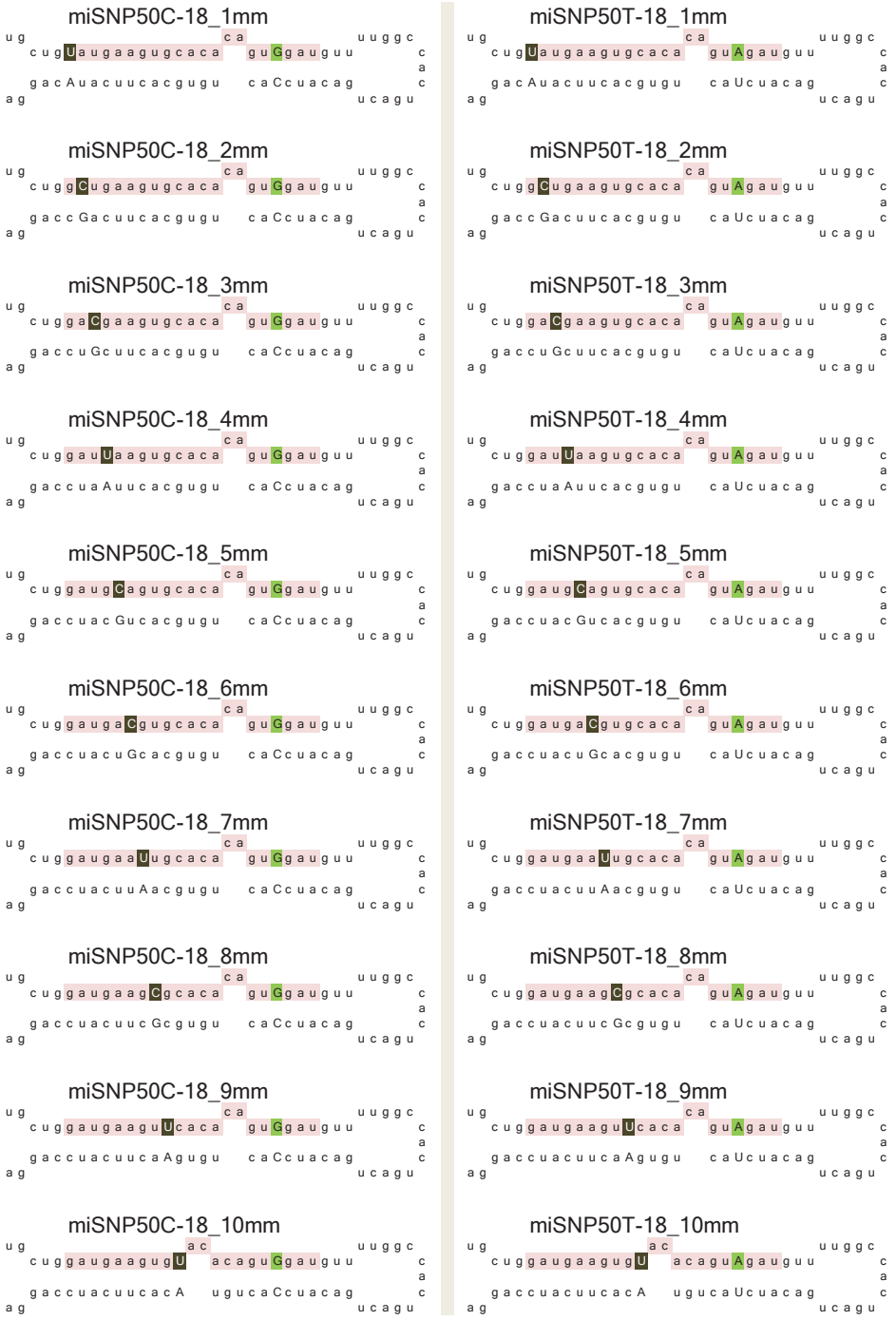
miSNP50C-21



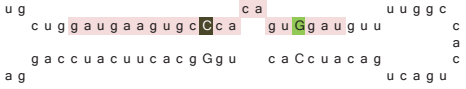
miSNP50T-21



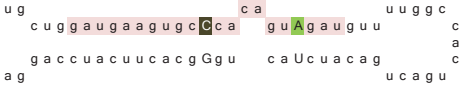
Inserted guide strand sequence
SNP matching nucleotide Secondary mismatch to the wtHTT
pre-miSNP50C-18 and pre-miSNP50T-18 folding was generated from (http://unafold.rna.albany.edu/?q=mfold)



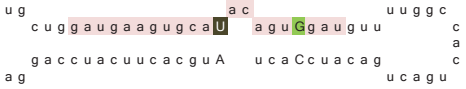
miSNP50C-18_11mm



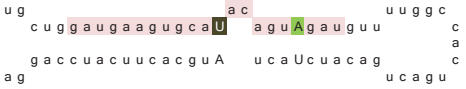
miSNP50T-18_11mm



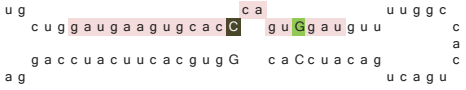
miSNP50C-18_12mm



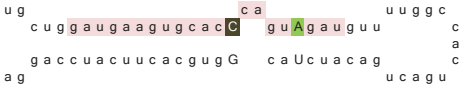
miSNP50T-18_12mm



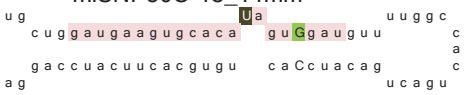
miSNP50C-18_13mm



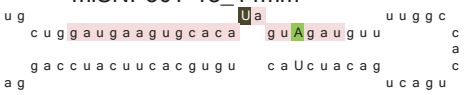
miSNP50T-18_13mm



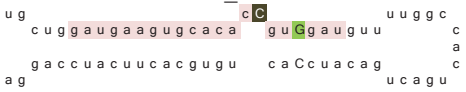
miSNP50C-18_14mm



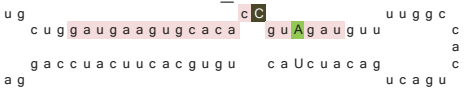
miSNP50T-18_14mm



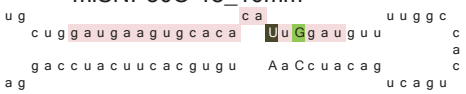
miSNP50C-18_15mm



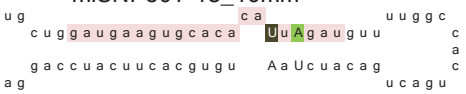
miSNP50T-18_15mm



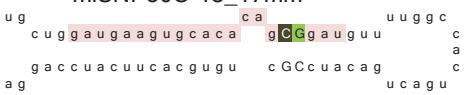
miSNP50C-18_16mm



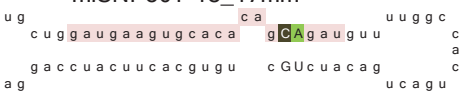
miSNP50T-18_16mm



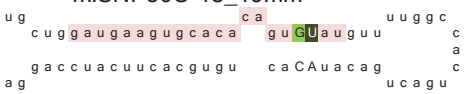
miSNP50C-18_17mm



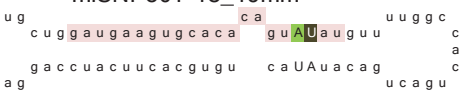
miSNP50T-18_17mm



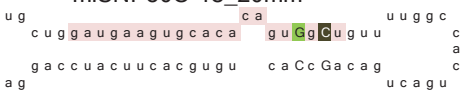
miSNP50C-18_19mm



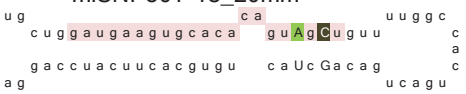
miSNP50T-18_19mm



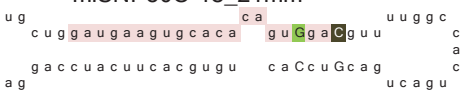
miSNP50C-18_20mm



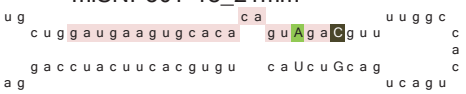
miSNP50T-18_20mm



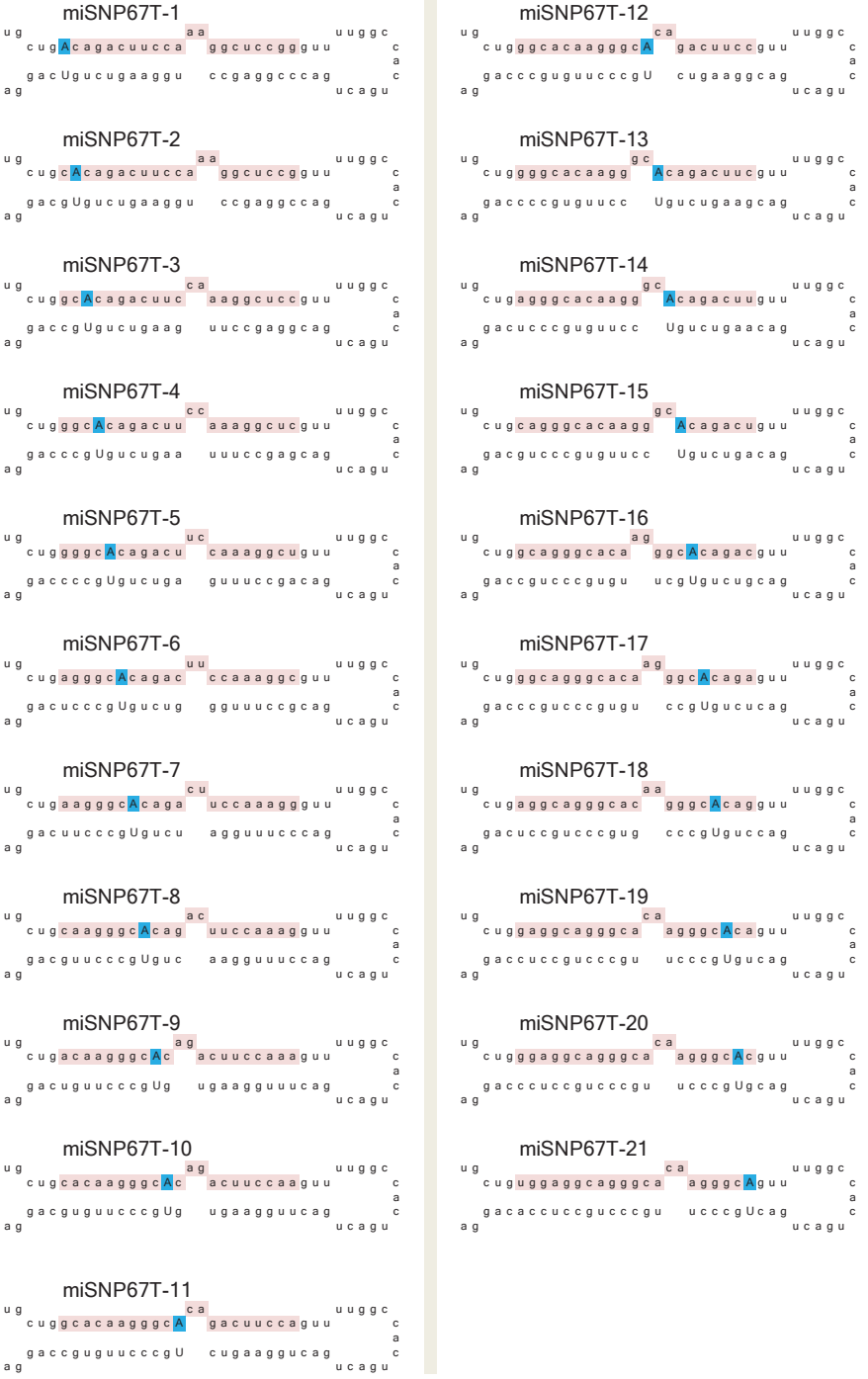
miSNP50C-18_21mm



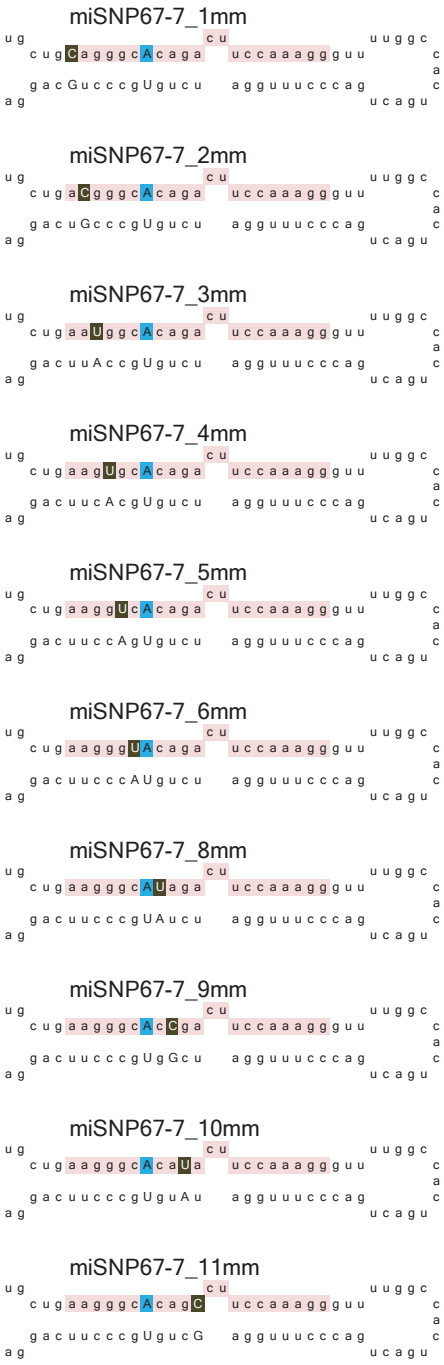
miSNP50T-18_21mm

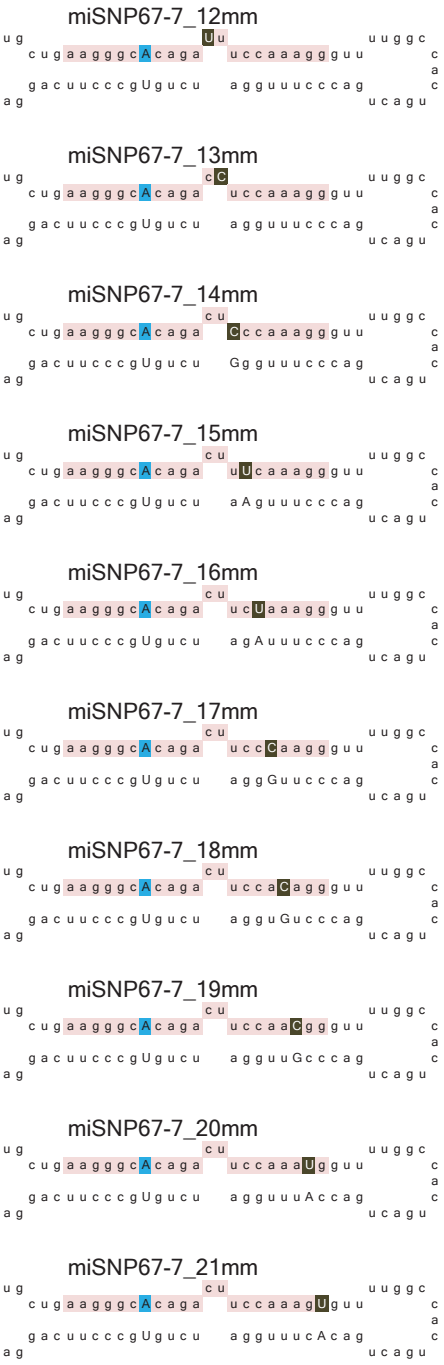


Inserted guide strand sequence
SNP matching nucleotide
pre-miSNP67T folding was generated from (http://unafold.rna.albany.edu/?q=mfold)



Inserted guide strand sequence
SNP matching nucleotide
Secondary mismatch to the wtHTT
pre-miSNP67T-7 folding was generated from (http://unafold.rna.albany.edu/?q=mfold)



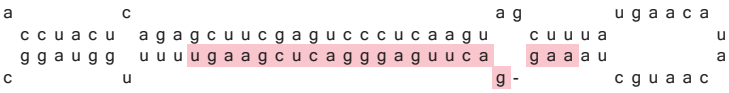


Predicted guide strand sequence from www.mirbase.org

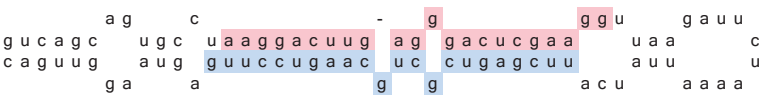
Predicted passender strand sequence from www.mirbase.org

pre-miH12 folding was generated from (http://unafold.rna.albany.edu/?q=mfold)

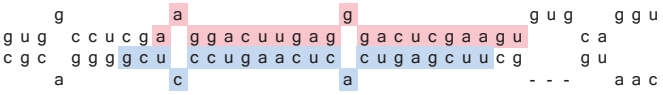
miH12-1



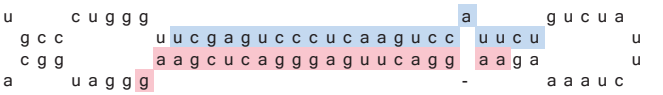
miH12-16



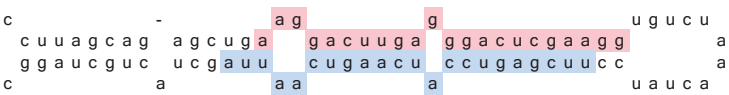
miH12-26



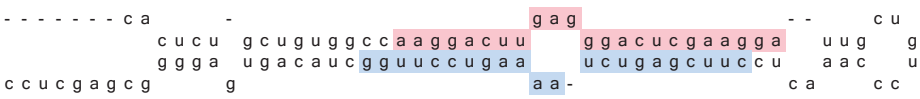
miH12-101



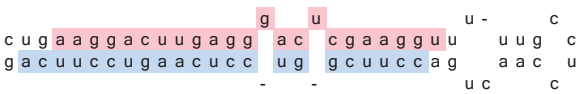
miH12-122



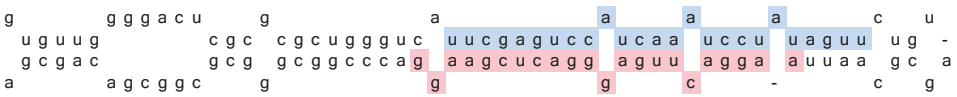
miH12-135



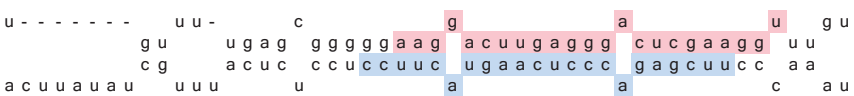
miH12-155



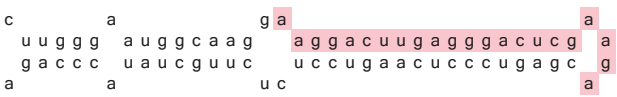
miH12-203



miH12-335

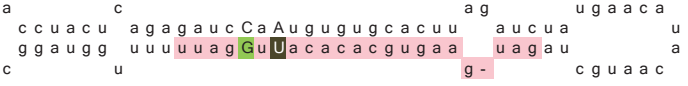


miH12-451

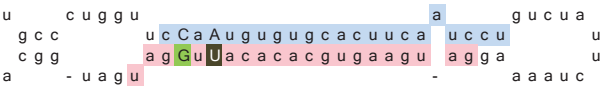


Predicted guide strand sequence from www.mirbase.org
Predicted passender strand sequence from www.mirbase.org
SNP matching nucleotide
Secondary mismatch to the wtHTT
pre-miSNP50C and pre-miSNP50T folding was generated from (http://unafold.rna.albany.edu/?q=mfold

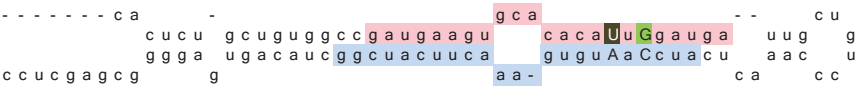
miSNP50C-1



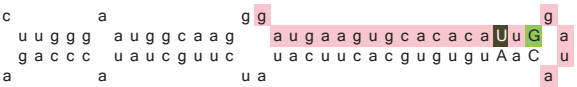
miSNP50C-101



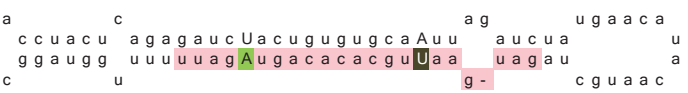
miSNP50C-135



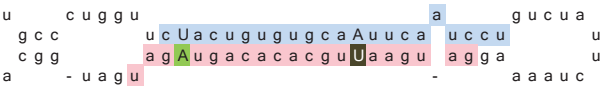
miSNP50C-451



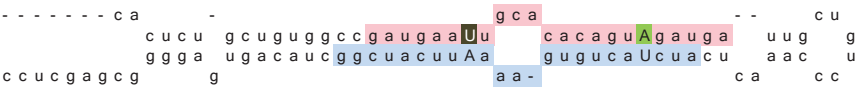
miSNP50T-1



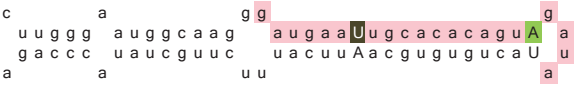
miSNP50T-101



miSNP50T-135



miSNP50T-451



3

AAV5-miHTT gene therapy demonstrates suppression of mutant huntingtin aggregation and neuronal dysfunction in a rat model of Huntington's disease

Jana Miniarikova[1,2], Virginie Zimmer[3,4], Raygene Martier[1,2], Cynthia C. Brouwers[1], Catherine Pythoud[3,4], Kevin Richetin[3,4], Maria Rey[3,4], Jacek Lubelski[1], Melvin M. Evers[1], Sander J. van Deventer[2], Harald Petry[1], Nicole Déglon[3,4], Pavlina Konstantinova[1]

[1]Department of Research & Development, uniQure, Amsterdam, the Netherlands
[2]Department of Gastroenterology and Hepatology, Leiden University Medical Center, Leiden, the Netherlands
[3]Neurosciences Research Center (CRN), LCMN, Lausanne University Hospital, 1011 Lausanne, Switzerland
[4]Department of Clinical Neurosciences, Laboratory of Cellular and Molecular Neurotherapies (LCMN), Lausanne University Hospital, 1011 Lausanne, Switzerland

*Gene Ther. (2017); **24**: 630–639*

ABSTRACT

Huntington's disease (HD) is a fatal progressive neurodegenerative disease caused by a mutation in the huntingtin (*HTT*) gene. To date, there is no treatment to halt or reverse the course of HD. Lowering of either total or only the mutant HTT expression is expected to have therapeutic benefit. This can be achieved by engineered micro (mi)RNAs targeting HTT transcripts and delivered by an adeno-associated viral (AAV) vector. We have previously showed a miHTT construct to induce total HTT knock-down in Hu128/21 HD mice, while miSNP50T and miSNP67T constructs induced allele-selective HTT knock-down *in vitro*. In the current preclinical study, the mechanistic efficacy and gene specificity of these selected constructs delivered by an AAV serotype 5 (AAV5) vector was addressed using an acute HD rat model. Our data demonstrated suppression of mutant HTT mRNA, which almost completely prevented mutant HTT aggregate formation, and ultimately resulted in suppression of DARPP-32-associated neuronal dysfunction. The AAV5-miHTT-451 construct was found to be the most efficient, although AAV5-miSNP50T demonstrated the anticipated mutant HTT allele selectivity and no passenger strand expression. Ultimately, AAV5-delivered-miRNA-mediated HTT lowering did not cause activation of microglia or astrocytes suggesting no immune response to the AAV5 vector or therapeutic precursor sequences. These preclinical results suggest that using gene therapy to knock-down HTT may provide important therapeutic benefit for HD patients and raised no safety concerns, which supports our ongoing efforts for the development of an RNAi-based gene therapy product for HD.

INTRODUCTION

Huntington's disease (HD) is a fatal, currently untreatable, neurodegenerative disorder with a prevalence rate of 1-10 in 100 000 individuals worldwide.[1] The presence of 40 and more CAG triplets in exon 1 of the huntingtin (*HTT*) gene has been identified as a fully penetrant trigger for the neuropathological process, which usually stretches over decades.[2,3] The resultant neuronal death affects primarily GABAergic medium spiny neurons in the early stage of HD, as well as neurons in other brain regions in the later stages.[4,5] The CAG expansion is translated into a polyglutamine (polyQ) tract in the N-terminus of the HTT protein, causing the mutant HTT to misfold and aggregate.[6] Growing evidence suggests that the mutant HTT disturbs multiple critical cellular pathways and that its aggregation is a prerequisite to neurodegeneration. Therefore, clearance of mutant HTT is currently accepted as being key for HD treatment.[7] Notably, Yamamoto et al. showed that conditional blockage of HTT expression after symptom onset results in clearance of HTT aggregates and behavioral improvements, suggesting that HD may be partially reversible.[8]

In contrast to other progressive neurodegenerative disorders, such as Alzheimer's or Parkinson's disease, the monogenic nature of HD allows for the development of disease-modifying therapies that aim to halt or suppress production of the aberrant HTT. The discovery of RNA interference (RNAi) in 1998 revolutionized the progress of therapeutic interventions focusing on gene silencing at the post-transcriptional level.[9] Since then, several groups, including ours, applied RNAi principles to design artificial small interfering (si)RNAs, short-hairpin (sh)RNAs, or micro (mi)RNAs that bind to the HTT transcript and reduce its translation.[10,11] To circumvent several challenges regarding the delivery and stable expression of RNAi products in the central nervous system (CNS), many studies have used viral vectors as delivery vehicles, which can be injected directly into the brain. reviewed in [12] Adeno-associated viral (AAV) vectors are the most common vehicles of choice and a large number of AAV capsid serotypes provide cell- and tissue- specific tropism. reviewed in [13] For the CNS, studies in rodents and non-human primates have shown AAV serotype 5 (AAV5) to be strong and effective in the brain, making it an attractive candidate for RNAi-based gene transfer.[14–17] Importantly, the AAV-delivered-miRNA-based gene therapy approach comprises continual expression of artificial miRNAs following a single administration of an AAV vector, resulting in long-term HTT lowering.

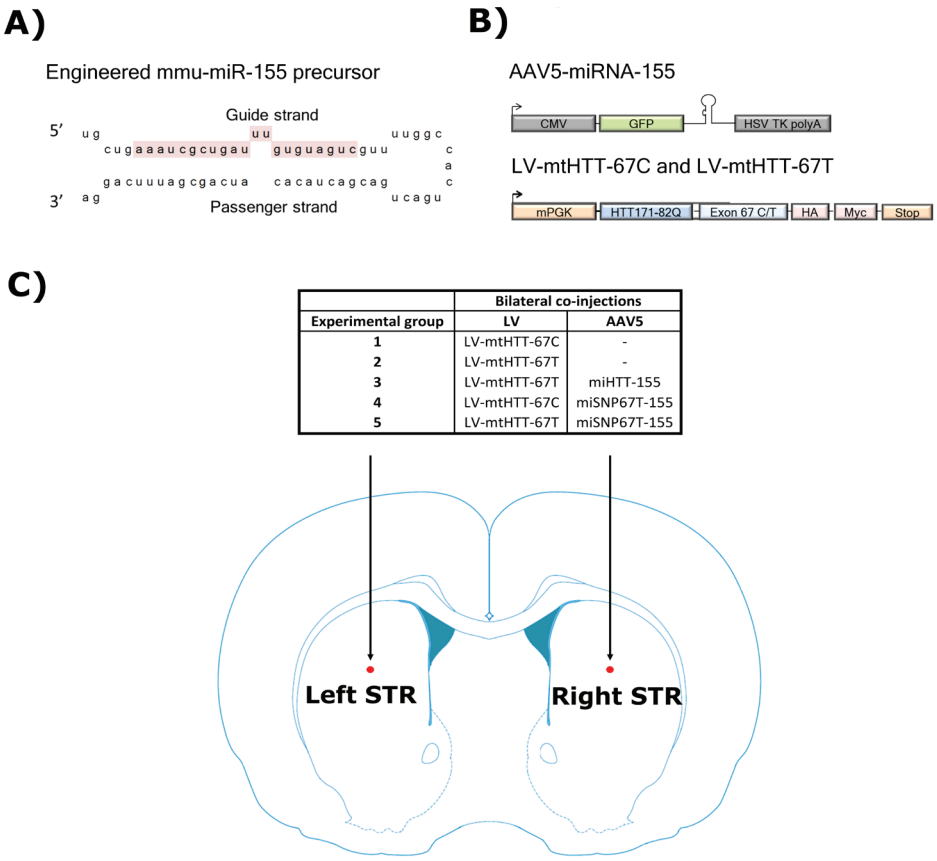
To develop a disease-modifying gene therapy for HD, we have previously designed several therapeutic miRNAs targeting either both "total" or preferentially the mutant HTT transcripts "allele-selective" and their HTT knock-down efficiency was addressed *in vitro* and in the humanized transgenic Hu128/21 HD mouse model.[18] Based on this study, we selected a miHTT construct that showed the strongest efficacy *in vitro* and induces a potent total HTT knock-down in the striatum and cortex of the humanized Hu128/21 HD mice.[18] For the allele-selective HTT knock-down, we selected the miSNP50T and miSNP67T constructs that showed strongest efficacy *in vitro*.

Although several transgenic or knock-in HD animal models have been established and used for preclinical testing, none completely recapitulates the neuropathology that occurs in HD patients.[19–21] Therefore, a combination of several *in vivo* preclinical studies is required to address the necessary treatment outcome and safety measures for HD. In respect to the latter, the present study was designed to evaluate the on-target efficacy of continuously expressed miHTT, miSNP50T and miSNP67T constructs in suppressing the neuropathology associated with HD using an acute lentiviral (LV) HD rat model. To generate the HD rat model, wild-type rats were injected intrastriatally with a LV expressing a chimeric mutant HTT fragment, which is shown to induce local formation of mutant HTT aggregates followed by severe neuronal dysfunction at two months post-infection.[22] Therefore, this model allowed us to address the HD treatment response downstream of the mutant HTT protein in a larger rodent brain. Moreover, the chimeric LV sequence enabled us to study both total and allele-selective approaches in the context of mechanistic efficacy and gene specificity.[23]

RESULTS

miHTT-155 delivered by an AAV5 vector suppressed mutant HTT aggregate formation and DARPP-32-associated neuronal dysfunction in HD rats

To assess distribution, mechanistic efficacy, and allele selectivity of the therapeutic miRNA sequences, we initiated a pilot study in the acute LV HD rat model using the miHTT construct for the total HTT knock-down and the miSNP67T construct for the allele-selective knock-down. Both miHTT and miSNP67T constructs were previously designed in the engineered mmu-miR-155 precursor, named miHTT-155 and miSNP67T-155 (**Figure 1a**). The miHTT and miSNP67T expression cassettes also contained a sequence encoding green fluorescent protein (GFP) to assess transduction efficiency (**Figure 1b**).[18]



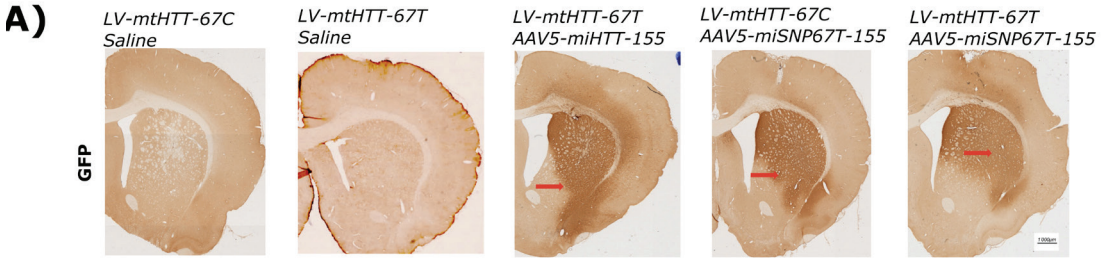
	Bilateral co-injections	
Experimental group	**LV**	**AAV5**
1	LV-mtHTT-67C	-
2	LV-mtHTT-67T	-
3	LV-mtHTT-67T	miHTT-155
4	LV-mtHTT-67C	miSNP67T-155
5	LV-mtHTT-67T	miSNP67T-155

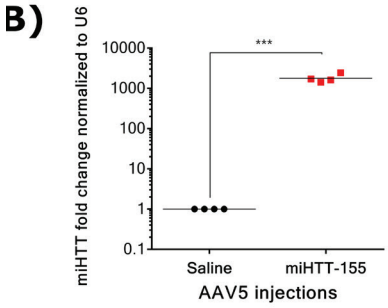
Figure 1. Design of proof-of-concept study using the AAV5-miHTT-155 and AAV5-miSNP67T-155 vectors in an acute HD rat model. **(a)** The structure and sequence of the engineered mmu-pre-miR-155 precursor used in the study with the highlighted guide strand in pink. **(b)** Schematic representation of the AAV5-miHTT-155 and AAV5-miSNP67T-155 expression cassettes; and LV-mtHTT-67C and LV-mtHTT-67T expressing the chimeric mutant HTT sequences. (c) Bilateral co-injections in the striatum (STR) of rats with LV-mtHTT-67C or LV-mtHTT-67T and AAV5-miHTT-155 or AAV5-miSNP67T-155 vectors. The experimental groups and injection sites are outlined.

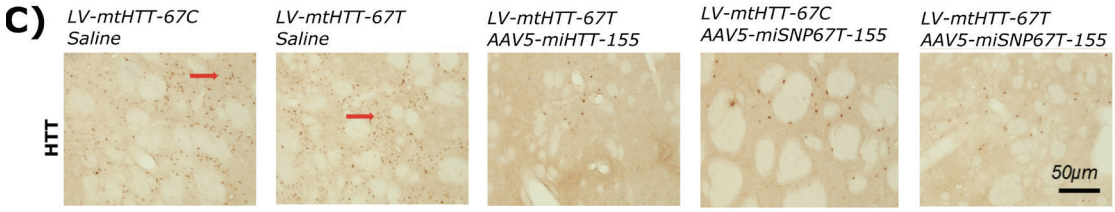
We generated AAV5 viruses carrying the miHTT and miSNP67T expression cassettes and co-injected each virus bilaterally in the striatum of rats with a LV vector encoding a chimeric human mutant HTT sequence (**Figure 1b,c**). The LV vector consisted of an 82-long glutamine (82Q) chain fused with the target regions for the miHTT and miSNP67T constructs, named LV-mtHTT-67T.[23] To address the allele-selective potential of the miSNP67T construct, we included in this study a second LV vector named LV-mtHTT-67C. The AAV5-miSNP67T-155 expression product perfectly matches LV-mtHTT-67T transcripts and has one nucleotide mismatch with LV-mtHTT-67C transcripts at the nucleotide polymorphism (SNP) rs362307. Therefore, this system enables us to test the allele-selectivity based on only a single SNP. The mutant HTT protein that is expressed from both LV vectors is known to cause HD-associated neuronal dysfunction.[22]

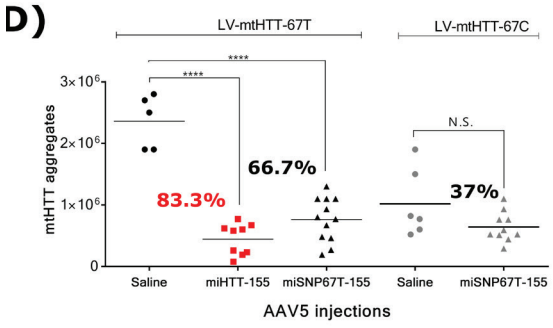
Two months post-injection, rats were sacrificed and the brain tissues were analyzed for AAV5 vector distribution, mature miHTT expression, on-target silencing efficiency measured by mutant HTT aggregate formation, and DARPP-32-associated neuronal dysfunction. To evaluate AAV5 vector distribution in the HD rat brain, we performed immunohistochemistry (IHC) against GFP on the fixed striato-cortical sections (**Figure 2a**). For all AAV5 constructs, we observed broad striatal with partial cortical GFP distribution. Consistent with the latter, we observed approximately 1800 times more miHTT molecules in the AAV5-miHTT-155-injected rats compared with the saline control (**Figure 2b**).

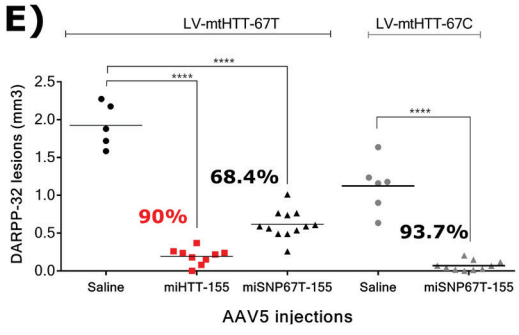
The accumulation of mutant HTT aggregates in the brain is a hallmark of the HD neuropathological process.[7] To validate on-target silencing efficiency of the AAV5-miHTT-155 and AAV5-miSNP67T-155 expression products, we performed IHC using an anti-HTT antibody that binds to the mutant HTT (**Figure 2c**). We observed significantly fewer mutant HTT aggregates in the HD rat striata injected with AAV5-miHTT-155 ($0.4x10^6 \pm 0.2x10^6$, $p \leq 0.0001$) or AAV5-miSNP67T-155 viruses ($0.8x10^6 \pm 0.3x10^6$, $p \leq 0.0001$) compared with the saline control ($2.4x10^6 \pm 0.4x10^6$) (**Figure 2d**). The AAV5-miSNP67T-155 showed no allele-selectivity as similarly low counts of mutant HTT aggregates were observed in both LV-mtHTT-67C- ($0.6x10^6 \pm 0.2x10^6$) and LV-mtHTT-67T-injected rats compared with the corresponding saline controls.


A)
LV-mtHTT-67C Saline
LV-mtHTT-67T Saline
LV-mtHTT-67T AAV5-miHTT-155
LV-mtHTT-67C AAV5-miSNP67T-155
LV-mtHTT-67T AAV5-miSNP67T-155
GFP


B)
miHTT fold change normalized to U6
10000
1000
100
10
1
0.1
***
Saline
miHTT-155
AAV5 injections


C)
LV-mtHTT-67C Saline
LV-mtHTT-67T Saline
LV-mtHTT-67T AAV5-miHTT-155
LV-mtHTT-67C AAV5-miSNP67T-155
LV-mtHTT-67T AAV5-miSNP67T-155
HTT
50μm


D)
LV-mtHTT-67T
LV-mtHTT-67C
mtHTT aggregates
3×10^6
2×10^6
1×10^6
0
****
****
N.S.
83.3%
66.7%
37%
Saline
miHTT-155
miSNP67T-155
Saline
miSNP67T-155
AAV5 injections


E)
LV-mtHTT-67T
LV-mtHTT-67C
DARPP-32 lesions (mm3)
2.5
2.0
1.5
1.0
0.5
0.0
****
****
****
90%
68.4%
93.7%
Saline
miHTT-155
miSNP67T-155
Saline
miSNP67T-155
AAV5 injections

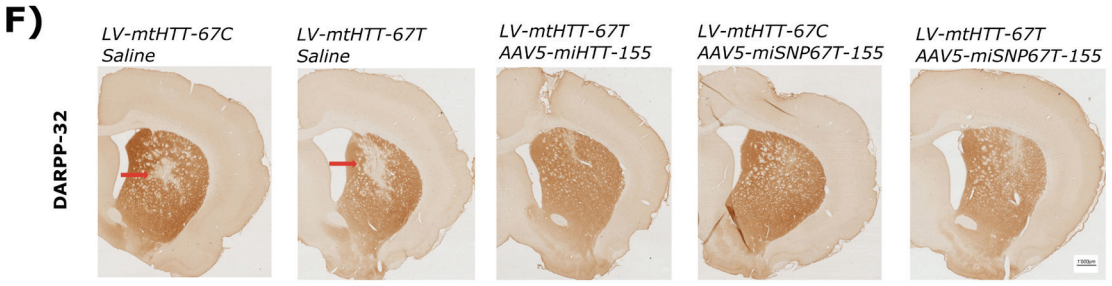

F)
LV-mtHTT-67C Saline
LV-mtHTT-67T Saline
LV-mtHTT-67T AAV5-miHTT-155
LV-mtHTT-67C AAV5-miSNP67T-155
LV-mtHTT-67T AAV5-miSNP67T-155
DARPP-32

Figure 2. Phenotypic improvement of HD neuropathology following AAV5-miHTT-155 and AAV5-miSNP67T-155 injections in HD rats. **(a)** IHC with an anti-GFP antibody showing AAV5 distribution. A representative picture of the right hemisphere is shown and GFP-positive areas are depicted by . **(b)** miHTT-specific TaqMan assay to determine miHTT fold change in the striatum of AAV5-miHTT-155 injected rats compared with the saline-treated rats (n=4). miHTT values are presented as the distribution plot with the mean of the values following normalization to U6 levels. **(c)** IHC with an anti-HTT antibody showing the mutant HTT aggregates. A representative picture of the right hemisphere is shown and mutant HTT aggregates are represented by . **(d)** Quantification of anti-HTT staining shows a reduction of mutant HTT aggregates induced by AAV5-miHTT-155 and AAV5-miSNP67T-155 vectors in the striatum (n=5-12). The reduction (%) of mutant HTT aggregates is relative to the saline control. **(e)** Quantification of DARPP-32 staining shows a reduction in neuronal dysfunction induced by AAV5-miHTT-155 and AAV5-miSNP67T-155 vectors in the striatum (n=5-12). The reduction (%) in neuronal dysfunction is relative to the saline control. **(f)** IHC against DARPP-32 showing neuronal dysfunction. A representative picture of the right hemisphere is shown and DARPP-32-negative areas are depicted by . All data were analyzed using one-way ANOVA. N.S., non-significant, $p > 0.05$; *, $p < 0.05$; **, $p < 0.01$; ***, $p < 0.001$; ****, $p \leq 0.0001$. The values were calculated as a mean ± standard deviation.

To address the effect of AAV5-miHTT-155 and AAV5-miSNP67T-155 treatments on HD-linked neuronal dysfunction, we stained for DARPP-32, a phosphoprotein widely expressed in medium spiny neurons.[24] Consistent with the low accumulation of mutant HTT aggregates, we observed a significant reduction of DARPP-32 lesion size two months after AAV5-miHTT-155 ($0.19mm^3 \pm 0.11$, $p \leq 0.0001$) or AAV5-miSNP67T-155 ($0.62mm^3 \pm 0.19$, $p \leq 0.0001$) treatments compared with the saline control ($1.92mm^3 \pm 0.29$) (**Figure 2 e,f).** AAV5-miHTT-155 was again shown to be the most effective. Moreover, consistent with the mutant HTT aggregate counts, AAV5-miSNP67T-155 showed no allele-selectivity as demonstrated by the similar DARPP-32 lesion size in both LV-mtHTT-67C- ($0.07mm^3 \pm 0.07$) and LV-mtHTT-67T-injected rats relative to the saline controls. These experiments enabled us to identify the miHTT guide sequence effectively targeting HTT, which resulted in a strong suppression of mutant HTT aggregate formation and neuronal dysfunction at two months post-injection.

Optimized miHTT-451 and miSNP50T-451 expressed from AAV5 vectors induced the mutant HTT mRNA knock-down in HD rats

Although the engineered mmu-miHTT-155 constructs generates the favorable miHTT effector sequence and is suitable for pilot experiments addressing efficacy and distribution, it is not optimal for clinical studies in humans due to a high risk of immune response to GFP and possibility of off-target silencing caused by the passenger strand.[18] Previously, we showed that the silencing efficacy and processing of the miHTT construct are influenced by the pre-miHTT precursor.[18] We identified the miHTT-451 precursor that showed no passenger strand *in vivo* opposite to the miHTT-101 and miHTT-135 precursors (**Figure 3a**). Moreover, the miHTT-451 construct showed efficacious HTT knock-down and no signs of toxicity. Therefore, in this study we included the miHTT-451 precursor for the total HTT knock-down. For the allele-selective approach, we optimized the miSNP50T construct designed to preferentially bind to HTT mRNA carrying the U isoform of SNP rs362331 in exon 50, which is associated at high frequencies with HD.[25] This miSNP50T construct, which exhibits stronger efficacy than miSNP67T *in vitro*, was not available when the pilot study was initiated and therefore,

it was introduced at this stage. Moreover, for both constructs the cytomegalovirus (CMV) promoter together with GFP was replaced by the strong CMV immediate-early enhancer fused to chicken β-actin (CAG) promoter, which has been shown to be effective in the brain.[26] The resultant constructs are named miHTT-451 and miSNP50T-451 (**Figure 3b**).

To further establish mechanistic efficiency, safety, as well as allele-selectivity *in vivo*, we generated AAV5-miHTT-451 and AAV5-miSNP50T-451 vectors and co-injected them bilaterally in the striatum of rats with a LV vector encoding a chimeric mutant HTT sequence with an 82Q chain and carrying target regions for the miHTT and miSNP50T constructs, named LV-mtHTT-50T (**Figure 3b,c**). In order to address the allele-selective potential of the miSNP50T construct, we included a second LV vector, named LV-mtHTT-50C. The AAV5-miSNP50T-451 expression product was designed to have one nucleotide mismatch with the LV-mtHTT-50T transcripts and two nucleotide mismatches with the LV-mtHTT-50C transcripts. Therefore, this system enabled us to test the allele-selectivity based on only a single SNP. As negative controls, we included a GFP expressed from the CAG promoter and saline control. Two months post-injection, rats were sacrificed and the brains were processed to assess on-target efficacy, HD-associated neuronal dysfunction, and immune reaction.

To measure AAV5 vector DNA in striata, we performed real-time qPCR with primers directed towards the CAG promoter (**Figure 3d**). We observed high and comparable vector DNA in the striatal homogenates from AAV5-GFP-, AAV5-miHTT-451-, and AAV5-miSNP50T-451-injected rats. Similar to TaqMan assays (data not shown), we detected a background level of~3000 genome copies in the saline control, which was considered for calculations of final vector DNA. Furthermore, the latter inversely correlated with the human-specific HTT mRNA knock-down from the same tissue homogenate demonstrated by TaqMan RT-qPCR (**Figure 3e**). We detected 62.3% ± 21.6% HTT mRNA knock-down in AAV5-miHTT-451- and 81% ± 4.3% HTT mRNA knock-down in AAV5-miSNP50T-451-injected rats as compared with the saline control. We observed similar HTT mRNA knock-down by AAV5-miSNP50T-451 in LV-mtHTT-50T-injected rats compared with LV-mtHTT-50C-injected rats where 65.5% ± 9.2% HTT mRNA reduction was detected.

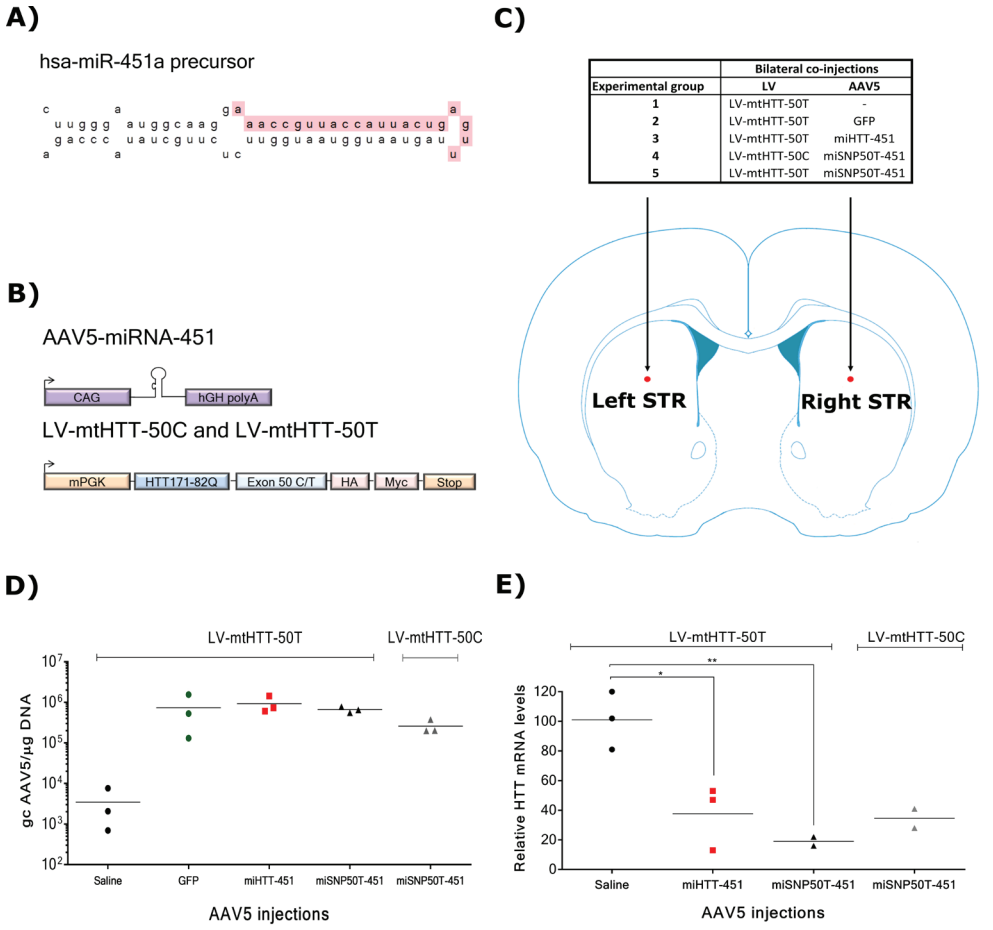


Figure 3. HTT mRNA knock-down induced by AAV5-miHTT-451 and AAV5-miSNP50T-451 vectors in the striatum of HD rats. **(a)** The structure and sequence of the hsa-pre-miR-451a precursor used in this study with the miRBase-predicted guide strand highlighted in pink (www.mirbase.org). **(b)** Schematic representation of the AAV5-miHTT-451 and AAV5-miSNP50T-451 expression cassettes; and LV-mtHTT-50C and LV-mtHTT-50T encoding a chimeric mutant HTT sequence with either C or T isoform of SNP rs362331. **(c)** Bilateral co-injections in the striatum (STR) of rats with LV-mtHTT-50C or LV-mtHTT-50T and AAV5-miHTT-451 or AAV5-miSNP50T-451 vectors. The experimental groups and injection sites are outlined. **(d)** qPCR to determine AAV5 genome copies (gc) in the striatum of AAV5-miHTT-451 and AAV5-miSNP50T-451 injected rats (n=3), two months post-injection. Primers directed to the CAG promoter were used and the gc values were calculated based on the standard curve and considering the background signal from the negative control. **(e)** TaqMan qPCR assay shows HTT mRNA knock-down in the striatum (n=2-3) induced by the AAV5-miHTT-451 and AAV5-miSNP50T-451 expression products. Human HTT-specific exon-spanning primers were used and HTT values were subsequently normalized to GAPDH, an internal control set at 100%. All data were analyzed using one-way ANOVA. *, $p < 0.05$; **, $p < 0.01$; ***, $p < 0.001$; ****, $p \leq 0.0001$. The values were calculated as a mean ± standard deviation.

On-target silencing efficiency of AAV5-miHTT-451 and AAV5-miSNP50T-451 correlates with suppression of DARPP-32-associated neuronal dysfunction in HD rats

To establish the ability of our optimized AAV5-miHTT-451 and AAV5-miSNP50T-451 vectors to suppress formation of mutant HTT aggregates, we analyzed striato-cortical sections by IHC using an anti-HTT antibody (**Figure 4a**). Here, in the AAV5-miHTT-451-injected rats almost no detectable mutant HTT aggregates were observed (843 ± 359, $p \leq 0.0001$), whereas the aggregates were abundant in the GFP ($3.6x10^4 \pm 2.9x10^4$) and saline ($4.4x10^4 \pm 2x10^4$) controls (**Figure 4b**). Based on the number of mutant HTT aggregates, AAV5-miSNP50T-451 showed stronger silencing of the matched LV-mtHTT-50T expression product ($1x10^4 \pm 0.8x10^4$, $p \leq 0.001$) compared with the mismatched LV-mtHTT-50C ($4.5x10^4 \pm 2.6x10^4$), suggesting allele-selective potential.

During development of symptomatic HD, the appearance of mutant HTT aggregates precedes the death of medium spiny neurons located in the striatum.[22] Therefore, we addressed the potential of our AAV5-miHTT-451 and AAV5-miSNP50T-451 vectors to suppress DARPP-32-associated neuronal dysfunction by performing IHC against DARPP-32 (**Figure 4c,d**). Consistent with lowering of mutant HTT aggregates, AAV5-miHTT-451 ($0.02mm^3 \pm 0.03$, $p \leq 0.0001$) and AAV5-miSNP50T-451 ($0.12mm^3 \pm 0.04$, $p \leq 0.0001$) treatments significantly suppressed the partial striatal lesion induced by the LV-mtHTT-SNP50T expression product compared with the GFP ($0.92mm^3 \pm 0.39$) and saline controls ($1.09mm^3 \pm 0.31$). In contrast, AAV5-miSNP50T-451 treatment did not show strong reduction in the size of DARPP-32 lesions in LV-mtHTT-SNP50C-injected rats ($0.96mm^3 \pm 0.29$), demonstrating allele-selectivity.

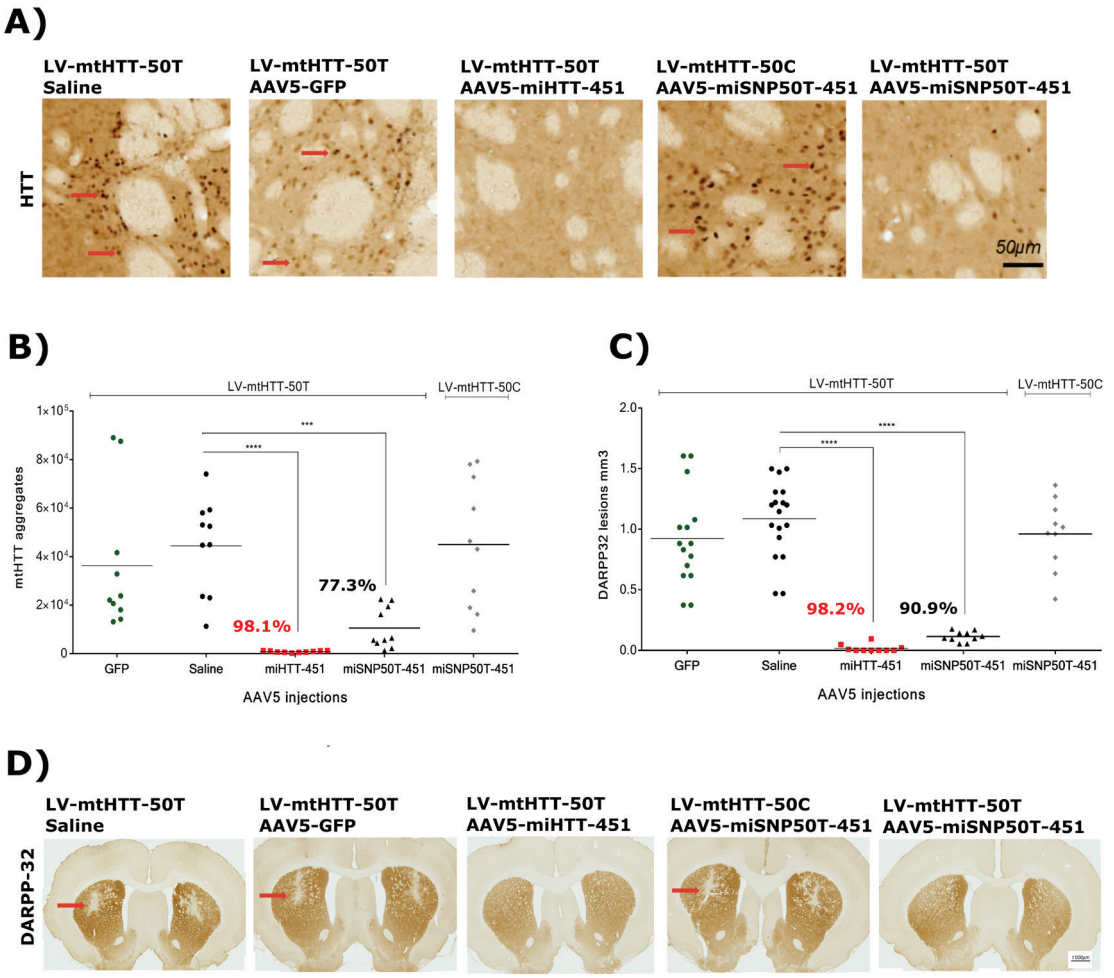


Figure 4. Phenotypic improvement of HD neuropathology following AAV5-miHTT-451 and AAV5-miSNP50T-451 injections in HD rats. (a) IHC using an anti-HTT antibody showing the mutant HTT aggregates. A representative picture of both hemispheres is shown and the mutant HTT aggregates are depicted by → . **(b)** Quantification of anti-HTT staining shows a reduction of mutant HTT aggregates induced by the AAV5-miHTT-451 and AAV5-miSNP50T-451 treatment in the striatum (n=10). The reduction (%) of mutant HTT aggregates is relative to the saline control. **(c)** Quantification of DARPP-32 staining shows reduced neuronal dysfunction following AAV5-miHTT-451 and AAV5-miSNP50T-451 injections in the striatum (n=10-18). The reduction (%) in neuronal dysfunction is relative to the saline control. **(d)** IHC against DARPP-32 showing neuronal dysfunction. A representative picture of both hemispheres is shown and DARPP-32-negative areas are depicted by → . All data were analyzed using one-way ANOVA. *, $p < 0.05$; **, $p < 0.01$; ***, $p < 0.001$; ****, $p \leq 0.0001$. The values were calculated as a mean ± standard deviation.

AAV5 viruses delivering the miHTT-451 or miSNP50T-451 precursors did not induce an overt immune response via GFAP and Iba1 activation

Although AAV-based gene therapy is an attractive approach for the delivery of gene products, such as therapeutic miRNAs, and overall has demonstrated low toxicity to date, activation of the immune response should be addressed for each therapeutic candidate in a given target tissue. To evaluate the immune response to our AAV5 vectors expressing therapeutic miRNA precursors in the brain, we analyzed the activation of microglia and infiltration of astrocytes in the injected areas by IHC using an anti-ionized calcium-binding adapter molecule 1 (Iba1) and anti-glial fibrillary acidic protein (GFAP) antibody, respectively (**Figure 5a,b**). We found similar levels of immunoreactivity in AAV5-miHTT-451- and AAV5-miSNP50T-451-treated rats compared to the saline control, indicating no apparent activation of immune reaction via microglia and astrocytes.

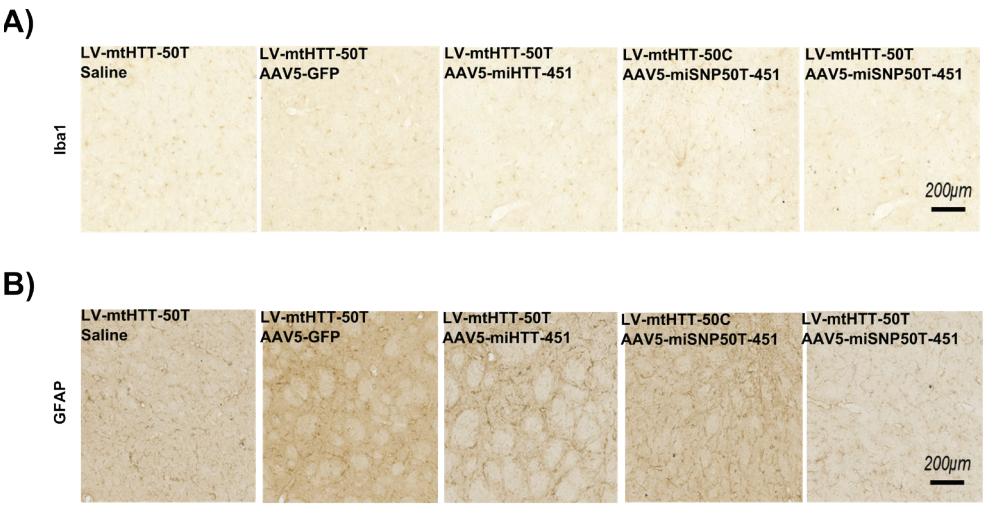


Figure 5. No apparent activation of microglia and astrocytes following AAV5-miHTT-451 and AAV5-miSNP50T-451 injections in HD rats. **(a)** IHC against Iba1 to show microglial activity. A representative picture of the right hemisphere is shown. **(b)** IHC against GFAP to show the astrocyte activity. A representative picture of the right hemisphere is shown.

AAV5-miHTT-451 and miSNP50T-451 constructs do not generate a passenger strand *in vivo*

Previously, we showed that the miHTT-451 construct does not generate a passenger strand and is not toxic probably due to higher specificity *in vivo* (**Figure 6a**).[18] The absence of the passenger strand from the miR-451 scaffold provides a better safety profile for therapeutic shRNAs or miRNAs since it reduces the chance for off-target suppression of other genes by the passenger strand.[18,27,28] To establish the absence of a passenger strand for the miSNP50T-451 construct *in vivo*, we analyzed the processing patterns in the striatum of AAV5-miSNP50T-451-injected rats by next-generation sequencing. We observed consistent processing patterns between the analyzed samples (**Figure 6b**). The most abundant reads were 23 nucleotides long and belonged to the miSNP50T guide strand (**Figure 6c**). We did not observe any reads belonging to the passenger strand, confirming the absence of a passenger strand associated with the miR-451 precursor.

Based on this study, we identify the AAV5-miHTT-451 construct as the most efficient candidate for the gene therapy approach targeting HTT by showing a robust suppression of crucial HD pathological features in the rat model of HD.

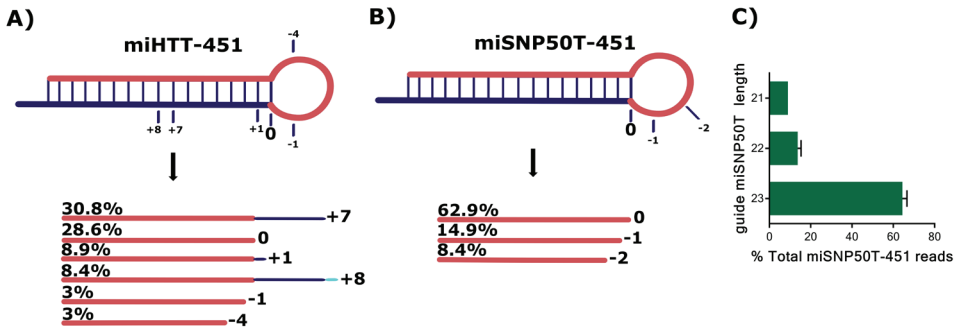


Figure 6. Next-generation sequencing analysis of the pre-miHTT-451 and pre-miSNP50T-451 processing patterns shows no passenger strand *in vivo*. (a) Sequence distribution (%) of reads mapping to pre-miHTT-451 *in vivo*.[18] The predicted guide strand is indicated in red and a mismatch with the reference sequence in light blue. **(b)** Sequence distribution (%) of reads mapping to pre-miSNP50T *in vivo*. The predicted guide strand is indicated in red and a mismatch with the reference sequence in light blue. **(c)** The length distribution of reads mapping to the pre-miSNP50T precursor (n=2). For the read alignments, up to 3 mismatches with the reference sequence were allowed. Reads represented with less than 3% were excluded from the figure.

DISCUSSION

In the current study, we have demonstrated the feasibility of total and allele-selective HTT silencing induced by therapeutic miRNAs delivered to the brain. Intracerebral administration of AAV5 vectors delivering the miHTT candidates for total HTT knock-down or the miSNP50T and miSNP67T candidates for an allele-selective approach resulted in suppression of mutant HTT aggregates and prevention of DARPP-32-associated neuronal dysfunction in rat striata. The AAV5-miHTT-451 construct recapitulated the *in vitro* observations by demonstrating the strongest efficacy *in vivo*.

The LV HD rat model very closely and rapidly reproduces the critical pathogenic features of HD: the mutant HTT aggregation and striatal neuronal dysfunction. Although this model does not permit study of improvement in HD-like behavioral symptoms, it provides a means to preselect therapeutic candidates to continue with high-cost preclinical studies in large animals that carry on for several months to years. Previous studies with shRNAs showed equivalent silencing efficacy of the chimeric HTT constructs in rats and HEK293T cells compared with silencing of the endogenous full-length human HTT in HD-derived neuronal cultures, suggesting that accessibility of silencing agents to the chimeric HTT constructs resembles the natural situation.[23] Moreover, the rapid severity of DARPP-32-associated neuronal dysfunction challenges the read-out efficacy; but on the other hand, it strengthens confidence in case efficacy is demonstrated.

Most HD patients are heterozygous at the HTT locus and therefore many studies attempt to target only the mutant HTT. However, the nature of the HD mutation makes allele-selective HTT silencing challenging. To distinguish between the mutant and heathy HTT alleles, most of the therapeutic interventions so far have focused on targeting the heterozygous HD-associated SNPs or CAG expansions.[23,25,29–33] However, not all HD patients have the identified common SNP isoforms linked to HD. Therefore, more than one product would be needed to fully address the HD patient population. For instance, one study showed that five therapeutic products targeting the isoforms of three different SNPs are required to treat three-quarters of the United States and European HD patient populations.[31] Moreover, as a personalized medicine, additional genotyping will be required to identify suitable HD candidates for a given clinical trial. Furthermore, the allele-selectivity based on targeting the CAG expansions depends on a difference between the consecutive CAGs located on the mutant and healthy HTT alleles. Nevertheless, it has not shown to be more efficacious than the SNP approach, when simultaneously tested.[18,32] Ultimately, the presence of CAG repeats in more than 66 genes increases the chance for off-targeting, making it a less attractive target for clinical testing.[34] Consequently, the allele-selective approach still faces obstacles to advance into clinical development.

In this study, we identified AAV5-miSNP50T-451 that showed allele-selective silencing of the HTT allele carrying the T isoform of SNP rs362331. The ongoing experiments with the

Hu128/21 mice that express full-length human HTT with the U isoform of SNP rs362331 will provide more insights into efficacy and allele-selectivity of AAV5-miSNP50T-451. The AAV5-miSNP67T-155 construct showed no allele-selectivity *in vivo*. mfold prediction analysis indicated that the secondary RNA structures of miHTT, miSNP67T and miSNP50T target sites do not form stable duplexes (data not shown), supporting their similar accessibility to the therapeutics. Previously, it has been reported that allele-selective potential of artificial miRNAs observed *in vitro* may not be retained *in vivo*.[35] In general, miRNA-mRNA interactions are determined by the sequence composition that influences the thermodynamics, such as the melting temperature, of the duplex RNA.[36] miSNP67T binds to 52%-rich GC region, which could enhance the miRNA:mRNA pairing stability and ultimately contribute to no allele-selectivity based on a single SNP observed *in vivo*.

Most HTT lowering strategies intend to suppress both HTT alleles and the first ongoing clinical trial with antisense oligonucleotides employs this approach (https://clinicaltrials.gov/). Preclinical studies using HD animal models and non-human primates indicate that there is a therapeutic window where total HTT knock-down is safe and yet beneficial for HD patients.[37–39] Importantly, this strategy would provide a treatment for all HD patients independent from their genotype. In this study, we showed that miHTT construct processed from miR-451 scaffold is able to strongly suppress mutant HTT aggregation and ultimately dramatically reduce the generation of striatal lesions at two months post-injection. Moreover, we did not observe immune reaction to the AAV5-miHTT-451 vector via astrocytes or microglia activation, suggesting a favorable safety profile.

Altogether, these data provide strong evidence for the therapeutic efficacy of AAV5-miHTT-451 vector by inducing functional improvements downstream in the HD pathological process without raising safety concerns in a rodent model of HD. These promising results support our ongoing efforts for the development of an HD-modifying treatment by silencing the human HTT gene.

MATERIALS AND METHODS

HTT target sequences

Homo sapiens HTT mRNA, complete CDS (gb|L12392.1|HUMHDA) obtained from http://blast.ncbi.nlm.nih.gov/Blast.cgi, was used to identify target sequences for the artificial miHTT located in exon 1, the miSNP50T construct binding to the U isoform of SNP rs362331, and the miSNP67T construct targeting the U isoform of SNP rs362307.

DNA constructs

To generate the miHTT-155 and miSNP67T-155 constructs, their guide sequences targeting HTT transcripts were embedded into the engineered murine pre-miR-155 backbone of pcDNA6.2-GW/EmGFP-miR (Invitrogen, Carlsbad, CA) by annealing complementary oligonucleotides (Qiagen, Valencia, CA) followed by ligation into the linearized pcDNA6.2 plasmid.[18]

To generate miHTT-451 and miSNP50T-451 constructs, the guide and passenger strand sequences were incorporated in the hsa-pri-miR-451a scaffold. 200 nucleotides long 5' and 3' encompassing flanking regions were included with EcoRV and BamHI restriction sites and the complete sequences were ordered from GeneArt® gene synthesis (Invitrogen). In these constructs, the CMV promoter was replaced by the CAG promoter (Inovio, Plymouth Meeting, PA),[18]

AAV5 vector production

AAV5 vectors expressing miHTT, miSNP50T, miSNP67T, and GFP were produced by baculovirus-based AAV production system (uniQure, Amsterdam, The Netherlands). The artificial miRNA cassettes were cloned in a transfer plasmid in order to generate an entry plasmid. The expression cassettes were inserted in a recombinant baculovirus vector by homologous recombination and clones were selected by plague purification. The recombinant baculovirus containing the cassettes were further amplified till the passage 6 and clones screened for the best production and stability by PCR and qPCR. To generate AAV5, infections with different recombinant baculoviruses containing the vector genome, the replicon enzyme and the capsid protein were performed. The cells were lysed 72hr after infection and the crude lysate was treated with Benzonase (50U/ ml) (Merck, Darmstadt, Germany) for 1 hour at 37°C. AAV5 was purified on AVB Sepharose column (GE Healthcare, Little Chalfont, UK) using AKTA Explorer purification system (GE Healthcare) and the genome copy titer was determined by qPCR.

Lentiviral vector production

LVs were produced in HEK-293T cells with the four-plasmid system, as previously described. [40] Human immunodeficiency virus type 1 (HIV-1) vectors were pseudotyped with the vesicular

stomatitis virus glycoprotein (VSV-G) envelope, concentrated by ultracentrifugation and resuspended in phosphate-buffered saline (PBS, Gibco, Life Technologies, Zug, Switzerland) supplemented with 1% bovine serum albumin (BSA, Sigma-Aldrcich, Buchs, Switzerland). The viral particle content of each batch was determined by p24 antigen enzyme-linked immunosorbent assay (p24 ELISA, RETROtek, Kampenhout, Belgium). Viral stocks were stored at -80°C. Lentiviral vectors encoding the mutant HTT fragments were used at 300 ng of p24. Based on transcriptional start site from the PGK promoter and the presence of polyA+ signal in the 3'LTR of the lentiviral vector, the mRNAs expressed from the LV-mtHTT-50T and LV-mtHTT-67 constructs are expected to be approximately 1993bp and 2059bp, respectively.[41]

Animals

Adult male Sprague Dawley rats (200g; OFA, Charles River, Oncins, France) were housed in a temperature-controlled room and maintained on a 12h day/night cycle. Food and water were available ad libitum. All experiments were carried out in accordance with the European Community directive (86/609/EEC) for the care and use of laboratory animals as well as the Swiss animal welfare laws under the authorization n° VD 2487 and 2889 from the Service de la consommation et des affaires vétérinaires du Canton de Vaud, Switzerland.

Stereotaxic injections

The animals were anesthetized using a solution containing 75mg/kg ketamine (Ketasol, Graeub, Bern, Switzerland) and 10mg/kg xylazine (Rompun, Bayer Health Care, Uznach, Switzerland) administered i.p. The rat was placed in the stereotaxic frame (model 963 Ultra Precise Small Animal Stereotaxic Instrument, Kopf, Tujunga, USA). Viral vectors were stereotaxically injected into the striatum of animals through a 34-gauge blunt-tip needle (Phymep, Paris, France) linked to a Hamilton syringe (Hamilton Medical AG, Bonaduz, Switzerland) by a polyethylene catheter. The stereotaxic coordinates for an intrastriatal injection were: 0.5 mm rostral to bregma, 3 mm lateral to midline and 5 mm from the skull surface. For the infections, 300 ng p24 antigen of lentiviral vectors were mixed with $6.5x10E^{10}$ gc of AAV5 in 4µl and injected at 0.2µl/min. The injections were not performed in a blind manner. The rats received 2mg/mL acetaminophen (Dafalgan®, UPSA, Agen, France) in water for the three days following the intervention.

Histology

The rats were sacrificed by an overdose of sodium pentobarbital 150 mg/kg (B-Braun Mediacal SA, Sempach, Switzerland) and transcardially perfused at a rate of 20 ml/min with 100 ml of 1 x PBS and then with 300 ml of 4% PFA. Brains were removed and post-fixed by incubation in 4% PFA for 24 h at 4°C and cryoprotected by incubation in 20% sucrose (Sigma-Aldrich, Buchs, Switzerland) in 1 x PBS for 24 h and in 30% sucrose in 1 x PBS for 24

h. Brains were frozen on dry ice and then stored at -80°C. For RNA analysis, the animals were sacrificed and the brains were snap-frozen in liquid nitrogen.

25 µm-thick coronal brain sections were cut on a sledge microtome with a freezing stage at -30°C (Leica SM2010R, Biosystems Switzerland, Nunningen, Switzerland). Sections throughout the striatum were collected and kept in tubes, as free-floating sections in anti-freeze solution (25% glycerol (Sigma-Aldrich, Buchs, Switzerland), 30% Ethylene glycol (Merck, Nottingham, UK), 25% 1X PBS and 20% nanopure water).

Immunostaining

Free-floating sections were washed three times, for 10 minutes each, in Tris-buffered saline (TBS, 10 mM Tris pH = 7.6 and 0.9% NaCl Sigma-Aldrich, Buchs, Switzerland). Non-specific peroxidases were inactivated by incubation in quenching solution (TBS supplemented with 3% H_2O_2 and 10% methanol, Sigma-Aldrich, Buchs, Switzerland) for 15 minutes at room temperature. Sections were washed twice, for 10 minutes each, in TBS, and then for 10 minutes in TBS-0.1% Triton X-100 (TBST). Sections were blocked by incubation in Tris-high salt- buffer (THST, 50 mM Tris pH = 7.6, 0.5 M Nacl, 0.5% Triton X-100,) for anti-HTT antibody or TBST-5% NGS for DARPP32 antibody during 1 h at room temperature and were then incubated overnight at 4°C in TBST-1% BSA with antibodies. The following primary antibodies were used: Goat polyclonal anti-HTT antibody (1/1000, Sicgen, Coimbra, Portugal), rabbit polyclonal anti-DARPP-32 antibody (1/1000, Cell Signaling Technology Europe, Leiden, The Netherlands), rabbit polyclonal anti-GFP antibody (1/100'000, Abcam, Cambridge, UK), rabbit polyclonal anti-Ibal antibody (1/25'000, Wako Chemicals, Richmond, USA), rabbit polyclonal anti-GFAP antibody (1/500, Dako, Baar, Switzeland). After incubation with the primary antibody, the sections were washed three times, for 10 minutes each, in TBS and then incubated for 1 h at room temperature in TBST-1% BSA with secondary antibodies. The following secondary antibodies were used: biotinylated donkey anti-goat IgG (1/1000, Jackson, Pennsylvania, USA) and biotinylated goat anti-rabbit IgG (1/400, Vector Lab Inc, Burlingame, USA). Sections were washed three times, for 10 minutes each, in TBST and incubated for 1 h at RT in ABC (Vector Lab Inc, Burlingame, USA). Samples were washed twice, for 10 minutes each, in TBS and were then incubated with nickel chloride and diaminobenzidine (DAB, Vector Lab Inc, Burlingame, USA) for antibody detection. Sections were mounted on Superfrost Ultraplus slides. Sections were allowed to dry in a laminar flow hood and were dehydrated (70% ethanol in nanopure water, 95% ethanol in nanopure water, 100% ethanol, 100% ethanol, xylene) before mounting in Eukitt (Kindler GmbH, Freiburg, Germany).

Image acquisition and quantification

Images were obtained with a digital camera (3CCD Hitachi HV-F202SCL) on a slide scanner microscope (x20 objective, Zeiss axioscan Z1). Measurements were made with Image J software (http://rsb.info.nih.gov/ij/, NIH, Bethesda, USA) for aggregates and Zeiss Zen Lite 2 (blue Edition) (Carl Zeiss AG, Germany) for DARPP32 lesion. An Image J macro was developed to count the number of aggregates. The aggregates were identified on the basis of their intensity relative to the background, their size and their circularity. The same intensity, size and circularity parameters were used for all samples.

Quantification of mtHTT aggregates and DARPP-32 lesions

The number of mutant HTT aggregates in striatum was automatically counted in 1 in 8 sections with analyze particle plugin on ImageJ. Cut-off with minimum size and maximum pixel area size was applied to exclude non-aggregates in the ROI. The total number of aggregates was estimated by multiplying these densities by 8. The loss of DARPP-32 expression was analyzed by collecting digitized images sections (1 in 8 sections separated by 200µm). Lesion areas in each section were determined as regions poor in DARPP-32 staining relative to the surrounding tissue. The lesion volume for each animal was quantified with the following formulae: lesion in mm^3 = (mean size in μm^2 x number of counted section x inter-section distance) / 1x10E9. Means and standard deviations were calculated for each group. The quantifications were performed in a blind manner.

Quantitative Real-Time PCR

Rat striata were crushed using CryoPrep System (Covaris, Woburn, MA) and the powder was divided for RNA and DNA analyses. For RNA isolation, the striatal powder was homogenized in Trizol using gentleMACS Dissociator (Miltenyi Biotec) and total RNA was isolated from Trizol according to the manufacturer's protocol (Invitrogen). To remove genomic DNA, RNA was treated with dsDNase (Thermo Scientific, Waltham, MA). Quantitative Real-Time PCR (qRT-PCR) reaction was performed to detect *HTT* mRNA knock-down using TaqMan gene expression assays (Applied Biosystems, Foster City, CA), human HTT (Hs00918134_m1), rat GAPDH (Rn01462662_g1); and miHTT expression levels using custom TaqMan microRNA expression assay or U6 snRNA (001973) (Applied Biosystems). The expression level of each gene was normalized to either endogenous GAPDH or U6 snRNA levels. Fold change/ percentages in HTT mRNA knock-down or miHTT expression were calculated based on 2^DDCT method.

For the genomic DNA isolation, the striatal powder was processed using DNeasy96 Blood and Tissue kit (Qiagen). qPCR reaction was performed to detect AAV5 vector titers using a standard line and SYBR Green protocol (Applied Biosystems). Forward primer sequence: GAGCCGCAGCCATTGC and reverse primer sequence: CACAGATTTGGGACAAAGGAAGT. Based on the standard line, genome copies per microgram DNA were calculated.

Next-generation sequencing data analysis

The raw sequencing data were produced as previously described.[18] small RNA raw data sets were analyzed using the CLC Genomics Workbench 6 (Qiagen). All reads containing ambiguity N symbols, reads shorter than 10 nucleotides, longer than 45 nucleotides and reads represented less than 10 times were discarded. The obtained unique small RNA reads were aligned to the reference sequences of the pre-miHTT and pre-miSNP50T constructs with a max. of 3 nucleotide mismatches allowed. The percentages of reads based on the total number of reads matching the reference sequences were calculated.

Sample sizes, calculations and statistical analysis

Sample sizes of Saline n=18, GFP n=16, AAV5-miHTT-155 n=18, AAV5-miHTT-451 n=16, AAV5-miSNP67T-155 n=16, and AAV5-miSNP50T-451 n=16 represent the number of striata injected per experimental group. The sample size was chosen to consider statistical variability due to surgical procedure based on previous studies. All experiments involving animals were performed once. The only exclusion criterion was if a problem was encountered during the injection procedure. The knock-down percentages were calculated using the following formula: Knock-down (%)= [AAV5-miRNA treatment] / [Saline treatment] x 100%. Data were analyzed using one-way ANOVA. *, $p < 0.05$; **, $p < 0.01$; ***, $p < 0.001$; ****, $p \leq 0.0001$. Differences were considered significant when $p < 0.05$. The values were calculated as a mean ± standard deviation.

Acknowledgments

The authors thank Dr. Eileen Sawyer and Dr. Olivier ter Brake for critically reviewing the manuscript.

Conflict of Interest

Jana Miniarikova, Raygene Martier, Cynthia C. Brouwers, Dr. Jacek Lubelski, Dr. Melvin M. Evers, Dr. Harald Petry, and Dr. Pavlina Konstantinova are employees and shareholders at uniQure. Prof. N. Déglon and CHUV have a collaborative agreement with uniQure. uniQure has sponsored a portion of the research performed in prof. N. Déglon's lab.

REFERENCES

1 Rawlins MD, Wexler NS, Wexler AR, Tabrizi SJ, Douglas I, Evans SJW *et al.* The prevalence of huntington's disease. *Neuroepidemiology* 2016; 46: 144–153.

2 Langbehn DR, Brinkman RR, Falush D, Paulsen JS, Hayden MR. A new model for prediction of the age of onset and penetrance for Huntington's disease based on CAG length. *Clin Genet* 2004; 65: 267–277.

3 Huntington T, Macdonald ME, Ambrose CM, Duyao MP, Myers RH, Lin C *et al.* A Novel Gene Containing a Trinucleotide That Is Expanded and Unstable on Huntington ' s Disease Chromosomes. 1993; 72: 971–983.

4 Ross C a., Tabrizi SJ. Huntington's disease: From molecular pathogenesis to clinical treatment. *Lancet Neurol* 2011; 10: 83–98.

5 Bates GP, Dorsey R, Gusella JF, Hayden MR, Kay C, Leavitt BR *et al.* Huntington disease. *Nat Rev Dis Prim* 2015; : 15005.

6 DiFiglia M, Sapp E, Chase KO, Davies SW, Bates GP, Vonsattel JP *et al.* Aggregation of huntingtin in neuronal intranuclear inclusions and dystrophic neurites in brain. *Science* 1997; 277: 1990–3.

7 Ross C a, Aylward EH, Wild EJ, Langbehn DR, Long JD, Warner JH *et al.* Huntington disease: natural history, biomarkers and prospects for therapeutics. *Nat Rev Neurol* 2014; 10: 204–16.

8 Yamamoto a, Lucas JJ, Hen R. Reversal of neuropathology and motor dysfunction in a conditional model of Huntington's disease. *Cell* 2000; 101: 57–66.

9 Fire A, Xu S, Montgomery MK, Kostas SA, Driver SE, Mello CC. Potent and specific genetic interference by double-stranded RNA in Caenorhabditis elegans. *Nature* 1998; 391: 806–811.

10 Boudreau RL, Rodríguez-Lebrón E, Davidson BL. RNAi medicine for the brain: Progresses and challenges. *Hum Mol Genet* 2011; 20: 21–27.

11 Aronin N, DiFiglia M. Huntingtin-lowering strategies in Huntington's disease: Antisense oligonucleotides, small RNAs, and gene editing. *Mov Disord* 2014; 29: 1455–1461.

12 Kantor B, Bailey RM, Wimberly K, Kalburgi SN, Gray SJ. *Methods for gene transfer to the central nervous system*. Elsevier, 2014 doi:10.1016/B978-0-12-800149-3.00003-2.

13 Srivastava A. In vivo tissue-tropism of adeno-associated viral vectors. *Curr Opin Virol* 2016; 21: 75–80.

14 Markakis EA, Vives KP, Bober J, Leichtle S, Leranth C, Beecham J *et al.* Comparative Transduction Efficiency of AAV Vector Serotypes 1–6 in the Substantia Nigra and Striatum of the Primate Brain. *Mol Ther* 2010; 18: 588–593.

15 Burger C, Gorbatyuk OS, Velardo MJ, Peden CS, Williams P, Zolotukhin S *et al.* Recombinant AAV viral vectors pseudotyped with viral capsids from serotypes 1, 2, and 5 display differential efficiency and cell tropism after delivery to different regions of the central nervous system. *Mol Ther* 2004; 10: 302–317.

16 Lin D, Fantz CR, Levy B, Rafi MA, Vogler C, Wenger DA *et al.* AAV2/5 vector expressing galactocerebrosidase ameliorates CNS disease in the murine model of globoid-cell leukodystrophy more efficiently than AAV2. *Mol Ther* 2005; 12: 422–430.

17 Samaranch L, Blits B, San Sebastian W, Hadaczek P, Bringas J, Sudhakar V *et al.* MR-guided parenchymal delivery of adeno-associated viral vector serotype 5 in non-human primate brain. *Gene Ther* 2017; 24: 253–261.

18 Miniarikova J, Zanella I, Huseinovic A, van der Zon T, Hanemaaijer E, Martier R *et al.* Design, Characterization, and Lead Selection of Therapeutic miRNAs Targeting Huntingtin for Development of Gene Therapy for Huntington's Disease. *Mol Ther Nucleic Acids* 2016; 5: e297.

19 Menalled L, Brunner D. Animal models of Huntington's disease for translation to the clinic: Best practices. *Mov Disord* 2014; 29: 1375–1390.

20 Ramaswamy S, Mcbride JL, Kordower JH. Animal Models of Huntington's Disease. .

21 Pouladi M a, Morton a J, Hayden MR. Choosing an animal model for the study of Huntington's disease. *Nat Rev Neurosci* 2013; 14: 708–21.

22 de Almeida LP, Ross CA, Zala D, Aebischer P, Deglon N. Lentiviral-mediated delivery of mutant huntingtin in the striatum of rats induces a selective neuropathology modulated by polyglutamine repeat size, huntingtin expression levels, and protein length. *J Neurosci* 2002; 22: 3473–3483.

23 Drouet V, Ruiz M, Zala D, Feyeux M, Auregan G, Cambon K *et al.* Allele-specific silencing of mutant huntingtin in rodent brain and human stem cells. *PLoS One* 2014; 9. doi:10.1371/journal.pone.0099341.

24 Ouimet CC, Langley-Gullion KC, Greengard P. Quantitative immunocytochemistry of DARPP-32-expressing neurons in the rat caudatoputamen. *Brain Res* 1998; 808: 8–12.

25 Lombardi MS, Jaspers L, Spronkmans C, Gellera C, Taroni F, Di Maria E *et al.* A majority of Huntington's disease patients may be treatable by individualized allele-specific RNA interference. *Exp Neurol* 2009; 217: 312–319.

26 Klein RL, Hamby ME, Gong Y, Hirko AC, Wang S, Hughes J a. *et al.* Dose and Promoter Effects of Adeno-Associated Viral Vector for Green Fluorescent Protein Expression in the Rat Brain. *Exp Neurol* 2002; 176: 66–74.

27 Ma H, Zhang J, Wu H. Designing Ago2-specific siRNA/shRNA to Avoid Competition with Endogenous miRNAs. *Mol Ther Nucleic Acids* 2014; 3: e176.

28 Herrera-carrillo E, Harwig A, Liu YP, Berkhout B. Probing the shRNA characteristics that hinder Dicer recognition and consequently allow Ago-mediated processing and AgoshRNA activity. *RNA* 2014; 20: 1–9.

29 Yu D, Pendergraff H, Liu J, Kordasiewicz HB, Cleveland DW, Swayze EE *et al.* Single-stranded RNAs use RNAi to potently and allele-selectively inhibit mutant huntingtin expression. *Cell* 2012; 150: 895–908.

30 Carroll JB, Warby SC, Southwell AL, Doty CN, Greenlee S, Skotte N *et al.* Potent and selective antisense oligonucleotides targeting single-nucleotide polymorphisms in the Huntington disease gene / allele-specific silencing of mutant huntingtin. *Mol Ther* 2011; 19: 2178–85.

31 Pfister EL, Kennington L, Straubhaar J, Wagh S, Liu W, Landwehrmeyer B *et al.* Five siRNAs targeting three SNPs in Huntingtin may provide therapy for three-quarters of Huntington's disease patients. 2009; 19: 774–778.

32 Kay C, Skotte NH, Southwell a L, Hayden MR. Personalized gene silencing therapeutics for Huntington disease. *Clin Genet* 2014; 86: 29–36.

33 Warby SC, Montpetit A, Hayden AR, Carroll JB, Butland SL, Visscher H *et al.* CAG expansion in the Huntington disease gene is associated with a specific and targetable predisposing haplogroup. *Am J Hum Genet* 2009; 84: 351–66.

34 Butland SL, Devon RS, Huang Y, Mead C-L, Meynert AM, Neal SJ *et al.* CAG-encoded polyglutamine length polymorphism in the human genome. *BMC Genomics* 2007; 8: 126.

35 Monteys AM, Wilson MJ, Boudreau RL, Spengler RM, Davidson BL. Artificial miRNAs Targeting Mutant Huntingtin Show Preferential Silencing In Vitro and In Vivo. *Mol Ther Acids* 2015; 4: e234.

36 Bartel DP, Lee R, Feinbaum R. MicroRNAs : Genomics , Biogenesis , Mechanism , and Function Genomics : The miRNA Genes. 2004; 116: 281–297.

37 Stiles DK, Zhang Z, Ge P, Nelson B, Grondin R, Ai Y *et al.* Widespread suppression of huntingtin with convection-enhanced delivery of siRNA. *Exp Neurol* 2012; 233: 463–471.

38 McBride JL, Pitzer MR, Boudreau RL, Dufour B, Hobbs T, Ojeda SR *et al.* Preclinical Safety of RNAi-Mediated HTT Suppression in the Rhesus Macaque as a Potential Therapy for Huntington's Disease. *Mol Ther* 2011; 19: 2152–2162.

39 Grondin R, Kaytor MD, Ai Y, Nelson PT, Thakker DR, Heisel J *et al.* Six-month partial suppression of Huntingtin is well tolerated in the adult rhesus striatum. *Brain* 2012; 135: 1197–209.

40 Hottinger AF, Azzouz M, Déglon N, Aebischer P, Zurn AD. Complete and long-term rescue of lesioned adult motoneurons by lentiviral-mediated expression of glial cell line-derived neurotrophic factor in the facial nucleus. *J Neurosci* 2000; 20: 5587–5593.

41 Adra CN, Boer PH, McBurney MW. Cloning and expression of the mouse pgk-1 gene and the nucleotide sequence of its promoter. *Gene* 1987; 60: 65–74.

Supplementary material and methods (S1). GAPDH and HTT expression values. CT values showing GAPDH and human HTT expression in rats injected with LV vectors and Saline, AAV5-miHTT-451, or AAV5-miSNP50T-451 vectors (n=2-3). Two uninfected rat striata were included as negative controls. Saline and AAV5-miHTT-451-treated striata were double-treated with DNase (Thermo Scientific, Waltham, MA) and 200ng input RNA was used. AAV5-miSNP50T-451 striata were treated one time with DNase (Thermo Scientific, Waltham, MA) and 400ng input RNA was used.

	GAPDH	**human HTT**
Treatment	**CT mean**	**CT mean**
Neg. Control 1 rat striatum	30.47	37.16
Neg. Control 2 rat striatum	30.52	39.14
LV-mtHTT-50T + Saline	30.40	30.78
LV-mtHTT-50T + Saline	30.46	30.50
LV-mtHTT-50T + Saline	30.15	29.96
LV-mtHTT-50T + AAV5-miHTT-451	29.69	30.67
LV-mtHTT-50T + AAV5-miHTT-451	23.35	26.33
LV-mtHTT-50T + AAV5-miHTT-451	30.35	31.52
LV-mtHTT-50T + AAV5-miSNP50T-451	23.02	25.76
LV-mtHTT-50T + AAV5-miSNP50T-451	23.07	25.35
LV-mtHTT-50C + AAV5-miSNP50T-451	22.97	24.87
LV-mtHTT-50C + AAV5-miSNP50T-451	23.08	24.44

Supplementary material and methods (S2). Image J Macro

```
setBatchMode(true);
imgArray = newArray(nImages);
for (i=0; i<nImages; i++) {
selectImage(i+1);
imgArray[i] = getImageID();
 }
for (i=0; i< imgArray.length; i++) {
selectImage(imgArray[i]);
run("8-bit");
setAutoThreshold("MaxEntropy dark");
//run("Threshold...");
setAutoThreshold("MaxEntropy dark");
//setThreshold(0, 88);
setOption("BlackBackground", false);
run("Convert to Mask");
run("Analyze Particles...", "size=10-160 summarize add")
```

4

THERAPEUTIC MICRORNAS TARGETING NUCLEAR HUNTINGTIN FOR A DEVELOPMENT OF A PERSONALIZED GENE THERAPY FOR HUNTINGTON'S DISEASE

Jana Miniarikova[1,2], Marina Sogorb-Gonzalez[1,2], Astrid Vallès[1], Melvin M. Evers[1], Harald Petry[1], Sander J. van Deventer[1,2], Pavlina Konstantinova[1]

[1]Department of Research & Development, uniQure, Amsterdam, the Netherlands

[2]Department of Gastroenterology and Hepatology, Leiden University Medical Center, Leiden, the Netherlands

ABSTRACT

Huntington's disease (HD) is a monogenic neurodegenerative disorder caused by an expansion of CAG repeats in the huntingtin (*HTT*) gene, resulting in a formation of a toxic mutant HTT protein. Currently, there is no disease-modifying treatment available. HTT lowering therapies targeting HTT DNA or RNA show a great promise since they offer a reduction of the HD culprit, the mutant HTT protein. One of the most preclinically advanced HTT lowering therapy is a micro (mi)RNA-based gene therapy delivered to target cells by adeno-associated viral (AAV) vectors and resulting in a long-term HTT lowering. The long-perceived theory of miRNA-based lowering occurring predominantly in the cytoplasm is nowadays being questioned, with emerging evidence of miRNAs being active also in the nucleus. A four-nucleotide deletion ΔACTT (rs72239206) in HTT intron 22 is often associated with the mutant HTT in HD patients of A1 haplotype. Here, we investigated the efficacy of therapeutic miRNAs targeting sequences in HTT intron 22 containing ΔACTT to induce nuclear allele-specific mutant HTT lowering. Our results demonstrate a strong mutant HTT protein lowering in HD patient neuronal cultures heterozygous for ΔACTT induced by the miACTT2 construct delivered by an AAV serotype 5 (AAV5) vector. This is a first preclinical evidence suggesting that a therapeutic miRNA can lower the nuclear disease-related transcripts and thereby prevent the translation into the toxic protein. Further experiments are required to confirm a broad applicability. This offers a new perspective on the general application of miRNA-based therapies and their competitiveness with therapies targeting nuclear disease-linked transcripts, such as antisense oligonucleotides.

INTRODUCTION

Huntington's disease (HD) is a neurodegenerative genetic disorder inherited in an autosomal dominant manner with a prevalence of 1-10 in 100.000 people worldwide.[1] HD pathology results from an expansion of CAG triplet nucleotides in exon 1 of the huntingtin (*HTT*) gene.[2] As a result, mutant HTT protein incorporates an extended polyglutamine (polyQ) chain at the N-terminus. Due to the presence of more than 39 glutamines in the polyQ chain, the mutant HTT misfolds and aggregates, which negatively affects several cellular pathways, causing cellular stress, and ultimately resulting in neuronal cell death over the years.[3,4] Although mutant HTT is expressed throughout the body and peripheral signs of the disease have been also reported, HD is predominantly a disease of the brain, in particular of the striatum and cortex.[5] In most cases, HD manifests in the prime of adulthood with a median survival of 15-18 years after motor symptom onset.[4] The progressive clinical symptoms of HD include motor, cognitive, and psychiatric disturbances.[6] Currently, there is no disease-modifying treatment available.

The gain of toxic function of the mutant HTT protein is widely accepted as a predominant cause of HD pathology.[7] Transgenic HD murine models expressing mutant HTT fragments, causing intracellular formation, develop HD-like neurodegeneration.[8,9] Interference with mutant HTT aggregation results in a suppression of neurodegeneration in HD rodent models.[10–14] Mutant HTT aggregates have been also found *post mortem* in HD human brains.[15,16] HTT lowering therapies that aim to suppress the production of the mutant HTT protein represent the main therapeutic approach towards HD.[17] Many studies in small and large animals have tested the efficacy of (mutant) HTT lowering technologies based on antisense oligonucleotides or RNA interference (RNAi).[Reviewed in 18–20] In contrast to antisense oligonucleotides that demonstrated short-term (in months) HTT lowering, RNAi molecules delivered by viral vectors offer an advantage of a continuous long-term (in years) HTT lowering.[17] One of the most advanced RNAi approaches applies intra-striatal delivery of adeno-associated viruses (AAVs) to express therapeutic micro (mi)RNA precursors.[11] These precursors are processed by the cellular RNAi machinery, generating a mature therapeutic that binds to HTT transcripts and suppresses HTT translation.[21] The safety and efficacy of various therapeutic miRNAs have been preclinically evaluated in rodent and large HD animal models and currently they are approaching clinical testing.[11,13,22–25]

The traditional concept of cellular miRNAs being active mainly in the cytoplasm has been challenged in recent years as systematic profiling analyses performed on RNA isolated from the nuclear and cytoplasmic fractions demonstrated that a majority of cellular miRNAs are present in the nucleus.[26–29] Moreover, the cardinal proteins enabling RNAi in the cytoplasm such as AGO2, Dicer1, TRBP2 and GW182 have been recently also found in the nucleus.[30] AGO2 catalytic activity is preserved in nuclear extracts, indicating the possible functionality of AGO2-bound miRNAs in the nucleus. This provides opportunities to design therapeutic miRNAs targeting nuclear disease-related transcripts.

As HD is a rare disease with a dominant inheritance, the homozygous HD mutation carriers are only occasional and most HD patients express the wild-type and mutant HTT.[31] Dozens of heterozygous single-nucleotide polymorphisms (SNPs) have been identified that are *in cis* with the HD mutation and largely annotate HD haplotypes.[32] These heterozygous SNPs allow for a design of miRNAs to induce the allele-specific lowering. Unfortunately, allele-specific lowering has limitations because 1) the treatment needs to be personalized and therefore, currently, it would be available only for specific subgroups of HD patients, and 2) the allele-selectivity-to-efficacy ratio does not outweigh the efficacy level induced by the non-selective approach, which is the deciding factor for the efficacy of current gene therapy approaches. Recently, a deletion of four nucleotides ΔACTT (rs72239206) in HTT intron 22 has been identified in the most frequent heterozygous HD haplotype A1 in Canadian Caucasian population.[32] ΔACTT is located in the intronic region, which suggests that most of the ΔACTT-containing transcripts are located in the nucleus, before the splicing occurs. Hence, the ΔACTT deletion offers the opportunity to simultaneously evaluate the allele-specific and nuclear HTT lowering.

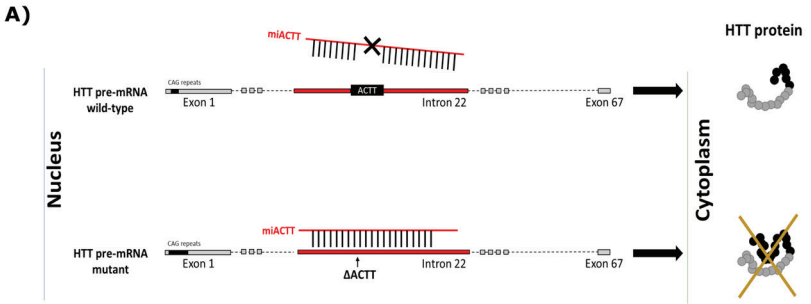
The aim of this study was to demonstrate the efficacy of therapeutic miRNAs to lower the nuclear mutant HTT transcripts. We designed therapeutic miRNAs (referred as miACTTs) to target mutant HTT sequences located in HTT intron 22 encompassing ΔACTT. We hypothesized that targeting ΔACTT will offer a greater mutant selectivity compared to the standard SNP-based approaches, which strongly depends on the number of nucleotides not matching to the wild-type HTT sequences. We designed two artificial miRNAs (miACTTs) embedded in five different endogenous pre-miRNA precursors, and their allele-selectivity was first addressed using luciferase reporter constructs. The HTT lowering activity of several miACTTs was evaluated in both nucleus and cytoplasm and we analyzed the processing of mature miACTT, allowing a selection of a candidate that was devoid of passenger strand activity. The efficacy and allele-selectivity of the most efficient miACTT2 candidate embedded in the hsa-miR-451 precursor delivered by an AAV5 vector was evaluated in induced pluripotent stem cells (iPSC)-derived HD neuronal cultures heterozygous for ΔACTT.

RESULTS

Therapeutic miRNAs show strong allele-selective lowering of luciferase reporters heterozygous for ΔACTT (rs72239206).

To design therapeutic miRNAs that effectively and selectively target ΔACTT (rs72239206) in HTT intron 22, we analyzed a sequence composition in the HTT gene region surrounding ΔACTT (**Figure 1a**). We searched for enriched AT motifs to identify the beginning of the 5'end of the guide strand while keeping ΔACTT binding either at the 3'end or in the center of the pre-miRNA. Enriched AT motifs at the beginning of a guide strand have been shown to reduce the production of the passenger strand during the pre-miRNA processing and reducing the odds of passenger strand-related unwanted off-target interactions.[11,20] Moreover, 3'end or central positions of the target nucleotides during the target miRNA-mRNA binding have been shown to improve the allele-selectivity of the artificial miRNAs by reducing thermodynamic stability between the miRNA and mismatch mRNAs.[11] We identified two regions that contain five nucleotide-long AT motifs with the ΔACTT binding starting at position 19 and 9 from the 5'end of the guide strand, named miACTT1 and miACTT2. We placed miACTT1 and miACTT2 guide strands in five scaffolds that we have previously evaluated with an artificial miRNA targeting HTT exon 1: hsa-miR-101, hsa-miR-122, hsa-miR-135, hsa-miR-155, and hsa-miR-451.[11] The passenger strands were corrected to maintain the original miRNA scaffolding. The resultant constructs are named miACTT1-101, miACTT1-122, miACTT1-135, miACTT1-155, miACTT2-101, miACTT2-122, miACTT2-135, miACTT2-155, and miACTT2-451 (**Figure 1b**). To address the efficacy of the miACTT constructs, we generated a renilla luciferase reporter expressing a luciferase gene fused with HTT intron 22 containing ΔACTT and the splicing sites, named Luc-ΔACTT (**Figure 1c**). To address the allele-selectivity of miACTTs, we generated a second renilla luciferase reporter containing HTT intron 22, named Luc-ACTT. All miACTT constructs perfectly match to Luc-ΔACTT and have a four-nucleotide mismatch with Luc-ACTT.

To evaluate the efficacy and allele-selectivity of the miACTT constructs, we co-transfected them with Luc-ACTT and Luc-ΔACTT reporters in HEK293T cells and quantified the luciferase activity. We observed 60-90% lowering of Luc-ΔACTT reporter activity as compared to 20-40% lowering of the Luc-ACTT activity by all miACTT constructs, demonstrating strong allele-selectivity (**Figure 1d**). Overall, miACTT1 constructs showed slightly stronger allele-selectivity compared to miACTT2 constructs, confirming that the 3'end terminal binding interaction between the miRNA and target mRNA is more potent to discriminate a four-nucleotide mismatch.


A)
miACTT
HTT protein
HTT pre-mRNA wild-type
CAG repeats
Exon 1
ACTT
Intron 22
Exon 67
Nucleus
Cytoplasm
miACTT
HTT pre-mRNA mutant
CAG repeats
Exon 1
ΔACTT
Intron 22
Exon 67


B)
miACTT1-101
miACTT1-122
miACTT1-135
miACTT1-155
miACTT2-101
miACTT2-122
miACTT2-135
miACTT2-155
miACTT2-451

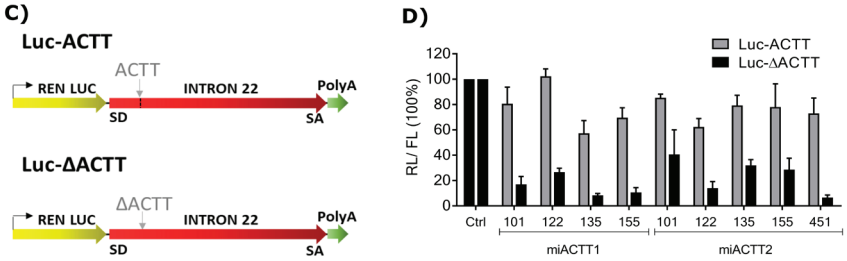


Figure 1. miACTT1 and miACTT2 precursors induce strong allele-selective lowering of luciferase reporters carrying HTT intron 22 with ΔACTT. (**A**) Proposed mechanism of action for miACTT1 and miACTT2 guide sequences targeting HTT intron 22 containing ΔACTT. miACTTs bind to HTT intron 22 with ΔACTT based on miRNA-mRNA complementarity in the nucleus. It results in an overall reduction of the mutant HTT protein in the cytoplasm. (**B**) The schematic of miACTT1 and miACTT2 guide sequences embedded in five human pre-miRNA scaffolds, named miACTT1-101, miACTT1-122, miACTT1-135, miACTT1-155, miACTT2-101, miACTT2-122, miACTT2-135, miACTT2-155, and miACTT2-451. Based on miRBase database (www.mirbase.org), the guide and passenger strands are represented in red and blue, respectively. (**C**) Schematic of luciferase reporters containing renilla luciferase gene (REN LUC) fused to HTT intron 22 with ACTT, named Luc-ACTT, and with the ACTT deletion, named Luc-ΔACTT. (**D**) Luc-ACTT and Luc-ΔACTT luciferase knock-down by miACTT1 and miACTT2 scaffolds in HEK293T cells.

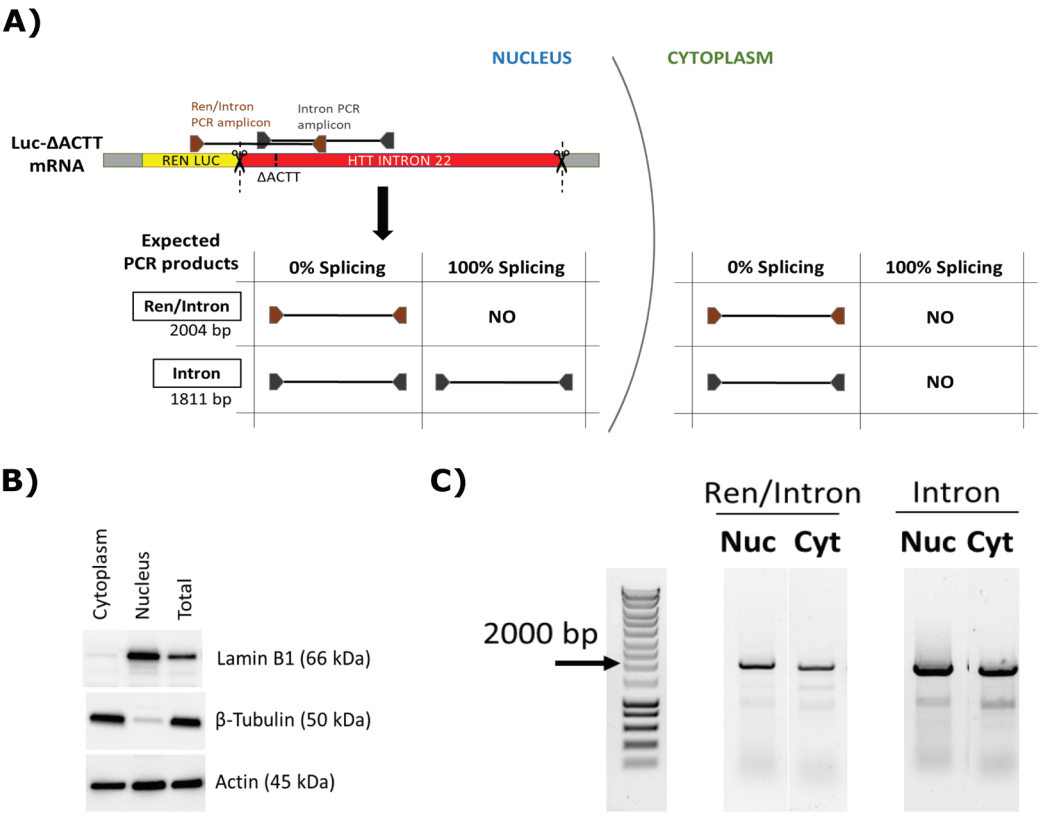
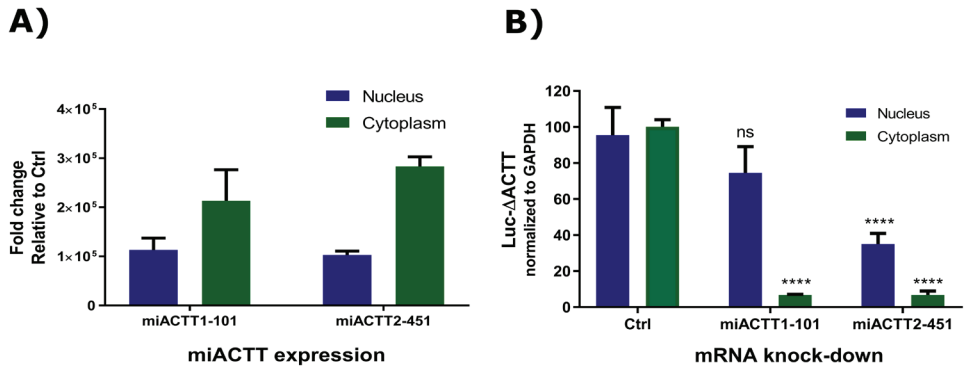


Figure 2. The Luc-ΔACTT reporter expresses renilla transcripts fused with HTT intron 22 in the cytoplasm. (**A**) The overview of expected PCR products in case 0% or 100% splicing of HTT intron 22 from the luciferase reporters occurs. Two PCR primer pairs were designed to amplify a fragment encompassing a portion of luciferase gene and HTT intron 22, named Ren/Intron, or a fragment within HTT intron 22, named Intron. (**B**) Western blotting showing a separation of the nuclear and cytoplasmic fraction. Lamin B1 is an exclusive nuclear protein, β-tubulin is an exclusive cytoplasmic protein, and Actin can be found in all fractions. (**C**) PCR products using Ren/Intron and Intron primers separated on an agarose gel.

The HTT intron 22 containing the splicing sites is located in the 3'UTR of the luciferase gene and this may interfere with effective splicing. Therefore, we analyzed the splicing efficacy of HTT intron 22 from the Luc-ΔACTT reporter by RT-PCR of the nuclear and cytoplasmic RNA fractions isolated from HEK293T cells (**Figure 2**). We used custom primers that generate an amplicon within the intron 22, named Intron, or an amplicon encompassing a part of the luciferase gene and intron 22, named Ren/Intron (**Figure 2a**). A separation of the nucleus and cytoplasm was evaluated by western blotting using nuclear marker Lamin B1 and cytoplasmic marker β-Tubulin (**Figure 2b)**. RT-PCR products were separated by electrophoresis on agarose gels (**Figure 2c**). We detected equal bands of unspliced variants in both cytoplasm and nucleus using both primer sets, suggesting that splicing does not occur or, at such a low rate, that it cannot be visualized on a gel. The inability of HTT intron

22 to be effectively spliced from the luciferase reporter can reflect its placement in the 3'UTR of the luciferase gene. This result indicates that the miACTTs evaluated in this system have the potential to target HTT mRNA in the nucleus and in the cytoplasm. Furthermore, this is also indicative that lowered mRNA in the cytoplasm can be the result of both nuclear and cytoplasmic lowering. To further establish whether the lowering efficacy of luciferase expression is a result of mRNA lowering in the nucleus, we conducted further experiments described below.



Mean CT values

	Nucleus			Cytoplasm		
	GAPDH	Ren/Intron*	Intron*	GAPDH	Ren/Intron*	Intron*
Ctrl	22.1	19.6	20.1	20.3	19.9	20.2
miACTT1-101	22.2	20.1	20.6	20.5	23.4	24
miACTT2-451	21.9	20.7	21.2	20.9	23.8	24.5
NTC	40	29.1	32	40	35.7	33.3

Figure 3. Luc-ΔACTT mRNA knock-down induced by the miACTT1-101 and miACTT2-451 construct in the nucleus and cytoplasm of HEK293T cells. (A) Differential expression of mature miACTT1 and miACTT2 molecules measured by RT-qPCR in the nuclear and cytoplasmic fraction using custom TaqMan small RNA probes. (**B**) TaqMan RT-qPCR analysis to evaluate the Luc-ΔACTT knock-down by miACTT1-101 and miACTT2-451 in the nucleus and cytoplasm of HEK239T cells. Mean CT values of Luc-ΔACTT mRNA measured by qPCR in the nuclear and cytoplasmic fractions using Ren/Intron* and Intron* TaqMan probes. GAPDH was used as an internal control. Ctrl represents a PBS group and NTC describes a non-template control. All data were analyzed using one-way ANOVA. Data are represented as the mean ± s.d. (error bars) ***, $p \leq 0.001$; ****, $p \leq 0.0001$; ns= non-significant.

miACTT1-101 and miACTT2-451 constructs induce mRNA lowering of luciferase reporters in the nucleus and cytoplasm.

We have previously shown that the miR-451 scaffold does not produce any passenger strand *in vitro* and *in vivo*. It limits the chance for off-target activity thereby providing better safety profiles.[10,11] Therefore, the miACTT2-451 construct was investigated in more detail, along with the miACTT1-101 construct that showed the strongest selective efficacy *in*

vitro. To further quantify the miACTT expression, HTT intron 22 splicing from the luciferase reporters, and lowering of luciferase reporters within different cellular compartments, we co-transfected miACTT1-101 and miACTT2-451 with the Luc-ΔACTT reporter in HEK293T cells and analyzed the expression of their transcripts. Both scaffolds induced ~$1x10^5$ levels of mature miACTT1-101 molecules in the nucleus when normalized to the scrambled negative control (**Figure 3a**). In the cytoplasm, the miACTT2-451 was slightly more abundant (~$2.8x10^5$) compared with miACTT1-101 (~$2.1x10^5$), when normalized to the negative scrambled control. To address the splicing and knock-down efficacy of the Luc-ΔACTT reporter, we performed RT-qPCR with TaqMan primers, named Intron* and Ren/Intron* (**Figure 3b**). We measured equal values of Luc-ΔACTT transcripts with both probes (data shown for Intron*), suggesting that the splicing of intron 22 from the luciferase reporter indeed does not occur or it is not detectable by RT-qPCR, and the knock-down efficacy should be evaluated separately in the nucleus and cytoplasm. Both miACTT1-101 and miACTT2-451 constructs induced a strong ~90% knock-down of Luc-ΔACTT transcripts in the cytoplasm. However, at an equal expression level within the nucleus, miACTT2-451 construct showed stronger ~65% silencing of the nuclear Luc-ΔACTT as compared to only ~25% silencing induced by the miACTT1-101 construct, suggesting that the silencing activity of the miACTT constructs in the nucleus is scaffold-dependent.

The miACTT2-451 construct does not generate a passenger strand *in vitro.*

The miACTT1-101 and miACTT2-451 constructs are embedded in different scaffolds and hence they generate different amounts of the guide and passenger strands. To address the processing patterns of these constructs, we performed small RNA next generation sequencing. The overview of the read alignments for the pre-miACTT1-101 and pre-miACTT2-451 constructs are presented in (**Figure 4a**). The analysis of the sequence length and composition revealed that the guide strands from both constructs were cleaved precisely at the predicted Drosha sites, whereas the further downstream Dicer cleavage generated all the variability in the sequence length (**Figure 4b**). This processing pattern is consistent with our previously published studies using different therapeutic miRNAs.[10,11] 47% reads processed from the miACTT1-101 scaffold were 22 nucleotides long. The miACTT2-451 processing generated variable lengths of the reads with 39% reads of 25 nucleotides in length. In case of the pri-miR-451 scaffold, the heterogenous 3'arm is a result of a cleavage by Argonaute 2 (AGO2) and further trimming by PARN.[33,34] With the regard to the miRNA activity, the crucial ''seed'' region recognizing the mRNA target is positioned in the 5'arm and therefore, the activity is preserved. We confirmed the absence passenger strands generated from the miACTT2-451 constructs, whereas we detected 8% of the passenger strand originating from the miACTT1-101 constructs. Based on the results above, we selected miACTT2-451 scaffold for further testing.

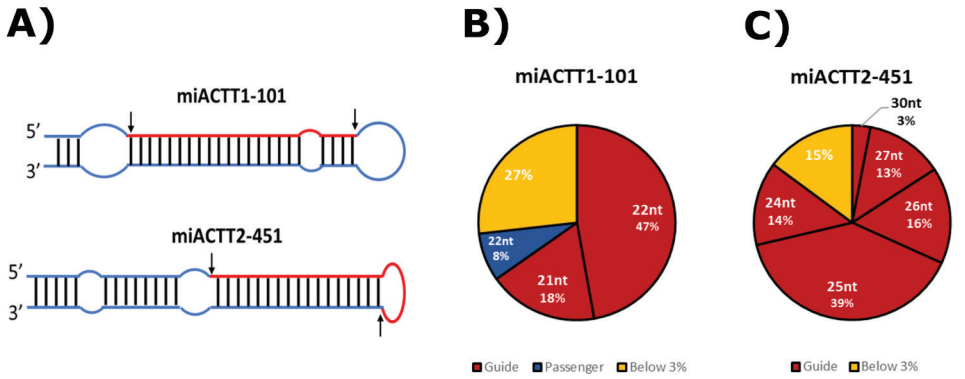


Figure 4. Next generation sequencing analysis of miACTT1-101 and miACTT2-451 processing in HEK293T cells. (A) Schematic representation of pre-miACTT1-101 and pre-miACTT2-451 scaffolds. Based on miRBase database (www.mirbase.org), the guide and passenger strands are represented in red and blue, respectively. Expected Drosha and Dicer guide cleavage sites are represented by arrows. **(B)** The length distribution of reads mapping to pre-miACTT1-101. For the read alignments, up to three mismatches with the references sequence were allowed. Reads represented with less than 3% were excluded from the figure. **(C)** The length distribution of reads mapping to pre-miACTT2-451. For the read alignments, up to three mismatches with the references sequence were allowed. Reads represented with less than 3% were excluded from the figure.

Genotyping and generation of HD patient-derived neuronal cultures heterozygous for ΔACTT

To gain more insights into the efficacy and allele-selectivity of lowering endogenous mutant HTT by the miACTT2-451 construct, we took advantage of recent protocols that enable generation of HD neuronal cultures from HD-derived iPSCs (**Figure 5a**). These iPSCs are reprogrammed from fibroblasts isolated from HD patients and can be differentiated into several neuronal lineages. To date, no HD-derived iPSCs have been reported to be heterozygous for ΔACTT. To identify candidate iPSCs for generation of HD neuronal cultures heterozygous for ΔACTT, seven different HD fibroblast cell lines were tested for ΔACTT heterozygosity: GM02147, GM02155, GM04022, GM04281, GM04717, GM09197, GM21756 (Coriell biorepository) (**Figure 5b**). We identified GM09197 with 180 CAG repeats as the only cell line heterozygous for ΔACTT and obtained iPSCs derived from these cells. As a negative control, not heterozygous for ΔACTT, we selected commonly used iPSCs originating from GM04281 fibroblasts containing 71 CAG repeats. HD neuronal cultures were induced and differentiated from iPSCs that were derived from GM09197 and GM04281 fibroblasts and confirmed differentiation into maturated neuronal cultures using the MAP2 marker (**Figure 5c**). The heterozygosity for ΔACTT in HD neuronal cultures was confirmed by performing RT-qPCRs with custom primers detecting ΔACTT or ACTT polymorphism (**Figure 5d**). We also analyzed the matured neuronal cultures for an additional heterozygous (C/T) SNP rs362307 that is also associated with the A1 haplotype and is localized in the 3'UTR of HTT mRNA. In contrast to the ΔACTT polymorphism, SNP rs362307 is localized in the region that is not spliced and thus, this SNP enabled us to test the allele-specific mutant HTT mRNA knock-

down in both the nucleus and cytoplasm. As expected, we detected the presence of both ACTT/ΔACTT and (C/T) rs362307 polymorphisms in neuronal cultures containing 180 CAGs (CAG180), but not in the neuronal cultures with 71 CAGs (CAG71).

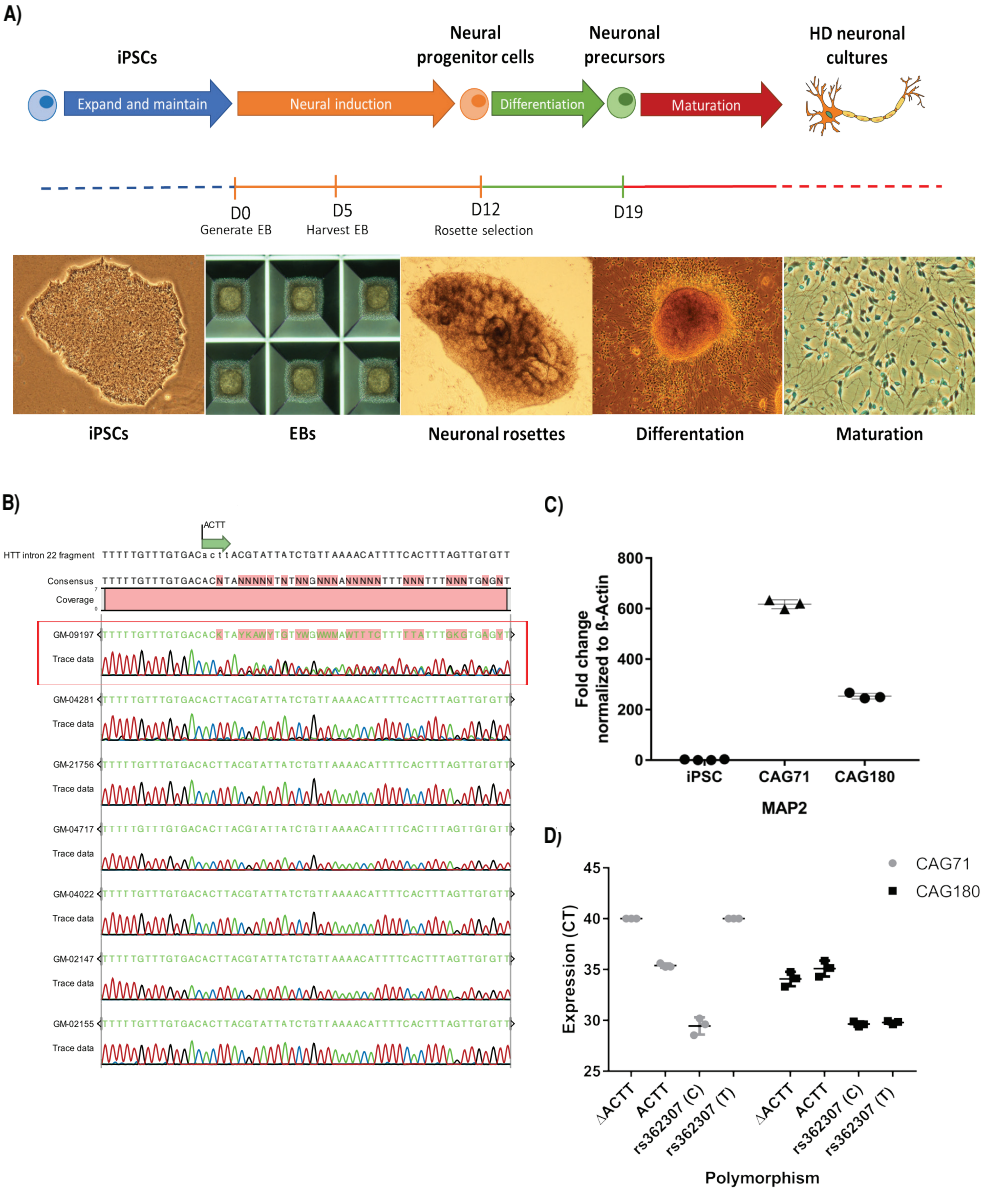


Figure 5. GM09197 fibroblasts are heterozygous for ΔACTT and identify a source of iPSCs to generate HD neuronal cultures heterozygous for ΔACTT. (A) An outline of a generation of matured HD-derived neuronal cultures from iPSCs. **(B)** Sanger sequencing of DNA isolated form seven HD fibroblast cell lines: GM02147, GM02155, GM04022, GM04281, GM04717, GM09197, GM21756. The region of interest is the sequence in HTT intron 22 containing ACTT/ΔACTT polymorphism. GM09197 positive for ΔACTT is highlighted in red. **(C)** MAP2 immunostainings of two-week matured CAG71 and CAG180 neuronal cultures. **(D)** RT-qPCR using custom TaqMan probes to evaluate ACTT/ΔACTT or (C/T) rs362307 heterozygosity in matured CAG71 and CAG180 neuronal cultures.

AAV5-miACTT2-451 construct induced nuclear HTT lowering in HD neuronal cultures. To evaluate the efficacy of endogenous mutant HTT lowering in HD neuronal cultures by the miACTT2-451, we generated an AAV5 virus to deliver the miACTT2-451 expression cassette, named AAV5-miACTT2-451. Three different doses of AAV5-miACTT2-451 (1e10, 1e11, and 1e12 total genomic copies (gc)) were used to transduce two-week matured CAG71 and CAG180 neuronal cultures (**Figure 6a**). Ten days post-transduction, we analyzed the transduction efficacy by measuring mature miACTT2 expression in the total cell lysates and separately in the cytoplasm and nucleus of CAG180 cells. We detected a dose-dependent increase of mature miACTT2-451 levels in the total cell lysates isolated from CAG71 and CAG180 cells (**Figure 6b**). We observed higher transduction efficacy of CAG71 cells compared with CAG180 cells. Mature miACTT2-451 molecules were ˜3 times more abundant (fold change ˜670) in the cytoplasm of CAG180 cells compared with the nuclear fraction (fold change ˜200), when normalized to the negative saline control (**Figure 6c**). To address the allele-selective mRNA knock-down by AAV5-miACTT2-451 constructs, we performed TaqMan mRNA assays (**Figure 6d**). We observed ˜40% selective mutant HTT mRNA knock-down at the highest dose of 1e12 gc AAV5-miACTT2-451. Ultimately, we addressed the mutant HTT protein knock-down in both CAG71 and CAG180 cells by Singulex assay (**Figure 6e**). All doses induced strong 50-60% mutant HTT knock-down in CAG180 cells and 5-10% knock-down in CAG71 cells. Hence, this is a first report suggesting that artificial miRNAs can be active in the nucleus and can lower the expression of a disease gene in human HD neuronal cultures.

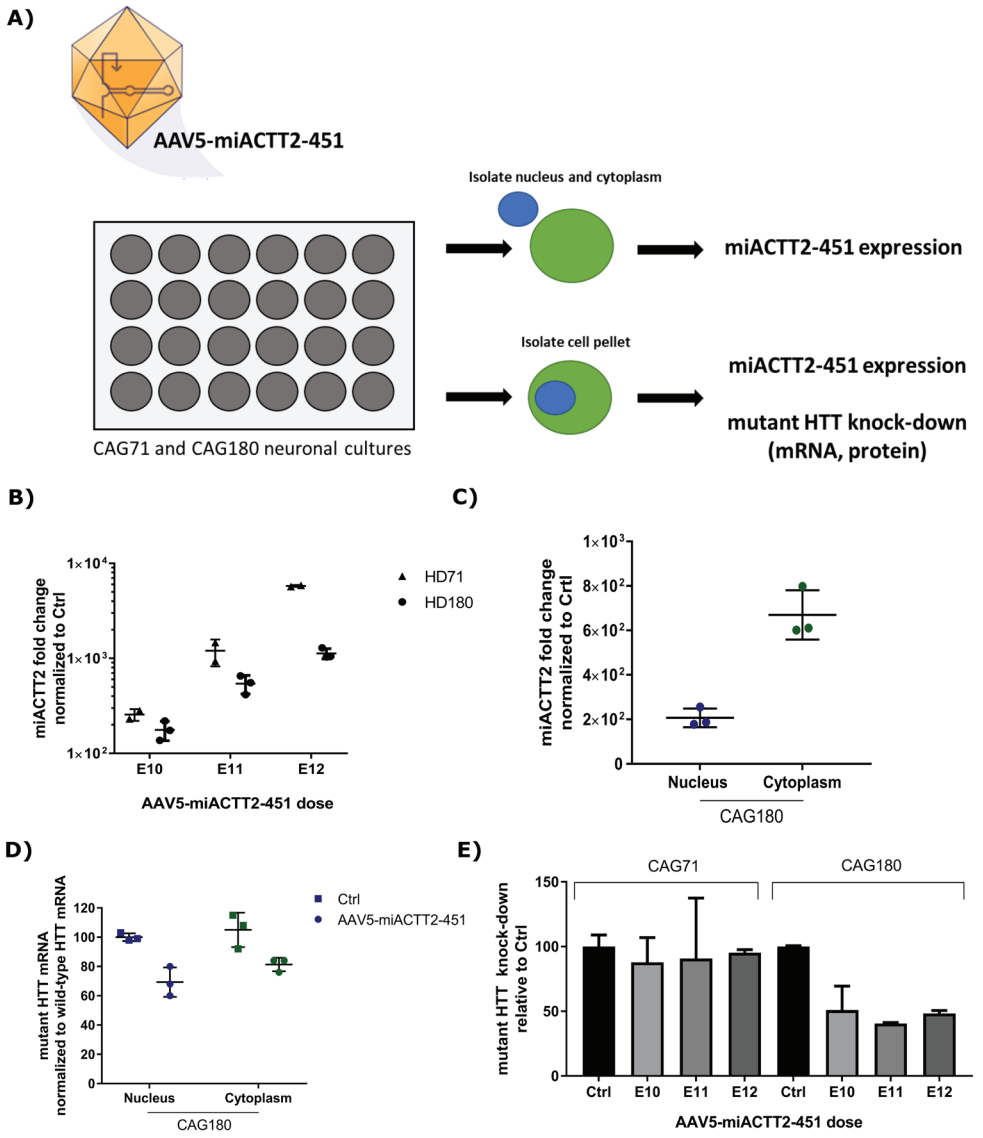


Figure 6. The mutant HTT lowering induced by the AAV5-miACTT2-451 construct in CAG180 neuronal cultures. **(A)** The experimental outline of AAV5 transductions and downstream analysis. **(B)** The miACTT2 expression in CAG71 and CAG180 cells transduced with E10, E11, and E12 genomic copies of AAV5-miACTT2-451 measured by small RNA TaqMan RT-qPCR. miACTT2 values are presented as a distribution plot with the mean of the values following normalization to U6 levels. **(C)** The miACTT2 expression in nucleus and cytoplasm of CAG180 cells transduced with E12 genomic copies of AAV5-miACTT2-451 measured by small RNA TaqMan RT-qPCR. The miACTT2 values are presented as a distribution plot with the mean of the values following normalization to U6 levels. (**D**) The mutant HTT mRNA knock-down in CAG180 cells measured by RT-qPCR using primers detecting (C/T) rs362307 heterozygosity. (**E**) Mutant HTT protein knock-down in CAG71 and CAG180 cells measured by Singulex SMC Immunoassay.

DISCUSSION

We here report an evidence of the allele-specific nuclear mutant HTT lowering by artificial miACTT1 and miACTT2 constructs, processed from the pre-miR-101 and pre-miR-451 precursors respectively, and targeting sequences in HTT intron 22 with ΔACTT (rs72239206) polymorphism. We detected mature miACTT1 and miACTT2 sequences in the nucleus and cytoplasm of HEK293T cells. In HD neuronal cultures heterozygous for ΔACTT, the miACTT2-451 construct delivered by the AAV5 vectors resulted in the selective lowering of mutant HTT mRNA and protein. This is a first evidence suggesting that artificial miRNAs can be designed to lower disease-related transcripts in the nucleus and supports further investigations.

There is accumulating evidence that cellular miRNAs and RISC proteins are present and active in the nucleus in many cells types.[35] Several profiling studies have shown that hundreds of miRNAs are present in the nucleus of human neural stem cells, rat neurons, and cancerous cell lines such as HeLa.[29,36,37] In general, nuclear miRNAs have been found two- or four-fold less abundant in the nucleus when compared with the cytoplasm.[28] This is consistent with our current results from HD neuronal cultures, where we found approximately three-fold lower miACTT2 concentrations when compared with the cytoplasm. However, the nuclear concentration of miACTT2 was sufficient to induce 50-60% lowering of mutant HTT protein. Noteworthy, we did not detect a strong HTT mRNA knock-down, which might be reflected by the experimental errata and further experiments are required to address levels of HTT mRNA knock-down in this setting.

miRNAs are a class of small RNAs known to regulate gene expression primarily in the cytoplasm by binding to transcripts and inducing either their degradation or translational repression.[38,39] In the canonical pathway, miRNA processing is initiated in the nucleus where the long pri-miRNA precursor is expressed and processed by Drosha to generate a shorter stem-loop pre-miRNA precursor.[40] The pre-miRNA is subsequently exported out of the nucleus by Exportin 5.[41] In the cytoplasm, a majority of pre-miRNA loops are cleaved by Dicer to generate a double-stranded mature miRNA that is analogous to an siRNA.[42,43] Based on the thermodynamic properties of the 5'ends of the double-stranded miRNA molecules, the passenger strand is selected and degraded by AGO2, enabling the guide strand to be functionally active.[44] In the noncanonical pathway, that has been so far reported for the pre-miR-451 scaffold, the pre-miR-451 stem loop is recognized directly by AGO2, cleaved precisely to generate a thirty-nucleotide long guide molecule and trimmed by PARN to further render a mature miR-451 guide strand.[33,34,45] The non-canonical pathway does not generate a passenger strand and thus, the pre-miR-451 scaffold has been recently proposed by several groups, including ours, for the miRNA and shRNA design since it limits the off-target effects by the passenger strand.[11,46,47] The target recognition and lowering efficacy between miRNA and target mRNA is based on the sequence and level of base-pair

complementarity.[48] In this study, we designed miACTT1 and miACTT2 constructs that have a perfect complementarity with HTT intron 22 carrying ΔACTT and a four-nucleotide mismatch when binding to HTT intron 22 carrying ACTT. Both miACTT constructs showed strong allele selectivity with miACTT1 constructs being slightly more efficient. This can reflect 3'end position of the miACTT1 binding to ΔACTT, which is consistent with our previous studies showing that the terminal binding to the polymorphism can enhance the allele-selectivity.[11] The miACTT2 construct processed from the pre-miR-451 scaffold showed stronger allele-selectivity of luciferase reporter mRNA in the nucleus, when compared to pre-miR-101 scaffold, and no passenger strand, which strongly supports the use of miR-451 scaffold for the therapeutic purposes.

Currently, the most advanced approaches of HTT lowering, including the first clinical trial initiated in 2015 (NCT02519036), target both HTT alleles and thus, provide a potential therapy for all HD patients. Lowering of both HTT alleles by antisense oligonucleotides or RNAi molecules has been shown so far to be an effective HTT-lowering approach and no adverse effects have been observed in in HD rodent or large animal models.reviewed[17,24,49,50] The ultimate goal of a personalized gene therapy by the selected miACTT2-451 construct is to exclusively lower the expression of the mutant HTT in HD patients and thus, to limit the potential safety concerns of non-selective HTT lowering. The preclinical development of a personalized gene therapy for HD requires to address the efficacy and safety of a therapeutic product in animals before entering the clinic. Although HD animal models are plentiful and commonly used for preclinical testing, the intronic ΔACTT mutation has been only recently discovered and no heterozygous animal model is available. HD patient-derived induced pluripotent stem cells (iPSCs) have emerged as a new disease model which more closely represent the disease genetic background as compared to HD rodents and large animals.[51] In this study, we have demonstrated the feasibility of selective mutant HTT lowering by miACTT2-451 construct delivered by the AAV5 vector in HD neuronal cultures heterozygous for ΔACTT. These results support further investigations using additional controls to provide the proof of mechanism and activity for the concept of miRNA-based transcript lowering in the nucleus.

MATERIAL AND METHODS

DNA plasmids

To generate the miACTT constructs, miACTT1 and miACTT2 guide sequences targeting HTT intron 22 pre-mRNAs were incorporated in the cellular pre-miRNA scaffolds of the human miR-101-1, miR-122, miR-135b, miR-155, and miR-451a scaffolds. 200 nucleotide-long 5' and 3' encompassing flanking regions were included with EcoRV and BamHI restriction sites and the full sequences were ordered from GeneArt® gene synthesis (Invitrogen, Carlsbad, CA). The constructs were expressed from the CAG promoter (Inovio, Plymouth Meeting, PA). The Mfold web server (http://mfold.rna.albany.edu/?q=mfold) was used to determine the pre-miACTT folding. For the generation of Luc-ACTT and Luc-ΔACTT, a complete HTT intron 22 sequences containing either ACTT or ΔACTT, respectively, were cloned in the 3'UTR of the renilla luciferase gene of the psiCHECK-2 vector (Promega, Madison, WI, USA).

AAV5 vector production

The AAV5-miACTT2 construct was produced by baculovirus-based AAV production system (uniQure, Amsterdam, The Netherlands) as previously described.[10] The miACTT2-451 expression cassette was inserted in a recombinant baculovirus vector by homologous recombination. The recombinant baculovirus was further amplified till the passage 6 and clones were screened for the best production and stability by PCR and qPCR. To generate AAV5, infections with different recombinant baculoviruses containing the vector genome, the replicon enzyme and the capsid protein were performed as described previously.[10]

Transfections of HEK293T cells

HEK293T cells were maintained at 37°C and 5% CO2 in Dulbecco's modified Eagle's medium (DMEM; Invitrogen) containing 10% fetal calf serum, 100 U/ml penicillin, and 100 U/ml streptomycin. For luciferase assays, cells were seeded in 24-well plates at $1.2*10^5$ per well and co-transfections were performed at 1:1 reporter:miACTT ratios. For qPCRs, HEK293T cells were seeded in 6-well plates at $0.5*10^5$ cells per well and co-transfections were performed at 2:1 reporter:miACTT ratios. For the next generation sequencing analysis, cells were seeded in 6-well plates at $0.5*10^5$ cells per well and 4µg of miACTT1-101 or miACTT2-451 was used for transfections. All transfections were performed with OptiMEM and Lipofectamine 2000 reagent according to manufacturer's instructions (Invitrogen).

Luciferase assays

The luciferase assays were performed using Dual-Luciferase Reporter Assay System, according to the manufacturer's instructions (Promega, Madison, WI, USA). Two days post-transfection, HEK293T cells were lysed in 100µl 1x passive lysis buffer by gentle rocking for 15min at room temperature. The cell lysates were centrifuged for 5min at 4000rpm and

10µl of the supernatant was used to measure renilla and firefly activities. Relative luciferase activity was calculated as the ratio between renilla and firefly signals.

Separation of the nucleus and cytoplasm

Two days post-transfection, the nucleus and cytoplasm were separated using Nuclei EZ Prep Isolation Kit according to the manufacturer's instructions (Sigma-Aldrich, St. Louis, Missouri, USA). Cells were washed with cold Dulbecco's PBS (Life Technologies, Carlsbad, CA, USA) and lysed using 500 µl of Nuclei EZ lysis buffer. Nuclei were harvested by centrifugation at 500 x g for 5mins at 4°C. A supernatant containing the cytoplasmic fraction was collected in a separate tube and nuclei pellet was additionally washed with lysis buffer in order to remove cytoplasmic residues. Both nuclei and cytoplasmic fractions were ultimately resuspended in appropriate buffers and stored at -80°C.

Next generation sequencing

Two days post-transfection, RNA was isolated from cells using Trizol according to the manufacturer's protocol (Invitrogen). Small RNA sequencing libraries for the Illumina sequencing platform were generated using the NEXTflex Small RNA Sequencing kit (Bioo Scientific, Austin, TX, USA). The libraries were multiplexed, clustered, and sequenced on an Illumina HiSeq 2000 (TruSeq v3 chemistry) with a single-read 36 cycles sequencing protocol and indexing. The sequencing run was analyzed with the Illumina CASAVA pipeline (v1.8.2) with demultiplexing based on sample-specific barcodes. The raw sequencing data produced was processed removing the sequence reads which were of too low quality (only "passing filter" reads were selected). In total, we generated between 7-12 million reads per sample. The raw sequencing data were produced as previously described.[11] Small RNA raw data sets were analyzed using the CLC Genomics Workbench 6 (Qiagen, Hilden, Germany). The obtained unique small RNA reads were aligned to the reference sequences of the pre-miACTT1-101 and pre-miACTT2-451 constructs with a max. of three nucleotide mismatches allowed. The percentages of reads based on the total number of reads matching the reference sequences were calculated.

PCR and quantitative PCR

Two days post-transfection, RNA was isolated from cells using Trizol according to the manufacturer's protocol (Invitrogen). To remove genomic DNA, RNA was treated with dsDNase (Thermo Scientific, Waltham, MA, USA). To measure mRNA knock-down and determine MAP2 expression, cDNA was generated using Maxima Synthesis Kit (Thermo Scientific). cDNA was analyzed by qPCR using custom probes named Ren/Intron* and Intron* and human GAPDH Hs02758991_g1 (Thermo Scientific). Maturation status of neuronal cultures was evaluated by measuring expression of genes associated with neural development using TaqMan qPCR for detection of MAP2 Hs00258900_m1 (Thermo

Scientific). To detect miACTT expression levels, RT-PCR and RT-qPCR were performed using TaqMan Fast Universal kit (Thermo Scientific). U6 snRNA (001973, Applied Biosystems) and custom miACTT probes for detection of mature miACTT1-101 and miACTT2-451 sequences were used (Thermo Scientific). The expression level of each gene was normalized to either endogenous GAPDH or U6 snRNA levels. Fold changes, percentages in mRNA knock-down, or miRNA expression were calculated based on 2^ΔΔCT method.

Protein isolation and western blotting

Protein content from nuclear and cytoplasmic fractions was isolated using RIPA lysis buffer (Sigma-Aldrich) supplemented with protein inhibitor cocktail (cOmplete™ ULTRA Tablet; Roche, Basel, Switzerland). Total protein concentration was quantified using a Bradford Protein Assay (Bio-Rad, Hercules, CA, USA) and absorbance was measured at 600 nm on the GloMax Discover System (Promega). Equal amounts of sample protein (10-30 µg) were incubated with β-mercaptoethanol and Laemmli buffer at 95°C for 5 min and separated using 4-20% Mini-Protean TGX Stain-Free Protein Gel (Bio-Rad). Samples were transferred to PVDF membranes by Trans-Blot Turbo Transfer system (Bio-Rad) using the "Mixed MW" protocol. Blot was incubated with 3% Blotting-Grade blocker (Bio-Rad) in 1x Tris Buffered Saline (TBS) for 1 hour at room temperature, followed by immunoblotting with selected primary antibody overnight at 4°C. Primary antibodies include the following: CD63 (System Biosciences), b-tubulin (Abcam), Actin (Abcam), Lamin B1 (Abcam) at 1:1000 dilution. Chromogenic signals were detected after 2 hours incubation with HRP-conjugated secondary antibodies (goat anti-rabbit, Abcam, 1:20000 or rabbit anti-mouse, Dako, Denmark, 1:20000) and 5 min incubation with SuperSignal Pico sensitivity Substrate (ThermoScientific) using ChemiDoc Touch Gel Imaging System (Bio-Rad).

Differentiation of forebrain HD neuronal cultures from human HD iPSCs

HD iPSCs (CS97iHD-180n2) containing 180 CAG repeats were ordered from (Cedars-Sinai Medical Center, Los Angeles, CA, USA). These cells were generated from human HD fibroblasts GM09197 (Coriell Institute Stem Biobank, New Jersey, USA) reprogrammed with six factors (OCT4, SOX2, KLF4, LMYC, LIN28, shRNA to P53) using episomal vectors. As a negative control, HD iPSCs (ND42229*B) containing 71 CAG repeats were ordered from (Coriell Institute Stem Biobank). These cells were generated from human HD fibroblasts GM04281 (Coriell Institute Stem Biobank) reprogrammed with six factors (OCT4, SOX2, KLF4, LMYC, LIN28, shRNA to P53) using episomal vectors. iPSCs were maintained on matrigel coating with mTeSR medium for several passages, following the manufacturer's instructions (StemCell Technologies, Vancouver, Canada). Non-differentiated colonies were released using ReLeSR reagent during each passage and diluted 1:5-20 (StemCell Technologies). For the neural induction, cells were plated onto AggreWellTM 800 plate at day 0 as 3x106 cells per well in STEMdiff™ Neural Induction Medium (StemCell Technologies). At day 5, embryoid

bodies were formed and replated onto poly-D-lysine/laminin coated 6-well plates. Coating was prepared with poly-D-lysine hydrobromide (0,1 mg/mL) and Laminin from Engelbreth-Holm-Swarm murine (0,1 mg/ml) (Sigma-Aldrich). At day 12, the neuronal rosettes were selected using STEMdiff™ Neural Rosette Selection Reagent (StemCell Technologies) and replated in poly-D-lysine/laminin coated plates. Next day, differentiation of neural progenitor cells was initiated using STEMdiff™ Neuron Differentiation Kit (StemCell Technologies). From day 19, cells were matured using STEMdiff™ Neuron Maturation Kit for a minimum of two weeks (StemCell Technologies).

SMC immunoassay for the mutant HTT protein quantification

Protein lysates were resuspended in dilution buffer (50 µl/well) containing 6% BSA, 0.8% Triton X-100, 750 mM NaCl, and complete protease inhibitor (catalog 04693116001; Roche) and added to a 96-conical assay plate (catalog P-96-450V-C; Axygen). MAB2166 antibody (Merck Millipore) diluted to 1:1000 with Erenna Assay Buffer (02-0474-00; Singulex) coupled with magnetic particles (03-0077-02; Singulex) at a ratio of 25 µg antibody per milligram magnetic particles was added to the plate and shaking (600 rpm; Heidolph Titramax 1000 Microplate Shaker) at room temperature for 1 hour. The plate was placed on a magnetic rack and washed four times with 200 µl 1× washing buffer (02-0111-00; Singulex). 20 µl/well of 0.5 ng/µl diluted MW1 detection antibody labeled with detection fluorophore (catalog 03-0076-02; Singulex) at a ratio of 15.7 pmol fluorophore per micrgram MW1 was added to the plate. The plate was incubated shaking (750 rpm) at room temperature for 1 hour. Plates were washed, and the antibody-antigen complex was transferred to a new 96-conical assay plate. After four washes with 200 µl 1× washing buffer and aspiration, elution buffer (acidic glycine solution, 0.1 M, pH 2.7) was added to the plate, and the plate was incubated shaking (1,000 rpm) for 5 minutes. The eluted detection antibody was transferred to a Nunc 384-well analysis plate (catalog 264573; Sigma-Aldrich) and neutralized with neutralization buffer (Tris, 1 M, pH 9). The analysis plate was spun down, sealed, and subsequently analyzed with the Erenna Immunoassay System (Singulex).

Statistics

Data were analyzed using un-paired Student's t-test (for two groups) or one-way ANOVA (for three or more groups) to determine statistically significances between samples. Tukey's post hoc test (α=0.05) was applied to analyzed differences between relevant groups. P-values are represented as: *p<0.05; **p<0.01; ***p<0.001; ****p<0.0001.

REFERENCES

1. Rawlins, MD, Wexler, NS, Wexler, AR, Tabrizi, SJ, Douglas, I, Evans, SJW, *et al.* (2016). The prevalence of huntington's disease. *Neuroepidemiology* **46**: 144–153.
2. Macdonald, ME, Ambrose, CM, Duyao, MP, Myers, RH, Lin, C, Srinidhi, L, *et al.* (1993). A Novel Gene Containing a Trinucleotide That Is Expanded and Unstable on Huntington's Disease Chromosomes. *Cell* **72**: 971–983.
3. Saudou, F and Humbert, S (2016). The Biology of Huntingtin. *Neuron* **89**: 910–926.
4. Bates, GP, Dorsey, R, Gusella, JF, Hayden, MR, Kay, C, Leavitt, BR, *et al.* (2015). Huntington disease. *Nat. Rev. Dis. Prim.* **1**: 1–21.
5. Marques Sousa, C and Humbert, S (2013). Huntingtin: Here, there, everywhere! *J. Huntingtons. Dis.* **2**: 395–403.
6. Ross, CA, Aylward, EH, Wild, EJ, Langbehn, DR, Long, JD, Warner, JH, *et al.* (2014). Huntington disease: natural history, biomarkers and prospects for therapeutics. *Nat. Rev. Neurol.* **10**: 204–16.
7. Mestre, TA and Sampaio, C (2017). Huntington Disease: Linking Pathogenesis to the Development of Experimental Therapeutics. *Curr. Neurol. Neurosci. Rep.* **17**: 1–8.
8. Difiglia, M, Sapp, E, Chase, KO, Davies, SW, Bates, GP, Vonsattel, JP, *et al.* (1997). Aggregation of huntingtin in neuronal intranuclear inclusions and dystrophic neurites in brain. *Science (80-.).* **277**: 1990–3.
9. Davies, SW, Turmaine, M, Scherzinger, E, Wanker, EE, Mangiarini, L and Bates, GP (1997). Formation of Neuronal Intranuclear Inclusions Underlies the Neurological Dysfunction in Mice Transgenic for the HD Mutation. *Cell* **90**: 537–548.
10. Miniarikova, J, Zimmer, V, Martier, R, Brouwers, CC, Pythoud, C, Richetin, K, *et al.* (2017). AAV5-miHTT gene therapy demonstrates suppression of mutant huntingtin aggregation and neuronal dysfunction in a rat model of Huntington's disease. *Gene Ther.* **24**: 630–639.
11. Miniarikova, J, Zanella, I, Huseinovic, A, van der Zon, T, Hanemaaijer, E, Martier, R, *et al.* (2016). Design, Characterization, and Lead Selection of Therapeutic miRNAs Targeting Huntingtin for Development of Gene Therapy for Huntington's Disease. *Mol. Ther. Acids* **5**: e297.
12. Southwell, AL, Skotte, NH, Kordasiewicz, HB, Ostergaard, ME, Watt, AT, Carroll, JB, *et al.* (2014). In vivo evaluation of candidate allele-specific mutant huntingtin gene silencing antisense oligonucleotides. *Mol. Ther.* **22**: 2093–2106.
13. Harper, SQ, Staber, PD, He, X, Eliason, SL, Martins, IH, Mao, Q, *et al.* (2005). RNA interference improves motor and neuropathological abnormalities in a Huntington's disease mouse model. *Proc. Natl. Acad. Sci. U. S. A.* **102**: 5820–5825.
14. Sánchez, I, Mahlke, C and Yuan, J (2003). Pivotal role of oligomerization in expanded polyglutamine neurodegenerative disorders. *Nature* **421**: 373–379.
15. Ehrnhoefer, DE, Sutton, L and Hayden, MR (2011). Small changes, big impact: Posttranslational modifications and function of huntingtin in Huntington disease. *Neuroscientist* **17**: 475–492.
16. Kim, YJ, Yi, Y, Sapp, E, Wang, Y, Cuiffo, B, Kegel, KB, *et al.* (2001). Caspase 3-cleaved N-terminal fragments of wild-type and mutant huntingtin are present in normal and Huntington's disease brains, associate with membranes, and undergo calpain-dependent proteolysis. *Proc. Natl. Acad. Sci. U. S. A.* **98**: 12784–12789.
17. Wild, EJ and Tabrizi, SJ (2017). Therapies targeting DNA and RNA in Huntington's disease. *Lancet Neurol.* **16**: 837–847.
18. Evers, MM, Toonen, LJA and van Roon-Mom, WMC (2015). Antisense oligonucleotides in therapy for neurodegenerative disorders. *Adv. Drug Deliv. Rev.* **87**: 90–103.

19. Chery, J (2016). RNA therapeutics: RNAi and antisense mechanisms and clinical applications. *Postdoc J.* **4**: 35–50.
20. Miniarikova, J, Evers, MM and Konstantinova, P (2018). Translation of MicroRNA-Based Huntingtin-Lowering Therapies from Preclinical Studies to the Clinic. *Mol. Ther.* **26**: 947–962.
21. Kantor, B, McCown, T, Leone, P and Gray, SJ (2014). *Clinical applications involving CNS gene transfer*. *Adv. Genet.* **87**, Elsevier, 71-124pp.
22. Drouet, V, Perrin, V, Hassig, R, Dufour, N, Auregan, G, Alves, S, *et al.* (2009). Sustained effects of nonallele-specific Huntingtin silencing. *Ann. Neurol.* **65**: 276–85.
23. Cambon, K, Zimmer, V, Martineau, S, Gaillard, M, Jarrige, M, Bugi, A, *et al.* (2017). Preclinical Evaluation of a Lentiviral Vector for Huntingtin Silencing. *Mol. Ther. Methods Clin. Dev.* **5**: 259–276.
24. McBride, JL, Pitzer, MR, Boudreau, RL, Dufour, B, Hobbs, T, Ojeda, SR, *et al.* (2011). Preclinical Safety of RNAi-Mediated HTT Suppression in the Rhesus Macaque as a Potential Therapy for Huntington's Disease. *Mol. Ther.* **19**: 2152–2162.
25. Stiles, DK, Zhang, Z, Ge, P, Nelson, B, Grondin, R, Ai, Y, *et al.* (2012). Widespread suppression of huntingtin with convection-enhanced delivery of siRNA. *Exp. Neurol.* **233**: 463–471.
26. Rasko, JEJ and Wong, JJ (2017). Nuclear microRNAs in normal hemopoiesis and cancer. *J. Hematol. Oncol.*: 1–8doi:10.1186/s13045-016-0375-x.
27. Jeffries, CD, Fried, HM and Perkins, DO (2011). Nuclear and cytoplasmic localization of neural stem cell microRNAs. *RNA* **17**: 675–686.
28. Roberts, TC (2014). The MicroRNA Biology of the Mammalian Nucleus. *Mol. Ther. - Nucleic Acids* **3**: e188.
29. Liao, JY, Ma, LM, Guo, YH, Zhang, YC, Zhou, H, Shao, P, *et al.* (2010). Deep sequencing of human nuclear and cytoplasmic small RNAS reveals an unexpectedly complex subcellular distribution of mirnas and tRNA 3' trailers. *PLoS One* **5**: e10563.
30. Redfern, AD, Colley, SM, Beveridge, DJ, Ikeda, N, Epis, MR, Li, X, *et al.* (2013). RNA-induced silencing complex (RISC) Proteins PACT, TRBP, and Dicer are SRA binding nuclear receptor coregulators. *Proc. Natl. Acad. Sci. U. S. A.* **110**: 6536–41.
31. Wexler, NS, Young, AB, Tanzi, RE, Travers, H, Starosta-Rubinstein, S, Penney, JB, *et al.* (1987). Homozygotes for Huntington's disease. *Nature* **326**: 194–7.
32. Kay, C, Skotte, N, Southwell, A and Hayden, M (2014). Personalized gene silencing therapeutics for Huntington disease. *Clin. Genet.* **86**: 29–36.
33. Cheloufi, S, Dos Santos, CO, Chong, MMW and Hannon, GJ (2010). A dicer-independent miRNA biogenesis pathway that requires Ago catalysis. *Nature* **465**: 584–589.
34. Cifuentes, D, Xue, H, Taylor, DW, Patnode, H, Mishima, Y, Cheloufi, S, *et al.* (2010). A novel miRNA processing pathway independent of Dicer requires Argonaute2 catalytic activity. *Science* **328**: 1694–1698.
35. Gagnon, KT, Li, L, Chu, Y, Janowski, BA and Corey, DR (2014). RNAi Factors are Present and Active in Human Cell Nuclei. *Cell Rep.* **6**: 211–221.
36. Jeffries, CD, Fried, HM and Perkins, DO (2011). Nuclear and cytoplasmic localization of neural stem cell microRNAs. *Spring*: 675–686doi:10.1261/rna.2006511.44.
37. Khudayberdiev, SA, Zampa, F, Rajman, M and Schratt, G (2013). A comprehensive characterization of the nuclear microRNA repertoire of post-mitotic neurons. *Front. Mol. Neurosci.* **6**: 1–19.
38. Gurtan, AM and Sharp, PA (2013). The role of miRNAs in regulating gene expression networks. *J. Mol. Biol.* **425**: 3582–3600.
39. Lochmatter, D and Mullis, P-E (2011). RNA interference in mammalian cell systems. *Horm. Res. pædiatrics* **75**: 63–9.

40. Han, J, Lee, Y, Yeom, K-H, Kim, Y-K, Jin, H and Kim, VN (2004). The Drosha-DGCR8 complex in primary microRNA processing. *Genes Dev.* **18**: 3016–27.

41. Bohnsack, MT, Czaplinski, K and Görlich, D (2004). Exportin 5 is a RanGTP-dependent dsRNA-binding protein that mediates nuclear export of pre-miRNAs Exportin 5 is a RanGTP-dependent dsRNA-binding protein that mediates nuclear export of pre-miRNAs: 185-191doi:10.1261/rna.5167604.Most.

42. Chendrimada, TP, Gregory, RI, Kumaraswamy, E, Norman, J, Cooch, N, Nishikura, K, *et al.* (2005). TRBP recruits the Dicer complex to Ago2 for microRNA processing and gene silencing. *Nature* **436**: 740–4.

43. Gu, S, Jin, L, Zhang, Y, Huang, Y, Zhang, F, Valdmanis, PN, *et al.* (2012). The loop position of shRNAs and pre-miRNAs is critical for the accuracy of Dicer processing in vivo. *Cell* **151**: 900–911.

44. Meijer, H a, Smith, EM and Bushell, M (2014). Regulation of miRNA strand selection: follow the leader? *Biochem. Soc. Trans.* **42**: 1135–40.

45. Yoda, M, Cifuentes, D, Izumi, N, Sakaguchi, Y, Suzuki, T, Giraldez, AJ, *et al.* (2013). Poly(A)-specific ribonuclease mediates 3'-end trimming of argonaute2-cleaved precursor microrna. *Cell Rep.* **5**: 715–726.

46. Ma, H, Zhang, J and Wu, H (2014). Designing Ago2-specific siRNA/shRNA to Avoid Competition with Endogenous miRNAs. *Mol. Ther. Nucleic Acids* **3**: e176.

47. Harwig, A, Kruize, Z, Yang, Z, Restle, T and Berkhout, B (2017). Analysis of AgoshRNA maturation and loading into Ago2. *PLoS One*: 1–15.

48. Bartel, DP (2009). MicroRNAs: target recognition and regulatory functions. *Cell* **136**: 215–33.

49. Evers, MM, Miniarikova, J, Juhas, S, Vallès, A, Bohuslavova, B, Juhasova, J, *et al.* AAV5-miHTT gene therapy demonstrates broad distribution and strong human mutant huntingtin lowering in a Huntington disease minipig model: Submitted to Neuron.

50. Pfister, E, Dinardo, N, Mondo, E, Borel, F, Conroy, F, Fraser, C, *et al.* (2017). Artificial miRNAs reduce human mutant Huntingtin throughout the striatum in a transgenic sheep model of Huntington's disease. *Hum. Gene Ther.*doi:10.1089/hum.2017.199.

51. Tousley, A and Kegel-gleason, KB (2016). Induced Pluripotent Stem Cells in Huntington's Disease Research : Progress and Opportunity. *J. Huntingtons. Dis.* **5**: 99–131.

5

MATURE MIHTT MOLECULES ARE PRESENT IN VESICLES ENRICHED FOR EXOSOMES AND SECRETED FROM HUNTINGTON'S DISEASE NEURONAL CULTURES TREATED WITH AAV5-MIHTT GENE THERAPY

Jana Miniarikova[1,2], Marina Sogorb-Gonzalez[1,2], Cynthia C. Brouwers[1], Sonay Keskin[1], Astrid Vallès[1], Melvin M. Evers[1], Harald Petry[1], Sander J. van Deventer[1,2], Pavlina Konstantinova[1]

[1]Department of Research & Development, uniQure, Amsterdam, the Netherlands

[2]Department of Gastroenterology and Hepatology, Leiden University Medical Center, Leiden, the Netherlands

ABSTRACT

Huntington's disease (HD) is a fatal neurodegenerative disorder caused by a single mutation in the huntingtin (*HTT*) gene. The resulting mutant HTT protein is considered to be the pathogenic culprit, affecting mainly the striatum and cortex in the HD brain. We have developed a gene therapy approach for HD that is based on a single intra-striatal delivery of an adeno-associated serotype 5 (AAV5) virus carrying an expression cassette of an engineered therapeutic micro (mi)RNA construct targeting HTT exon 1 (miHTT). The preclinical development of HD requires pharmacokinetic/pharmacodynamic (PK/PD) modeling measures and biomarkers from easily obtainable biofluids. More specifically, a PK/PD measure that is informative of the expression of therapeutic miRNA in the brain of AAV5-miHTT-treated patients is needed to enable proper correlations between the treatment dose and efficacy. In recent years, exosomes isolated from biofluids have emerged as carriers of endogenous miRNA-based biomarkers such as miRNAs, long noncoding RNAs, and proteins. In this study, we have investigated the presence of expressed mature miHTT molecules in exosomes secreted from AAV5-miHTT-treated neuronal cultures originating from an HD patient. We confirmed the presence of mature miHTT molecules within vesicles enriched for exosomes and secreted from the HD neuronal cultures. This study indicates that the miHTT may be a suitable PK/PD candidate measure for the AAV5-miHTT gene therapy approach to treat HD. Further ongoing studies addressing the detection of mature miHTT in the cerebrospinal fluid of the AAV5-miHTT-treated cell and animals models will provide more information on the use of therapeutic miRNA as a PK/PD measure for gene therapy approaches.

INTRODUCTION

Huntington's disease (HD) belongs to a group of neurodegenerative disorders commonly referred as proteinopathies, which include also Alzheimer's (AD) and Parkinson's disease (PD).[1] HD is exceptional in that it has an autosomal dominant monogenic cause which offers a unique opportunity for a design of therapeutic strategies that target the pathogenic culprit.[2] HD usually manifests in midlife and potential carriers can be genetically screened, allowing for therapeutic interventions to be applied in the premanifest stages.[3] In HD, the toxic mutant protein is encoded by the huntingtin (*HTT*) gene, and the disease has a full penetrance when the expansion exceeds 39 CAG repeats.[2] Mutant HTT protein has been reported to undergo proteolytic cleavage, posttranslational modifications, and aggregation, which resulted in toxicity when tested in HD animal models.[4] The cell death is a result of prolonged cellular dysfunction caused by the mutant HTT disturbing pathways such as apoptosis, protein degradation, transcription, and mitochondrial activity.[5] Mutant HTT protein is ubiquitously expressed, but the pathology is almost completely restricted to the central nervous system (CNS).[6] The corticostriatal circuitry has been implicated as the most affected brain area in HD neurodegeneration, largely contributing to abnormal body movements, cognitive and psychiatric disturbances.[7] On average, an HD patient dies approximately 15-20 years after onset, in many cases, from fatal aspiration pneumonia.[8] Currently, there is no treatment for HD, but therapies aiming to lower the toxic HTT protein are under development.[9]

The most investigated HTT lowering therapies apply molecules that bind and reduce HTT transcripts (RNA-targeting) either through RNase-H or RNA interference (RNAi) pathways and thus, prevent the formation of the malfunctional protein.[10,11] Current HTT RNA-targeting therapies can be categorized based on the duration of the treatment as short-term and long-term.[9] The first of such clinical trials started in 2015 and delivers antisense oligonucleotides in the cerebrospinal fluid (CSF) of HD patients through lumbar punctures to induce short-term HTT lowering in the CNS (https://clinicaltrials.gov/: NCT02519036). First results from an ongoing phase I/IIa study are encouraging, reporting a reduction of mutant HTT protein in the CSF. However, it remains unknown why the mutant HTT is secreted and from which brain areas the mutant HTT recovered in CSF originates.[12] Other, long-term, HTT RNA-targeting therapies are planned to enter the clinic in a near future. Micro (mi)RNA-based gene therapy approaches are among the most advanced long-term HTT lowering strategies. These are based on the adeno-associated viral (AAV) vector delivery of therapeutic engineered miRNA precursors directly into the CNS to induce a reduction of mutant HTT in the striatum and cortex.[13,14] The therapeutic effect of gene therapy is to be long-term (years) as oppose to antisense technology (months). Recently, we have demonstrated proof-of-principle and proof-of-mechanism for a miHTT construct targeting HTT exon 1, delivered by AAV serotype 5 (AAV5) to the striatum of various HD animal models.[13] Importantly, we have shown a dose-dependent distribution of the AAV5-miHTT in the HD minipig model which correlated with

the observed reduction of the human mutant HTT protein (Evers et al., submitted).

Clinical development of HTT lowering would greatly benefit from biomarkers and pharmacokinetic/pharmacodynamic PK/PD measures, preferably in more easily obtainable biomaterial than brain, which would not only be indicative of disease progression, but also of the treatment efficacy and dose response. Recently, exosomes have been investigated for their potential to carry diagnostic, prognostic and treatment efficacy biomarkers, which can be relatively easily obtained from biofluids such as serum or CSF. Exosomes are lipid bilayer membrane-enveloped nanovesicles of 40-100nm in size, extracellularly released from virtually all cells to all biological fluids, such as CSF, blood, and urine and have been shown to carry a vast number of RNAs, DNAs, and proteins.[15–18] The specific molecular cargo found in distinct exosomes is considered a fingerprint of the exosome-releasing cell.

Exosomes carry RNA species, including mRNAs, rRNAs, miRNAs, long non-coding RNA, and other small non-coding RNAs.[17,19] Next generation sequencing (NGS) analysis of plasma-derived exosomal RNAs suggests that miRNAs are the most enriched exosomal RNAs.[20] Some miRNAs are more abundant in the exosomes than others.[21,22] The composition and sorting of miRNAs in the exosomes is complex with constantly emerging new data and insights. For instance, in human B cells, 3' end-uridylated miRNAs were more abundant in the exosomes as compared with 3' end-adenylated miRNAs, which implies that post-transcriptional modifications might influence the sorting of miRNAs into the exosomes.[23] Chaperones that recognize specific miRNA sequence motifs may also control the loading of miRNAs into the exosomes.[24] Squadrito et al. recently demonstrated that the presence of the miRNA in the exosomes is influenced by the abundance of endogenous target mRNAs and the relative miRNA:target concentrations.[25] Overexpressing of artificial miRNAs in macrophages promotes sorting of the artificial miRNAs into the exosomes. Interestingly, overexpressed artificial miRNAs present in secreted exosomes may be functionally active in the recipient cells.[26–30]

As a first step to develop an AAV5-miHTT-specific PK/PD measure, we have investigated the presence of therapeutic miHTT in exosomes secreted by AAV5-miHTT-transduced HD patient-derived neuronal cultures. For this purpose, we generated and characterized HD patient induced pluripotent stem cells (iPSCs)-derived neuronal cultures carrying 71 CAG repeats. First, we established the efficacy of AAV5-miHTT in these human cells by measuring the HTT mRNA and protein lowering two weeks post-transduction. The processing patterns of the pre-miHTT precursor were analyzed using NGS to identify the most abundant mature miHTT guide sequence for further design of TaqMan detection probes. We then analyzed the miHTT abundance in exosomes isolated from the medium of HD neuronal cultures that were transduced with the AAV5-miHTT construct. Our results suggest that an exosomal miRNA-based test may be developed as a surrogate PK/PD marker in patients treated with the AAV5-miHTT.

RESULTS

Generation and characterization of mature HD patient-derived neuronal cultures

To established that miHTT molecules are secreted within the vesicles enriched for exosomes HD patient cells, we generated human HD patient-derived neuronal cultures from iPSCs. HD iPSCs were expanded, differentiated and matured into forebrain neurons through a process that comprises all major stages of neuronal development from stem cells, neuronal progenitor cells to mature neurons (**Figure 1a**). To characterize two-week matured neuronal cultures, we performed immunofluorescence cytochemistry. A general cellular marker α-tubulin was used to identify cells (**Figure 1b**). To detect matured neuronal cells and astrocytes, we stained for microtubule-associated protein 2 (MAP2) and glial fibrillary acidic protein (GFAP), respectively (**Figure 1c**). Both neurons and astrocytes were detected in all neuronal cultures, estimated at 50% respectively. The maturation status was further evaluated by measuring the expression of genes that are exclusively active in the matured neurons by TaqMan quantitative polymerase chain reaction (qPCR). Being involved in dendritic and axonal development, MAP2 and tubulin beta class III (TUBB3) have been used extensively as markers of mature neuronal cells. Significantly higher levels of MAP2 (48.7-fold, $p<0.05$) and TUBB3 (5.8-fold, $p<0.05$) were observed in two-week matured neuronal cultures when compared with iPSCs of their origin (n=2-3) (**Figure 1d**).

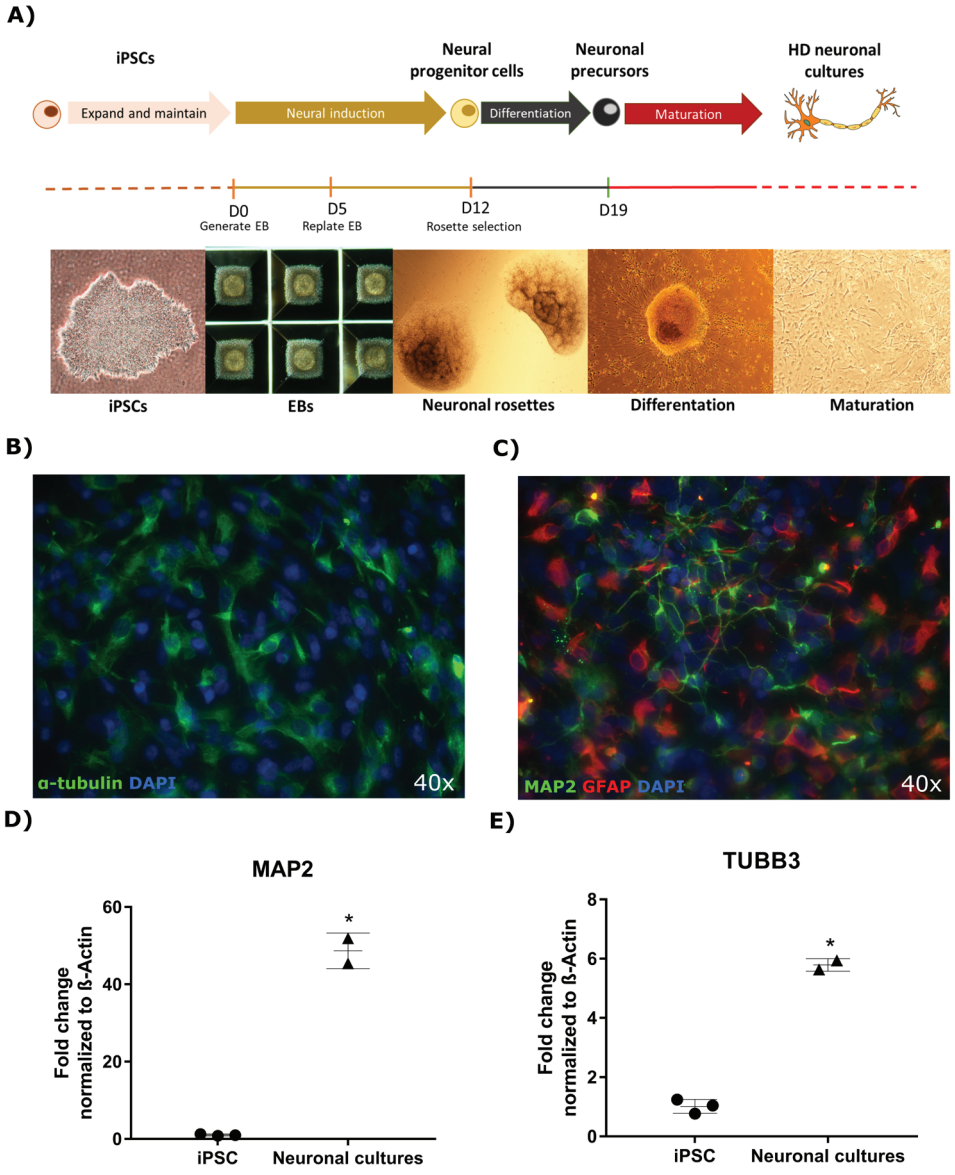
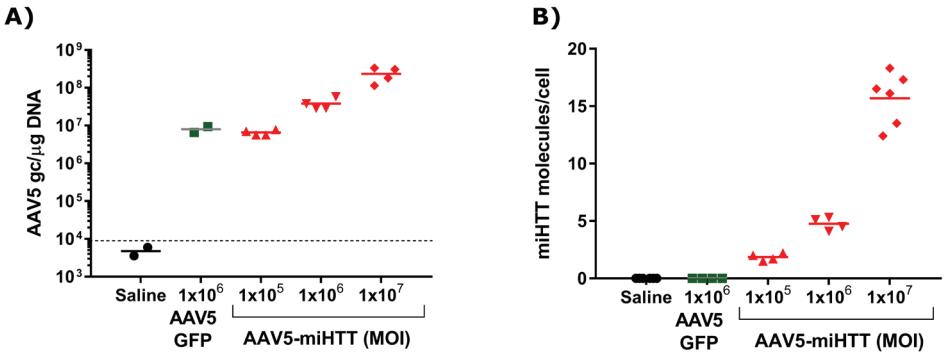


Figure 1. iPSC-derived HD neuronal cultures express the neural maturation markers. (**A**) Schematic representation of a standardized protocol that describes a generation of embryoid bodies (EB) from HD patient-derived iPSCs and subsequent differentiation to neural progenitor cells, and maturation to HD neuronal cultures. The timeline in days (D) is indicated. (**B**) Immunofluorescence cytochemistry (ICC) of two-week matured HD neuronal cultures using anti-αtubulin and anti-DAPI antibodies to show neuronal cell cultures in green and nuclei in blue, respectively. (**C**) ICC of HD neuronal cultures using anti-MAP2, anti-GFAP, and anti-DAPI antibodies to show mature neurons in green, astrocytes in red and nuclei in blue, respectively. (**D**) TaqMan assays to demonstrate differential expression of MAP2 in HD-patient derived iPSCs and two-week matured HD neuronal cultures. (**E**) TaqMan assays to demonstrate differential expression of β3-tubulin (TUBB3) in HD-patient derived iPSCs and two-week matured HD neuronal cultures. One-way ANOVA: P-values are represented as *p<0.05.

Mature miHTT molecules are dose-dependently expressed in HD neuronal cultures following AAV5-miHTT gene transfer

To address the transduction efficacy and cellular processing of the AAV5-miHTT construct in HD neuronal cultures, we transduced two-week matured HD neuronal cultures with three doses of AAV5-miHTT $1x10^5$, $1x10^6$, $1x10^7$ MOI (**Figure 2a**). An AAV5-GFP construct ($1x10^6$ MOI) and vehicle were used as negative controls. To quantify viral copies, we isolated DNA and measured vector genome copies (gc) by SYBR Green qPCR, expressed as gc/µg of input DNA. A dose-dependent increase of AAV5-miHTT gc was detected, with the highest dose generating 2.34E8 gc/µg of input DNA (N=4). The transduction efficacy of the AAV5-GFP ($1x10^6$ MOI) was lower compared with the AAV5-miHTT ($1x10^6$ MOI). To quantify mature miHTT expression, TaqMan small RNA qPCR was performed using custom probes that detect mature miHTT molecules. Molecules/cell were calculated based on the miHTT standard curve. We detected a dose-dependent expression of miHTT molecules with the highest dose resulting in an average of 16 molecules of miHTT per cell (N=4-6) (**Figure 2b**).

We previously reported that the miHTT-451 construct does not generate a passenger strand in the murine and rat HD model. The absence of a passenger strand eliminates the chance for off-target effects induced by the passenger strand, which ultimately enhances the safety profile.[31–33] Hence, during clinical development, it is important to establish cellular processing of a drug in the target human tissue. For this reason, we analyzed the miRNA processing patterns in HD neuronal cultures transduced with the AAV5-miHTT by NGS. We have detected a typical variability in the read length (19-30 nucleotides) occurring when the miR-451 precursor is intracellularly processed.[34] The most abundant reads were 24 nucleotides long and belonged to the miHTT guide strand (**Figure 2c**). We did not observe any reads belonging to the passenger strand, confirming the absence of a passenger strand associated with the miR-451 precursor also in the human HD patient cells.



C)

	Small RNA read	Counts	Length	%Total reads	miHTT-451 precursor
1	AAGGACTTGAGGGACTCGAAGACG	297466	24	45.7%	
2	AAGGACTTGAGGGACTCGAAGACGAGTCCC	104239	30	16.0%	
3	AAGGACTTGAGGGACTCGAAGAC	74819	23	11.5%	
4	AAGGACTTGAGGGACTCGAAGA	53978	22	8.3%	
5	AAGGACTTGAGGGACTCGAAGACGA	31640	25	4.9%	
6	AAGGACTTGAGGGACTCGAAG	20263	21	3.1%	
7	AAGGACTTGAGGGACTCGAAGACGAGT	14692	27	2.3%	
8	AAGGACTTGAGGGACTCGA	10260	19	1.6%	
9	AAGGACTTGAGGGACTCGAAGACGAGTCCCT	7176	31	1.1%	
10	AAGGACTTGAGGGACTCGAA	6227	20	1.0%	

Figure 2. AAV5-miHTT transduction efficacy and miHTT processing in HD neuronal cultures. (**A**) qPCR to determine AAV5 genome copies (gc)/ug DNA isolated from AAV5-miHTT-transduced HD neuronal cultures. AAV5-GFP and Saline were used as negative controls. Different AAV doses are indicated. (**B**) Small RNA TaqMan assay to determine miHTT molecules per cell in the AAV5-miHTT-transduced HD neuronal cultures. AAV5-GFP and Saline were used as negative controls. (**C**) Sequence distribution (%) of reads mapping to the pre-miHTT sequence. The predicted guide strand is indicated in red. No passenger strand detected. For the read alignments, up to 3 mismatches with the reference sequence were allowed. Reads represented with less than 1% were excluded from the figure.

A dose-dependent HTT mRNA and protein lowering in HD neuronal cultures transduced with the AAV5-miHTT construct

To evaluate the efficacy in which the mature miHTT molecules engages with endogenous HTT transcripts, we measured HTT mRNA lowering by TaqMan qPCR. We observed significant dose-dependent HTT mRNA lowering by the AAV5-miHTT construct with the highest dose inducing the strongest 56.2% ($p \leq 0.0001$) knock-down when compared with the AAV5-GFP

and saline negative controls ($p \leq 0.0001$) (**Figure 3a**). HTT protein lowering was measured by single molecule counting (SMC) immunoassay assay (**Figure 3b**). Total HTT protein was lowered in a dose-dependent manner with the highest dose inducing the strongest 67.5% ($p<0.001$) lowering, in line with the miHTT expression and HTT mRNA lowering. Hence, the AAV5-miHTT construct induced clinically relevant HTT protein lowering in HD-patient neuronal cells, confirming that it is capable of targeting HTT in humans.

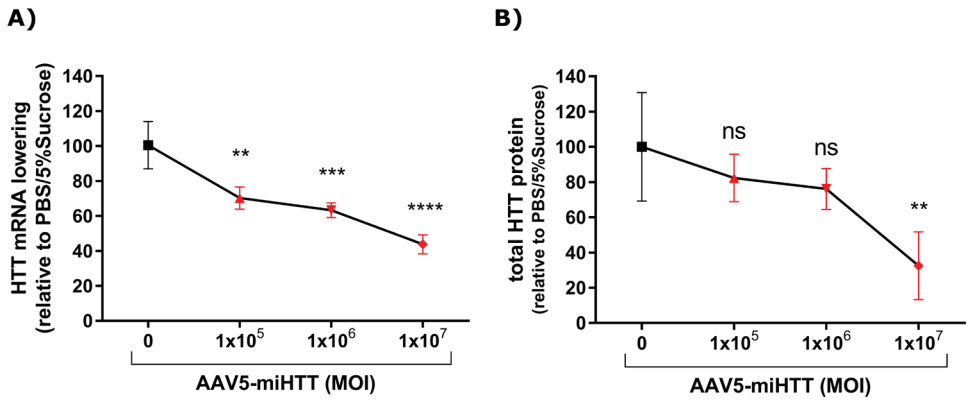


Figure 3. The AAV5-miHTT construct induces HTT mRNA and protein lowering in HD neuronal cultures. (**A**) Dose-dependent HTT mRNA knock-down in AAV5-miHTT transduced cells measured by TaqMan qPCR (n=4). (**B**) Dose-dependent HTT protein lowering measured by SMC immunoassay (n=4). Data are presented as the mean ± s.d. (error bars). One-way ANOVA: ns, non-significant. P-values are represented as **p<0.01; ***p<0.001; ****p<0.0001.

Detection of mature artificial miHTT molecules in extracellular vesicles enriched for exosomes

To determine whether mature miHTT molecules can be released within exosomes secreted from HD mature neuronal cultures, we designed an experiment that allowed for an isolation of a larger number of exosomes from culture media (**Figure 4a**). First, we transduced HD neuronal cultures in T75-flask format with the AAV5-miHTT ($3.3x10^7$ MOI) or the AAV5-GFP ($3.3x10^5$ MOI) and saline as negative controls. Five days post-exposure, the transduction efficiency was estimated microscopically to be 90% based on GFP fluorescence (**Figure 4b**). Twenty days post-transduction, neuronal cultures were harvested and separated for molecular analysis. To quantify mature miHTT molecules, we performed TaqMan small RNA qPCR (**Figure 4c**). We observed 10^4-fold more molecules in the AAV5-miHTT-transduced cells as oppose to saline or AAV5-GFP negative controls. To characterize the exosomal content released from HD neuronal cultures, media were harvested, cells and cellular debris were discarded, and the media were precipitated to enrich for exosomes.

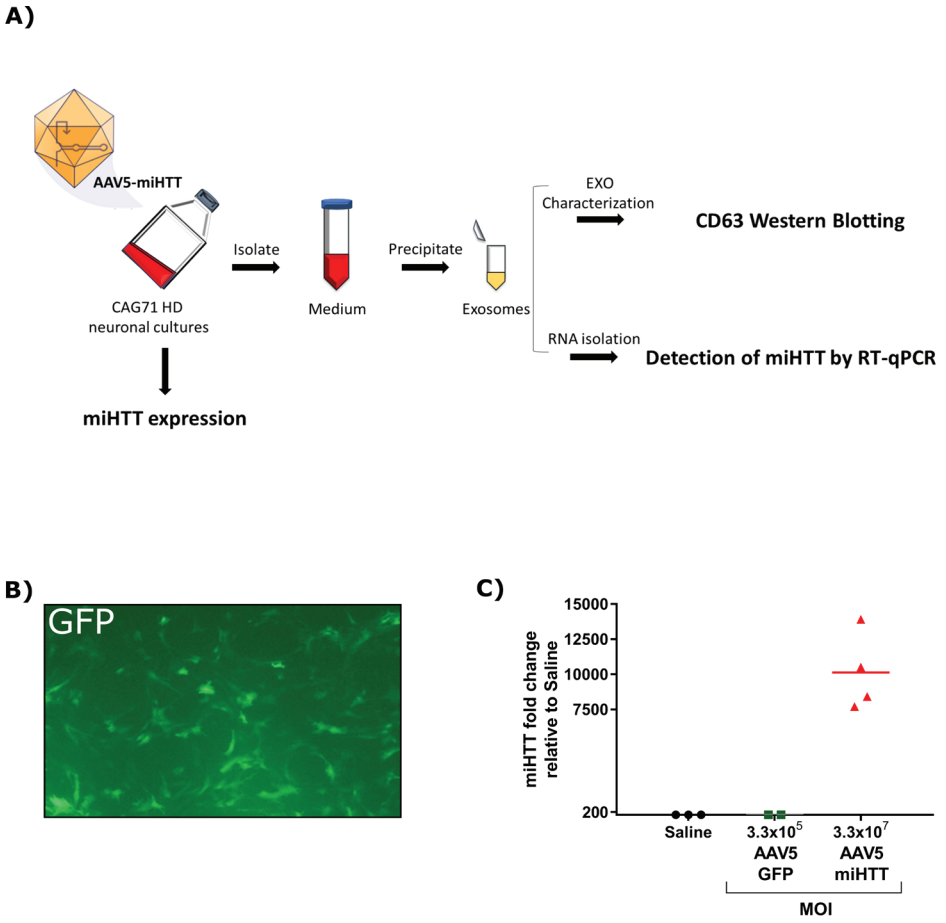


Figure 4. The experimental outline for a detection of Exo-miHTT in vesicles secreted from HD neuronal cultures. (**A**) Experimental outline to detect miHTT in exosomes secreted from AAV5-miHTT transduced HD neuronal cultures. (**B**) GFP expression in HD neuronal cultures five days post-transductions with the AAV5-miHTT. (**C**) Small RNA TaqMan assay to determine miHTT molecules in the AAV5-miHTT-transduced HD neuronal cultures (N=4). AAV5-GFP and Saline were used as negative controls (N=2-3).

To evaluate the presence of exosomal vesicles in the precipitated samples, we performed western blotting using CD63 antibody, a tetraspanin classically used as an exosomal marker. All samples isolated from the AAV5-miHTT (from now referred as exo-miHTT)- and the AAV5-GFP (from now referred as exo-GFP)-transduced HD neuronal cultures were shown to be enriched for exosomes (**Figure 5a**). To further quantify the abundance of mature miHTT molecules in the isolated exosomes, we performed TaqMan small RNA qPCR (**Figure 5B**) and demonstrated that exo-miHTT, but not exo-control or exo-GFP were enriched ($4.6x10^3$-fold increase) for miHTT molecules.

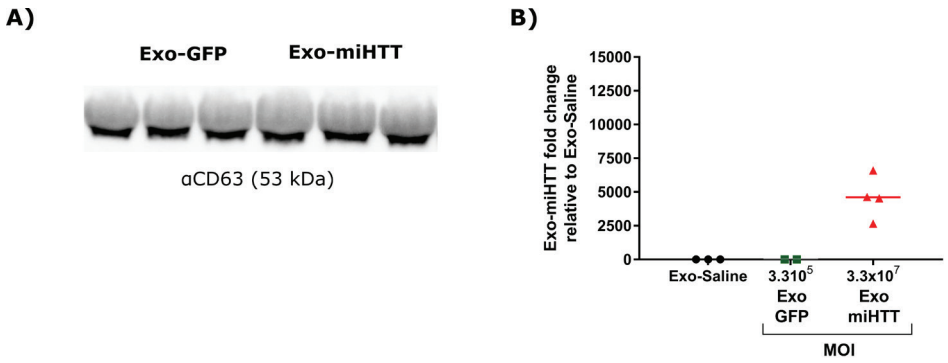


Figure 5. Mature miHTT molecules detected in the vesicles expressing exosomal markers and secreted from HD neuronal cultures. (**A**) Western blotting to detect the exosomal marker CD63 in samples isolated from conditioned media of AAV5-GFP-transduced cells (Exo-GFP, N=3) and AAV5-miHTT-transduced cells (Exo-miHTT, N=3). (**B**) Quantification of miHTT molecules in exosomes released by transduced cells by small TaqMan qPCR (n=2-4).

DISCUSSION

We report that mature miHTT molecules are secreted from HD patient cells within vesicles that are enriched for exosomes. We hypothesize that miHTT molecules are likely present within exosomes secreted into biofluids of AAV5-miHTT-treated animals and patients. If this can be confirmed in large HD animal models, the miRNA concentration in the CSF could become a PK/PD measure for miRNA-based drugs in the CNS, having a major impact on the preclinical and clinical development of RNAi therapeutics for CNS indications. Establishing a PK/PD profile of a therapeutic miRNA in an accessible biofluid that reflects the miRNA expression in the CNS, would allow for a more accurate analysis of dose-response relationships.

The exosome biogenesis starts with the formation of an endosome through invagination of the plasma membrane.[35] The endosome continues budding inside the cell, which gives rise to a late endosome. At this stage, intraluminal vesicles (ILVs) carrying diverse molecular cargos become part of the endosome.[35] As late endosomes contain many ILVs, they are often referred to as multivesicular bodies (MVBs). MVBs either fuse with lysosomes that degrade ILVs and their content, or fuse with the cell membrane and release ILVs into the extracellular space as exosomes.[18,36] The MVB origin of exosomes is reflected in their cargos and the secreted particles are enriched for tetraspanins such as CD63 or CD81, and heat shock proteins which are often used as exosomal markers.[37] We demonstrated the enrichment for the CD63 marker in the precipitate isolated from the HD neuronal culture media. Although this suggest an enrichment for the exosomes, but it does not exclude other vesicles potentially associated with miHTT molecules. Three types of extracellular vesicles are known to carry miRNAs in biofluids: exosomes (40-100nm), macrovesicles (50-2000nm) and apoptotic bodies (500-4000nm).[38] All three systems are secreted into the body fluids and their biogenesis is very different. Therefore, further experiments need to be performed to either exclude or include other extracellular source of miHTT in the culture media and possibly in the biofluids of the AAV5-miHTT-injected large species.

Because most of the miRNA-containing vesicles are thought not to cross the intact blood-brain-barrier (BBB), quantification of the therapeutic miRNA in the CSF seem to be a more appropriate source for the PK/PD measurement. Due to the limitations of CSF sampling volumes from rodents, further evaluation of the potential of CSF as a source of therapeutic miRNAs as diagnostic or PK/PD biomarkers requires additional preclinical studies in large animals.

Our data show a potential to use therapeutic miRNA not only as a PK/PD measure for CNS indications but also trigger new hypotheses. We postulate that the miHTT can spread in the CNS and further by other than viral means, for instance by using an ”infective” exosomal pathway. Through this mechanism, the efficacy of miHTT gene therapy for HD could be extended beyond the initial viral distribution. The ability of exosomes to incorporate and

transfer functional miRNAs is currently used as a non-viral alternative approach to gene therapy. Several reports indicate that therapeutic RNAi molecules can be delivered to the target cells when enveloped into exosomes.[15,39–41] Moreover, viruses employ exosome-linked machineries, like ESRT, to induce escapism via viral budding of the plasma membrane.[42] If the AAV-based gene therapy for HD would induce exosome-dependent spreading of the silencing effect, this might provide important additional therapeutic benefit.

In conclusion, we have demonstrated a release of miHTT in exosome-enriched particles secreted from HD neuronal cultures. This opens the way for further development of a PK/PD biomarker for therapeutic miRNA expression in HD patients. We hypothesize that the exosomal spread of miHTT potentially may contribute to therapeutic silencing beyond cells initially targeted by the AAV5-miHTT.

MATERIAL AND METHODS

Differentiation of forebrain CAG71 neuronal cultures from human HD iPSCs

HD iPSCs (ND42229*B) containing 71 CAG repeats were ordered from (Coriell Institute Stem Biobank, passage 25). These cells were generated from human HD fibroblasts GM04281 (Coriell Institute Stem Biobank) reprogrammed with six factors (OCT4, SOX2, KLF4, LMYC, LIN28, shRNA to P53) using episomal vectors. iPSCs were maintained on matrigel coating with mTeSR medium for several passages, following the manufacturer's instructions (StemCell Technologies, Vancouver, Canada). Non-differentiated colonies were released using ReLeSR reagent during each passage and diluted 1:5-20 (StemCell Technologies). For the neural induction, cells were plated onto AggreWellTM 800 plate at day 0 as 3x106 cells per well in STEMdiff™ Neural Induction Medium (StemCell Technologies). At day 5, embryoid bodies were formed and replated onto poly-D-lysine/laminin coated 6-well plates. Coating was prepared with poly-D-lysine hydrobromide (0,1 mg/mL) and Laminin from Engelbreth-Holm-Swarm murine (0,1 mg/ml) (Sigma-Aldrich). At day 12, the neuronal rosettes were selected using STEMdiff™ Neural Rosette Selection Reagent (StemCell Technologies) and replated in poly-D-lysine/laminin coated plates. Next day, differentiation of neural progenitor cells was initiated using STEMdiff™ Neuron Differentiation Kit (StemCell Technologies). From day 19, cells were matured using STEMdiff™ Neuron Maturation Kit for a minimum of two weeks (StemCell Technologies).

AAV5 vector production

An AAV5 vector expressing miHTT construct was produced by baculovirus-based AAV production system (uniQure, Amsterdam, The Netherlands) as previously described.[43] The miHTT expression cassette was inserted in a recombinant baculovirus vector by homologous recombination. To generate AAV5, infections with different recombinant baculoviruses containing the vector genome, the replicative enzymes and the capsid proteins were performed as described previously.[43]

Next generation sequencing

RNA was isolated from cells using Trizol according to the manufacturer's protocol (Invitrogen). Small RNA sequencing libraries for the Illumina sequencing platform were generated using the NEXTflex Small RNA Sequencing kit (Bioo Scientific, Austin, TX, USA). The libraries were multiplexed, clustered, and sequenced on an Illumina HiSeq 2000 (TruSeq v3 chemistry) with a single-read 36 cycles sequencing protocol and indexing. The sequencing run was analyzed with the Illumina CASAVA pipeline (v1.8.2) with demultiplexing based on sample-specific barcodes. In total, we generated between 8-15 million reads per sample. The raw sequencing data were produced as previously described.[31] Small RNA raw data sets were analyzed using the CLC Genomics Workbench 6 (Qiagen, Hilden, Germany). The obtained

unique small RNA reads were aligned to the reference sequences with a max. of three nucleotide mismatches allowed. The percentages of reads based on the total number of reads matching the reference sequences were calculated.

Quantitative polymerase chain reaction

RNA was isolated from cells using Trizol according to the manufacturer's protocol (Invitrogen). To remove genomic DNA, RNA was treated with dsDNase (Thermo Scientific, Waltham, MA, USA). To measure mRNA knock-down, cDNA was generated using Maxima Synthesis Kit (Thermo Scientific). cDNA was analyzed by qPCR using probes: human HTT Hs00918134_m1 and human GAPDH Hs02758991_g1 (Thermo Scientific). To detect miHTT expression levels, RT-qPCR was performed using TaqMan Fast Universal kit (Thermo Scientific). U6 snRNA (001973, Applied Biosystems) and custom miHTT probes (Thermo Scientific). The expression level of each gene was normalized to either endogenous GAPDH or U6 snRNA levels. Fold changes, percentages in mRNA knock-down, or miRNA expression were calculated based on 2^ΔΔCT method. miRNA expression was calculated based on a standard line.

Maturation status of neuronal cultures was evaluated by measuring expression of genes associated with neural development using TaqMan qPCR for detection of MAP2 (Hs00258900_m1) and TUBB3 (Hs00801390_m1).

For the viral DNA isolation, neuronal cultures were processed using DNeasy Blood & Tissue Kit (Qiagen, Valencia, CA, USA) following manufacturer's protocol. AAV5 vector genome copies were measured by qPCR reaction using SYBR Green protocol (Applied Biosystems, Foster City, CA, USA) and validated standard line for detection of CAG promoter. Forward primer sequence: GAGCCGCAGCCATTGC and reverse primer sequence: CACAGATTTGGGACAAAGGAAGT. The standard line was used to calculate the genome copies per DNA microgram.

Protein isolation and Western blotting

Exosomal precipitates were lysed using RIPA lysis buffer (Sigma-Aldrich) supplemented with protein inhibitor cocktail (cOmplete™ ULTRA Tablet; Roche, Basel, Switzerland). Total protein concentration was quantified using a Bradford Protein Assay (Bio-Rad, Hercules, CA, USA) and absorbance was measured at 600 nm on the GloMax Discover System (Promega). Equal amounts of sample protein (10-30 µg) were incubated with β-mercaptoethanol and Laemmli buffer at 95°C for 5 min and separated using 4-20% Mini-Protean TGX Stain-Free Protein Gel (Bio-Rad). Samples were transferred to PVDF membranes by Trans-Blot Turbo Transfer system (Bio-Rad) using the 'Mixed MW' protocol. Blot was incubated with 3% Blotting-Grade blocker (Bio-Rad) in 1x Tris Buffered Saline (TBS) for 1 hour at room temperature, followed by immunoblotting with selected primary antibody overnight at 4°C.

Primary antibody CD63 (System Biosciences) was diluted at 1:1000 dilution. Chromogenic signals were detected after 2 hours incubation with HRP-conjugated secondary antibodies (goat anti-rabbit, Abcam, 1:20000) and 5 min incubation with SuperSignal Pico sensitivity Substrate (ThermoScientific) using ChemiDoc Touch Gel Imaging System (Bio-Rad).

SMC immunoassay

Protein lysates were resuspended in dilution buffer (50 µl/well) containing 6% BSA, 0.8% Triton X-100, 750 mM NaCl, and complete protease inhibitor (catalog 04693116001; Roche) and added to a 96-conical assay plate (catalog P-96-450V-C; Axygen). MAB2166 antibody (Merck Millipore) diluted to 1:1000 with Erenna Assay Buffer (02-0474-00; Singulex) coupled with magnetic particles (03-0077-02; Singulex) at a ratio of 25 µg antibody per milligram magnetic particles was added to the plate and shaking (600 rpm; Heidolph Titramax 1000 Microplate Shaker) at room temperature for 1 hour. The plate was placed on a magnetic rack and washed four times with 200 µl 1× washing buffer (02-0111-00; Singulex). 20 µl/well of 0.5 ng/µl diluted MW1 detection antibody labeled with detection fluorophore (catalog 03-0076-02; Singulex) at a ratio of 15.7 pmol fluorophore per micrgram MW1 was added to the plate. The plate was incubated shaking (750 rpm) at room temperature for 1 hour. Plates were washed, and the antibody-antigen complex was transferred to a new 96-conical assay plate. After four washes with 200 µl 1× washing buffer and aspiration, elution buffer (acidic glycine solution, 0.1 M, pH 2.7) was added to the plate, and the plate was incubated shaking (1,000 rpm) for 5 minutes. The eluted detection antibody was transferred to a Nunc 384-well analysis plate (catalog 264573; Sigma-Aldrich) and neutralized with neutralization buffer (Tris, 1 M, pH 9). The analysis plate was spun down, sealed, and subsequently analyzed with the Erenna Immunoassay System (Singulex).

Exosome precipitation

Medium from transduced neuronal cultures was collected every second or third day and centrifuged at 3000g for 15 min to remove cells and cell debris. The exosomes were isolated with ExoQuick-TC (System Bioscience, California, USA) according to manufacturer's protocol. 3 ml of ExoQuick buffer was added to 10 ml of conditioned medium and incubated at 4°C overnight. Next day, the exosomes were collected at 1500 x g for 30 minutes and the supernatant was discarded. The residual solution was additionally centrifuged at 1500 x g for 10 minutes. The exosome pellets were re-suspended in appropriate buffers and stored at -80°C for further experiments.

Immunocytochemistry

Two-week mature neuronal cultures were plated on Nunc™ Lab-Tek™ 4-chamber slides (Thermo Scientific). At day 7, cells were fixed in 4% paraformaldehyde for 10 minutes at room temperature. Cells were washed 3 times with 1x PBS and permeabilized with 0.25%

Tween for 5 minutes. After blocking with 5% bovine serum albumin (BSA) for 30 minutes, cells were labeled with different primary antibodies overnight at 4°C. Primary antibodies include: ms MAP2 (Merk Millipore MAB364, 1:500), rb GFAP (StemCell technologies, 1:250), ms α-tubulin (Abcam, Cambridge, UK, 1:1000). Next, cells were incubated in fluorescently-tagged secondary antibodies for 60 minutes at room temperature. Secondary antibodies include: Donkey anti-mouse Alexa Fluor 488 (Invitrogen, Carlsbad, CA, 1:1000) and Goat anti-rabbit Alexa Fluor 568 (Life Technologies, Zug, Switzerland, 1:1000). Coverslips were mounted with ProLong® Gold Antifade Mountant with DAPI (Life Technologies) and images were acquired using Leica DM2500 fluorescence microscope.

Statistics

Data were analyzed using un-paired Student's t-test (for two groups) or one-way ANOVA (for three or more groups) to determine statistically significances between samples. Tukey's post hoc test (α=0.05) was applied to analyzed differences between relevant groups. P-values are represented as: *p<0.05; **p<0.01; ***p<0.001; ****p<0.0001.

REFERENCES

1. Jucker, M and Walker, LC (2013). Self-propagation of pathogenic protein aggregates in neurodegenerative diseases. *Nature* **501**: 45–51.
2. Macdonald, ME, Ambrose, CM, Duyao, MP, Myers, RH, Lin, C, Srinidhi, L, *et al.* (1993). A Novel Gene Containing a Trinucleotide That Is Expanded and Unstable on Huntington's Disease Chromosomes. *Cell* **72**: 971–983.
3. Ross, CA and Tabrizi, SJ (2011). Huntington's disease: From molecular pathogenesis to clinical treatment. *Lancet Neurol.* **10**: 83–98.
4. Zielonka, D, Mielcarek, M and Landwehrmeyer, GB (2015). Update on Huntington's disease: Advances in care and emerging therapeutic options. *Park. Relat. Disord.* **21**: 169–178.
5. Bates, GP, Dorsey, R, Gusella, JF, Hayden, MR, Kay, C, Leavitt, BR, *et al.* (2015). Huntington disease. *Nat. Rev. Dis. Prim.* **1**: 1–21.
6. Saudou, F and Humbert, S (2016). The Biology of Huntingtin. *Neuron* **89**: 910–926.
7. Tabrizi, SJ, Langbehn, DR, Leavitt, BR, Roos, RAC, Durr, A, Craufurd, D, *et al.* (2013). Biological and clinical manifestations of Huntington's disease in the longitudinal TRACK-HD study: cross-sectional analysis of baseline data. *Lancet Neurol.* **8**: 791–801.
8. Heemskerk, A and Roos, RAC (2012). Aspiration pneumonia and death in Huntington's disease. *PLOS Curr.* **Version 2**: 1–4.
9. Wild, EJ and Tabrizi, SJ (2017). Therapies targeting DNA and RNA in Huntington's disease. *Lancet Neurol.* **16**: 837–847.
10. Mestre, TA and Sampaio, C (2017). Huntington Disease: Linking Pathogenesis to the Development of Experimental Therapeutics. *Curr. Neurol. Neurosci. Rep.* **17**: 1–8.
11. Miniarikova, J, Evers, MM and Konstantinova, P (2018). Translation of MicroRNA-Based Huntingtin-Lowering Therapies from Preclinical Studies to the Clinic. *Mol. Ther.* **26**: 947–962.
12. Ross, CA, Aylward, EH, Wild, EJ, Langbehn, DR, Long, JD, Warner, JH, *et al.* (2014). Huntington disease: natural history, biomarkers and prospects for therapeutics. *Nat. Rev. Neurol.* **10**: 204–16.
13. Evers, MM, Miniarikova, J, Juhas, S, Vallès, A, Bohuslavova, B, Juhasova, J, *et al.* AAV5-miHTT gene therapy demonstrates broad distribution and strong human mutant huntingtin lowering in a Huntington disease minipig model: Submitted to Neuron.
14. Pfister, E, Dinardo, N, Mondo, E, Borel, F, Conroy, F, Fraser, C, *et al.* (2017). Artificial miRNAs reduce human mutant Huntingtin throughout the striatum in a transgenic sheep model of Huntington's disease. *Hum. Gene Ther.*doi:10.1089/hum.2017.199.
15. Barile, L and Vassalli, G (2017). Exosomes: Therapy delivery tools and biomarkers of diseases. *Pharmacol. Ther.* **174**: 63–78.
16. Properzi, F, Logozzi, M and Fais, S (2013). Exosomes: the future of biomarkers in medicine. *Biomark. Med.* **7**: 769–78.
17. Ragusa, M, Barbagallo, C, Cirnigliaro, M, Battaglia, R, Brex, D, Caponnetto, A, *et al.* (2017). Asymmetric RNA Distribution among Cells and Their Secreted Exosomes: Biomedical Meaning and Considerations on Diagnostic Applications. *Front. Mol. Biosci.* **4**: 1–14.
18. Colombo, M, Raposo, G and Théry, C (2014). Biogenesis, Secretion, and Intercellular Interactions of Exosomes and Other Extracellular Vesicles. *Annu. Rev. Cell Dev. Biol.* **30**: 255–289.
19. Li, M, Zeringer, E, Barta, T, Schageman, J, Cheng, A and Vlassov, A V. (2014). Analysis of the RNA content of the exosomes derived from blood serum and urine and its potential as biomarkers. *Philos. Trans. R. Soc. B Biol. Sci.* **369**: 1–8.

20. Huang, X, Yuan, T, Tschannen, M, Sun, Z, Jacob, H, Du, M, *et al.* (2013). Characterization of human plasma-derived exosomal RNAs by deep sequencing: 1–14.

21. Pigati, L, Yaddanapudi, SCS, Iyengar, R, Kim, DJ, Hearn, SA, Danforth, D, *et al.* (2010). Selective release of MicroRNA species from normal and malignant mammary epithelial cells. *PLoS One* **5**.

22. Nolte'T Hoen, ENM, Buermans, HPJ, Waasdorp, M, Stoorvogel, W, Wauben, MHM and 'T Hoen, PAC (2012). Deep sequencing of RNA from immune cell-derived vesicles uncovers the selective incorporation of small non-coding RNA biotypes with potential regulatory functions. *Nucleic Acids Res.* **40**: 9272–9285.

23. Koppers-Lalic, D, Hackenberg, M, Bijnsdorp, I V., van Eijndhoven, MAJ, Sadek, P, Sie, D, *et al.* (2014). Nontemplated nucleotide additions distinguish the small RNA composition in cells from exosomes. *Cell Rep.* **8**: 1649–1658.

24. Villarroya-Beltri, C, Gutiérrez-Vázquez, C, Sánchez-Cabo, F, Pérez-Hernández, D, Vázquez, J, Martin-Cofreces, N, *et al.* (2013). Sumoylated hnRNPA2B1 controls the sorting of miRNAs into exosomes through binding to specific motifs. *Nat. Commun.* **4**: 1–10.

25. Squadrito, ML, Baer, C, Burdet, F, Maderna, C, Gilfillan, GD, Lyle, R, *et al.* (2014). Endogenous RNAs Modulate MicroRNA Sorting to Exosomes and Transfer to Acceptor Cells. *Cell Rep.* **8**.

26. Ong, S-G, Lee, WH, Huang, M, Dey, D, Kodo, K, Sanchez-Freire, V, *et al.* (2014). Cross talk of combined gene and cell therapy in ischemic heart disease: role of exosomal microRNA transfer. *Circulation* **130**: S60-9.

27. Ke, X, Yan, R, Sun, Z, Cheng, Y, Meltzer, A, Lu, N, *et al.* (2017). Esophageal Adenocarcinoma–Derived Extracellular Vesicle MicroRNAs Induce a Neoplastic Phenotype in Gastric Organoids. *Neoplasia (United States)* **19**: 941–949.

28. Sruthi, T V, Edatt, L, Raji, GR, K, H, Shankar, SS, Shankar, V, *et al.* (2017). Horizontal transfer of miR-23a from hypoxic tumor cell colonies can induce angiogenesis. *J Cell Physiol*: 1–17doi:10.1002/jcp.26202.

29. Guenat, D, Hermetet, F, Prétet, JL and Mougin, C (2017). Exosomes and other extracellular vesicles in HPV transmission and carcinogenesis. *Viruses* **9**: 1–17.

30. Potrich, C, Lunelli, L, Vaghi, V, Pasquardini, L and Pederzolli, C (2017). Cell transfer of information via miR-loaded exosomes: a biophysical approach. *Eur. Biophys. J.* **46**: 803–811.

31. Miniarikova, J, Zanella, I, Huseinovic, A, van der Zon, T, Hanemaaijer, E, Martier, R, *et al.* (2016). Design, Characterization, and Lead Selection of Therapeutic miRNAs Targeting Huntingtin for Development of Gene Therapy for Huntington's Disease. *Mol. Ther. Acids* **5**: e297.

32. Ma, H, Zhang, J and Wu, H (2014). Designing Ago2-specific siRNA/shRNA to Avoid Competition with Endogenous miRNAs. *Mol. Ther. Nucleic Acids* **3**: e176.

33. Herrera-Carrillo, E, Harwig, A, Liu, YP and Berkhout, B (2014). Probing the shRNA characteristics that hinder Dicer recognition and consequently allow Ago-mediated processing and AgoshRNA activity. *RNA* **20**: 1410–1418.

34. Cifuentes, D, Xue, H, Taylor, DW, Patnode, H, Mishima, Y, Cheloufi, S, *et al.* (2010). A novel miRNA processing pathway independent of Dicer requires Argonaute2 catalytic activity. *Science* **328**: 1694–1698.

35. El Andaloussi, S, Mäger, I, Breakefield, XO and Wood, MJA (2013). Extracellular vesicles: Biology and emerging therapeutic opportunities. *Nat. Rev. Drug Discov.* **12**: 347–357.

36. Bobrie, A, Colombo, M, Raposo, G and Théry, C (2011). Exosome Secretion: Molecular Mechanisms and Roles in Immune Responses. *Traffic* **12**: 1659–1668.

37. Kowal, J, Tkach, M and Théry, C (2014). Biogenesis and secretion of exosomes. *Curr. Opin. Cell Biol.* **29**: 116–125.

38. Hessvik, NP, Sandvig, K and Llorente, A (2013). Exosomal miRNAs as biomarkers for prostate cancer. *Front. Genet.* **4**: 1–9.

39. Lin, J, Li, J, Huang, B, Liu, J, Chen, X, Chen, X-M, *et al.* (2015). Exosomes: Novel Biomarkers for Clinical Diagnosis. *Sci. World J.* **2015**: 1–8.

40. Shahabipour, F, Barati, N, Johnston, TP, Derosa, G, Maffioli, P and Sahebkar, A (2017). Exosomes: Nanoparticulate tools for RNA interference and drug delivery. *J. Cell. Physiol.* **232**: 1660–1668.

41. Alvarez-Erviti, L, Seow, Y, Yin, H, Betts, C, Lakhal, S and Wood, MJA (2011). Delivery of siRNA to the mouse brain by systemic injection of targeted exosomes. *Nat. Biotechnol.* **29**: 341–345.

42. Meckes, DG and Raab-Traub, N (2011). Microvesicles and Viral Infection. *J. Virol.* **85**: 12844–12854.

43. Miniarikova, J, Zimmer, V, Martier, R, Brouwers, CC, Pythoud, C, Richetin, K, *et al.* (2017). AAV5-miHTT gene therapy demonstrates suppression of mutant huntingtin aggregation and neuronal dysfunction in a rat model of Huntington's disease. *Gene Ther.* **24**: 630–639.

6

GENERAL DISCUSSION

Jana Miniarikova[1,2]**, Melvin M. Evers**[1]**, Pavlina Konstantinova**[1]
[1]Department of Research & Development, uniQure, Amsterdam, the Netherlands
[2]Department of Gastroenterology and Hepatology, Leiden University Medical Center, Leiden, the Netherlands

Mol. Ther. (2018); ***26****: 947–962*

INTRODUCTION

The main objective of this thesis is to demonstrate a preclinical efficacy of an adeno-associated virus (AAV)-delivery of micro (mi)RNA-based gene therapy for the treatment of Huntington's disease (HD). For this purpose, we have designed and tested various therapeutic miRNAs targeting different regions in the mutant HTT transcripts to achieve overall lowering of the neurotoxic HTT protein in HD rodent models and induced pluripotent stem cell (iPSC)-derived HD patient neuronal cultures. Excitingly, we have demonstrated HTT lowering efficacy by the AAV5-miHTT in all HD models tested so far with no undesired events, which strongly supports the continuation of preclinical testing in large animals. Furthermore, we provided an evidence suggesting that therapeutic miRNAs can be also active in the nucleus, extending their range of applicability. To ultimately treat the patients, the possibility to use exosomes as carriers of pharmacokinetic/pharmacodynamic (PK/PD) candidate measures for the AAV5-miHTT gene therapy approach, that would signal the presence of the active therapeutic miRNAs in the brain, was further explored in preparation for a first clinical trial in humans.

Our gene therapy approach is based on a delivery of an AAV vector carrying an expression cassette of a therapeutic miRNA that lowers HTT mRNA in target cells. We have already discussed HTT RNA lowering strategies in detail in the introduction. The alternatives to this approach would be modifications of *HTT* DNA and some efforts have been spent to directly target HTT protein. The latter, however, have had limited success so far. Here bellow, we will discuss HTT DNA-targeting and protein-targeting approaches into more detail.

RNAi vs. other HTT lowering approaches

HTT DNA-targeting

At the moment, three gene-editing tools showed efficacy in early preclinical testing, resulting in lowering of toxic HTT protein *in vitro* and *in vivo*: zinc finger nucleases (ZFNs), transcription activator-like effectors nucleases (TALENs), and clustered regularly interspaced short palindromic repeats (CRISPR-Cas9).[1–6] All three systems of engineered nucleases are similar in that they contain a catalytic and DNA-recognizing domain. The later can be engineered to target specific DNA sequences and thus, providing a valuable therapeutic tool that enables editing or deleting target disease-related sequences. ZFNs, TALENs, and CRISPR-Cas9 differ in a mode of action and additional requirements for their activity.[7] The major concerns for a use of reprogrammed nucleases are: the off-target editing of other genes that can disable their function or activate oncogenes, the stimulation of the immune response, and how to achieve an exclusive expression in the disease-associated cells.[7,8] Similar to RNA interference (RNAi), gene editing tools operate based on sequence complementarity with the target genes. However, the off-target safety concerns regarding the use of gene editing tools are aggravated because it largely results in permanent and

complete deactivation of gene expression, opposite to transcript lowering induced by RNAi-based drugs. If the designed gene editing approach is not highly specific, this could have detrimental consequences for the patient in the future. Most of emerging gene-editing tools are in the early HD preclinical development addressing the allele-specificity, off-targeting, and stimulation of the immune system *in vivo*.[5] If proven efficacious, selective, and safe, administrating gene-editing therapeutics could ideally provide an advantageous permanent switch-off of the mutant HTT expression while maintaining the wild-type HTT levels intact. Nevertheless, this strategy is still in its crude state.

HTT protein-targeting

A discovery of the prerequisite role of the mutant HTT aggregation in HD neuropathology set off a development of therapies aimed to lower levels of the mutant HTT protein.[9] Several groups generated specific intrabodies (iAbs) that bind to different HTT domains to reduce abnormal mutant HTT misfolding that contributes to aggregation.[10] iAbs are intracellularly expressed recombinant fragments that can be delivered by AAV vectors and that are able to recognize different epitopes or conformations of the same protein.[9] A number of anti-HTT iAbs showed a certain degree of reduction of mutant HTT aggregation in few murine models.[11–13] However, the intrabodies as a potential drug for HD is less recognized compared to therapies targeting directly HTT RNA and DNA.[14]

Lowering disease-related transcripts in the nucleus by the AAV-miRNA gene therapy

RNAi, as a regulatory mechanism of gene expression functionally-restricted mainly in the cytoplasm, has been assumed by many researchers for two decades. The role of RNAi in the nucleus, however, has been largely ignored and it is only recently that a number of studies challenge the exclusivity of cytoplasmic RNAi functions as a whole.[15,16] The restrained progress in studies addressing nuclear RNAi is also due to the skepticism in fractionation techniques that separate the cytoplasm and nucleus, but these hurdles are being nowadays experimentally overcome by demonstrating an absence of impurities. The data from current studies provide evidence that miRNAs and RISC proteins are present and active in the nucleus in many cells types. For instance, several profiling studies have shown that hundreds of miRNAs are present in the nucleus of human neural stem cells, rat neurons, and cancerous cell lines such as HeLa.[17–19] Endogenous human AGO2 has been shown to be also nuclear.[16,20] Gagnon et al. showed recently a functional activity of RNAi proteins such as AGO2, Dicer, TRBP, and GW182 in the nuclei of multiple human cell lines.[21] Moreover, they showed that small RNAs associate with these proteins and induce gene silencing in the nucleus. Földes-Papp et al. demonstrated shuttling of endogenous miR-122 from the cytoplasm to the nucleus by optoporation and using superquencher molecular probes complementary the guide strand in live liver cells.[22] The overall functions of nuclear miRNAs have been reported in post-transcriptional and transcriptional gene silencing, epigenetics, and alternative

splicing.[15,23] Together, these data open a venue for new therapeutic approaches using RNAi to target nuclear disease-related transcripts. Based on this knowledge, in chapter 4, we have designed several therapeutic miRNAs that target sequences located in the nuclear pre-mRNA HTT transcripts. We have shown first indications that miRNA-based gene therapy can induce lowering of HTT transcripts in the nucleus of HD iPSC-patient derived neuronal cultures. We have demonstrated lowering of HTT carrying a four-nucleotide deletion of ACTT in HTT intron 22. For the treatment of HD, it would be advantageous to target both the nuclear and cytoplasmic mutant HTT transcripts, since some level of mutant HTT RNA toxicity has been reported.[24]

Finally, the data showing that RNAi can participate in alternative splicing suggest that the RNAi approaches do not have to be restricted only to lower the levels of malfunctional proteins, but they could be designed to induce alternative splicing of toxic RNAs to prevent the pathology.[25] For instance, siRNAs targeting pre-mRNAs of genes involved in the pathology of spinal muscular atrophy and Duchenne muscular dystrophy demonstrated therapeutic efficacy by exon inclusion and skipping of the relevant exons.[26] Thus, developing AAV-miRNA-based gene therapies for spinal muscular atrophy and Duchenne muscular dystrophy might become therapeutic targets in the future.

Exosomes: potential carriers of quantifiable PK/PD measures for an AAV-miRNA-based gene therapy

In chapter 5 of this thesis, we have shown first indications that mature miHTT molecules can be found in the exosomes secreted from HD-patient derived neuronal cultures and we expressed a need to perform further experiments to support these results. Our ongoing studies with large animals will determine whether the mature therapeutic miHTT can be indeed secreted encapsulated in exosomes into biofluids *in vivo*.

The exosomal miRNA cargo reflects the miRNA expression profile of the secreting cell and therefore enables the identification of a potential pathology. This provides another perspective to use exosomes as a source of biomarkers. Exocarta, EVpedia, or Vesiclepedia are useful databases that continuously accumulate data from studies focusing on the characterization of exosomal content.[27–29] Several studies showed that profiles of the circulating miRNAs isolated from the exosomes are similar to those of their originating cancer cells.[30–33] Moreover, the recent data demonstrated that toxic proteins involved in the pathology of several neurodegenerative disorders are transported via the exosomes and can contribute to disease propagation within the CNS.[34–36] For instance, huntingtin, PrP^{Sc} prion, β-amyloid peptide and α-synuclein have been found in exosomes and are currently investigated as diagnostic biomarkers for HD, prion disease, Alzheimer's disease, and Parkinson's disease, respectively.[34,37–40] Exosomes can also propagate neurotoxic molecules between species. The interesting work of Jeon et al. recently showed that injecting exosomes secreted from HD patient derived iPSCs and fibroblasts into neonatal mice was sufficient

to induce HD-like neurodegeneration in those mice.[36] Therefore, besides evaluating the presence of miHTT molecules in exosomes isolated from the CSF of AAV5-miHTT-injected animals, it would be important to quantify the mutant HTT mRNA and protein levels in these extracellular vesicles. Moreover, the miHTT treatment is resulting in a cleavage in exon 1 of the HTT mRNA and by that, it prevents the production of the mutant HTT protein. We underline the importance to investigate whether the cleaved HTT mRNA transcripts can be found in the vesicles isolated from the biofluids of different species treated with the AAV5-miHTT gene therapy as an ideal treatment-efficacy biomarker.

Pursuits for valid clinical biomarkers

The therapeutic goal of an AAV-miRNA gene therapy is to delay disease onset and/or slow down disease progression. The ultimate success of a clinical trial strongly depends on a robust validation of on-target efficacy and proof-of-principle. This is difficult to achieve without engaging and sampling the treated biochemical environment. In case of HD, brain biopsies are possible but highly risky. Not fully described HD natural history and heterogeneity of clinical symptoms present major obstacles for identifying clinical efficacy endpoints for HD treatment. Characterization of quantifiable and treatment-responsive biomarkers that correlate with HD neurodegeneration is heavily investigated.[41] Biomarkers need to be established for each treatment paradigm and subsequently validated in clinical studies, ideally based on results from preclinical models. Although no biomarker has been currently validated for a clinical outcome in HD, there are several high potential candidates that are incorporated as exploratory end points in HD clinical studies (https://clinicaltrials.gov: NCT02215616, NCT02197130, NCT02519036).

TRACK-HD and PREDICT-HD studies involving large groups of HD patients have investigated a wide range of neuroimaging, movement-based, and biofluid-based biomarkers for HD. [42–48] The results from these studies suggest the potential use of neuroimaging and biofluid-based biochemical markers to measure responses to therapeutic interventions, such as AAV-miRNA gene therapies. For instance, structural (MRI) can assess reductions in the striatal volume during HD progression.[42] Disease-specific changes of metabolite patterns have been observed using magnetic resonance spectroscopy and positron emission tomography.[49–53]

Perhaps the most promising is the quantification of biofluid-based disease-associated markers that allow monitoring of HD progression following administration of the AAV-miRNA gene therapy.[54,55] The soluble mutant HTT concentration in the CSF correlates with disease severity which suggests that this may become a biomarker to track the effectiveness of HTT lowering.[56,57] Major progress has been made in the development of assays that quantify soluble mutant HTT in the CSF.[56] It should be noted that the source of mutant HTT in the CSF is not fully understood and therefore its significance as a clinical biomarker for the HTT lowering efficacy needs robust evaluations. The mutant HTT in the CSF is not linked to functional readouts, ergo, reduced HTT in the CSF doesn't directly mean

functional improvements in patients. Interestingly, the ongoing clinical trial with antisense oligonucleotides recently reported mutant HTT lowering in the CSF in a completed phase I/IIa (https://clinicaltrials.gov: NCT02519036). Next to the mutant HTT, other biomarkers such as tau, interleukin-6, interleukin-8, and clusterin isolated from CSF and neurofilament light chain (NFL) isolated from plasma, were strongly investigated.[55–60] A recent study reported that the plasma NFL concentration in HD patients correlated with clinical and magnetic resonance spectroscopy findings in the three-year international TRACK-HD study. Hence, plasma NFL and mutant HTT in the CSF show so far the strongest potential to become sensitive biomarkers to the AAV-miRNA gene therapy for HD.[58]

In addition to clinical biomarkers, cross-species biomarkers would be very useful to translate preclinical results into clinical studies in humans. Cortical metabolites, sleep and quantitative electroencephalographic measures have been proposed as potential biomarkers in R6/2 and zQ175 mice.[61–63] Longitudinal brain atrophy has been detected in N171-82Q mice by structural MRI that allows study of improvements upon treatment. The mutant HTT protein has been detected in the CSF of HD rodents and minipigs (M.M.E. et al., unpublished data).[57,64–66] Unfortunately, there is still a poor translatability of the imaging and biofluid-based biomarkers between the HD animal models and humans. There is an urgent need for studies that more precisely establish the cross-species biomarkers

Safety issues specific for AAV-delivered miRNA-based HTT lowering therapies

Safety is a major aspect of drug development and because of the long-term and irreversible nature of gene therapy, evaluation of short- and long-term toxicity is critical. Besides the routine safety studies that will not be discussed in this review, an AAV-miRNA gene therapy should be appropriately evaluated to: **1)** rule out a possible immune response to the AAV capsid or vector DNA, **2)** exclude potential off-target activity by overexpression of the therapeutic miRNA precursors, and **3)** demonstrate tolerability to long-term HTT lowering.

Immune response

AAV capsids as well as therapeutic DNA expression cassettes can provoke immune responses and novel gene therapy approaches expressing miRNA precursors need to address the potential of activating the immune system in the preclinical studies.[67] Neurophysiology and immunophysiology of HD animal models should be taken into account when designing such preclinical studies, especially as neurodegenerative disorders are known to induce a primed immune response, which is a result of a cascade of events following the presence of a toxic protein.[68] HD patients were shown to have mutant HTT-related activation of microglial cells in the striatum with cytokine upregulation in the body fluids.[69–71] Preclinical models of HD are also characterized by abnormal immune activation and in several HD mouse models microglial activation in the striatum has been demonstrated.[70,72,73] Transgenic HD minipigs display changes in the cytokine levels in the CNS, CSF, and serum as compared to healthy

littermates.[74] Therefore, these animal models provide a great opportunity to investigate a potential immune reaction to an AAV-miRNA gene therapy in the HD background.

AAV1, AAV2, and AAV5 transduce preferentially neurons and astrocytes after intracranial injection, whereas AAV9 more efficiently transduces astrocytes after intravenous delivery.[75–78] This cellular tropism has qualitative and quantitative consequences on the activation of immune response in the CNS. Intraparenchymal delivery of AAV1-miRNA to nonhuman primates has resulted in a dose-dependent mild microglial response and astrogliosis around the tip of injection, very likely due to a local injury caused by the needle.[79] Likewise, cytokines released from astrocytes and microglia were found to be transiently upregulated after intracranial delivery of the AAV5-miRNA gene therapy in a transgenic HD minipig model (M.M.E. et al., unpublished data). Next to local inflammatory and immune responses in the putamen, cell-mediated and humoral responses should be carefully evaluated to exclude that the AAV-miRNA gene therapy results in a constitutive activation of a peripheral immune response. A recent publication has shown a transient mild cytokine increase in the CSF after administrating the AAV5-miHTT in tgHD minipigs up to two weeks (M.M.E. et al., unpublished data). The cytokine increase returned to zero and remained as such till the termination of the study at three months. Therefore, the results from the above studies suggest a possibility of transient immune activation in the periphery shortly after the drug administration without causing adverse events.

Prediction and evaluation of miRNA on- and off-target activities

A general safety concern for RNAi therapeutics are unwanted side effects caused by expressing artificial miRNA precursors that lower HTT. These can be categorized as (**1**) negative on-target effects, which can result in dysregulation of genes due to lower HTT levels and (**2**) off-target effects caused by nonspecific binding of the miRNA to other mRNAs resulting in a prevention of translation.[80–82] There are cases showing that overexpression of shRNAs and miRNAs can cause toxicity and off-target activity caused by saturation of the RNAi machinery related to cellular processing of therapeutic precursors, or resulting from miRNA target sequence similarity with other genes.[83–85] In general, miRNA-induced gene silencing effect is based on 7-8 nucleotide homology between the so-called “seed” region of the miRNA and the 3’UTR of the gene. To date, all miRNAs that showed preclinical efficacy to lower the HTT mRNA were designed *in silico* and they vary in the length and sequence composition. The roles of specific miRNA sequences in the context of efficacy in target lowering are heavily studied but so far, the exact formulas enabling the design of highly efficient therapeutic miRNAs are largely missing. In the case of HTT silencing, the artificial miRNAs are being designed with a complete homology to induce sufficient HTT silencing, but they might also bind and lower the expression of other genes.[86] Off-targeting can be minimized by adopting a stringent design filter for both guide and passenger strands of the RNAi effector molecules. This approach has been validated for RNAi therapeutics targeting

HTT, where off-target effect was significantly minimized by avoiding partial complementarity of siRNAs to 3'UTR regions of nontargeted genes, whereas a strong lowering of HTT was maintained. [87–89] Notably, miRNAs are more accurately processed by Dicer compared with shRNAs, which increases their specificity to the target region.[90] Importantly, a specific precursor backbone was recently identified for the artificial miRNA and shRNA design that does not generate a passenger strand by avoiding Dicer processing and thus, a possibility of off-target silencing due to the passenger strand can be eliminated.[88,91,92]

The analysis of potential off-target activities caused by the RNAi therapeutics is rather complex in the HD background. HTT has been implicated in the transcriptional regulation and changes in gene expression patterns have been detected in HD animal models.[93] Off-target effects may be predicted by seeking for genomic sequences with partial homology to the artificial miRNA targets and addressing the potential gene expression changes in HD animal and cell models.[84,94]

Long-term wild-type HTT lowering

Most HTT lowering therapies do not discriminate between HTT alleles and the potential toxicity of long-term HTT lowering is therefore a major safety concern. Wild-type HTT is highly conserved and has important physiological functions in neuronal development, axonal transport, transcriptional regulation and protection from cell death. [Reviewed in 93] The long-term consequences of interfering with these processes in the adult HD context is largely unknown. Complete elimination of wild-type HTT is embryonically lethal in mice and negatively impacts adult neuronal function by reduction of neurotrophic factors, hampered mitochondrial trafficking, and increased production of reactive oxygen species.[95–97] Thus, silencing of the wild-type HTT must be done with a recognition that residual gene expression should be maintained at safe levels. Heterozygous Htt knockout mice are phenotypically normal and humans with only one copy of HTT (50% reduction of normal HTT production) show no abnormal behavioral deficits.[98–100] Recent studies have demonstrated that depletion of Htt in adult neurons is non-deleterious and HTT without N-terminal region is functional suggesting that silencing of HTT expression can be achieved within a certain therapeutic window in an adult human brain.[96,101]

A suitable system to study the long-term effects of HTT lowering would be a large animal brain. Current safety studies are lacking measurements beyond six months post injections (M.M.E. et al., unpublished data)..[79,102–104] The evaluation of consequences of long-term (> six months) 50% HTT lowering in large animals should be included in the preclinical portfolio before entering the clinic.

In summary, results from small and large HD animal studies suggest that a local (striatal), long-term (in months), and partial inactivation of endogenous HTT in adult brains can be achieved without important toxicity.[105] Notably, in most rodent models except for the humanized mice, the safety of wild-type HTT silencing cannot be studied as the human

HTT is expressed on the background of the murine Htt copies and in order to silence both HTT expressing genes, the target region needs to have enough sequence conservation. Further investigations are needed to evaluate if long-term wild-type HTT lowering affects neuronal function and whether compensatory changes in brain occur to prevent abnormal neurological functions.[105]

Dose finding

Dose finding in gene therapy studies is complex because it is not ethical to expose patients to either a non-active dose or to a potentially toxic dose. The initial dose for a phase I/IIa is calculated based on a conversion factor that translates results from preclinical animal and cell studies to the human brain. Several variables should be accounted for, including the differences in size and volume between animal and human brains, the spread of the volume delivered, and the AAV genomic copy number. Our studies showed linear correlations between the injected AAV vector DNA copies, miRNA expression, and HTT lowering efficacy, and we demonstrated that a minimal number of miRNA molecules per cell is required to reach 50% mutant HTT mRNA reduction (M.M.E. et al., unpublished data).[88,104,106] Nonetheless, the translation of preclinical results acquired in a relatively small animal brain to a large HD patient brain remains challenging. For instance, intra-striatal injections of AAV-miRNA gene therapy in small murine HD brains resulted in a widespread AAV distribution and HTT lowering throughout the brain.[83,88] On the other hand, intra-striatal delivery of AAV-miRNA gene therapy in nonhuman primates and transgenic HD minipigs resulted in a strong local transduction using lower viral doses and a more widespread AAV transduction and HTT lowering with an increasing viral load (M.M.E. et al., unpublished data).[79] AAVs preferentially make use of anterograde transport, whereas retrograde transport can be achieved with higher concentration of virus, suggesting that distribution patterns can be dose-dependent.[77] An additional layer of complexity is added by the HD neuropathology, with progressive white matter degeneration that is thought to reduce connectivity between the putamen and the motor cortex and thus, influencing the viral spread.[107] This further underlines the importance of proper dose-range finding studies in large HD animal models to close the gap between the preclinical research in HD rodents and clinical research in humans.

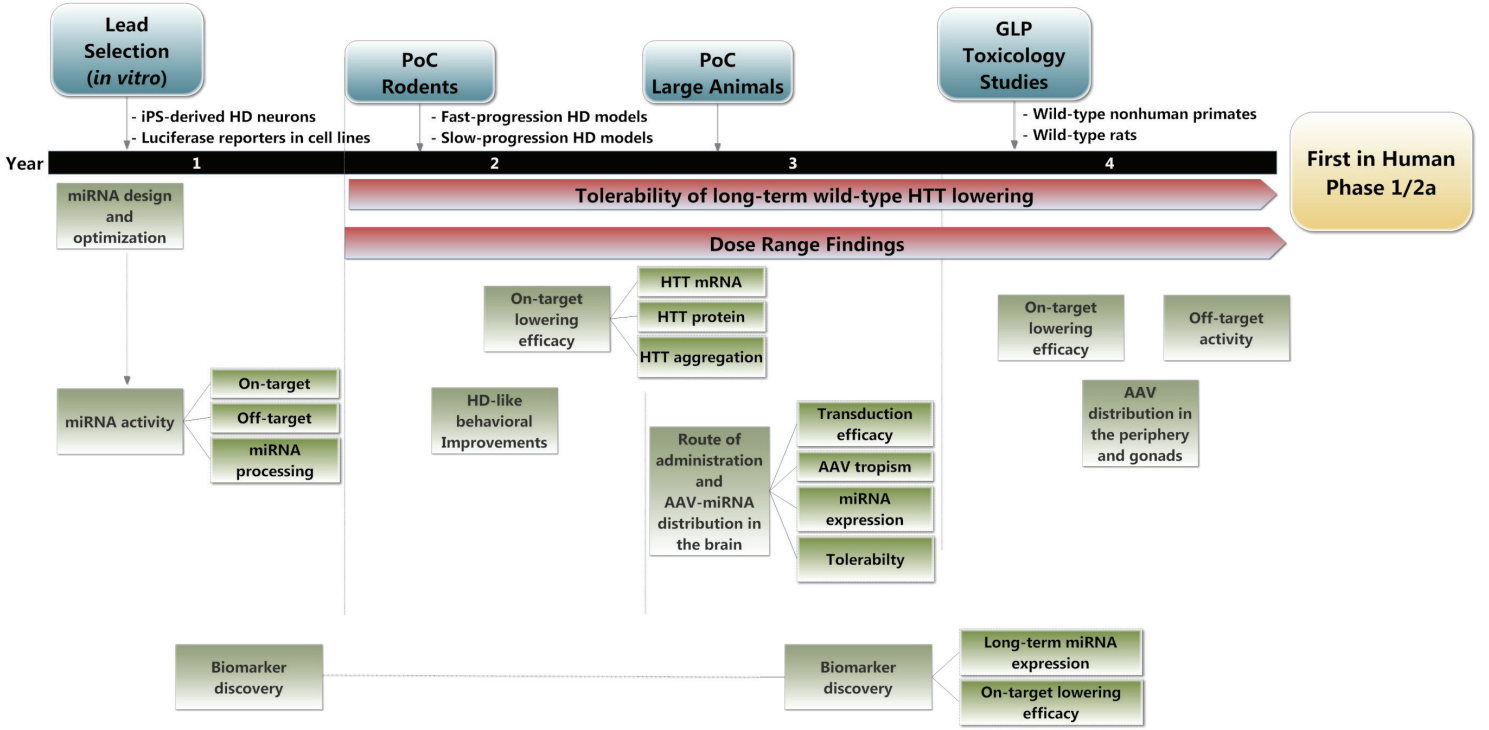

Lead Selection (in vitro)
PoC Rodents
PoC Large Animals
GLP Toxicology Studies
- iPS-derived HD neurons
- Luciferase reporters in cell lines
- Fast-progression HD models
- Slow-progression HD models
- Wild-type nonhuman primates
- Wild-type rats
Year
1
2
3
4
First in Human Phase 1/2a
miRNA design and optimization
Tolerability of long-term wild-type HTT lowering
Dose Range Findings
On-target lowering efficacy
HTT mRNA
HTT protein
HTT aggregation
On-target lowering efficacy
Off-target activity
miRNA activity
On-target
Off-target
miRNA processing
HD-like behavioral Improvements
AAV distribution in the periphery and gonads
Route of administration and AAV-miRNA distribution in the brain
Transduction efficacy
AAV tropism
miRNA expression
Tolerabilty
Biomarker discovery
Biomarker discovery
Long-term miRNA expression
On-target lowering efficacy

Figure 1. A preclinical framework for an AAV-miRNA gene therapy to treat HD. An overview of preclinical studies addressing clinically relevant aspects for HD treatment in various animal and cell models. Four major proof-of-concept (PoC) studies involve *in vitro* lead candidate selection using either luciferase reporters or iPSC-derived neuronal cultures, rodent and large animal studies addressing major efficacy and safety measures, and good laboratory practice (GLP) toxicology studies. Additionally, tolerability of long-term nonselective HTT lowering in a large animal should be explored.

Future perspectives on the HTT lowering gene therapy for HD

It has been difficult to translate therapeutic HD paradigms into disease-modifying treatments of this devastating disorder. Many studies have failed because of the incomplete preclinical characterization of the mechanism of action, and animal studies being poorly designed or underpowered.[108] In order to improve the odds of clinical success of gene-silencing therapies for HD, we propose a preclinical framework that addresses, using multiple HD cell and animal models, preclinical measures that are specific for therapies using AAVs as delivery vehicles in order to achieve gene silencing in the corticostriatal circuitry of the brain. The framework includes four main preclinical research phases (**Figure 1**): **1)** a lead selection using *in vitro* cell systems, **2)** proof of concept studies in rodents, **3)** proof of concept studies in large animals, and **4)** good laboratory practice toxicology studies. These areas are interdependent and timewise overlapping. The correlations between the outcomes of different preclinical studies should be made for each preclinical measure (e.g. a mode of action) with various readouts (e.g. lowering of HTT mRNA, protein, and aggregation) and they should be evaluated in terms of the translational power to clinical trials in HD patients. The overall aim of these studies is to gain sufficient knowledge on the efficacy and safety of an AAV-miRNA gene therapy approach. Once establishing a consistent miRNA activity across multiple species, we highlight the importance of careful selection of the AAV serotype together with a route of delivery to achieve safe but efficacious HTT lowering in the striatum and cortex. Importantly, the preclinical studies should strongly focus on the biomarker discovery specific for RNAi therapeutics to facilitate the translation into the clinic. In the near future it will be also important to integrate results from the repeated short-term HTT lowering clinical studies and the long-term HTT lowering preclinical studies in large HD animals to better address the consequences of the non-selective HTT lowering gene therapy in HD patients. Finally, a generation of a humanized large animal model that would express both human HTT copies and no endogenous animal HTT would be of a great interest to more accurately translate post-treatment preclinical results to humans. To conclude, it is exciting to observe fast preclinical progress of miRNA-based gene therapy approaches and to witness AAV-miRNA products being currently on a doorstep of clinical trials.

REFERENCES

1. Fink, KD, Deng, P, Gutierrez, J, Anderson, JS, Torrest, A, Komarla, A, *et al.* (2016). Allele-specific reduction of the mutant huntingtin allele using transcription activator- like effectors in human Huntington's disease fibroblasts Allele-Specific Reduction of the Mutant Huntingtin Allele Huntington's Disease Fibroblasts. *Cell Transplant*. **25**: 677–686.
2. Monteys, AM, Ebanks, SA, Keiser, MS and Davidson, BL (2017). CRISPR/Cas9 Editing of the Mutant Huntingtin Allele In Vitro and In Vivo. *Mol. Ther.* **25**: 12–23.
3. Shin, JW, Kim, K-H, Chao, MJ, Atwal, RS, Gillis, T, MacDonald, ME, *et al.* (2016). Permanent inactivation of Huntington's disease mutation by personalized allele-specific CRISPR/Cas9. *Hum. Mol. Genet*. **0**: 1–11.
4. Garriga-canut, M, Agustín-pavón, C, Herrmann, F, Sánchez, A, Dierssen, M, Fillate, C, *et al.* (2012). Synthetic zinc finger repressors reduce mutant huntingtin expression in the brain of R6/2 mice. *Proc. Natl. Acad. Sci.* **109**: E3136–E3145.
5. Malkki, H (2016). Selective deactivation of Huntington disease mutant allele by CRISPR–Cas9 gene editing. *Nat. Rev. Neurol.* **12**: 614–615.
6. Yang, S, Chang, R, Yang, H, Zhao, T, Hong, Y, Kong, HE, *et al.* (2017). CRISPR / Cas9-mediated gene editing ameliorates neurotoxicity in mouse model of Huntington ' s disease. *J. Clin. Invest.* **127**: 1–6.
7. Malankhanova, TB, Malakhova, AA, Medvedev, SP and Zakian, SM (2017). Modern Genome Editing Technologies in Huntington's Disease Research. *J. Huntingtons. Dis.* **6**: 19–31.
8. Ghosh, R and Tabrizi, SJ (2017). Gene suppression approaches to neurodegeneration. *Alzheimers. Res. Ther.* **9**: 82.
9. Messer, A and Joshi, SN (2013). Intrabodies as Neuroprotective Therapeutics. *Neurotherapeutics* **10**: 447–458.
10. Marschall, ALJ and Dübel, S (2016). Antibodies inside of a cell can change its outside: Can intrabodies provide a new therapeutic paradigm? *Comput. Struct. Biotechnol. J.* **14**: 304–308.
11. Amaro, IA and Henderson, LA (2016). An Intrabody Drug (rAAV6-INT41) Reduces the Binding of N-Terminal Huntingtin Fragment (s) to DNA to Basal Levels in PC12 Cells and Delays Cognitive Loss in the R6/2 Animal Model **2016**: 1–10.
12. Snyder-Keller, A, McLear, JA, A. Hathorn, T, Messer, A, Hathorn, T and Messer, A (2010). Early or Late-Stage Anti-N-Terminal Huntingtin Intrabody Gene Therapy Reduces Pathological Features in B6.HDR6/1 Mice. *J. Neuropathol. Exp. Neurol.* **69**: 1078–1085.
13. Southwell, AL, Ko, J and Patterson, PH (2009). Intrabody gene therapy ameliorates motor, cognitive, and neuropathological symptoms in multiple mouse models of Huntington's disease. *J. Neurosci.* **29**: 13589–13602.
14. Wild, EJ and Tabrizi, SJ (2017). Therapies targeting DNA and RNA in Huntington's disease. *Lancet Neurol.* **16**: 837–847.
15. Roberts, TC (2014). The MicroRNA Biology of the Mammalian Nucleus. *Mol. Ther. - Nucleic Acids* **3**: e188.
16. Gagnon, KT and Corey, DR (2012). Argonaute and the nuclear RNAs: new pathways for RNA-mediated control of gene expression. *Nucleic Acid Ther.* **22**: 3–16.
17. Jeffries, CD, Fried, HM and Perkins, DO (2011). Nuclear and cytoplasmic localization of neural stem cell microRNAs. *Spring*: 675–686doi:10.1261/rna.2006511.44.
18. Khudayberdiev, SA, Zampa, F, Rajman, M and Schratt, G (2013). A comprehensive characterization of the nuclear microRNA repertoire of post-mitotic neurons. *Front. Mol. Neurosci.* **6**: 1–19.
19. Liao, JY, Ma, LM, Guo, YH, Zhang, YC, Zhou, H, Shao, P, *et al.* (2010). Deep sequencing of human nuclear and cytoplasmic small RNAS reveals an unexpectedly complex subcellular distribution of mirnas and tRNA 3' trailers. *PLoS One* **5**: e10563.

20. Chu, Y, Yue, X, Younger, ST, Janowski, BA and Corey, DR (2010). Involvement of argonaute proteins in gene silencing and activation by RNAs complementary to a non-coding transcript at the progesterone receptor promoter. *Nucleic Acids Res.* **38**: 7736–7748.
21. Gagnon, KT, Li, L, Chu, Y, Janowski, BA and Corey, DR (2014). RNAi Factors are Present and Active in Human Cell Nuclei. *Cell Rep.* **6**: 211–221.
22. Földes-Papp, Z, König, K, Studier, H, Bückle, R, Breunig, HG, Uchugonova, A, *et al.* (2009). Trafficking of mature miRNA-122 into the nucleus of live liver cells. *Curr. Pharm. Biotechnol.* **10**: 569–78.
23. Zovkic, IB, Guzman-Karlsson, MC and Sweatt, JD (2013). Epigenetic regulation of memory formation and maintenance. *Learn. Mem.* **20**: 61–74.
24. Chan, HYE (2014). RNA-mediated pathogenic mechanisms in polyglutamine diseases and amyotrophic lateral sclerosis. *Front. Cell. Neurosci.* **8**: 1–12.
25. Alló, M, Buggiano, V, Fededa, JP, Petrillo, E, Schor, I, de la Mata, M, *et al.* (2009). Control of alternative splicing through siRNA-mediated transcriptional gene silencing. *Nat. Struct. Mol. Biol.* **16**: 717–724.
26. Liu, J, Hu, J and Corey, DR (2012). Expanding the action of duplex RNAs into the nucleus: Redirecting alternative splicing. *Nucleic Acids Res.* **40**: 1240–1250.
27. Mathivanan, S and Simpson, RJ (2009). ExoCarta: A compendium of exosomal proteins and RNA. *Proteomics* **9**: 4997–5000.
28. Kim, DK, Kang, B, Kim, OY, Choi, DS, Lee, J, Kim, SR, *et al.* (2013). EVpedia: An integrated database of high-throughput data for systemic analyses of extracellular vesicles. *J. Extracell. Vesicles* **2**.
29. Kalra, H, Simpson, RJ, Ji, H, Aikawa, E, Altevogt, P, Askenase, P, *et al.* (2012). Vesiclepedia: A Compendium for Extracellular Vesicles with Continuous Community Annotation. *PLoS Biol.* **10**: 8–12.
30. Reclusa, P, Taverna, S, Pucci, M, Durendez, E, Calabuig, S, Manca, P, *et al.* (2017). Exosomes as diagnostic and predictive biomarkers in lung cancer. *J. Thorac. Dis.* **9**: S1373–S1382.
31. Valentino, A, Reclusa, P, Sirera, R, Giallombardo, M, Camps, C, Pauwels, P, *et al.* (2017). Exosomal microRNAs in liquid biopsies: future biomarkers for prostate cancer. *Clin. Transl. Oncol.* **19**: 651–657.
32. Cheng, L, Wu, S, Zhang, K, Qing, Y and Xu, T (2017). A comprehensive overview of exosomes in ovarian cancer: emerging biomarkers and therapeutic strategies. *J. Ovarian Res.* **10**: 73.
33. Fesler, A, Jiang, J, Zhai, H and Ju, J (2014). Circulating microRNA testing for the early diagnosis and follow-up of colorectal cancer patients. *Mol. Diagnosis Ther.* **18**: 303–308.
34. Bellingham, S a, Guo, BB, Coleman, BM and Hill, AF (2012). Exosomes: vehicles for the transfer of toxic proteins associated with neurodegenerative diseases? *Front. Physiol.* **3**: 124.
35. Morales, R, Duran-Aniotz, C, Castilla, J, Estrada, LD and Soto, C (2012). De novo induction of amyloid-β deposition in vivo. *Mol. Psychiatry* **17**: 1347–1353.
36. Jeon, I, Cicchetti, F, Cisbani, G, Lee, S, Li, E, Bae, J, *et al.* (2016). Human-to-mouse prion-like propagation of mutant huntingtin protein. *Acta Neuropathol.* **132**: 577–592.
37. Soria, FN, Pampliega, O, Bourdenx, M, Meissner, WG, Bezard, E and Dehay, B (2017). Exosomes, an unmasked culprit in neurodegenerative diseases. *Front. Neurosci.* **11**: 1–12.
38. Deleo, AM and Ikezu, T (2017). Extracellular Vesicle Biology in Alzheimer ' s Disease and Related Tauopathy.
39. Vella, LJ, Hill, AF and Cheng, L (2016). Focus on extracellular vesicles: Exosomes and their role in protein trafficking and biomarker potential in Alzheimer's and Parkinson's disease. *Int. J. Mol. Sci.* **17**.
40. Tsunemi, T, Hamada, K and Krainc, D (2014). ATP13A2/PARK9 Regulates Secretion of Exosomes and -Synuclein. *J. Neurosci.* **34**: 15281–15287.
41. Mestre, TA and Sampaio, C (2017). Huntington Disease: Linking Pathogenesis to the Development of Experimental Therapeutics. *Curr. Neurol. Neurosci. Rep.* **17**: 1–8.

42. Tabrizi, SJ, Langbehn, DR, Leavitt, BR, Roos, RAC, Durr, A, Craufurd, D, *et al.* (2013). Biological and clinical manifestations of Huntington's disease in the longitudinal TRACK-HD study: cross-sectional analysis of baseline data. *Lancet Neurol.* **8**: 791–801.

43. Warner, J and Sampaio, C (2016). Modeling Variability in the Progression of Huntington's Disease A Novel Modeling Approach Applied to Structural Imaging Markers from TRACK-HD. *CPT Pharmacometrics Syst. Pharmacol.* **5**: 437–445.

44. Moss, DJH, Pardiñas, AF, Langbehn, D, Lo, K, Leavitt, BR, Roos, R, *et al.* (2017). Identification of genetic variants associated with Huntington's disease progression: a genome-wide association study. *Lancet Neurol.* **4422**: 1–11.

45. Long, JD, Paulsen, JS and Investigators, P-H (2015). Multivariate Prediction of Motor Diagnosis in Huntington's Disease: 12 Years of PREDICT-HD. *Mov. Disord.* **30**: 1664–1672.

46. Paulsen, JS, Long, JD, Johnson, HJ, Aylward, EH, Ross, C a, Williams, JK, *et al.* (2014). Clinical and Biomarker Changes in Premanifest Huntington Disease Show Trial Feasibility: A Decade of the PREDICT-HD Study. *Front. Aging Neurosci.* **6**: 1–11.

47. Sturrock, A, Laule, C, Wyper, K, Milner, RA, Decolongon, J, Santos, RD, *et al.* (2015). A Longitudinal Study of Magnetic Resonance Spectroscopy Huntington's Disease Biomarkers. *Mov. Disord.* **30**: 393–401.

48. Li, K, Furr-stimming, E, Paulsen, J, Luo, S and Investigators, P-H (2017). Dynamic Prediction of Motor Diagnosis in Huntington's Disease Using a Joint Modeling Approach. *J. Huntingtons. Dis.* **6**: 127–137.

49. Sturrock, A, Laule, C, Decolongon, J, Santos, R, Coleman, A, Creighton, S, *et al.* (2010). Magnetic resonance spectroscopy biomarkers in premanifest and early Huntington disease. *Neurology* **75**: 1702–1710.

50. Unschuld, PG, Edden, RAE, Carass, A, Liu, X, Shanahan, M, Wang, X, *et al.* (2012). Brain Metabolite Alterations and Cognitive Dysfunction in Early Huntington's Disease. *Mov. Disord.* **27**: 895–902.

51. Rosas, H, Chen, I, Doros, G, Salat, D, Chen, N, Kwong, K, *et al.* (2012). Alterations in Brain Transition Metals in Huntington Disease. *Arch Neurol.* **69**: 887–893.

52. Shin, H, Kim, MH, Lee, SJ, Lee, K, Kim, M, Kim, JS, *et al.* (2013). Decreased Metabolism in the Cerebral Cortex in Early-Stage Huntington's Disease: A Possible Biomarker of Disease Progression? *J Clin Neurol* **9**: 21–25.

53. Tang, CC, Feigin, A, Ma, Y, Habeck, C, Paulsen, JS, Leenders, KL, *et al.* (2013). Metabolic network as a progression biomarker of premanifest Huntington's disease. *JCI* **123**: 4076–4088.

54. Byrne, LM and Wild, EJ (2016). Cerebrospinal Fluid Biomarkers for Huntington's Disease. *J. Huntington's Dis.* **5**: 1–13.

55. Rodrigues, FFB, Byrne, L, McColgan, P, Robertson, N, Tabrizi, SSJ, Leavitt, BBR, *et al.* (2016). Cerebrospinal fluid total tau concentration predicts clinical phenotype in Huntington's disease. *J. Neurochem.* **139**: 22–25.

56. Wild, EJ, Boggio, R, Langbehn, D, Robertson, N, Haider, S, Miller, JRC, *et al.* (2015). Quantification of mutant huntingtin protein in cerebrospinal fluid from Huntington's disease patients. *JCI* **125**: 1979–1986.

57. Southwell, AL, Smith, SEP, Davis, TR, Caron, NS, Villanueva, EB, Xie, Y, *et al.* (2015). Ultrasensitive measurement of huntingtin protein in cerebrospinal fluid demonstrates increase with Huntington disease stage and decrease following brain huntingtin suppression. *Sci. Rep.* **5**: 1–11.

58. Byrne, LM, Rodrigues, FB, Blennow, K, Durr, A, Leavitt, BR, Roos, RAC, *et al.* (2017). Neurofilament light protein in blood as a potential biomarker of neurodegeneration in Huntington's disease: a retrospective cohort analysis. *Lancet Neurol.* **4422**: 1–9.

59. Rodrigues, F, Byrne, L, McColgan, P, Robertson, N, Tabrizi, S, Leavitt, B, *et al.* (2016). Cerebrospinal fluid total tau concentration predicts clinical phenotype in Huntington's disease. *J. Neurochem.* **139**: 22–25.

60. Rodrigues, FB, Byrne, LM, Mccolgan, P, Robertson, N, Tabrizi, SJ, Zetterberg, H, *et al.* (2016). Cerebrospinal Fluid Inflammatory Biomarkers Reflect Clinical Severity in Huntington's Disease. *PLoS One* **11**: e0163479.

61. Zacharoff, L, Tkac, I, Song, Q, Tang, C, Bolan, PJ, Mangia, S, *et al.* (2012). Cortical metabolites as biomarkers in the R6/2 model of Huntington's disease. *J. Cereb. Blood Flow Metab.* **32**: 502–514.
62. Leuchter, AF, Donzis, EJ, Cepeda, C, Hunter, AM, Estrada-Sánchez, AM, Cook, IA, *et al.* (2017). Quantitative electroencephalographic Biomarkers in Preclinical and Human Studies of Huntington's Disease: Are They Fit-for-Purpose for Treatment Development ? *Front. Neurol.* **8**: 1–12.
63. Fisher, SP, Schwartz, MD, Wurts-Black, S, Thomas, AM, Chen, T-M, Miller, MA, *et al.* (2016). Quantitative electroencephalographic analysis provides an early-stage indicator of disease onset and progression in the zQ175 knock-in mouse model of Huntington's disease. *Sleep* **39**: 379–391.
64. Aggarwal, M, Duan, W, Hou, Z, Rakesh, N, Peng, Q, Ross, CA, *et al.* (2012). Spatiotemporal mapping of brain atrophy in mouse models of Huntington's disease using longitudinal in vivo magnetic resonance imaging. *Neuroimage* **60**: 2086–2095.
65. Cheng, Y, Peng, Q, Hou, Z, Aggarwal, M, Zhang, J, Mori, S, *et al.* (2011). Structural MRI detects progressive regional brain atrophy and neuroprotective effects in N171-82Q Huntington's disease mouse model. *Neuroimage* **56**: 1027–1034.
66. Tan, Z, Dai, W, Van Erp, TGM, Overman, J, Demuro, A, Digman, MA, *et al.* (2015). Huntington's disease cerebrospinal fluid seeds aggregation of mutant huntingtin. *Mol. Psychiatry* **20**: 1286–1293.
67. Murlidharan, G, Samulski, RJ and Asokan, A (2014). Biology of adeno-associated viral vectors in the central nervous system. *Front. Mol. Neurosci.* **7**: 1–9.
68. Richards, RI, Robertson, SA, Keefe, LVO, Fornarino, D, Scott, A, Lardelli, M, *et al.* (2016). The Enemy within: Innate Surveillance-Mediated Cell Death, the Common Mechanism of Neurodegenerative Disease. *Front. Neurosci.* **10**: 1–20.
69. Björkqvist, M, Wild, EJ, Thiele, J, Silvestroni, A, Andre, R, Lahiri, N, *et al.* (2008). A novel pathogenic pathway of immune activation detectable before clinical onset in Huntington's disease. *J. Exp. Med.* **205**: 1869–1877.
70. Simmons, DA, Casale, M, Alcon, B, Pham, N, Narayan, N and Lynch, G (2007). Ferritin Accumulation in Dystrophic Microglia is an Early Event in the Development of Huntington's Disease. *Glia* **55**: 1074–1084.
71. Rocha, NP, Ribeiro, FM, Furr-stimming, E and Teixeira, AL (2016). Neuroimmunology of Huntington's Disease: Revisiting Evidence from Human Studies. *Hindawi Publ.* **2016**: 1–10.
72. Crotti, A, Benner, C, Kerman, BE, Gosselin, D, Lagier-tourenne, C, Zuccato, C, *et al.* (2014). Mutant Huntingtin promotes autonomous microglia activation via myeloid lineage-determining factors. *Nat. Neurosci.* **17**: 513–524.
73. Franciosi, S, Ryu, JK, Shim, Y, Hill, A, Connolly, C, Hayden, MR, *et al.* (2012). Age-dependent neurovascular abnormalities and altered microglial morphology in the YAC128 mouse model of Huntington disease. *Neurobiol. Dis.* **45**: 438–449.
74. Valekova, I, Jarkovska, K, Kotrcova, E, Bucci, J, Ellederova, Z, Juhas, S, *et al.* (2016). Revelation of the IFNα, IL-10, IL-8 and IL-1β as promising biomarkers reflecting immuno-pathological mechanisms in porcine Huntington's disease model. *J. Neuroimmunol.* **293**: 71–81.
75. Tenenbaum, L, Chtarto, A, Lehtonen, E, Velu, T, Brotchi, J and Levivier, M (2004). Recombinant AAV-mediated gene delivery to the central nervous system. *J Gene Med* **6**: 212–222.
76. Burger, C, Gorbatyuk, OS, Velardo, MJ, Peden, CS, Williams, P, Zolotukhin, S, *et al.* (2004). Recombinant AAV viral vectors pseudotyped with viral capsids from serotypes 1, 2, and 5 display differential efficiency and cell tropism after delivery to different regions of the central nervous system. *Mol. Ther.* **10**: 302–317.
77. Samaranch, L, Blits, B, San Sebastian, W, Hadaczek, P, Bringas, J, Sudhakar, V, *et al.* (2017). MR-guided parenchymal delivery of adeno-associated viral vector serotype 5 in non-human primate brain. *Gene Ther.* **24**: 253–261.
78. Vagner, T, Dvorzhak, A, Maria, A, Harms, C and Grantyn, R (2016). Systemic application of AAV vectors targeting GFAP-expressing astrocytes in Z -Q175-KI Huntington's disease mice. *Mol. Cell. Neurosci.* **77**: 76–86.

79. McBride, JL, Pitzer, MR, Boudreau, RL, Dufour, B, Hobbs, T, Ojeda, SR, *et al.* (2011). Preclinical Safety of RNAi-Mediated HTT Suppression in the Rhesus Macaque as a Potential Therapy for Huntington's Disease. *Mol. Ther.* **19**: 2152–2162.
80. Jackson, AL and Linsley, PS (2010). Recognizing and avoiding siRNA off-target effects for target identification and therapeutic application. *Nat. Rev. Drug Discov.* **9**: 57–67.
81. Singh, S, Narang, AS and Mahato, RI (2011). Subcellular fate and off-target effects of siRNA, shRNA, and miRNA. *Pharm. Res.* **28**: 2996–3015.
82. Cullen, BR (2006). Enhancing and confirming the specificity of RNAi experiments. *Nat. Methods* **3**: 677–681.
83. McBride, JL, Boudreau, RL, Harper, SQ, Staber, PD, Monteys, AM, Martins, I, *et al.* (2008). Artificial miRNAs mitigate shRNA-mediated toxicity in the brain: implications for the therapeutic development of RNAi. *Proc. Natl. Acad. Sci. U. S. A.* **105**: 5868–5873.
84. Monteys, AM, Spengler, RM, Dufour, BD, Wilson, MS, Oakley, CK, Sowada, MJ, *et al.* (2014). Single nucleotide seed modification restores in vivo tolerability of a toxic artificial miRNA sequence in the mouse brain. *Nucleic Acids Res.* **42**: 13315–13327.
85. Grimm, D, Streetz, KL, Jopling, CL, Storm, T a, Pandey, K, Davis, CR, *et al.* (2006). Fatality in mice due to oversaturation of cellular microRNA/short hairpin RNA pathways. *Nature* **441**: 537–541.
86. Bartel, DP, Lee, R and Feinbaum, R (2004). MicroRNAs : Genomics , Biogenesis , Mechanism , and Function **116**: 281–297.
87. Maczuga, P, Koornneef, A, Borel, F, Petry, H, van Deventer, S, Ritsema, T, *et al.* (2012). Optimization and comparison of knockdown efficacy between polymerase II expressed shRNA and artificial miRNA targeting luciferase and Apolipoprotein B100. *BMC Biotechnol.* **12**: 1–12.
88. Miniarikova, J, Zanella, I, Huseinovic, A, van der Zon, T, Hanemaaijer, E, Martier, R, *et al.* (2016). Design, Characterization, and Lead Selection of Therapeutic miRNAs Targeting Huntingtin for Development of Gene Therapy for Huntington's Disease. *Mol. Ther. Acids* **5**: e297.
89. Davidson, BL, Boudreau, RL, Rodrı, E, Rodríguez-Lebrón, E and Davidson, BL (2011). RNAi medicine for the brain: Progresses and challenges. *Hum. Mol. Genet.* **20**: 21–27.
90. Gu, S, Jin, L, Zhang, Y, Huang, Y, Zhang, F, Valdmanis, PN, *et al.* (2012). The loop position of shRNAs and pre-miRNAs is critical for the accuracy of Dicer processing in vivo. *Cell* **151**: 900–911.
91. Herrera-Carrillo, E, Harwig, A, Liu, YP and Berkhout, B (2014). Probing the shRNA characteristics that hinder Dicer recognition and consequently allow Ago-mediated processing and AgoshRNA activity. *RNA* **20**: 1410–1418.
92. Ma, H, Zhang, J and Wu, H (2014). Designing Ago2-specific siRNA/shRNA to Avoid Competition with Endogenous miRNAs. *Mol. Ther. Nucleic Acids* **3**: e176.
93. Saudou, F and Humbert, S (2016). The Biology of Huntingtin. *Neuron* **89**: 910–926.
94. Cambon, K, Zimmer, V, Martineau, S, Gaillard, M, Jarrige, M, Bugi, A, *et al.* (2017). Preclinical Evaluation of a Lentiviral Vector for Huntingtin Silencing. *Mol. Ther. Methods Clin. Dev.* **5**: 259–276.
95. Zuccato, C, Valenza, M and Cattaneo, E (2010). Molecular Mechanisms and Potential Therapeutical Targets in Huntington's Disease. *Physiol Rev* **90**: 905–981.
96. Wang, G, Liu, X, Gaertig, MA, Li, S and Li, X-J (2016). Ablation of huntingtin in adult neurons is nondeleterious but its depletion in young mice causes acute pancreatitis. *Proc. Natl. Acad. Sci.* **113**: 1–6.
97. Nasir, J, Floresco, S and O'Kusky, J (1995). Targeted disruption of the Huntington's disease gene results in embryonic lethality and behavioral and morphological changes in heterozygotes. *Cell* **81**: 811–823.
98. Ross, CA and Tabrizi, SJ (2011). Huntington's disease: From molecular pathogenesis to clinical treatment. *Lancet Neurol.* **10**: 83–98.
99. Duyao, MP, Auerbach, AB, Ryan, A, Persichetti, F, Glenn, T, Mcneil, SM, *et al.* (1995). Inactivation of the Mouse Huntingto's Disease Gene Homolog Hdh. *Science (80-.).* **269**: 407–410.

100. Ambrose, CM, Duyao, MP, Barnes, G, Bates, GP, Lin, CS, Srinidhi, J, *et al.* (1994). Structure and expression of the Huntington's disease gene: Evidence against simple inactivation due to an expanded CAG repeat. *Somat. Cell Mol. Genet.* **20**: 27–38.

101. Liu, X, Wang, C, Hong, Y, Zhao, T, Wang, G, Gaertig, MA, *et al.* (2016). N-terminal Huntingtin Knock-In Mice: Implications of Removing the N-terminal Region of Huntingtin for Therapy. *PLoS Genet.* **12**: 1–21.

102. Grondin, R, Kaytor, MD, Ai, Y, Nelson, PT, Thakker, DR, Heisel, J, *et al.* (2012). Six-month partial suppression of Huntingtin is well tolerated in the adult rhesus striatum. *Brain a J. Neurol.* **135**: 1197–1209.

103. Hadaczek, P, Stanek, L, Ciesielska, A, Sudhakar, V, Samaranch, L, Pivirotto, P, *et al.* (2016). Widespread AAV1- and AAV2-mediated transgene expression in the nonhuman primate brain: implications for Huntington's disease. *Mol. Ther. Methods Clin. Dev.* **3**: 16037.

104. Evers, MM, Miniarikova, J, Juhas, S, Vallès, A, Bohuslavova, B, Juhasova, J, *et al.* AAV5-miHTT gene therapy demonstrates broad distribution and strong human mutant huntingtin lowering in a Huntington disease minipig model: Submitted to Neuron.

105. Liu, J-P and Zeitlin, SO (2017). Is Huntingtin Dispensable in the Adult Brain? *J. Huntington's Dis.* **6**: 1–17.

106. Miniarikova, J, Zimmer, V, Martier, R, Brouwers, CC, Pythoud, C, Richetin, K, *et al.* (2017). AAV5-miHTT gene therapy demonstrates suppression of mutant huntingtin aggregation and neuronal dysfunction in a rat model of Huntington's disease. *Gene Ther.* **24**: 630–639.

107. Ross, CA, Aylward, EH, Wild, EJ, Langbehn, DR, Long, JD, Warner, JH, *et al.* (2014). Huntington disease: natural history, biomarkers and prospects for therapeutics. *Nat. Rev. Neurol.* **10**: 204–16.

108. Travessa, A, Rodrigues, F, Mestre, T and Ferreira, J (2017). Fifteen Years of Clinical Trials in Huntington's Disease: A Very Low Clinical Drug Development Success Rate. *J. Huntingtons. Dis.* **6**: 157–163.

A

ADDENDUM

ENGLISH SUMMARY

Huntington's disease (HD) is a devastating neurodegenerative disease caused by a single mutation, a CAG expansion, in the huntigntin (*HTT*) gene. The resultant mutant HTT protein has been shown to be the predominant toxic entity in the HD pathogenesis and therapeutic strategies that aim to lower the mutant HTT show a great promise. Micro (mi)RNAs are a class of small cellular RNAs that bind to target mRNAs based on the base-pair complementarity to mainly supress mRNA translation into a protein. Thus, miRNAs offer a therapeutic tool to lower the expression of disease genes such as *HTT*. For clinical applications, the expression cassette of therapeutic miRNAs can be delivered to the target tissue by the AAV vectors to achieve a long-term (in years) expression of miRNA precursors. These precursors are being further processed by the cellular RNA interference (RNAi) machinery to render mature a miRNA molecule that recognizes a specific sequence in the disease transcript and enables the reduction of toxic HTT protein, HTT lowering.

In **chapter 1**, we describe a current knowledge on the HD pathogenesis, HTT RNA-lowering treatment strategies, and HD cell and animal models enabling the preclinical development. We positioned the AAV-delivered-miRNA-based HTT gene therapy among currently investigated HTT lowering strategies. We provide a description of the efficacy outcome measures in the preclinical cell and animal HD models that present the proof-of-concept and proof-of-principle that are necessary to be addressed before the initiation of a clinical trial.

In **chapter 2,** we describe the pilot proof-of-concept study using the miRNA-based gene therapy approach. We have designed and tested *in vitro* and *in vivo* the efficacy of different miRNAs targeting various sequences in *HTT* exon 1, 50, and 67. Based on the generated results, we selected the miHTT construct targeting a sequence located one nucleotide upstream from the CAG expansion in exon 1 for further preclinical development. The miHTT construct showed the strongest efficacy *in vitro* and in the humanized HD 128/21 mouse model. Furthermore, as first in the HD field, we tested several pri-miRNA precursors to optimize the processing patterns of the selected miHTT to enhance the safety profile. We identified the human pre-miR-451 precursor as the only scaffold that does not produce the passenger strand both *in vitro and in vivo* thus, the use of this precursor offers a prevention of the unwanted off-target effects associated with the passenger strand.

To further establish the proof-of-mechanism, we addressed the efficacy of the miHTT-451 construct on supressing the downstream pathological HTT aggregation and neurodegeneration. In **chapter 3,** we injected the miHTT-451 construct delivered by AAV5 vectors bilaterally in the striatum of the lentiviral HD rat model to measure a therapeutic response. We showed strong reduction of HTT aggregation, which supressed the neuronal dysfunction at two months post injections. This study demonstrated a functional efficacy of the AAV5-miHTT-451 construct affecting downstream pathological events caused by

the mutant HTT protein. These results further supported the continuation of preclinical studies in large animals, which are beyond the scope of this thesis. Currently, the miHTT-451 construct is the product candidate AMT-130 in the development pipeline of uniQure, N.V. In October 2017, AMT-130 received the orphan drug designation in HD by the U.S. Food and Drug Administration. In January 2018, AMT-130 received an Orphan Medicinal Product Designation (OMPD) in HD from the European Medicines Agency, making it the first investigational AAV-gene therapy in HD to receive such designation. AMT-130 is expected to enter the clinical development in 2019.

The role of miRNAs in the cytoplasm is well established, however their functions in the nucleus are only recently being described. Lowering of HTT transcripts in the nucleus is intriguing because some level of HTT RNA toxicity in the nucleus has been reported. Moreover, extending the therapeutic effect of miRNAs to the nucleus could offer new applications for other indications in the future. In **chapter 4**, we designed miRNAs that specifically target a newly identified polymorphic sequence linked to the mutant HTT intron 22 with a deletion of four nucleotides, ΔACTT. This heterozygous polymorphism is largely characteristic for A1 haplogroup of HD patients and therefore it offers simultaneously an evaluation of allele-specific and nuclear HTT lowering. We showed a strong 90% HTT lowering of mutant protein in HD neuronal cultures heterozygous for ΔACTT and almost 0% lowering in ΔACTT-negative HD cultures, demonstrating the strongest allele-selective efficacy so far. Interestingly, these data challenge the traditional concept of mature miRNAs acting mainly in the cytoplasm. We propose the general concept of targeting nuclear disease-related genes by therapeutic miRNAs and we recommend further preclinical validation studies.

To enable the translation of HD gene therapy to the patients, it is important to identify informative pharmacokinetic/pharmacodynamic (PK/PD) measures, in easily obtainable biofluids such CSF or blood, which would correlate the expression of active AAV-miRNA vectors in the brain of treated HD patients with the efficacy and long-term effects. In **chapter 5,** we showed first indications that therapeutic miRNAs can be secreted within vesicles enriched for exosomes from human HD patient neuronal cultures. These findings are substantial and not only for the HD field. Having a therapy-specific PK/PD measure, which can be applicable to other CNS indications, will significantly impact the preclinical and clinical development of RNAi-based gene therapies currently facing these challanges. Further invistigations are ongoing beyond the scope of this thesis in order to provide better understandings on the mechanism of action and a possibility of the 'exosomal spread' of HTT silencing *in vivo*. Finally, in **chapter 6**, we summarize the current knowledge on HTT DNA and protein-lowering strategies, provide an overview of the safety preclinical measures for miRNA-based gene therapy and its future perspectives. To conclude, data presented in this thesis resulted in three first-author publications, one patent, and fuelled further preclinical and clinical development of AMT-130 gene therapy for HD.

DUTCH SUMMARY / NEDERLANDSE SAMENVATTING

De ziekte van Huntington (ZvH) is een ernstige hersenaandoening die veroorzaakt wordt door een CAG-verlenging in het huntingtine (HTT) gen. Het is bewezen dat het schadelijke mutante HTT-eiwit de voornaamste oorzaak is van ZvH en therapeutische strategieën die gericht zijn op het verlagen van het schadelijke HTT eiwit zijn veelbelovend. Micro (mi) RNA's zijn korte cellulaire RNAs die aan een complementair stukje boodschappermolecuul, messenger RNA (mRNA) genaamd, kunnen binden om zo de translatie tot eiwit te stoppen. Door gebruik te maken van deze eigenschap kunnen miRNAs worden ontworpen welke in een expressieplasmide gekloneerd zijn om de expressie van ziekte genen zoals HTT te verlagen.

De miRNA-coderende plasmide wordt vervolgens verpakt in niet delende, niet in het humane genoom integrerende virussen, genaamd AAVs. Het verpakken van therapeutische genen in een AAV wordt gentherapie genoemd. Deze onschadelijke AAVs worden afgeleverd aan de desbetreffede weefsels, opgenomen door de cellen, gaan naar de celkern resulterend in lange termijn (in jaren) expressie van precursor miRNA (pre-miRNA). Deze pre-miRNAs worden verder verwerkt door het cellulaire RNA-interferentie (RNAi) mechanisme tot een "gematureerd" miRNA molecuul. Het "gematureerde" miRNA molecuul kan aan een complementaire stukje HTT mRNA binden met vervolgens een reductie in het schadelijke HTT-eiwit als gevolg: HTT gen-uitschakeling.

In **hoofdstuk 1** wordt de huidige kennis en ontwikkelingen beschreven over de pathogenese van de ZvH, behandelstrategieën om het schadelijke HTT uit te schakelen en het gebruik van cellulaire en diermodellen in preklinische studies. Daarnaast wordt de strategie van AAV gentherapie tegen de ZvH bescherven in dit proefschrift vergeleken met andere strategieën die gebruikt worden om HTT te verlagen. Ook wordt er een beschrijving gegeven van de voorafgaande preklinische studies in cellulaire en diermodelen die noodzakelijk zijn als "proof-of-concept" en "proof-of-principle" om met een klinische studie te kunnen beginnen.

In **hoofdstuk 2** wordt een proof-of-concept studie beschreven van gentherapie door middel van miRNAs resulterend in HTT gen-uitschakeling. Verschillende miRNA's werden ontworpen tegen HTT-exon 1, 50 en 67 en getest *in vitro* en *in vivo*. Op basis hiervan hebben we het miHTT-construct geselecteerd voor verdere preklinische ontwikkeling. Het geselecteerde miHTT-construct bindt één nucleotide vóór de CAG-expansie in exon 1 en gaf het sterkste effect *in vitro* en *in vivo* in een gehumaniseerd ZvH muismodel, Hu128/21. Daarnaast hebben we als eerste in het ZvH-veld verschillende primaire-miRNA moleculen zowel *in vitro* als *in vivo* getest om zo het productieproces van miHTT in cellen te optimaliseren en het veiligheidsprofiel te verbeteren. We hebben vastgesteld dat de humane miR-451 precursor als enige primaire-miRNA molecuul geen extra tweede tegenovergesteld molecuul, genaamd passagiersstreng produceerd. Door deze miRNA precursor te gebruiken

kunnen dus de ongewenste effecten die geassocieerd worden met de passagiersstreng worden uitgesloten. Het werk beschreven in hoofdstuk 2 heeft geresulteerd in de selectie van één therapeutische kandidaat, genaamd AAV5-miHTT-451.

Voor een verder mechanistisch bewijs hebben we gekeken naar de effecten van het miHTT-451-construct om formatie van HTT-aggregatie en neurodegeneratie te onderdrukken. In **hoofdstuk 3** werd AAV5-miHTT-451 bilateraal geintjecteerd in het striatum van een lentivirale ZvH rat model en detherapeutische effecten werden bestudeerd. Een sterke vermindering in aggregatie van het schadelijke HTT eiwit werd aangetoond, wat vervolgens leidde tot onderdrukking van neuronaal dysfunctioneren van het ZvH rat model. Deze studie bevestigd een functioneel therapeutishe effect van AAV5-miHTT-451 op de ZvH pathologie dat veroorzaakt wordt door het mutante HTT-eiwit. Deze resultaten ondersteunen verdere ontwikkelingen van preklinische studies in grotere dieren, die buiten het kader van dit proefschrift vallen. Momenteel is het miHTT-451-construct de definieve productkandidaat AMT-130 in de ontwikkelingspijplijn van uniQure, N.V. In oktober 2017 ontving AMT-130 de “orphan drug designation” onderscheiding in ZvH door de “Amerikaanse Food and Drug Administration”. In januari 2018 ontving AMT-130 een “Orphan Medicinal Product Designation” (OMPD) onderscheiding in ZvH van “European Medicines Agency”, als eerste AAV-gentherapie voor ZvH. Er wordt verwacht dat AMT-130 in 2019 de klinische ontwikkeling zal ingaan.

De rol van miRNAs in het cytoplasma is uitvoerig onderzocht, maar hun mogelijke functies in de celkern zijn pas recent beschreven. Verlaging van HTT-transcripten in de celkern is interessant omdat hier ook een kleine hoeveelheid van het schadelijke HTT-RNA actief is. Bovendien zou therapeutische effecten van miRNAs in de kern nieuwe kansen kunnen bieden in de toekomst voor andere ziektes. In **hoofdstuk 4** wordt beschrven hoe miRNAs ontworpen zijn om specifiek tegen een recent geïdentificeerde polymorfisme sequentie dat gekoppeld is aan het mutante allel. Deze polymorphisme bevindt zich in HTT-intron 22 en bestaat uit een deletie van vier nucleotiden; ACTT en is grotendeels uniek voor de A1-haplogroep van ZvH-patiënten en biedt daarom een mogelijkheid voor een allel-specifieke en nucleare strategie om HTT te onderdrukken. Gebruik makend van miRNAs is een zeer sterke reductie van 90% aangetoond van de mutante HTT eiwit in ZvH-neuronale cellijnen die heterozygoot zijn voor ΔACTT. In ΔACTT-negatieve neuronale cellijnen geen verlaging was aangetoond, wat tot nu toe de sterkste allel-speciefieke reductie is beschreven in de literatuur. Deze bevindingen dienen als bewijs dat miRNA’s ook in de celkern actief kunnen zijn en gebruikt kunnen worden in preklinische validatiestudies tegen andere schadelijke mRNA moleculen welke tot hersenaandoeningen leiden en die specifiek in de celkern tot expressie komen.

Om verder ontwikkelingen in een ZvH-gentherapie in patiënten te ondersteunen, is het belangrijk om wat het lichaam doet met het medicijn en wat het medicijn doet met het lichaam (PK/PD)-metingen te verrichten in lichaamsvloeistoffen die gemakkelijk te verkrijgen

zijn, zoals hersenvocht of bloed. Hiermee kan een verband gelegd worden van de aanwezige hoeveelheid miRNA moleculen in de hersenen met de klinische langetermijn effecten in ZvH-patienten. In **hoofdstuk 5** worden de bevindingen beschreven dat therapeutische miRNA's in neuronale cellijnen van ZvH-patiënten uitgescheiden kunnen worden in vesikels verrijkt met exosomen. Deze bevindingen zijn van groot belang voor de ZvH veld en andere ziekte indicaties. Het hebben van een specifieke PK/PD-metingen, die van toepassing kunnen zijn op andere CNS-indicaties, zal een aanzienlijke invloed hebben op de preklinische en klinische ontwikkeling van gentherapieën op basis van gen-uitschakeling die momenteel met deze uitdagingen worden geconfronteerd. Verdere studies worden gedaan buiten het kader van dit proefschrift om een beter inzicht te krijgen van het mechanisme en mogelijkheid van de 'exosomale verspreiding' van HTT gen-uitschakeling *in vivo*.

Tot slot, in **hoofdstuk 6**, wordt de huidige kennis over reductie van HTT-mRNA en eiwit strategieën samengevat. Verder wordt er een overzicht gegeven van de preklinische veiligheidsmaatregelen voor gentherapie op basis van miRNA en de mogelijkheden voor de toekomst.

SLOVAK SUMMARY / ZHRNUTIE V SLOVENČINE

Huntingtonova choroba (Huntington's disease, HD) patrí k doposiaľ nevyliečiteľným neurodegeneratívnym ochoreniam vykazujúcim autozómovo dominantnú dedičnosť. Samotnou príčinou ochorenia je nadpočetné opakovanie C-A-G kodónu, v počte 40 a viac, v géne kódujúcom proteín huntingtín (*HTT*). Expanziou C-A-G trípletu dochádza k vzniku mutantnej formy huntigtínu a celkovej zmene jeho funkcie v organizme. Zmutovaný HTT proteín sa ukázal byť prevládajúcou toxickou entitou, ktorá podmieňuje vznik HD patogenézy v mozgu. Veľký význam sa preto prikladá vývoju terapeutických stratégií, ktorých cieľom je znížiť hladinu zmutovaného HTT proteínu. Mikro (mi)RNA patria do triedy malých bunkových RNA, ktoré sa na základe komplementarity báz viažu na príslušné mRNA a tým potláčajú ich transláciu do proteínu. miRNA môžu potenciálne slúžiť ako terapeutický nástroj na zníženie expresie mutantného *HTT* génu. V klinických aplikáciach je expresná kazeta kódujúca danú terapeutickú miRNA doručená do mozgu za pomoci adeno-asociovaných vírusov (AAV), kde zaručí dlhodobú expresiou miRNA prekurzorov a to v priebehu niekoľkých rokov. Tieto prekurzory sú ďalej spracovávané mechanizmom bunkovej RNA interferencie (RNAi) za vzniku maturovanej miRNA molekuly, ktorá rozpoznáva špecifickú sekvenciu v HTT mRNA a zabezpečí zníženie produkcie toxického HTT proteínu.

V prvej kapitole opisujeme súčasné poznatky o Huntingtonovej patogenéze, terapeutických stratégiách, ktoré znižujú hladinu zmutovaného HTT, a bunkové a živočíšne modely umožňujúce preklinický výskum tohto ochorenia. Zaradili sme génovú terapiu využívajúcu miRNA doručovaných pomocov AAV vírusov medzi, v súčasnosti študované, terapeutické metódy znižovania hladiny zmutovaného HTT. Popisujeme experimentálne poznatky získané z predklinických štúdií na bunkových a zvieracích modeloch Huntingtonovej choroby, ktoré sú dôkazom potenciálnej účinnosti génovej terapie na liečenie Huntingtonovej choroby, a potrebným predpokladom pred začiatkom klinickej štúdie.

V druhej kapitole opisujeme pilotnú štúdiu využívajúcu génovú terapiu na základe miRNA. Navrhli a testovali sme účinnosť rôznych terapeutických miRNA zacielených na rôzne sekvencie v HTT exónoch 1, 50 a 67 *in vitro* a *in vivo*. Na základe získaných výsledkov sme pre ďalší predklinický výskum vybrali miHTT konštrukt zacielený na sekvenciu umiestnenú jeden nukleotid *upstream* od začiatku CAG opakovania v exóne 1. miHTT konštrukt vykazoval najsilnejšiu účinnosť *in vitro* a v humanizovanom myšacom modeli (hu128/21). Okrem toho sme ako prví v oblasti výskumu Huntingtonovej choroby testovali niekoľko pre-miRNA prekurzorov s cieľom zvýšiť bezpečnosť lieku. Identifikovali sme pre-miR-451 ako jediný prekurzor, ktorý neprodukuje opozitný reťazec *in vitro* a *in vivo*, a preto zlepšuje profil bezpečnosti lieku.

V nadväznosti na predchádzajúcu štúdiu sme sa rozhodli otestovať účinnosť génovej terapie využívajúcej miHTT-451 konštrukt na potlačenie agregácie HTT proteínu a neurodegenerácie. **V tretej kapitole** sme injektovali AAV5 vektory nesúce miHTT-451

konštrukt bilaterálne do prúžkovaného telesa (striatum) potkanov, ktoré reprezentujú lentivírusoý model Huntingtonovej choroby a následne sme merali terapeutickú odpoveď. Ukázali sme výrazné zníženie počtu HTT agregátov, čo viedlo k potlačeniu neuronálnej dysfunkcie dva mesiace po injektovaní. Táto štúdia preukázala funkčnú účinnosť AAV5-miHTT-451 konštruktu na potlačenie patologických príhod spôsobených zmutovaným HTT proteínom. Naše výsledky podporili pokračovanie predklinických štúdií na ďalších zvieracích modeloch, ktoré sú mimo rozsahu tejto práce. V súčasnej dobe je miHTT-451 konštrukt sľubným kandidátom (AMT-130) v uniQure pre liečenie Huntingtonovej choroby. V októbri 2017 bola AMT-130 génová terapia označená organizáciou FDA (Food and Drug Administration) v USA ako „*Orphan Drug*“ a v januári 2018 organizáciou EMA (European Medicines Agency) ako *„Orphan Medicinal Product Designation”* (OMPD), vďaka čomu sa stala prvou študovanou AAV génovou terapiou, ktorá prijala toto označenie na poli Huntingtonovej choroby. Očakáva sa, že AMT-130 vstúpi do klinického vývoja v roku 2019.

Úloha miRNA v cytoplazme je pomerne dobre popísaná, ale ich funkcia v jadre bunky začala byť objasňovaná iba nedávno. Zaujímavé je znižovanie HTT mRNA v jadre, pretože v jadre bola hlásená určitá úroveň toxicity spôsobená HTT mRNA. Okrem toho rozšírenie terapeutického účinku miRNA do jadra bunky by mohlo v budúcnosti ponúknuť nové možnosti v aplikácach aj pre iné ochorenia. **V štvrtej kapitole** sme navrhli miRNA, ktoré sú špecificky zamerané na nedávno identifikovanú polymorfnú sekvenciu s deléciou štyroch nukleotidov, ΔACTT, ktorá sa nachádza v intróne 22 zmutovaného HTT mRNA. Tento heterozygotný polymorfizmus je vo veľkej miere charakteristický pre pacientov Huntingtonovej choroby haploskupiny A1 a preto je možné súčasne zabezpečiť alelovú špecificitu a zníženie hladiny jadrového HTT pre liečbu Huntingtonovej choroby. V tejto kapitole sme ukázali 90% zníženie zmutovaného HTT proteínu v ľudských neuronálnych bunkových kultúrach Huntingtonovej choroby heterozygotných pre ΔACTT, a takmer 0% zníženie v ΔACTT-negatívnych kultúrach, čo ukazuje najsilnejšiu selektívnu účinnosť génovej terapie do súčasnosti vôbec. Zaujímavé je, že tieto údaje spochybňujú tradičný koncept zmaturovaných miRNA, ktoré pôsobia predovšetkým v cytoplazme. Preto sme navrhli všeobecnú koncepciu znižovania expresie génov v jadre bunky, ktoré spôsobujú iné ochorenia, za pomoci terapeutických miRNA a odporúčame ďalšie predklinické validačné štúdie.

Klinické štúdie predstavujú pokročilú fázu vývoja nového lieku. Aby bolo možné zavedenie výsledkov génovej terapie z preklinických štúdii k pacientom s Huntingtonovou chorobou, dôležitou zložkou výskumu je identifikácia farmakokinetických/farmakodynamických markerov. Ideálne sú tieto markery merané na ľahko získateľných biologických tekutinách ako je krv alebo cerebrospinálna tekutina a ukazujú koreláciu medzi expresiou účinných AAV-miRNA vektorov a dlhodobou účinnosťou u pacientov s Huntingtonovou chorobou liečených génovou terapiou. **V piatej kapitole** sme ukázali prvé náznaky, že terapeutické miRNA môžu byť vylučované vo vezikulách obohatených o exozómy z ľudských neuronálnych bunkových kultúr pacientov s Huntingtonovou chorobou. Tieto zistenia sú významné

nielen pre oblasť Huntingtonovej choroby. Použitie terapeutických miRNA ako špecifických farmakokinetických/farmakodynamických markerov pre génovou terapiu môže byť aplikovateľné aj pre iné neurálne ochorenia a bude mať významný vplyv na predklinický a klinický vývoj génových terapií založených na RNAi. Ďalšie štúdie pokračujú nad rámec tejto práce za účelom objasnenia mechanizmu účinku a možnosti „exosomálneho šírenia" znižovania hladiny HTT *in vivo*.

Napokon, **v šiestej kapitole** sumarizujeme súčasné poznatky o géne pre HTT a stratégiách znižovania hladiny mutantného huntingtínu, poskytujeme prehľad predklinických bezpečnostných opatrení pre génovú terapiu založenú na miRNA a jej budúce perspektívy. Na záver, výsledky prezentované v tejto práci viedli k trom publikáciam prvého autora, jeden patent a ďalší predklinický a klinický vývoj génovej terapie s AMT-130 na liečbu Huntingtonovej choroby.

LIST OF ABBREVIATIONS

3'UTR	3' untranslated region
AAV	adeno-associated virus
AD	Alzheimer's disease
Ago	Argonaute protein
BBB	blood brain barrier
CAG	cytomegalovirus immediate-early enhancer fused to chicken β-actin promoter
CMV	cytomegalovirus
CNS	central nervous system
CSF	cerebrospinal fluid
dsRNA	double-stranded DNA
gDNA	genomic DNA
GFAP	glial fibrillary acidic
GFP	green fluorescent protein
HD	Huntington's disease
HTT	huntingtin
ICV	intracerebroventricular
ITR	inverted terminal repeat
miRNA	microRNA
MRI	magnetic resonance imaging
NGS	next generation sequencing
NHP	nonhuman primate
Nt	nucleotide
ORF	open reading frame
pA	polyadenylation signal
PD	Parkinson's disease
PK/PD	pharmacokinetic/pharmacodynamic
polyQ	polyglutamine
pre-miRNA	precursor miRNA
pri-miRNA	primary precursor miRNA

qRT-PCR	quantitative real-time polymerase chain reaction
RNAi	RNA interference
RNAse H	ribonuclease H
RT-PCR	real-time polymerase chain reaction
shRNA	short hairpin RNA
siRNA	small interfering RNA
SNP	single nucleotide polymorphism
SOD1	superoxide dismutase 1
ss-siRNA	single-stranded silencing RNA
3'UTR	3' untranslated region

CURRICULUM VITAE

Jana Miniariková was born on 26-07-1988 in Bratislava, Slovakia. In 2003, she entered Bilingual High School Metodova in Bratislava, Slovakia with a focus on Natural Sciences. She graduated with a majority of subjects in French. In 2008, she started her bachelor studies in Biology at Comenius University in Bratislava, Slovakia. She graduated with a major in Genetics. During these studies, she lived one year in Málaga, Spain as an exchange student having all subjects thought in Spanish. In 2012, she moved to Rotterdam, Netherlands to study Molecular Medicine at Erasmus Medical Center Rotterdam. During her internship at the Department of Hematology, she investigated the biology of cellular microRNAs and their roles in hematologic malignancies. During these studies, she realized the clinical applicability of microRNAs to treat genetic disorders. In 2014, she pursued actions to translate the basic knowledge into a preclinical development as a doctoral researcher at Leiden University Medical Center, Leiden, Netherlands. The work described in this thesis was performed at uniQure, Amsterdam, Netherlands under a daily supervision of Dr. Pavlina Konstantinova and her promoter Prof. Dr. Sander J. van Deventer. In 2018, while approaching to her graduation date, she joined ttopstart, Utrecht, Netherlands. As a ttopstart consultant, she appreciates the opportunity to combine science, business, creativity and innovation, while reaching a wide audience. She yearns to work with the brightest mind to reinvent biotech and contribute to the society.

LIST OF PUBLICATIONS AND PATENTS

Martier, R, Liefhebber, J, Evers, MM, van der Zon, T, Snapper, J, **Miniarikova, J**, *et al.* MicroRNAs targeting C9ORF72 have the potential to reduce gain of toxicity in ALS and FTD patients. *Submitted to Mol. Ther. Nucleic Acids.*

Evers, MM, **Miniarikova, J**, Juhas, S, Vallès, A, Bohuslavova B, Juhasova, J, Kupcova, H *et al*. **(2018)**. AAV5-miHTT gene therapy demonstrates broad distribution and strong mutant huntingtin lowering in a Huntington's disease minipig model. *Mol. Ther.* ***26****(9):2163-2177.*

Miniarikova, J, Evers, MM and Konstantinova, P (**2018**). Translation of MicroRNA-Based Huntingtin-Lowering Therapies from Preclinical Studies to the Clinic. *Mol. Ther.* **26**: 947–962.

Miniarikova, J, Zimmer, V, Martier, R, Brouwers, CC, Pythoud, C, Richetin, K, *et al.* (**2017**). AAV5-miHTT gene therapy demonstrates suppression of mutant huntingtin aggregation and neuronal dysfunction in a rat model of Huntington's disease. *Gene Ther.* **24**: 630–639.

Cambon, K, Zimmer, V, Martineau, S, Gaillard, M, Jarrige, M, Bugi, A, **Miniarikova, J**, *et al.* (**2017**). Preclinical Evaluation of a Lentiviral Vector for Huntingtin Silencing. *Mol. Ther. Methods Clin. Dev.* **5**: 259–276.

Miniarikova, J, Zanella, I, Huseinovic, A, van der Zon, T, Hanemaaijer, E, Martier, R, et al. (**2016**). Design, Characterization, and Lead Selection of Therapeutic miRNAs Targeting Huntingtin for Development of Gene Therapy for Huntington's Disease. *Mol. Ther. Nucleic Acids* 5: e297. *Selected as 'the best of 2016' in the journal of Molecular Therapy: Family of Journals.*

Konstantinova P and **Miniarikova J**. RNAI INDUCED HUNTINGTIN GENE SUPRESSION. Patent filed on Dec 23, 2015. de 15817385.6-1401.

LIST OF PRESENTATIONS

2014 **NVGCT**, Lunteren, The Netherlands, Poster presentation
2014 **EHDN**, Barcelona, Spain, Poster presentation
2014 **ESGCT**, The Hague, The Netherlands, Poster presentation
2015 **ESGCT**, Helsinki, Finland, Oral presentation
2015 **OTS**, Leiden, The Netherlands, Poster presentation
2015 **HD Dutch Meeting**, Groningen, The Netherlands, Oral presentation
2016 **Small RNA meeting**, Keystone, CO, USA, Poster presentation
2016 **EHDN**, The Hague, The Netherlands, Poster presentation
2017 **CHDI**, St Julian's, Malta, Poster presentation

ACKNOWLEDGEMENTS

Here I am, at end of my PhD track, still trying to understand the lessons I have learned. From the beginning, I understood that it would be a very challenging task: PhD track in a growing company. Nevertheless, I am very grateful for this experience. This journey made me realized that, as a synchronized community with a common goal to find cures for patients, we work more efficiently and achieve results faster, as opposed to fragmented units competing among each other. This work would have hardly seen the print without a contribution from others. With a great pleasure and gratitude, I would like to dedicate some words of thanks to those relevant.

One of the most important people to thank is my daily supervisor: **Dr. Pavlina Konstantinova**. Dear Pavlina, you have started this journey with me five years ago and witnessed me through my scientific and personal growth, good or challenging. As one of the few PhD students in the company, you have personally provided me with enough safe space to learn, scientifically grow, and become independent. I realize how much of your time and patience you have invested in me in order to deliver better science in the midst of a constant change within the organization. I believe, we contributed to a therapy that will reach the HD patient at the end. I am hoping this will open possibilities for other future treatments based on RNAi. Thank you for everything. To my promoter **Prof. Dr. Sander J. van Deventer,** thank you for being critical, constructive, and supportive. Dear Sander, I appreciate the scientific tips, discussions, and positive attitude towards our research along the way. I further really appreciate your interest in culture and discussions about Eastern Europe. This made me less homesick and more welcome in the company. Thank you, **Dr. Harald Petry**, for leading the research team of uniQure during my PhD and especially, for your strong support for the HD project. Your involvement, mentorship, and useful advices allowed this project to grow rapidly.

To all members of this **thesis committee**, thank you for your time and suggestions. I am very grateful to have you in my thesis committee.

Dear **Marina**, although you have been with me only during the last two years of my journey, you became one of the most important part of it. We started as a mentor and a student. Now, I consider you as my little sister. I am so grateful you entered my life: our constant jokes, your understanding that I am not a morning person, funny impressions, singing in the lab, your “almost’’ panic attacks when the cells grew a bit differently, for “finding exosomes within exosomes”, and for our master experiments with “just enough” virus and cells. You have provided me the support, easiness, and cheerfulness that was necessary to finalize my PhD. I am very happy that your PhD project is based on the work that we started

together, the mesmerizing exosomes. You are very smart and skilful. I have no doubt you will make great and fast discoveries in this or any other field. MSG forever. Dear **Rudy**, my sense-two, you have been my partner in crime for almost the whole period of my PhD. Starting as a colleague, you became my friend, best friend, landlord, money supervisor, travel companion and more to come. I got to know you as an intelligent, caring, and very supportive person. You have helped me to develop my obsession for plants, smells, world travelling as *international sensations*, and money problems. I am very grateful to have you as my paranymph, not only to assure that I will make it on time for the graduation, but the fact that you will be standing next to me during this important day. Cheers to our future and I hope to keep building the community. Dear **Kasia**, there is so much to say and so little space. You have been my best friend since I entered the Netherlands. We have been through thick and thin. We started the techno club together, dinners, nights out, and crazy adventures. You have been the most important part of my personal growth. You have a gift to energize everything around you with wit and smart, while being kind and supportive. You are my family and I have tremendous respect for you. You have been a paranymph to many people and I feel privileged that you have accepted to stand next to me as well during this important moment of my life. Cheers pumpkin.

Dear **Raygene**, I am so thankful to have you in the research group. You are one of the few people who offers help without asking, who puts others' needs before his own, and who is always supportive. You are an amazing person, scientist, and congratulations for becoming a father. Dear **Kimberley**, thank you for sharing ideas and approaches. I admire your strong personality, keep it up girl. Dear **Ilaria**, my first master student -an experiment on its own. I appreciate your help and being the sunshine during the busy days. Hopefully, see you soon. Dear **Melvin**, thank you for all your suggestions and help. You joined the team in the middle of the company relocation and structural changes, and yet you managed to add a great value. Cheers. Dear **Tom**, thank you for your help with the *amazing master plans* and experiments in the lab. You made the bad lab days bearable and fun. Good news: no more *Zalando* boxes in the office. Dear **Cynthia** and **Sonay**, thank you for being kind and always positive. You make uniQure a lovely place to work in. Dear **Jolanda S.** thank you for the lab control and keeping the freezers organized.

Dear **Valerie**, **Bas**, and **Jacek**, when I started, you formed the backbone of the research team in uniQure. I have learned so much from the discussions with you and presentations. Good luck with everything. Dear **Olivier** and **Wim**, thank you for teaching me about IP. Dear **Eileen,** thank you for reviewing chapters of this thesis and your valuable input. Dear **Lisa** and **Martin**, thank you for the useful input on the nonclinical matters. Dear **Jolanda L.**, **Ying Poi, Anna, Francois**, **Astrid,** and **Erich**, it was a great learning experience to see you scientifically grow and establishing yourselves in the company. Good luck with your projects. Dear **Karin**

and **Bas**, thank you for your technical input whenever I needed it. Dear Karin, I will miss your singing and laughing in the corners of uniQure. Dear **Sumiati**, **Nikki**, **Lucas**, **Betty**, **Vanessa**, and **Richard.** I appreciate your advices, energy, and discussions. Keep it up guys. Dear **Lisa, LaVaLL,** I am grateful for your always positive attitude and assisting the research team. I love your clothing ideas and fashion. Keep up the good vibe. Dear IT team: **Christian**, **Dennis** and **Pascal**, thank you for helping me with all those cables, tables, computers, IT stuff and fun energy. You guys are awesome. To all **uniQurians**, thank you for everyday activities and being a part of the team. Cheers to you.

To all my friends, thank you. Please, see the extended version.

Dear **mom** and **dad**, you have given me the greatest things a child can receive: support, confidence, love, and understanding. This is the base that is crucial to be able to live as an expat and fulfil my dreams. I keep you in my heart everywhere I go. I am so happy for the family we have created together. I love you. Dear **Ika**, my twin sister, because of you, I had to fight the world only five minutes alone. Thank you for being with me my whole life. You are my counterpart, you are my mirror, and my constant support. I love you and I am so excited about our family to grow.

Thank you and much love to all of you.